Exploring Kardar-Parisi-Zhang universality class : from the dynamics of exciton-polariton condensates to stochastic interface growth with temporally correlated noise

Davide Squizzato

Communauté
UNIVERSITÉ Grenoble Alpes

THÈSE

Pour obtenir le grade de

DOCTEUR DE LA COMMUNAUTE UNIVERSITE GRENOBLE ALPES

Spécialité : **Physique Théorique**

Arrêté ministériel : 25 mai 2016

Présentée par

Davide SQUIZZATO

Thèse dirigée par **Léonie CANET**, Professeure, UGA
et codirigée par **Anna MINGUZZI,** Directrice de Recherche, CNRS

préparée au sein du **Laboratoire Laboratoire de Physique et de Modélisation des Milieux Condensés**
dans l'**École Doctorale Physique**

Exploring Kardar-Parisi-Zhang universality class: from the dynamics of exciton-polariton condensates to stochastic interface growth with temporally correlated noise.

Exploration des propriétés universelles Kardar-Parisi-Zhang: de la dynamique des condensats d'exciton-polariton à la croissance stochastique d'interfaces avec un bruit temporellement corrélé.

Thèse soutenue publiquement le **9 octobre 2019**,
devant le jury composé de :

Monsieur Eric BERTIN
Directeur de Recherche, CNRS, Président
Monsieur Alberto BRAMATI
Professeur, Sorbonne université, Examinateur
Madame Léonie CANET
Professeure, UGA, Directrice de thèse
Madame Anna MINGUZZI
Directrice de Recherche, CNRS, Co-Directrice de thèse
Monsieur Dominique MOUHANNA
Professeur, Sorbonne université, Rapporteur
Monsieur Grégory SCHEHR
Directeur de Recherche, Université de Paris-Sud et CNRS, Rapporteur

Acknowledgements

I would like to thank the members of the jury Dominique Mouhanna, Grégory Schehr, Eric Bertin and Alberto Bramati for accepting to review the following manuscript.
This thesis is the result of almost three years of work. In this period i had the pleasure to share, discuss and learn a lot from two sunny and cheerful people, Léonie and Anna, which supervised the development of this work. I have to warmly thank them because, besides all the work we did together and all the good moment shared besides physics, they left me the freedom i need. I also have to thank all the people from the Laboratoire de Physique et de Modélisation des Milieux Condensés, with whom i shared the daily life. From the secretaries, Habiba and Camille, who were fundamental in covering my bureaucratic inadequacy and with whom i had the pleasure to laugh and joke, to Jean-Daniel, to whom i am indebted for all the help he gave me on the informatics side with the happiness that distinguishes him, to the permanent staff. Of course i also have to thank all the non-permanent people of the lab that i met in these years, most of them good friends rather then just colleagues.
This work would have been impossible without all the people i met besides physics and all the friends i shared the life with. I am eternally grateful to them for all the good moments we passed through, all the good (and less good) beers we had, the mountains we climbed and skied, the waves we surfed and, more importantly, for all the discussions we had and all the questions they triggered in me.
The last, biggest, thank goes to my family, that always supported me and taught me the quest of knowledge, the willing to travel and being enriched by different cultures, and the importance of solidarity.

To social struggle and libertarian socialism,
that are the only means to free science and humanity
from capitalism and selfishness.

Table of Contents

Introduction

Many physical phenomena in nature exhibit common features at the macroscopic scale, despite having extremely different microscopic description. A prominent and long studied example is the analogy between the paramagnetic to ferromagnetic phase-transition in magnets at the Curie temperature and the gas to liquid phase transition in a molecular gas at the critical point. Usually, such a universal description of a-priori different physical apparati appears in the scaling limit, when they become invariant under a change in the scale at which they are observed. In this regime the correlations between distant degrees of freedom behave as a power law. This regime is often referred to as critical, since it is related to a phase transition in which the system changes its properties in a dramatic way. At criticality, the correlation length diverges and the fluctuations between two different parts of the system are correlated over all the scales, signalling the appearance of long-range order in the system. In this regime, different correlations decay with different power-laws, characterized by the critical exponents. The set of these critical exponents defines the Universality Class of the model, which characterizes the universal properties of different microscopic models when the critical point is reached.

Following these arguments, even if a system possesses many quantities which strongly depend on the microscopic scale Λ at which we analyse it, to assess and study universal properties we are interested in the observables that are smooth and slowly varying with Λ. Such observables are usually related to conserved, and hence slowly varying, quantities of the system. The set of conserved quantities of the model is determined by the set of transformations that leave it invariant. Physical systems obeying different symmetries will be described by different slowly varying fields and by different critical exponents in the scaling regime: we will say that they belong to different universality classes. The formal analysis of such universal phenomena can be performed using tools coming from statistical mechanics, which studies physical systems with a large number of degrees of freedom. Our goal is to explain the critical behaviour of such systems using as few as possible relevant quantities. Hence we want to get reliable predictions on the scaling properties of a model while being as ignorant as possible about its microscopic details.

In equilibrium statistical mechanics, the microscopic dynamics is fully reversible and detailed balance condition is fulfilled. There, one usually has to fine-tune the control parameters of the model at the scale Λ in order to reach the critical behaviour at large scales. Relaxing the equilibrium condition by allowing drive and dissipation in the system, and hence breaking the reversibility of the microscopic dynamics, the situation can change drastically. To describe the out-of-equilibrium dynamics of slowly varying fields, one accepts to be ignorant about the microscopic phenomena generating the driven-dissipative nature of the system and models these effects by an effective noise term responsible for the fluctuations. The coarse-grained fields under study thus become random variables, or random fields, following a stochastic evolution, usually determined by a Langevin-type equation. This equation is assumed to well describe the underlying dynamics at not too small distances and times. Since the eighties many non-equilibrium systems described by a Langevin equation showed generic scale invariance, *i.e.* diverging correlation

length and power law behaviours of the correlations in both time and space for arbitrary values of the microscopic parameters. These systems are often referred to as self-critical, because they develop critical properties in their dynamical evolution no matter the initial conditions [1]. In general, from simple arguments, one expects models with conserved dynamics accompanied by non-conservative noise, to be self critical [2]. For systems with conservative noise the argument is more subtle but one can also show that without detailed balance, *i.e.* being out-of-equilibrium, a generic power-law behaviour in the correlation is attained. Forcing the detailed balance condition suddenly implies exponential, and hence non critical, decay of the correlations for generic microscopic parameters [3].

In the last sixty years a lot of effort has been devoted to trying to investigate these universal properties at the theoretical level. More precisely, the task addressed has been to start from a microscopic formulation of a theory and to look if it ever reaches a critical regime as the observing scale κ is changed. While κ flows, the contribution coming from the irrelevant microscopic parameters is supposed to be washed out, leaving only the one of relevant parameters. If it ever reaches a scaling regime, the goal is to know to which broader universality class this effective model belongs to in this scaling regime. Once we find the universality class, the critical exponents and scaling functions associated to it, are enough to characterize the behaviour of all the physical observables. This procedure of following the behaviour of a theory as the observing scale κ is changed, in order to understand which parameters survive in the long distance and time regime, is called renormalization. All these scale transformations are hence called renormalization group (RG) transformations. The application of the renormalization idea to statistical physics was first introduced by Kadanoff [4] and then refined by Wilson [5, 6], borrowing the idea of renormalization of the coupling constants already present in quantum field theories [7, 8, 9, 10]. The idea of RG is to get a set of equations describing how the different couplings evolve as the scale κ is varied, which are the Callan-Symanzik beta functions [11, 12]. The critical behaviour is reached at the fixed-point, where the beta functions stop to flow under a scale transformations. This is the signature of scale invariance. The critical exponents defining the universality classes can then be assessed by looking at how the system approaches the fixed point of the theory.

This concept of RG introduced in equilibrium statistical physics, has been extended to out-of-equilibrium by Hohenberg and Halperin [13]. The appropriate framework to implement a RG is a field theory. A procedure to recast the Langevin description into a path integral formalism has been proposed. It consists in introducing an additional field, also known as response field, for each field in the Langevin equation. This method is often referred to as Martin-Siggia-Rose-Janssen-De Dominicis (MSRJD) formalism [14, 15, 16]. Even if the formal derivation is different, the MSRJD formalism is analogous to the closed-time-path (CTP) formalism introduced by Schwinger and Keldysh in quantum mechanics for non-equilibrium systems [17, 18].
In interacting field theories, computing the RG flow of an observable at the analytical level is an extremely difficult task. What is usually done is to study how the free theory is modified by the inclusion of the desired interaction, at a chosen order in this perturbation. When the interacting fixed points are connected smoothly to the non-interacting (Gaussian) ones, this perturbative analysis allows to grasp insights into the critical exponents of the interacting theory. A good example in this sense is the Wilson-Fisher fixed point in the ϕ^4 theory, which controls the critical properties of the paramagnetic to ferromagnetic continuous phase transition mentioned previously. This fixed point is Gaussian in $d = 4$ and can be described perturbatively for small $\epsilon = 4 - d$. However, there are theories where no connection exists between the Gaussian and the interacting fixed points. A paradigmatic example is the Kardar-Parisi-Zhang (KPZ) equation we will study in this manuscript. In KPZ, all the properties of the interacting (strong-coupling) fixed point in $d \neq 1$ cannot be accessed by perturbation theory. One thus

needs non perturbative techniques to tackle this theory. An alternative formulation of the RG procedure was first introduced by Polchinski, by generalizing the Kadanoff-Wilson picture [19]. In Polchinski's RG scheme one finds exact flow equations for the effective Hamiltonian of the system. A reformulation of Polchinski's RG for the effective average action was proposed some years later by Wetterich, Morris and Ellwanger separately [20, 21, 22]. This exact flow for the effective average action is the basis of the non-perturbative renormalization group (NPRG) formalism used in this work. This approach, initially formulated for physical systems at equilibrium, has recently been extended to study out of equilibrium universal properties [23].

Motivated by the fascinating properties of out-of-equilibrium dynamics and the concept of universality, in this thesis we study two models related to the KPZ equation. The first system is a driven-dissipative quantum system composed by excitons interacting with photons confined in a cavity. In the strong-coupling regime, this interaction gives rise to a bosonic quasi-particle, the exciton-polariton. Due to the losses of the photons out of the cavity, the system needs to be constantly pumped by a laser field in order to generate a steady state of exciton-polaritons. Under these conditions, Bose-Einstein condensation (BEC) of exciton-polaritons has been demonstrated experimentally [24]. Quite remarkably, the nature of this condensate is different from the equilibrium BEC. In particular it has been shown that the phase of the condensate in the steady state shows critical properties which are described by the KPZ equation [25]. The second model under study describes classical growing surfaces in which the underlying microscopic dynamics is correlated in time. This leads to a KPZ equation with temporal memory effects. This time correlation spoils one of the fundamental symmetry of the system and can in principle modify all the critical properties of the pure theory.

This manuscript is organized as follows. We first settle the notation used in the rest of the text. Then, in Chapter 1 we introduce the main features of the KPZ equation. In Chapter 2 we review the first physical system investigated, the Exciton-Polaritons. In the following two Chapters, 3 and 4, we present our original results on exciton-polaritons. We first use the Schwinger-Keldysh formalism to obtain new analytical results which demonstrate the EP to KPZ mapping beyond the homogeneous case, and then give some numerical results concerning the phase distribution of exciton-polaritons in the homogeneous case and the scaling in the inhomogeneous one. In the last part of the thesis, Chapter 5, we use NPRG techniques to tackle the KPZ equation with time-correlated noise. We study the one and two dimensional case with either short or long range correlations. All the technical details of the calculations presented in the main text are given in the subsequent Appendices.

The work of this thesis is presented in the following articles:

- Squizzato, Davide and Canet, Léonie and Minguzzi, Anna, "Kardar-Parisi-Zhang universality in the phase distributions of one-dimensional exciton-polaritons", Phys. Rev. B **97**, 195453 (2018)
- Squizzato, Davide and Canet, Léonie, "Non-Perturbative Renormalization Group Approach to Kardar-Parisi-Zhang Equation with Temporally-Correlated Noise", to be submitted (2019)

Notation

In this chapter we introduce the notation used in the rest of the manuscript.

Variables and Integrals

In the thesis we will be interested in both static and dynamical properties of physical systems; the space variable will be usually denoted by $\vec{x}$, which is a d-dimensional vector

$$\vec{x} = \{x_1, \dots, x_d\}. \tag{i}$$

In general, the modulus of any vector $\vec{a}$ will be indicated by the symbol a. The modulus of the space vector will thus be

$$x = |\vec{x}| = \sqrt{\sum_{i=1}^{d} x_i^2}. \tag{ii}$$

The time variable will be usually addressed to as t. For the sake of simplicity a space-time coordinate

$$\mathbf{x} = (\vec{x}, t) \tag{iii}$$

is introduced; any bold variable is then meant to be a space-time(or momentum-frequency) variable. A generic integral of a function $f(Y)$ over a set of variables $Y = \{y_1, \dots, y_N\}$ is denoted as

$$\int \left(\prod_{i=1,\dots,N} \mathrm{d}y_i \right) f(y_1, \dots, y_N) \equiv \int_Y f(y_1, \dots, y_N) \tag{iv}$$

The symbol $\int_{\mathbf{x}} \cdot$ thus means the integral over space-time coordinate.
The integrals we will compute in the NPRG approach have the form

$$I(\bar{\omega}, p) = \int_{\mathbf{q}} f(\omega, q) g(\bar{\omega} + \omega, |\vec{p} + \vec{q}|). \tag{v}$$

In $d \geq 2$ we can reduce this $(d+1)-$dimensional integral to a $3-$dimensional integral, by exploiting rotational symmetry. Going to hyperspherical coordinates we indeed have

$$I(\bar{\omega}, p) = \frac{S_{d-1}}{(2\pi)^{d+1}} \int_{-\infty}^{\infty} \mathrm{d}\omega \int_0^{\pi} \mathrm{d}\psi \sin(\psi)^{d-2} \int_0^{\infty} \mathrm{d}q\, q^{d-1} f(\omega, q)\, g\left(\bar{\omega} + \omega, \sqrt{p^2 + q^2 + 2\cos(\psi)} \right) \tag{vi}$$

where $S_d = 2\pi^{d/2}/\Gamma(d/2)$ is the d-dimensional solid angle. Here we used the fact that the $d-$dimensional solid angle element $\mathrm{d}\Omega$ can be written as

$$\begin{aligned} \mathrm{d}\Omega &= \sin(\psi_1)^{d-2} \sin(\psi_2)^{d-3} \dots \sin(\psi_{d-2})\, \mathrm{d}\psi_1 \dots \mathrm{d}\psi_{d-1} \\ &= S_{d-1} \sin(\psi_1)^{d-2} \mathrm{d}\psi_1 \end{aligned} \tag{vii}$$

and we rotated the system such that $\vec{p} \cdot \vec{q} = pq\cos(\psi_1)$.

Fourier Transform

In the NPRG context we will frequently switch back and forth from real to Fourier space. Given a function $f(\mathbf{x}) = f(\vec{x}, t)$ in real-space, its Fourier transform $\tilde{f}(\mathbf{p}) = \tilde{f}(\vec{p}, \omega)$ is defined as

$$\tilde{f}(\mathbf{p}) = \mathcal{F}[f(\mathbf{x})](\mathbf{p}) = \int_{\mathbf{x}} f(\mathbf{x}) e^{-i(\vec{p}\cdot\vec{x}-\omega t)} \tag{viii}$$

while the inverse Fourier transform will be

$$f(\mathbf{x}) = \mathcal{F}^{-1}[\tilde{f}(\mathbf{p})](\mathbf{x}) = \int_{\mathbf{p}} \tilde{f}(\mathbf{p}) e^{i(\vec{p}\cdot\vec{x}-\omega t)} \tag{ix}$$

with $\int_{\mathbf{p}} \cdot = \frac{1}{(2\pi)^{d+1}} \int \mathrm{d}\vec{p}\mathrm{d}\omega \cdot$.

Averages and Observables

In the main text we will always deal with stochastic systems, *i.e.* physical systems which undergo a random dynamics. In general we are interested in quantities that are averaged over different realizations of such dynamics, in order to exclude spurious effects linked to a single realization. Usually the randomness of the system is embodied by a noise term which takes into account all the microscopic effects to which we do not have access and which influence the mesoscopic dynamics in a unpredictable way. Given a noise term $\eta(\mathbf{x})$ we will indicate physical observables $\mathcal{O}$ averaged over different realizations as

$$\langle \mathcal{O} \rangle_\eta = \int \mathcal{D}[\eta] \mathcal{O}[\eta] \mathcal{P}[\eta] \tag{x}$$

with $\mathcal{P}[\eta]$ being the noise distribution, which in general is a functional, and $\mathcal{D}[\,\cdot\,]$ being the functional measure. Besides noise-averaged quantities we are also interested in averaging over, for example, space- and time-windows in which realizations of the observable are supposed to be independent from one window to the other, in order to reduce statistical fluctuations. An observable averaged over different realizations of the noise and over different space domains will read

$$\langle \mathcal{O} \rangle_{\eta,x} = \langle \left(\prod_{i=1}^{d} \frac{1}{L_i} \right) \int_{\vec{x}} \mathcal{O}(\vec{x}) \rangle_\eta \tag{xi}$$

with $x_i \in [0, L_i]$.

Correlations and Generating Functionals

Dealing with stochastic fields $\varphi(\mathbf{x})$ we are interested in different space-time correlations. In out-of-equilibrium systems, differently from the equilibrium situation, the probability distribution for the field φ is in general not known. We can however write down a generating functional for the different correlations. We define the equivalent of the partition function Z as

$$Z = \int \mathcal{D}[\varphi] e^{S[\varphi]} \tag{xii}$$

From this quantity we can in general extract $n-$point correlation functions $\langle \varphi(\mathbf{x}_1) \cdot \varphi(\mathbf{x}_n) \rangle$ via the introduction of an external source linearly coupled to the field φ,

$$Z[J] = \int \mathcal{D}[\varphi] e^{S[\varphi] + \int_x J\varphi} \tag{xiii}$$

and then differentiation with respect to the external source,

$$\langle \varphi(\mathbf{x}_1) \dots \varphi(\mathbf{x}_n) \rangle = \frac{1}{Z[J=0]} \frac{\delta^n Z[J]}{\delta J(\mathbf{x}_1) \dots \delta J(\mathbf{x}_n)} \bigg|_{J=0} . \tag{xiv}$$

As in the equilibrium case, we can define the analogue of the Helmholtz free-energy, $W[J] = \ln Z[J]$. The functional $W[J]$ generates the so-called connected correlation functions,

$$\langle \varphi(\mathbf{x}_1) \dots \varphi(\mathbf{x}_n) \rangle_c = \frac{\delta^n W[J]}{\delta J(\mathbf{x}_1) \dots \delta J(\mathbf{x}_n)} \bigg|_{J=0} , \tag{xv}$$

which are the analogous of the cumulants of a stochastic variable.

1 Kardar-Parisi-Zhang Equation and Universality Class

In this chapter we introduce the central topic of the thesis, the Kardar-Parisi-Zhang equation. The KPZ equation has been intensively studied after its formulation and we refer to the many available reviews (among others [26, 27, 28]) for learning its details and all its applications to other domains of physics. In this chapter we will focus on its universal features and on some particular properties which will be useful in the following sections of the manuscript. We will first introduce the model and its scaling properties and then analyse its linear version, the Edwards-Wilkinson equation. We will then investigate the strong-coupling nature of the KPZ fixed-point and discuss its consequences. Switching to the field-theoretical formalism we will be able to discuss the symmetries and their implications. We will then focus on the one-dimensional case and the geometrical sub-classes that emerge, together with interesting effects due to finite-size. At the end, we will briefly mention two important related models which will be useful as benchmarks for the results presented in Chapter 5.

1.1 Non-Conservative Growth Processes

We here present a general framework to describe non-conservative growth processes, based on [29]. We are interested in the description of a moving interface which could be for instance the line separating two isotropic thermodynamic phases. To describe the system we introduce a vector in $d+1$ dimensions $\vec{r}(\underline{s},t) = \{r_\alpha(\underline{s},t)\}_{\alpha=1}^{D+1}$ which spans the surface as $\underline{s} = \{s_\alpha\}_{\alpha=1}^{D}$ varies in parameters space. The growth of the surface can be triggered either by a non-conserved dynamics, *e.g.* the deposition of external particles or the growth of one phase against the other, or by a mass-conservative process, *e.g.* formation of gradients in the chemical potential on the surface due to modulations of the profile. In both cases the (deterministic) dynamics can be described by

$$\frac{\partial}{\partial t}\vec{r}(\underline{s},t) = \hat{n}\, v_n[\vec{r}(\underline{s},t)] \tag{1.1}$$

where

$$\hat{n} = \frac{1}{\sqrt{g}}\frac{\partial}{\partial s_1}\vec{r}\times\cdots\times\frac{\partial}{\partial s_D}\vec{r} \tag{1.2}$$

is the normal unite vector to the surface at point $\vec{r}$ and g is the determinant of the metric tensor.

1.1.1 The Monge Parametrization

A usual choice of parametrization is the Monge form $\vec{r} = (\vec{x}, h(\vec{x}))$ which assumes a flat background and no overhangs in the single-valued surface $h(\vec{x})$, oriented along the z direction perpendicular to $\vec{x}$. Using this parametrization we get

$$g = 1 + (\vec{\nabla}h(\vec{x}))^2, \quad \hat{n} = \left[1 + \left(\vec{\nabla}h(\vec{x})\right)^2\right]^{-1/2}(-\vec{\nabla}h(\vec{x}), 1) \tag{1.3}$$

and (1.1) becomes

$$\begin{aligned} \partial_t \vec{x}(\underline{s}, t)_\alpha &= n_\alpha v_n[h], \quad \alpha = 1, \dots, D \\ \partial_t h(\underline{s}, t) &= n_z v_n[h] \end{aligned} \tag{1.4}$$

This description is at fixed $\underline{s}$ while we are interested in the surface evolution at fixed $\vec{x}$:

$$\partial_t h(\underline{s}, t) = \partial_t h(\mathbf{x}) + \vec{\nabla} h \cdot \partial_t \vec{x}(\underline{s}, t) = \partial_t h(\mathbf{x}) + \vec{\nabla} h \cdot \partial_t \vec{x}(\underline{s}, t) \tag{1.5}$$

This leads to [29]

$$\partial_t h(\mathbf{x}) - \frac{v_n}{\left[1 + \left(\vec{\nabla} h(\mathbf{x})\right)^2\right]^{1/2}} \vec{\nabla} h \cdot \vec{\nabla} h = \frac{v_n}{\left[1 + \left(\vec{\nabla} h(\mathbf{x})\right)^2\right]^{1/2}} \tag{1.6}$$

and thus to

$$\partial_t h(\mathbf{x}) = v_n \left[1 + \left(\vec{\nabla} h(\mathbf{x})\right)^2\right]^{1/2} \tag{1.7}$$

The effective velocity v_n of the front depends on the microscopic dynamics.

1.1.2 Non-conserved dynamics

For non-conservative dynamics,

$$v_n = -\Gamma \mu = -\Gamma \frac{\delta \mathcal{F}}{\delta h} \tag{1.8}$$

where Γ is the effective mobility of the interface, μ is the chemical potential and $\mathcal{F}$ is the free-energy of the system, which in the case of a non-conserved growth is given by

$$\mathcal{F}[h] = \int_{\vec{x}} \sigma \sqrt{g} - \mu_0 \int_{\vec{x}} h(\vec{x}) \tag{1.9}$$

where σ is the effective surface tension and μ_0 gives the direction and intensity of the external field. This implies

$$\mu = -\frac{\sigma \vec{\nabla}^2 h(\vec{x})}{\left[1 + \left(\vec{\nabla} h(\vec{x})\right)^2\right]^{3/2}} - \mu_0 \tag{1.10}$$

and thus

$$\frac{\partial}{\partial t} h(\mathbf{x}) = \Gamma \mu_0 \left[1 + \left(\vec{\nabla} h(\mathbf{x})\right)^2\right]^{1/2} + \Gamma \sigma \frac{\vec{\nabla}^2 h(\mathbf{x})}{\left[1 + \left(\vec{\nabla} h(\mathbf{x})\right)^2\right]^2} \tag{1.11}$$

It's instructive to look at the $\left(\vec{\nabla} h(\mathbf{x})\right)^2 \ll 1$ limit. At first order we obtain

$$\frac{\partial}{\partial t} h(\mathbf{x}) = \nu \vec{\nabla}^2 h(\mathbf{x}) + \frac{\lambda}{2} \left(\vec{\nabla} h(\mathbf{x})\right)^2 \tag{1.12}$$

with $\nu = \Gamma \sigma$, $\lambda = \Gamma \mu_0$ and we neglected both $\vec{\nabla}^2 h \left(\vec{\nabla} h\right)^2$ and constant contributions.

1.2 The KPZ Equation

Kardar, Parisi and Zhang in 1986 [30] introduced a non-linear Langevin equation aimed to describe the transition to roughness of stochastic growing processes which do not conserve the total mass; this Partial-Differential-Equation(PDE), later referred to as KPZ-equation, is given by

$$\partial_t h(\mathbf{x}) = \nu \nabla^2 h(\mathbf{x}) + \frac{\lambda}{2}\left(\vec{\nabla} h(\mathbf{x})\right)^2 + \sqrt{D}\eta \tag{1.13}$$

with $\langle \eta(\mathbf{x}) \rangle = 0$, $\langle \eta(\mathbf{x})\eta(\mathbf{x}') \rangle = \delta(\mathbf{x} - \mathbf{x}')$. With respect to the deterministic equation (1.12), the equation (1.13) takes into account a noise term coming from the effects of the environment on the surface. As we saw in the previous section, the non-linear term in (1.13) is the most relevant quantity that comes out when taking into account lateral growth of a surface and has a key role in the roughening process. By properly rescaling the time and the height field as

$$t \to t/\nu, \quad h \to h\sqrt{\frac{D}{\nu}} \tag{1.14}$$

the original KPZ equation, containing three parameters ν, λ, D, reduces to a one-parameter equation

$$\partial_t h(\mathbf{x}) = \nabla^2 h(\mathbf{x}) + \frac{\sqrt{g}}{2}\left(\vec{\nabla} h(\mathbf{x})\right)^2 + \eta \tag{1.15}$$

where $g = \lambda^2 \frac{D}{\nu^3}$ is the effective non-linearity of the theory. This non-linear Langevin equation is very general and its universal features appear to be relevant in different domains such as growing of bacterial colonies, spreading of fire fronts and turbulent liquid-crystals [31, 32, 33].

1.2.1 Family-Vicsek Scaling

As usual in statistical mechanics one is interested in studying fluctuations of observables of the system. Historically the most investigated quantity in KPZ equation is the standard deviation w^2 of the height profile within a window of spatial extension L often referred to as roughness,

$$w^2(L,t) = \left\langle h(\mathbf{x}) - \langle h(\mathbf{x}) \rangle_x^2 \right\rangle_{x,\eta} \tag{1.16}$$

where $\langle \cdot \rangle_x = \frac{1}{L}\int_x \cdot$ and $\langle \cdot \rangle_\eta$ is the average over different realizations of the noise η, and we restricted to one dimension for the sake of simplicity. Motivated by the exact results obtained for the linear version of (1.15), see Chap. 1.2.2, Family and Vicsek proposed the following scaling behaviour for the roughness [34]

$$w(L,t) \sim t^{\beta} F_w(Lt^{-1/z}) \sim \begin{cases} L^{\chi}, & L \ll \xi(t) \\ t^{\beta} & L \gg \xi(t) \end{cases} \tag{1.17}$$

where χ and z are referred to as the roughness and dynamical critical exponent respectively and $\beta = \chi/z$, $F_w(\cdot)$ being a universal scaling function. Here $\xi(t) \sim t^{1/z}$ is a typical length scale taking into account the emergence of coherence within the L-sized growing surface. For a finite-size system one thus observes a power-law behaviour for the roughness up to a saturation time $T_s \sim t^z$ where it saturates to a value $w^2(L, T_s) \sim L^{2\chi}$ (see Fig. 1.1). Another interesting quantity is the two-point height-height connected correlation function,

$$C(\mathbf{x}) = \langle h(\mathbf{x})h(0,0) \rangle_c \equiv \langle h(\mathbf{x})h(0,0) \rangle - \langle h(\mathbf{x}) \rangle \langle h(0,0) \rangle \tag{1.18}$$

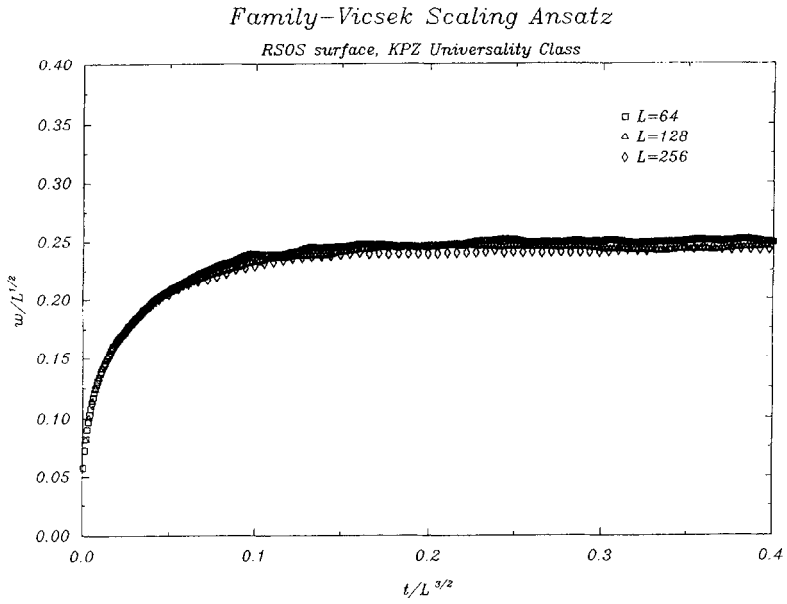

Figure 1.1: Scaling of the roughness for one-dimensional restricted-solid-on-solid (RSOS) growth process of different sizes L; RSOS belongs to the KPZ universality class [26].

which in the long-distance long-time limit $(t, x) \to \infty$ behaves as

$$C(\mathbf{x}) \sim x^{2\chi} F_C(t/x^z) \tag{1.19}$$

where $F_C(y)$ is a universal function characterized by two different asymptotic regimes,

$$F_C(y) \sim \begin{cases} F_0, & y \to 0 \\ F_\infty y^{2\chi/z}, & y \to \infty \end{cases}. \tag{1.20}$$

These power-law behaviours of correlations hold for any value of the coefficients in (1.13), which implies that no fine-tuning is required to get a critical system, or, equivalently, that KPZ equation describes fluctuations of self-similar growing surfaces.

1.2.2 The Edwards-Wilkinson Equation

The case $\lambda = 0$ is known in the literature as the Edwards-Wilkinson equation (EW) [35] and can be reduced to a perfectly equilibrium problem which can be solved exactly. Indeed the solution to the equation

$$\partial_t h(\mathbf{x}) = \nu \nabla^2 h(\mathbf{x}) + \sqrt{D}\eta \tag{1.21}$$

can be computed exactly by means of several approaches; we here recall two of them.

Fokker-Planck Solution of EW

The Fokker-Planck formulation of (1.21) reads

$$\partial_t P[h(\mathbf{x})] = -\int \mathrm{d}\vec{x} \frac{\delta}{\delta h} \left(\nu \nabla^2 h(\mathbf{x}) \right) P[h(\mathbf{x})] + \frac{D}{2} \int \mathrm{d}\vec{x} \frac{\delta^2}{\delta h^2} P[h(\mathbf{x})]. \tag{1.22}$$

Its stationary solution is given by

$$P[h(\vec{x})] \propto \exp\left(-\int d\vec{x}\frac{\nu}{D}(\vec{\nabla}h)^2\right) \tag{1.23}$$

which is a Gaussian distribution for the height-field h, typical of non-interacting systems. In such cases the anomalous dimension η associated to the scaling of the field variable h is $\eta = 0$ and we can easily find the scaling exponents from the behaviour of (1.21) under a scale transformation; if we re-scale $\vec{x} \to b\vec{x}$, $t \to b^z t$, $h \to b^\chi h$ and we ask (1.21) to be scale-invariant, we find

$$z = 2, \quad \chi = \frac{2-d}{2} \tag{1.24}$$

which are the exponents defining the EW universality class.

Solution of EW in Fourier Space

Another way of finding the EW exponents, which will be useful in the following for the perturbative RG analysis of KPZ equation, is to formulate the EW equation in Fourier space,

$$h(\mathbf{p}) = \frac{\sqrt{D}}{(-i\omega + \nu p^2)}\eta(\mathbf{p}) \equiv G_0(p)\eta(\mathbf{p}) \tag{1.25}$$

or equivalently using a diagrammatic representation,

(1.26)

This representation will be useful in the perturbative expansion of the non-linear case $\lambda \neq 0$. Equation (1.25) implies that

$$C(\mathbf{p}) = \langle h(\mathbf{p})h(-\mathbf{p})\rangle_c = \frac{D}{\omega^2 + \nu^2 p^4} = p^{-4}\frac{D}{\nu^2\left(1 + \frac{\omega^2}{\nu^2 p^4}\right)}, \tag{1.27}$$

using $\langle\eta(\mathbf{p})\rangle = 0$. Recalling that the usual scaling form for the correlation in dynamical critical phenomena reads [36]

$$C(\mathbf{p}) \sim p^{-z-2+\eta}\tilde{C}(\frac{\omega}{p^z}) \tag{1.28}$$

one deduces that $z = 2$ and $\eta = 0$. Furthermore from the comparison between the Fourier transform of (1.28) and the ansatz (1.19), we find that

$$\chi = \frac{-d+2-\eta}{2} \tag{1.29}$$

which combined to $\eta = 0$ gives $\chi = 1/2$ in $d = 1$; we recover the results of the previous section. For a generic interacting out-of equilibrium system the evolution in Fourier space cannot be solved exactly and one needs to build proper approximation schemes.

1.2.3 Strong Coupling Fixed-Point and the Failure of Perturbation Theory

While the linearity of EW implies that one can solve the equation in Fourier space, the non-linear term in KPZ equation prevents from finding an exact solution to the model in any dimension. This can be immediately seen by writing KPZ equation in Fourier space, as we did before for (1.25),

$$\begin{aligned} h(\mathbf{p}) =& h_0(\mathbf{p}) - \frac{\lambda}{2} G_0(p) \int_{\mathbf{k}} \vec{k} \cdot (\vec{p} - \vec{k}) h(\mathbf{k}) h(\mathbf{p} - \mathbf{k}) \\ \equiv& G(p)\eta(\mathbf{p}) \end{aligned} \tag{1.30}$$

with $h_0(\mathbf{p}) = G_0(p)\eta(\mathbf{p})$ being the solution of EW equation (1.25) and $G(p)$ the full propagator of the theory; we see that with respect to the EW case we have an additional term that cannot be computed exactly. Using the diagrammatic notation introduced before in (1.26), equation (1.30) reads

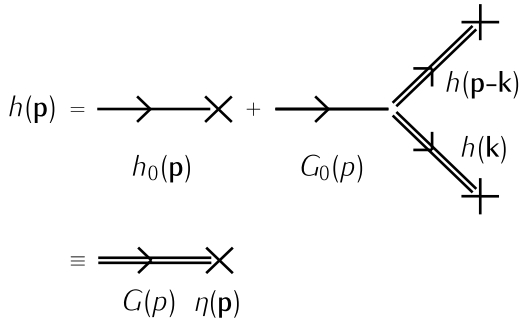

(1.31)

with

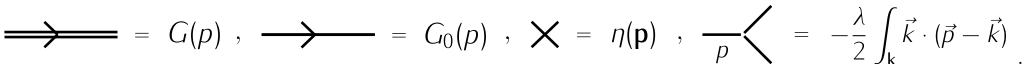

(1.32)

We see that the full solution of KPZ equation, $h(\mathbf{p})$, can be diagrammatically drawn as a double line with an arrow, symbolizing the full propagator $G(p)$, times a cross symbolizing the noise vertex $\eta(\mathbf{p})$, in analogy with (1.26) where the solution $h(\mathbf{p}) \equiv h_0(\mathbf{p})$ was a single line with an arrow, symbolizing the bare propagator $G_0(p)$, times the cross standing for the noise vertex $\eta(\mathbf{p})$. Using this formalism we see that we can try to solve KPZ equation by substituting the full solution in the integral on the $r.h.s$ with its approximate solution at the desired order in the non-linear vertex λ. This is the basic idea behind the dynamical RG (DRG) approach.

The DRG Approach to KPZ at One Loop

The dynamical Renormalization Group approach is a combination of the idea of perturbation theory and of Wilson's momentum-shell RG extended to out-of-equilibrium systems [37, 38]. For the KPZ equation it consists in a small-λ expansion around the exact non-interacting EW solution h_0 followed by an integration over an infinitesimal momentum-frequency shell [30]. Once we have an approximate solution of (1.30) we can compute observables and physical quantities by averaging over the noise η, exploiting the fact that an arbitrary Gaussian correlator splits into product of two-point correlations $\langle \eta\eta' \rangle$, whose statistical properties are known. This iterative procedure can be done more intuitively by using diagrammatic procedure, as shown in Fig. 1.2. If we restrict the momentum integral inside a shell $e^{-\ell}\Lambda < p < \Lambda$, for small enough ℓ, we can look for the renormalization of a given observable, at the chosen approximation order, under an infinitesimal scale transformation: this procedure is the key step

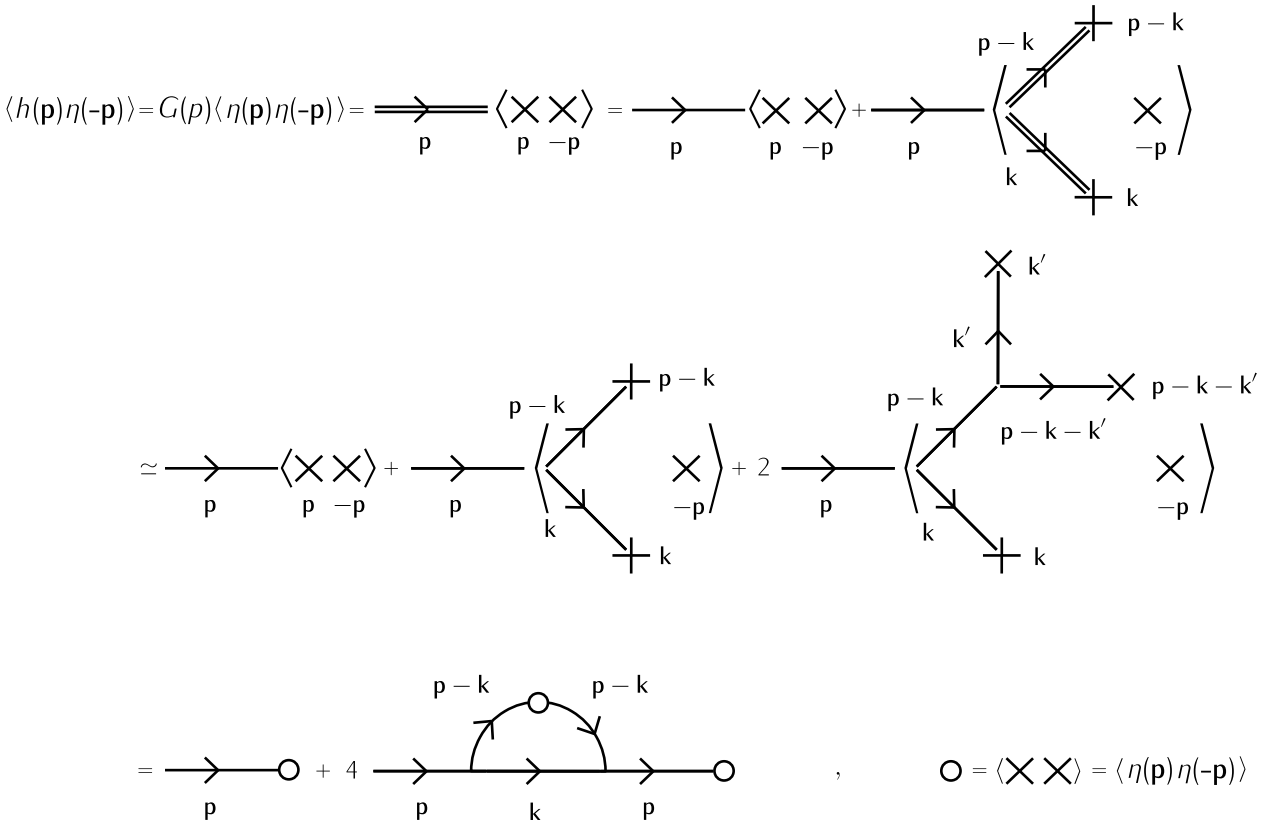

Figure 1.2: We here see an example of the DRG iterative procedure. If we choose as observable the quantity $\langle h(\mathbf{p})\eta(-\mathbf{p})\rangle$, that as we can see in the first line of the figure above will give the corrections to the bare propagator G_0, we have to multiply (1.31) by the term $\eta(-\mathbf{p})$, represented by a cross (see (1.32)) and to take the average over the noise η. Next we have to substitute in an iterative way the full solution in the $r.h.s$ of the first line, pictured as a double line with a cross, by the approximate solution h_0 plus corrections. If we stop at the $\mathcal{O}(\lambda^2)$ order we get the second line in the figure above. The averaging procedure will then consist in combining couples of crosses and use the fact that $\langle \eta(\mathbf{p})\eta(\mathbf{p}')\rangle = \delta(\mathbf{p}+\mathbf{p}')$; all the odd products of η will give a vanishing contribution because of its Gaussian statistics. In the third line we see that the chosen observable gives the first order correction to the bare propagator and hence renormalizes the bare coupling ν.

of DRG. Depending on the chosen observable we will have the renormalization contribution to different couplings (see Fig. 1.2). If we stop to the order λ^2 and look for only one-loop corrections we find [30]

$$\frac{\mathrm{d}\nu(\ell)}{\mathrm{d}\ell} = \nu\left[z - 2 + K_d\, g\, \frac{2-d}{4d}\right] \tag{1.33a}$$

$$\frac{\mathrm{d}D(\ell)}{\mathrm{d}\ell} = D\left[z - d - 2\chi + K_d \frac{g}{4}\right] \tag{1.33b}$$

$$\frac{\mathrm{d}\lambda(\ell)}{\mathrm{d}\ell} = \lambda[z + \chi - 2] \tag{1.33c}$$

where $K_d \equiv S_d/(2\pi)^d$ and $S_d \equiv 2\pi^{d/2}/\Gamma(d/2)$ is the angular volume in d dimension. As we will see in the following section Galilean invariance implies that the flow of λ is zero: this result holds to any order in perturbation theory. The flows of ν, D both depend on only one relevant parameter g, the effective non-linearity introduced in 1.15. Recalling that $\sqrt{g} = \lambda\sqrt{D/2\nu^3}$, its RG flow can be easily calculated from the ones above,

$$\frac{\mathrm{d}g(\ell)}{\mathrm{d}\ell} = (2-d)g + K_d \frac{2d-3}{2d} g^2. \tag{1.34}$$

We are interested in fixed point solutions of this equation, *i.e.* value of g^* such that $\mathrm{d}g(\ell)/\mathrm{d}\ell|_{g=g^*} = 0$. It is important to note that $d = 2$ is what would be called the marginal dimension in equilibrium systems, because the linear correction vanishes and only logarithmic renormalization occurs; we can read from (1.34) that the coupling g is marginally relevant in this dimension, because it grows under rescaling. The two fixed point solutions of (1.34) are:

$$g^*_{EW} = 0, \qquad g^*_{KPZ} = K_d^{-1}(d-2)\frac{2d}{2d-3}. \tag{1.35}$$

The stability analysis around the two FP then gives:

$$\frac{\mathrm{d}}{\mathrm{d}g}\left(\frac{\mathrm{d}g(\ell)}{\mathrm{d}\ell}\right)\bigg|_{g^*_{EW}} = 2 - d, \qquad \frac{\mathrm{d}}{\mathrm{d}g}\left(\frac{\mathrm{d}g(\ell)}{\mathrm{d}\ell}\right)\bigg|_{g^*_{KPZ}} = d - 2. \tag{1.36}$$

In $d = 1$ the only stable fixed point is the KPZ one. In $d = 2$ we have that g is marginally relevant and a small-perturbation around $g = 0$ will explode; a possible strong-coupling FP is thus inaccessible at this level of perturbation theory. For $d > 2$ we have a different scenario: for small enough perturbation the solution g^*_{EW} is stable and we recover the EW physics. However for strong enough initial values the quadratic term dominates and the flow will diverge, making any strong-coupling fixed point unreachable. Remarkably, it was shown that the same result is obtained at any order of perturbation theory [39]. This strong-coupling nature of the KPZ fixed point will motivate us in using NPRG approach, which is intrinsically non-perturbative and allows to reach the true KPZ fixed point in any dimension.

1.3 KPZ Action and Symmetries

Due to its scaling properties the KPZ equation appears as the right playground for investigating out-of-equilibrium universal features. To this aim it is important to understand the symmetries. A field-theoretical description of the model is then appropriate. One can use the Martin-Siggia-Rose-Janssen-De Dominicis (MSRJD) formalism (see App. A for details) to write a classical action associated to equation (1.13), ending with

$$S[h, \tilde{h}] = \int_{\mathbf{x}} \left\{ \tilde{h}\left(\partial_t h - \nu\nabla^2 h - \frac{\lambda}{2}(\nabla h)^2\right) - D\tilde{h}^2 \right\} \tag{1.37}$$

where $\tilde{h}$ is usually referred to as the response field. It is useful to look at the canonical (engineering) dimension, denoted $[\cdot]$, of the different terms for future RG applications; physically this quantity tells how an observable scales when the observation scale in a free (Gaussian) theory is varied. By defining $[\vec{x}] = -d$ and requiring $[\nu] = [D] = 0$, *i.e.* that the diffusivity and the noise strength do not get renormalized when changing the scale in a free theory, we get

$$[t] = -2, \quad [h] = \frac{d-2}{2}, \quad [\tilde{h}] = \frac{d+2}{2}, \quad [\lambda] = \frac{2-d}{2} \tag{1.38}$$

which also implies $[g] = (2-d)$. We see that the non-linearity becomes marginal at $d = 2$.

1.3.1 Symmetries

Besides the translational and rotational invariance, the KPZ action possesses three more exact symmetries: invariance under a constant shift of the height field, invariance under an infinitesimal tilt of the surface and invariance under time reversal of the dynamics; the latter is an accidental symmetry which holds only in one dimension.

- **Shift Symmetry**
  It is easy to check that the transformation

  $$h(\mathbf{x}) \to h'(\mathbf{x}) = h(\mathbf{x}) + c \tag{1.39}$$

  is an exact symmetry of (1.37).

- **Galilean Invariance**(GI)
  A key symmetry of (1.37) is the invariance under an infinitesimal tilt of the surface

  $$\begin{aligned} h(\mathbf{x} \to h'(\mathbf{x}) &= \vec{x} \cdot \vec{v} + h(t, \vec{x} + \lambda \vec{v} t) \\ \tilde{h}(\mathbf{x}) \to \tilde{h}'(\mathbf{x}) &= \tilde{h}(t, \vec{x} + \lambda \vec{v} t) \end{aligned} \tag{1.40}$$

  which corresponds to a Galilean transformation on the velocity field $\vec{v} = \vec{\nabla} h$. When a system is Galilean invariant, the standard Lagrangian derivative $\partial_t + \vec{v} \cdot \vec{\nabla}$, is preserved along the flow and hence gets renormalized in a multiplicative way under a change of scale $x \to bx$. Such a consideration implies a scaling relation between the roughness and dynamical exponent, which is exact in any dimension. Indeed taking

  $$x \to bx, \quad t \to b^z t, \quad h \to b^\chi h \tag{1.41}$$

  we get that

  $$D_t \to b^{-z} \partial_t + b^{\chi - 2} \vec{v} \cdot \vec{\nabla} \tag{1.42}$$

  which implies $z + \chi = 2$. This holds also for the covariant derivative in the KPZ equation, defined as $D_t = \partial_t - \lambda \vec{v} \cdot \vec{\nabla}$. Furthermore, since in this case λ is the structure constant of the transformation (1.40), it is not renormalized under a change of scale. For what follows it is important to note that this transformation is a symmetry only in the case in which the noise is delta-correlated in time. The KPZ equation indeed changes under (1.40) as

  $$\partial_{t'} h' = \nu \nabla'^2 h' + \frac{\lambda}{2} (\nabla' h')^2 + \eta' \tag{1.43}$$

with

$$\langle \eta'(\mathbf{x}_1)\eta'(\mathbf{x}_2)\rangle = \langle \eta(\vec{x}_1 + \lambda\vec{v}t_1, t_1)\eta(\vec{x}_2 + \lambda\vec{v}t_2, t_2)\rangle = F(\vec{x}_1 - \vec{x}_2 + \lambda\vec{v}(t_1 - t_2), t_1 - t_2) \tag{1.44}$$

The form of the general correlation $F(\mathbf{x}_1 - \mathbf{x}_2)$ is preserved only if $F(\mathbf{x}_1, \mathbf{x}_2) = \delta(t_1 - t_2)G(\vec{x}_1 - \vec{x}_2)$, indeed

$$\begin{aligned}\langle \eta'(\mathbf{x}_1)\eta'(\mathbf{x}_2)\rangle &= \delta(t_1 - t_2)G(\vec{x}_1 - \vec{x}_2 + \lambda\vec{v}(t_1 - t_2)) = \delta(t_1 - t_2)G(\vec{x}_1 - \vec{x}_2) \\ &= \langle \eta(\mathbf{x}_1)\eta(\mathbf{x}_2)\rangle\end{aligned} \tag{1.45}$$

which is not true anymore for any non-local correlation in time. Breaking the GI implies that λ is not any longer a structure constant of a symmetry of the system and in principle can flow under a change of scale.

- **Times Reversal Symmetry**
  Another important symmetry of the KPZ action is a discrete symmetry under time reversal,

$$\begin{aligned} h(\mathbf{x}) &\to h'(\mathbf{x}) = -h(-t, \vec{x}) \\ \tilde{h}(\mathbf{x}) &\to \tilde{h}'(\mathbf{x}) = \tilde{h}(-t, \vec{x}) + \frac{\nu}{D}\nabla^2 h(-t, \vec{x}) \end{aligned} \tag{1.46}$$

The variation in (1.37) due to such a transformation is $\delta S = \int_{\mathbf{x}} (\nabla^2 h)(\vec{\nabla} h)^2$ which is in general non-zero. However in one dimension

$$\delta S = \int_{\mathbf{x}} \partial_x^2 h(\partial_x h)^2 = \int_{\mathbf{x}} \partial_x(\partial_x h)(\partial_x h)^2 = \int_{\mathbf{x}} \partial_x(\partial_x h)^3 = 0 \tag{1.47}$$

under suitable boundary conditions. This symmetry holds also for the EW equation (1.21) and it yields a fluctuation-dissipation theorem. A consequence of this symmetry is that the roughness exponent χ is equal to the EW one in $d = 1$, $\chi_{KPZ} = \chi_{EW} = 1/2$. Thanks to GI we also have that $z_{KPZ} = 2 - \chi_{KPZ} = 3/2$. Hence the symmetries are enough to fix the KPZ exponents in $d = 1$.

1.4 KPZ Universality in One Dimension and its Geometrical Sub-Classes

We here focus on the one dimensional case. Following the scaling properties of the height fluctuations it is natural to express the asymptotic height profile as

$$h(\mathbf{x}) \overset{t\to\infty}{\sim} v_\infty t + (\Gamma t)^\beta \tilde{h}(\mathbf{x}) \tag{1.48}$$

where $\tilde{h}(\mathbf{x})$ is a random variable and $\beta = \chi/z = 1/3$ in one dimension. The first quantity on the RHS is the self-averaging contribution, while the second one keeps track of the non-trivial KPZ scaling of the fluctuations of the height profile; v_∞, Γ are non-universal quantities depending on the parameters in (1.13) via [40, 41]

$$v_\infty = \lambda, \qquad \Gamma = \frac{1}{2}\frac{D^2\lambda}{\nu^2}. \tag{1.49}$$

A very important analytical progress has been achieved in the last decades concerning the probability distribution $P(\tilde{h}(\mathbf{x}))$. Interestingly, it has first been shown [42], and then proven using the mapping to Directed Polymers in Random Media [43, 44, 45, 46, 47], that this probability distribution depends on the geometry, or equivalently on the initial conditions, of the problem:

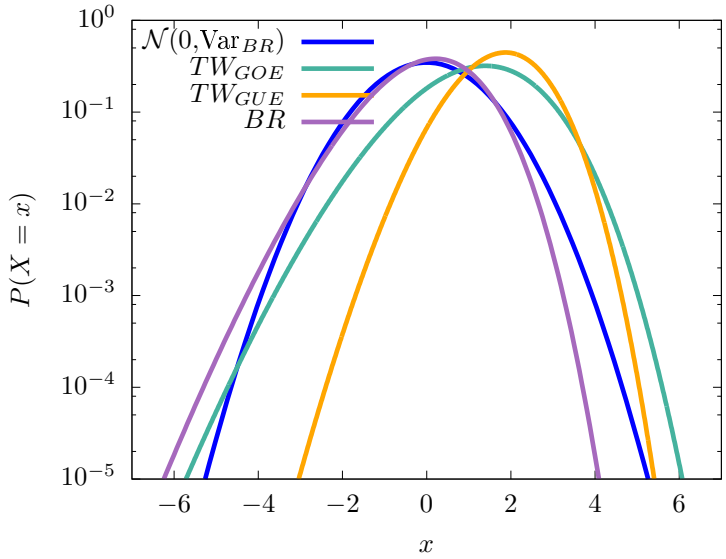

Figure 1.3: The three different distributions TW_{GOE}, TW_{GUE} and BR, together with a Gaussian distribution with zero mean and BR variance.

- Flat Initial Conditions
  Given a $h(x, t = 0) = h_0$, the distribution of $\tilde{h}(\mathbf{x})$ is the Tracy-Widom(TW) distribution associated to the probability of the largest eigenvalue of random matrices in the Gaussian orthogonal ensemble(GOE), TW_{GOE} [48].

- Sharp-Wedge Initial Conditions
  Given a $h(x, t = 0) = -\lim_{a\to\infty} a|x|$, the distribution of $\tilde{h}(\mathbf{x})$ is the Tracy-Widom(TW) distribution associated to the probability of the largest eigenvalue of random matrices in the Gaussian unitary ensemble(GUE), TW_{GUE}.

- Stationary Initial Conditions
  In Chap. 1.3.1 we saw that in one dimension the KPZ roughness exponent is the same as the one in EW universality class, due to an accidental fluctuation-dissipation theorem. One can also show that the stationary distribution for $h(\mathbf{x})$ is the same as the EW one. EW dynamics is a Brownian motion dumped by diffusive effects and has a Gaussian stationary distribution. Taking such a distribution as an initial condition for the growing interface, one finds that $\tilde{h}(\mathbf{x})$ is distributed according to the Baik-Rains (BR) distribution [49].

The three distributions introduced above are all highly non-Gaussian, see Fig 1.3; their non-Gaussianity can be measured by looking at the cumulants, that for a generic random variable X are defined as

$$\kappa_n = \frac{\partial^n}{\partial t^n} \log\left(\langle e^{tX}\rangle\right)|_{t=0}. \tag{1.50}$$

For a Gaussian distribution only κ_1, the Mean, and κ_2, the Variance(Var), are non-zero. Two important quantities related to the cumulants are the Skewness(Skew) and Excess-Kurtosis(ExKurt), defined as

$$\mathrm{Skew}(X) = \frac{\kappa_3}{\kappa_2^{3/2}} = \frac{\mu_3}{\mu_2^{3/2}}, \quad \mathrm{ExKurt}(X) = \frac{\kappa_4}{\kappa_2^2} = \frac{\mu_4}{\mu_2^2} - 3. \tag{1.51}$$

where $\mu_n = \langle (X - \langle X \rangle)^n \rangle$ is the nth central moment. The skewness and excess Kurtosis vanishes for a Gaussian distribution. Both these dimensionless quantities describe properties of the tails of the distribution: the skewness characterizes the asymmetry of the tails while the excess-kurtosis quantifies their size. For TW_{GOE}, TW_{GUE} and BR these quantities are known numerically to arbitrary precision and they are reported in Table 1.1. This geometry-dependent universal behaviour has been recently observed in experiments in the context of liquid-crystal turbulence [33, 51].

1.4.1 Finite Size and Cross-over to BR

All the analytical approaches that have led to the discovery of the KPZ geometrical sub-classes rely on the fact that the system is in its thermodynamic limit. When its finiteness is taken into account, interesting effects can be observed. When the KPZ dynamics is present, the correlation length ξ between different points on the surface grows as $\xi \sim t^{1/z}$. As the correlation length becomes comparable with the size of the system we approach the stationary regime of the interface. An appropriate quantity to study the spreading of such correlations was introduced in [52], and is defined as

$$\Delta q(x, t_0, \Delta t) = \frac{\delta h(x, t_0 + \Delta t) - \delta h(x, t_0)}{(\Gamma \Delta t)^{1/3}}, \quad \delta h(\mathbf{x}) = h(\mathbf{x}) - \langle h(\mathbf{x}) \rangle. \tag{1.52}$$

Starting from either flat or sharp-wedge initial conditions in a finite-size system we thus expect a transition to the stationary sub-class before finite-size effects start to dominate. If the system is large enough, this transition can be traced by looking at the evolution of the probability distribution of $\tilde{h}(x, t)$: a cross-over from either a TW_{GOE} or TW_{GUE}, depending on the initial conditions, to BR is expected in $P_{\Delta q}$:

$$P_{\Delta q} = \begin{cases} TW_{GOE,GUE}, & \Delta t / t_0 \to \infty \\ BR, & \Delta t / t_0 \to 0 \end{cases}. \tag{1.53}$$

This cross-over has recently been observed in experiments by Takeuchi and Sano [52].

1.5 Some Related Models

KPZ equation is related to several different models, both discrete and continuous. We here report two examples that, for different reasons, play an important role in the following.

1.5.1 Directed Polymers in Random Media(DPRM)

By performing a Cole-Hopf transformation $Z(\mathbf{x}) = \exp(\frac{\lambda}{2\nu} h(\mathbf{x}))$ we find that the dynamics of this new variable is ruled by

$$\partial_t Z(\mathbf{x}) = \nu Z(\mathbf{x}) + \frac{\lambda}{2\nu} \eta(\mathbf{x}) Z(\mathbf{x}). \tag{1.54}$$

	Mean	Var	Skew	ExKurt
TW_{GOE}	-0.76007	0.63805	0.2935	0.1652
TW_{GUE}	-1.77109	0.81320	0.2241	0.09345
BR	0	1.15039	0.35941	0.28916

Table 1.1: Mean, Var, Skew and ExKurt calculated from numerical integration of Painlevé II [50, 42].

This equation is sometimes called Stochastic Heat equation(SHE). Differently from KPZ equation, which is a non-linear PDE with additive noise, SHE is linear but with multiplicative noise. Being linear, one can easily find its solution using Feynman-Kac theorem,

$$Z(\mathbf{x}) = \int_{0,0}^{\mathbf{x}} \mathcal{D}[y(\tau)] \exp\left(-\frac{1}{2\nu}\int_0^t \mathrm{d}t\left[\frac{\partial_\tau y(\tau)^2}{2} - \lambda\,\eta(y(\tau),\tau)\right]\right). \tag{1.55}$$

This is the sum over all possible paths in the τ direction starting from a $\tau = 0$ and ending at $\tau = t$ at a point $y(t) = x$, through a disordered landscape of intensity η and at a temperature $T = 2\nu$, *i.e.* the partition function of a DPRM. Many analytical results for KPZ universality presented above, were found by exploiting this mapping; the strong disorder phase of DPRM corresponds indeed to the strong coupling regime of KPZ equation [26]. The analogy between DPRM and KPZ has also been exploited to theoretically understand the effects of breaking the tilt invariance onto the KPZ exponents z, χ [53]. To this aim it is important to introduce the relation between the usual set of exponents studied in DPRM and the KPZ ones. The introduction of a random potential $\eta(\mathbf{x})$ renders the partition function a random variable and we will thus have two different averages to perform in the system: the first is the thermal average, denoted by $\langle\cdots\rangle$, which we can perform also in the absence of the disorder and the second is the disorder average, denoted by $\overline{\cdots}$. The first scaling exponent is related to the spatial extent of the polymer at a distance t from the starting point $\tau = 0$,

$$\overline{\langle (x(t) - x(0))^2\rangle} \sim t^{2\zeta}. \tag{1.56}$$

For the free polymer, $\eta = 0$, the evolution is a simple random-walk and $\zeta = 1/2$. The second exponent is related to the fluctuations of the free-energy due to the presence of the random disorder,

$$\overline{\langle \ln Z(t)^2\rangle} \sim t^{2\theta} \tag{1.57}$$

with $\theta = 0$ for the $\eta = 0$ case. Recalling the relation between h and Z we immediately deduce that

$$\theta = \beta = \chi/z, \quad \zeta = 1/z \tag{1.58}$$

and that the relation imposed by GI, $z + \chi = 2$, translates into

$$\theta = 2\zeta - 1. \tag{1.59}$$

This relation can also be found by equating the scaling of the free-energy and of the elastic energy in (1.55).

1.5.2 Burgers Equation

If we consider the dynamics of the velocity $\vec{v}(\mathbf{x}) = -\lambda\vec{\nabla}h(\mathbf{x})$ we find that it is described by the equation

$$D_t\vec{v}(\mathbf{x}) = \nu\nabla^2\vec{v}(\mathbf{x}) + \lambda\vec{\nabla}\eta(\mathbf{x}) \tag{1.60}$$

where $D_t[\cdot]$ is the usual Lagrangian time-derivative. This equation is known as stochastic Burgers equation (SBE), and corresponds to a Navier-Stokes (NSE) equation without pressure and with a stochastic forcing [54, 55]. The deterministic version of SBE has been used to study shock waves, which naturally arise due to the non-linearity, while SBE is known to be a toy-model for investigating turbulence of incompressible fluids [56, 57]. For what follows it is important to note that the tilt transformation on the field $h(\mathbf{x})$ becomes the physically better understood Galilean invariance on the velocity field

$$v(\mathbf{x}) \to v_0 + v'(x - v_0 t) \tag{1.61}$$

which corresponds to looking at the fluid in the moving reference frame.

2 Large distance properties of Exciton-Polaritons and the Relation to KPZ Equation

In this chapter we review the dynamics of a homogeneous driven-dissipative Bose-Einstein condensate of Exciton-Polaritons and show that its phase dynamics follows the KPZ dynamics introduced in the previous chapter. In the first part we introduce the physical system and its effective mean-field description, both from phenomenological and field-theoretical approaches. After this introduction we focus on the dynamics of the phase and show that it follows the KPZ equation. We then see how the mapping works in both the phenomenological and field-theoretical approaches. We then extend the mapping to the non-adiabatic case.

2.1 Physical system: Exciton-Polaritons

Before discussing the model we will investigate in the first part of the manuscript, it is important to introduce the physical system and the state of the art of the experimental platforms.

2.1.1 Excitons in Semiconductor Structures

Semiconductors are materials whose band structure possesses a finite energy gap Δ between the valence band and the conduction band. In the ground state, all the electrons fill the valence band, leaving the conduction band empty. However, due to the small amplitude of the gap, one electron in the valence band can be excited to the conduction band if it gains an energy larger than Δ. In this case the valence band lacks a single negative charge; this lack can be described by a single quasi-particle of positive charge, usually referred to as hole. The hole in the valence band and the excited electron are particles of opposite charges and interact through Coulomb interaction, that allows to form an electron-hole bound-state known as exciton [58]. The energy structure of the ground state of the semiconductor and the exciton is illustrated in Fig. 2.1.

2.1.2 Bragg-Mirrors and Confined Photons

A fundamental ingredient of the physical system we will study are the Bragg mirrors, which are periodic stack of dielectric layers with two different refraction indices; this setup is also referred to as Distributed Bragg Reflectors (DBR). With proper choice of the optical thickness, *i.e.* the product between the physical thickness of the layer and its refraction index, the DBR acts as a mirror with a high reflectivity over a broad range of wavelength, called stop band [60]. A useful implementation of DBR is a microcavity made by two DBR separated by a distance L_C, which is usually called Brag mirror microcavity. For such setup, the reflectivity gets a very narrow dip of width $\Delta\lambda_C$ at the center of the stop band (see Fig. 2.2(a)), around a wavelength λ_C; this implies that inside the microcavity the electromagnetic field gets amplified for wavelength $\lambda \in \Delta\lambda_C$ (see Fig. 2.2(b)), while being reflected almost ideally by the DBR at the boundary. The result is that the photon with $\lambda \simeq \lambda_C$ is confined along the axis perpendicular to the

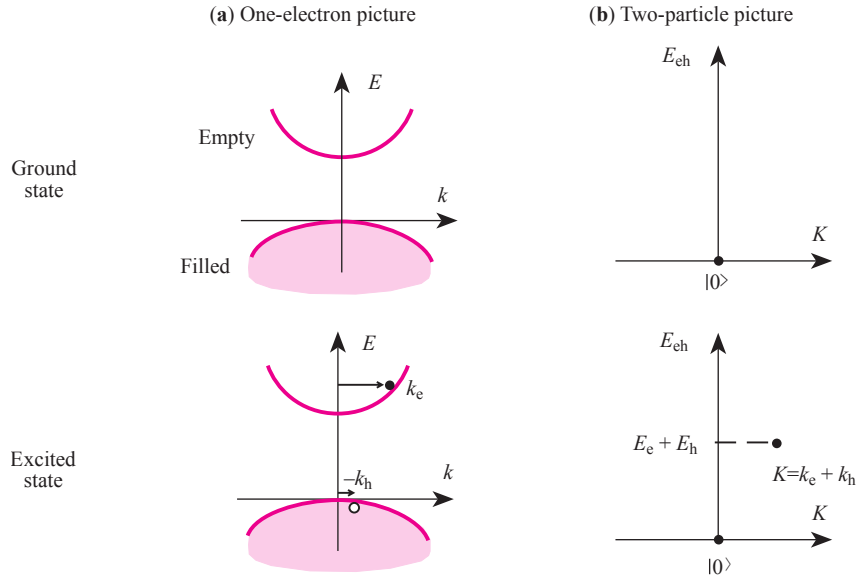

Figure 2.1: Energy difference between the ground state and a phonon excited electron-hole coupling in (a) the one electron band picture and (b) the two-particle picture. Picture adapted from [58].

DBR, z. The number of round trips the photon makes inside the microcavity before it escapes (because of non ideal reflectivity of DRB) can be estimated by the quality factor $\mathcal{Q}$, defined as

$$\mathcal{Q} = \frac{\lambda_C}{\Delta\lambda_C} \,. \tag{2.1}$$

Because of the confinement, the photon acquires an effective mass. Indeed, its dispersion relation inside the cavity has the form

$$\omega_C(k) = c|\vec{k}| = c\sqrt{k_{||}^2 + k_z^2} \,, \tag{2.2}$$

where c is the speed of light. The confinement in the z direction implies that k_z is quantized,

$$k_z = \frac{2\pi}{L_C} j \,, \tag{2.3}$$

where j takes integer values. In the small $k_{||}$ regime the dispersion behaves quadratically, and thus the cavity photon acquires a finite mass for the in-plane motion. This mass is proportional to c^{-1} and hence is very small, usually of the order of $m_c \simeq 10^{-5} m_{el}$ [61].

2.1.3 Exciton-Polaritons

The electron-hole quasi-particle forms a dipole which interacts with an electromagnetic field. The underlying mechanism is light-matter interaction, which can be model by microscopic Hamiltonian of the type

$$H_{int} = -\frac{e}{m_{el}} \vec{p} \cdot \vec{A} \,, \tag{2.4}$$

where $-e$ is the charge of an electron of mass m_{el} and momentum $\vec{p}$, and $\vec{A}$ is the magnetic vector potential of the electromagnetic radiation. An exciton can thus be created by a photon absorption or,

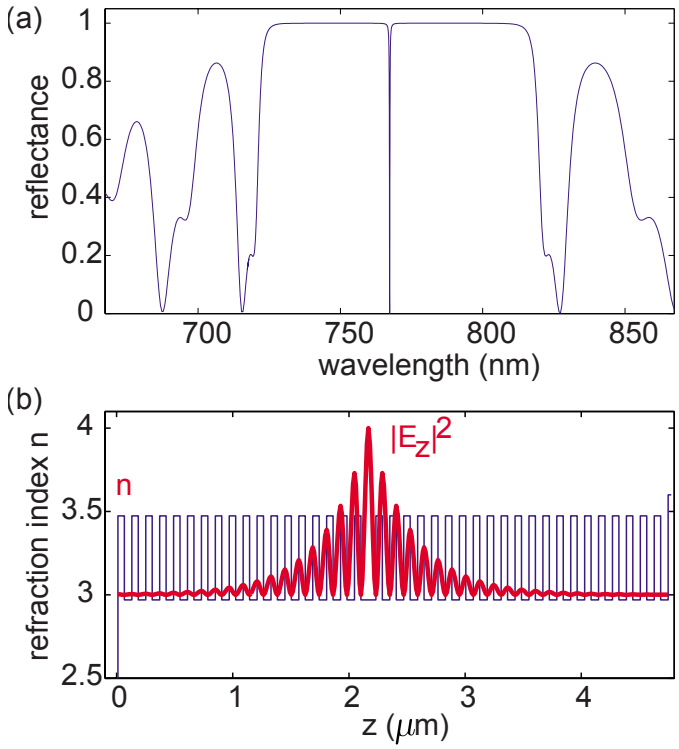

Figure 2.2: (a) Reflectance of an empty high quality microcavity and (b) the intensity of the field distribution of the resonant mode. Picture taken from [59].

conversely, a photon can be emitted by the the electron-hole recombination, with some finite probability given by

$$P_{int} \propto |\langle \text{exc}|H_{int}|0\rangle|^2 . \tag{2.5}$$

where $|\text{exc}\rangle$ denotes the excitonic state. It is interesting to note that, if the emitted photon is confined in some way, multiple excitation-emission processes can take place. As we discussed in the previous section, a confined photon can do several round trips inside the cavity before escaping. We now introduce a semiconductor layer in a cavity made by two DBR. If the resonant frequency of the cavity is the same as the frequency of the excitation of the semiconductor between the two DBR, this means that several excitation-emission events can take place before the photon leaks out. The coherent transfer of excitations between the cavity photons and the semiconductor excitons is called Rabi oscillation. This regime corresponds to a strong coupling between the excitons and the photons, where the eigenstates of the resulting system is a superposition of the bare excitons and photons. These hybridized bosonic quasi-particles stemming out from the strong coupling between excitons and photons confined in a cavity are called Exciton-Polaritons (EP). For an exhaustive review on the optical properties of polaritons the reader is addressed to [62]. The effective mass of EP is extremely low, of the order of the m_c introduced above, and opens the possibility to observe purely quantum effects up to at room temperature. It is important to stress that here by temperature we mean the one of the experimental environment into which the physical sample is placed. Indeed, due to the unavoidable leakages of the cavity, the system is fully out of equilibrium, and its temperature cannot be defined. In order to reach a steady state, the system needs a continuous injection of photons. The formation of a macroscopically-coherent state of these quasi-particles, analogous to the Bose-Einstein condensation (BEC) in equilibrium systems was first proposed theoretically in the late nineties [63]. The first experimental results showing long-range

first order correlations in EP were found in systems with resonant pumping [64, 65] in which a parametric oscillation linked to the breaking of $U(1)$ symmetry appears [66, 67, 68, 69]. In the case of non-resonant pumping, the condensation in the minimum of the dispersion and the off-diagonal long-range order have been observed experimentally [24] in the steady-state regime (see Fig. 2.3). In the following we will focus on the second case of non-resonant pumping, where the phase of the pumping laser does not affect directly the one of the condensate. For a more complete treatment of the resonant and non-resonant pumping, the review [61] is available. Since the first experimental observation of BEC, much work on the theoretical and experimental side has been done, leading, among all, to the observation of quantized vortices [70], superfluidity [71, 72] and solitons [73]. However, the nature of the transition to macroscopically occupied states in EP is still under debate. Indeed it has been conjectured that, rather than a non-equilibrium BEC transition, EP undergo either an out-of-equilibrium Berezinskii-Kosterlitz-Thouless (BKT) transition [74, 75, 76], or a BEC at thermodynamic equilibrium [77, 78]. The investigation of KPZ scaling in the phase distribution of EP, and hence, as we will see, the stretched exponential behaviour of its two-point correlation function, will also contribute to the characterization of the nature of the phase transition in the EP system.

2.2 A Model for Exciton-Polaritons

A phenomenological description of the dynamics of Exciton-Polaritons under incoherent pumping was introduced in [79, 80]. The polaritons in the lower band are described by a classical field $\psi(\mathbf{x})$ satisfying a complex generalization of the non-linear Schrödinger equation, coupled to a rate-equation for the polaritonic reservoir density n_R,

$$i\hbar\partial_t\psi = \left[-\frac{\hbar^2}{2m_{LP}}\nabla^2 + g|\psi|^2 + 2g_R n_R + \frac{i\hbar}{2}(R\, n_R - \gamma)\right]\psi + \mathcal{F} \tag{2.6a}$$

$$\partial_t n_R = P - (\gamma_R + R|\psi|^2)n_R \tag{2.6b}$$

where $\mathcal{F}$ is an effective noise taking into account both pumping and loss effects and is in general taken as a delta-correlated Gaussian-distributed random variable of strength F, $\langle\mathcal{F}(t,x)\mathcal{F}(t',x')\rangle \mathrm{d}t = F^2\delta(t-t')\delta(x-x')$. Equation (2.6) describes the non-linear dynamics of the lower polaritons, with an effective mass m_{LP}, which interact with the background mean-field density via a coupling strength g, as in the usual equilibrium Gross-Pitaevskii equation [81]. In this model, moreover, the system interacts with a high-energy reservoir, whose density n_R increases due to a constant pumping P and is depleted both by unavoidable leakages, on a time-scale γ_R, and by stimulated emission of strength R in the lower polariton branch. The population of the EP band is taken into account by an imaginary positive term in the dynamics of ψ. As in the reservoir, there are leakages of EP on a time-scale γ. Conservative effects due to interactions with the reservoir are taken into account via a coupling g_R between ψ and n_R.

2.2.1 Hopfield Model and the Dispersion Relation of Exciton-Polaritons

The first term in the r.h.s of (2.6a) comes from the usual parabolic approximation of the EP dispersion relation $E_{LP}(k)$. The full dispersion relation of the lower-polaritons band coming from the hybridization of the photonic band with the excitonic one can be computed by taking into account the quantum dynamics of excitons, denoted by $\hat{a}_X^{(\dagger)}$ annihilation (creation) operator, interacting with cavity photons, denoted by $\hat{a}_C^{(\dagger)}$ annihilation (creation) operator within the Hopfield model [82, 61]:

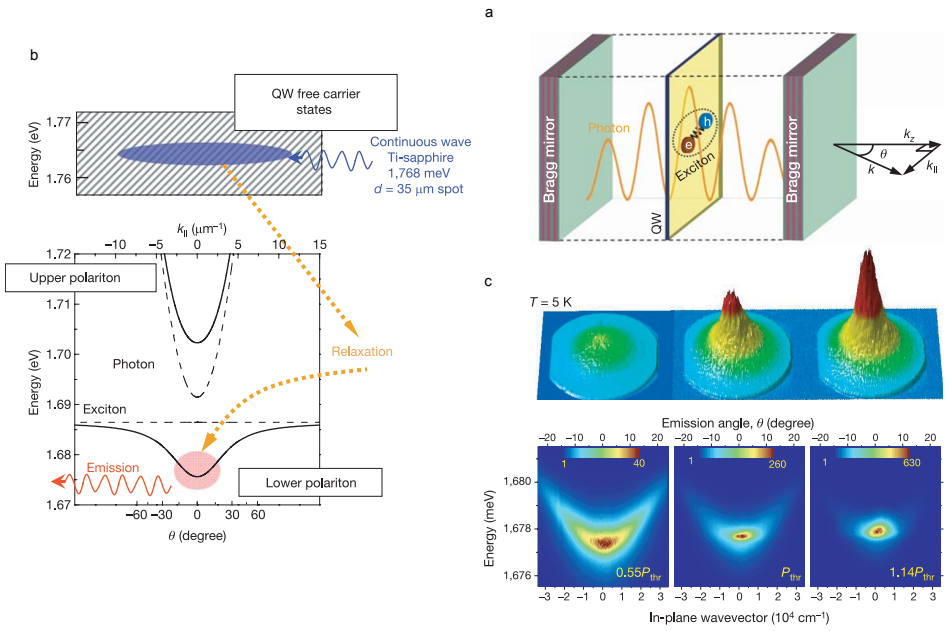

Figure 2.3: Some figures from the seminal work [24]: a) a schematic representation of the physical process leading to the creation of EP; b) (black solid lines) the dispersion relation of lower and upper polaritons, resulting from the coupling between (black dashed lines) the confined photon and the excitons in the quantum well; c) far-field emission spectra, resolved in angle(top) and energy(bottom), showing the condensation of EP at $T = 5K, p = 1.14$.

$$H_{EP} = H_C + H_X = \hbar \int_{\vec{k}} \left\{ \omega_C(\vec{k}) \hat{a}_C^\dagger(\vec{k}) \hat{a}_C(\vec{k}) + \omega_X(\vec{k}) \hat{a}_X^\dagger(\vec{k}) \hat{a}_X(\vec{k}) + \Omega_R \left[\hat{a}_C^\dagger(\vec{k}) \hat{a}_X(\vec{k}) + \hat{a}_X^\dagger(\vec{k}) \hat{a}_C(\vec{k}) \right] \right\} \tag{2.7}$$

where Ω_R is usually referred to as Rabi splitting. We can diagonalize this system by introducing linear combinations of $\hat{a}_X$, $\hat{a}_C$

$$\hat{a}_{LP}(\vec{k}) = X(\vec{k}) \hat{a}_X(\vec{k}) + C(\vec{k}) \hat{a}_C(\vec{k}), \quad \hat{a}_{UP}(\vec{k}) = -C(\vec{k}) \hat{a}_X(\vec{k}) + X(\vec{k}) \hat{a}_C(\vec{k}) \tag{2.8}$$

where X, C are known as Hopfield coefficients [82]. After this transformation we get

$$H_{EP} = \hbar \int_{\vec{k}} \left\{ E_{LP}(\vec{k}) \hat{a}_{LP}^\dagger(\vec{k}) \hat{a}_{LP}(\vec{k}) + E_{UP}(\vec{k}) \hat{a}_{UP}^\dagger(\vec{k}) \hat{a}_{UP}(\vec{k}) \right\} \tag{2.9}$$

with

$$E_{LP}(\vec{k}) = \frac{\hbar}{2} \left(\omega_C(\vec{k}) + \omega_X(\vec{k}) \right) - \hbar \sqrt{\frac{(\omega_C(\vec{k}) - \omega_X(\vec{k}))^2}{4} + \Omega_R^2} \tag{2.10a}$$

$$E_{UP}(\vec{k}) = \frac{\hbar}{2} \left(\omega_C(\vec{k}) + \omega_X(\vec{k}) \right) + \hbar \sqrt{\frac{(\omega_C(\vec{k}) - \omega_X(\vec{k}))^2}{4} + \Omega_R^2} \tag{2.10b}$$

and

$$|X(\vec{k})|^2 = \frac{1}{2}\left(1 + \frac{\omega_X(\vec{k}) - \omega_C(\vec{k})}{\sqrt{\omega_X(\vec{k}) - \omega_C(\vec{k}) + 4\Omega_R^2}}\right) \tag{2.11a}$$

$$|C(\vec{k})|^2 = \frac{1}{2}\left(1 - \frac{\omega_X(\vec{k}) - \omega_C(\vec{k})}{\sqrt{\omega_X(\vec{k}) - \omega_C(\vec{k}) + 4\Omega_R^2}}\right). \tag{2.11b}$$

Due to the huge difference in the effective mass of exciton and cavity photons, the momentum dependence in the dispersion of the excitons is usually neglected, $\omega_X(\vec{k}) \equiv \omega_{X,0}$. A particular regime is the one in which we take the minimum of the cavity photon dispersion, $\omega_C(\vec{k} = \vec{0})$, to coincide with $\omega_{X,0}$: this is known as the zero-detuning regime, onto which we will focus in the following. In this case $|X(\vec{k} = \vec{0})|^2 = |C(\vec{k} = \vec{0})|^2 = 1/2$ and LP and UP bands are populated by an equal mixture of cavity photons and excitons at $k = 0$. In the phenomenological model (2.6), the full dispersion is usually expanded around this point and takes the form of a parabola of effective mass m_{LP}; in the following we are also interested in the zone around the inflection point of the LP band. This requires to include quartic corrections to the lower-polariton dispersion,

$$E_{LP}(k) \simeq \frac{\hbar^2 k^2}{2m_{LP}} - \frac{1}{2\Omega_R}\left(\frac{\hbar^2 k^2}{2m_{LP}}\right)^2 \tag{2.12}$$

When going to higher $k = |\vec{k}|$, the population in LP starts to be imbalanced,

$$|X(\vec{k})|^2 > 1/2, \quad |C(\vec{k})|^2 < \frac{1}{2} \tag{2.13}$$

and thus the excitonic component in the LP increases. When taking into account the excitonic contribution, new loss phenomena that are usually momentum-dependent start to appear; to well reproduce them we introduce a k-dependent loss term to γ,

$$\gamma(k) = \gamma_0 + \gamma_2 k^2 \tag{2.14}$$

where the coefficient γ_2 can be estimated in the experiments from the width of the dispersion branches. This momentum-dependent loss term yields the appearance of a complex coefficient for the Laplacian in Eq. (2.6).

2.2.2 Steady State Solutions

We look for a solution for the LP wavefunction and for the reservoir density in the stationary regime, of the form $\psi(x,t) = e^{-i\mu_T t/\hbar}\psi_0$, $n_R(x,t) = n_R^{(0)}$. This implies

$$\begin{cases} \mu_T = g|\psi_0|^2 + 2g_R n_R^{(0)} + \dfrac{i}{2}(R\, n_R^{(0)} - \gamma_0) \\ n_R^{(0)} = \dfrac{P}{\gamma_R + R|\psi_0|^2} \end{cases} \tag{2.15}$$

and thus

$$\mu_T = g|\psi_0|^2 + 2\frac{g_R P}{\gamma_R + R|\psi_0|^2} + \frac{i}{2}\left(\frac{RP}{\gamma_R + R|\psi_0|^2} - \gamma_0\right). \tag{2.16}$$

We see that the we can have two different scenarii for the dynamical stability of the system:

(i) For small pumping intensity P, the dynamical stable solution is $|\psi_0|^2 = 0, n_R^{(0)} = \frac{P}{\gamma_R}$

(ii) For pumping at the threshold value $P \equiv P_{th} = \frac{\gamma_R \gamma_0}{R}$: $|\psi_0|^2 = 0$ solution becomes unstable and a macroscopic condensate appears with $|\psi_0|^2 \neq 0$. This is a non-equilibrium phase transition.

We define the steady state of the condensate as the regime in which no net gain (in time) occurs and the reservoir density is clamped at the threshold value $n_R^{(0)} \equiv n_R^{(th)} = \gamma_0/R$. In this regime we have a macroscopic phase μ_T and a condensate density $|\psi_0|^2$ which are equal to

$$\mu_T = g|\psi_0|^2 + 2\frac{g_R}{\hbar R}\gamma_0, \quad |\psi_0|^2 = \frac{\gamma_R}{R}\left(\frac{PR}{\gamma_R\gamma_0} - 1\right) = \frac{\gamma_r}{R}\left(\frac{P}{P_{th}} - 1\right) = \frac{\gamma_r}{R}(p-1) \tag{2.17}$$

respectively, with $P_{th} = PR/(\gamma_R\gamma_0)$, $p = P/P_{th}$. This implies that the condensate grows as the pump strength is increased, with a reservoir density clamped to its threshold value.

2.2.3 Plugging Fluctuations In

In the case in which the dynamics of the reservoir is much faster than the one of the polariton condensate one can integrate out adiabatically the former, ending with an effective equation for the dynamics of the low-energy polariton wavefunction in the adiabatic approximation:

$$i\hbar\partial_t\psi = \left[\left(-\frac{\hbar^2}{2m_{LP}} + i\frac{\gamma_2}{2}\right)\nabla^2 + g|\psi|^2 + 2\frac{g_R P}{\gamma_R + R|\psi|^2} + \frac{i\hbar}{2}\left(\frac{RP}{\gamma_R + R|\psi|^2} - \gamma_0\right)\right]\psi + \mathcal{F}. \tag{2.18}$$

By re-scaling space, time and the condensate density by

$$\hat{x}^2 = \frac{\hbar}{2|m_{LP}|\gamma_0}, \quad \hat{t} = \gamma_0^{-1}, \quad \hat{\psi}^2 = \frac{|\psi_0|^2}{p} = \frac{\gamma_R}{R}\frac{p-1}{p} \tag{2.19}$$

we can rewrite (2.18) in a dimensionless form,

$$\begin{aligned} i\tilde{\partial}_t\tilde{\psi} = \Bigg[&\left(-\mathrm{sgn}(m_{LP}) + i\frac{\gamma_2|m_{LP}|}{\hbar^2}\right)\tilde{\nabla}^2 + \frac{g}{\hbar R}\frac{\gamma_R}{\gamma_0}\frac{p-1}{p}|\tilde{\psi}|^2 + 2\frac{g_R}{\hbar R}\frac{p}{1+\frac{p-1}{p}|\tilde{\psi}|^2} \\ &+\frac{i}{2}\left(\frac{p}{1+\frac{p-1}{p}|\tilde{\psi}|^2} - 1\right)\Bigg]\psi + \tilde{\mathcal{F}}, \end{aligned} \tag{2.20}$$

with $\mathrm{sgn}(x) = x/|x|$, $\tilde{\psi} = \psi/\hat{\psi}$, $\tilde{t} = t/\hat{t}$, and $\tilde{x} = x/\hat{x}$. Accordingly, we rescale the noise strength as

$$\langle\tilde{\mathcal{F}}(\tilde{t},\tilde{x})\tilde{\mathcal{F}}^*(\tilde{t}',\tilde{x}')\rangle \mathrm{d}\tilde{t} = \frac{F^2}{\hat{\psi}^2\hat{x}\hbar^2}\delta(\tilde{t}-\tilde{t}')\delta(\tilde{x}-\tilde{x}') \hat{=} \tilde{F}^2\delta(\tilde{t}-\tilde{t}')\delta(\tilde{x}-\tilde{x}'). \tag{2.21}$$

The mass of the EP has been allowed to get negative values, *i.e.* negative curvature of the lower-polaritons band, for the sake of completeness and due to recent experimental results on which we will focus in the following [83]. From now on, for simplicity we will drop the tildes on dimensionless space, time and wave-function. For a small condensate amplitude, *i.e.* $\frac{p-1}{p}|\psi|^2 \ll 1$, we obtain an effective non-linear Schrödinger equation for the evolution of the condensate wavefunction ψ by expanding $\frac{p}{1+\frac{p-1}{p}|\psi|^2} \simeq p-(p-1)|\psi|^2$

$$\begin{aligned} i\partial_t\psi &= \left[\left(-\mathrm{sgn}(m_{LP}) + i\frac{\gamma_2|m_{LP}|}{\hbar^2}\right)\nabla^2 + \frac{g}{\hbar R}\frac{\gamma_R}{\gamma_0}\frac{p-1}{p}|\psi|^2 + 2\frac{g_R}{\hbar R}\left(p-(p-1)|\psi|^2\right)\right. \\ &\quad \left. + \frac{i}{2}(p-1)\left(1-|\psi|^2\right)\right]\psi + \tilde{\mathcal{F}} \\ &= \left[\left(-\mathrm{sgn}(m_{LP}) + i\frac{\gamma_2|m_{LP}|}{\hbar^2}\right)\nabla^2 + 2\frac{g_R}{\hbar R}p + \frac{g_R}{\hbar R}\frac{p-1}{p}\left(\frac{g}{g_R}\frac{\gamma_R}{\gamma_0} - 2p\right)|\psi|^2\right. \\ &\quad \left. + \frac{i}{2}(p-1)\left(1-|\psi|^2\right)\right]\psi + \tilde{\mathcal{F}} \\ &= \left[\left(-\overline{K}_c + i\,\overline{K}_d\right)\nabla^2 + \overline{r}_c + u_c|\psi|^2 + i\left(\overline{r}_d - \overline{u}_d|\psi|^2\right)\right]\psi + \tilde{\mathcal{F}} \end{aligned} \tag{2.22}$$

where in the last step we defined

$$\begin{aligned} \overline{K}_c = \mathrm{sgn}(m_{LP}), \quad \overline{r}_c = 2\frac{g_R}{\hbar R}p, \quad \overline{u}_c = \frac{g_R}{\hbar R}\frac{p-1}{p}\left(\frac{g}{g_R}\frac{\gamma_R}{\gamma_0} - 2p\right), \\ \overline{K}_d = \frac{\gamma_2|m_{LP}|}{\hbar^2}, \quad \overline{r}_d = \frac{1}{2}(p-1), \quad \overline{u}_d = \frac{1}{2}(p-1). \end{aligned} \tag{2.23}$$

2.3 Keldysh Field Theory for Exciton-Polaritons

In the previous section we have presented a phenomenological description of the EP system which, when the reservoir dynamics can be integrated out adiabatically, leads to a generalization of the usual Gross-Pitaevskii equation including drive and dissipation. This effective dynamics can also be derived starting from a pure quantum picture *via* the Keldysh formalism (see App. B). To do so we first have to define the coherent- and dissipative-part in the evolution of the open quantum system of interest. In the case of EP the coherent dynamics is the one of a Bose gas with contact interactions while the dissipative dynamics takes into account one- and two-body losses together with pumping from the reservoir; these two contributions appear in the Lindblad master equation

$$\partial_t\rho = -i[H_{LP},\rho] + \mathcal{L}\rho \hat{=} \mathscr{L}\rho \tag{2.24}$$

as

$$H_{LP} = \int_{\vec{x}}\left[\hat{\psi}^\dagger(\vec{x})\left(\omega^0_{LP} - \frac{\nabla^2}{2m_{LP}}\right)\hat{\psi}(\vec{x}) + u_c\hat{\psi}^\dagger(\vec{x})^2\hat{\psi}(\vec{x})^2\right] = \int_{\vec{x}} h_{LP}(\vec{x}) \tag{2.25}$$

and

$$\mathcal{L}\rho = \int_{\vec{x}}\left(\gamma_p\mathcal{D}[\hat{\psi}(\vec{x})^\dagger]\rho + \gamma\mathcal{D}[\hat{\psi}(\vec{x})]\rho + 2u_d\mathcal{D}[\hat{\psi}(\vec{x})^2]\rho\right) \tag{2.26}$$

respectively, with the super-operator $\mathcal{D}[\cdot]$ acting on the system density matrix ρ as

$$\mathcal{D}[L]\rho = L\rho L^\dagger - \frac{1}{2}\{L^\dagger L, \rho\}. \tag{2.27}$$

The Keldysh action associated to Lindblad master equation for such a system can be written as [84] (see App. B)

$$\begin{aligned} S = \int_{\mathbf{x}} \{ & \phi_q^*(i\partial_t + (K_c + iK_d)\nabla^2 - r_c + ir_d)\phi_c + c.c. - \left[(u_c - iu_d)(\phi_q^*\phi_c^*\phi_c^2 + \phi_q^*\phi_c^*\phi_c^2) + c.c.\right] \\ & + i2(\gamma + 2u_d\phi_c^*\phi_c)\phi_q^*\phi_q\}, \end{aligned} \tag{2.28}$$

where we have set $K_c \hat{=} \frac{1}{2m_{LP}}$, $r_c \hat{=} \omega_{LP}^0$ and $\gamma \hat{=} \frac{\gamma+\gamma_p}{2}$ is the effective noise strength, $r_d \hat{=} \frac{\gamma-\gamma_p}{2}$ is the gap from saturation and $c.c$ stands for the complex-conjugate. It is important to note that in using the Lindblad master equation (2.24) to describe the quantum dynamics we assumed the reservoir to be Markovian, which physically translates into the absence of back-action of the system onto the reservoir; this corresponds to the adiabatic limit described in the previous section. The effective description given by the gGPE is a particular limit of the full-quantum evolution given by the action (2.28). As for equilibrium systems indeed, the classical-field description of the dynamics holds when one particular state is macroscopically occupied and a large-scale coherence develops in the system; this is the case of the EP condensate in the steady-state. This condition translates into a large-scale limit of (2.28) around the point $r_d = 0$, *i.e.* $\gamma = \gamma_p$, which is the threshold for the steady steady to appear. After performing such a limit in one dimension one gets (see App. B)

$$i\partial_t\phi_c = \left[-(K_c + iK_d)\partial_x^2 + r_c - ir_d + (u_c - iu_d)|\phi_c|^2\right]\phi_c + \xi \tag{2.29}$$

with

$$\langle \xi(\mathbf{x})\xi^*(\mathbf{x}')\rangle = 2\left[(\gamma + 2u_d|\phi_c(\mathbf{x})|^2)(\gamma + 2u_d|\phi_c(\mathbf{x}')|^2)\right]^{1/2}\delta(\mathbf{x} - \mathbf{x}'). \tag{2.30}$$

It is useful to note that using the convention for r_d given in (2.28), which was introduced in the seminal paper [84] and is the usual notation for Keldysh formulation of driven-dissipative quantum system, we get a minus sign in front of the linear dissipative term (and hence on the complex diffusion coefficient) with respect to (2.22). Equation (2.29) for the condensate field ϕ_c is analogous to (2.22) for the condensate field ψ, with an additional multiplicative contribution in the noise; such a term is due to quantum fluctuations and becomes irrelevant in higher dimensions. Furthermore, to derive (2.22) from the phenomenological model (2.6) we made the assumption $(p-1)/p|\tilde{\psi}|^2 \ll 1$. If we recall that $u_d|\psi|^2 = (p-1)/2|\tilde{\psi}|^2$ and assume that $p = \mathcal{O}(1)$, which is in general the case in real experiments, we see that the multiplicative contribution is negligible. From now on we will then neglect this contribution in the calculations in order to be able to compare the results with the gGPE coming from the phenomenological description (2.22). We will then consider a complex noise ξ with correlation

$$\langle \xi(\mathbf{x})\xi^*(\mathbf{x}')\rangle = 2\gamma\delta(\mathbf{x} - \mathbf{x}'). \tag{2.31}$$

The complete case is reported in App. B.

2.4 From Exciton-Polaritons to KPZ

As we anticipated at the beginning of this chapter, the long-time and large-distance dynamics of the phase of the condensate wavefunction for EP is described by the KPZ equation. To understand how this mapping works out we can start either from the phenomenological description (2.22) or from the full Keldysh action (2.28). The advantage of the latter is that we can easily modify the homogeneous case to include more realistic effects, such as disorder and thermal effects. In the next chapter we will analyse both phenomenological and field-theoretical approaches; for all the details and the calculations concerning the Keldysh formalism we refer to App. B.

2.4.1 Dynamics of the Phase in the gGPE

To study the dynamics of the phase, it is useful to switch to the modulo-phase representation of the condensate wavefunction, $\phi_c(\mathbf{x}) = \rho(\mathbf{x})^{1/2}\exp(i\theta(\mathbf{x}))$. We thus have

$$\begin{aligned}\partial_t\phi_c(\mathbf{x}) =&\phi_c(\mathbf{x})\left(\frac{1}{2}\rho(\mathbf{x})^{-1}\partial_t\rho(\mathbf{x}) + i\partial_t\theta(\mathbf{x})\right)\\ \equiv&\phi_c(\mathbf{x})D_1[\rho,\theta] \qquad (2.32a)\\ \nabla^2\phi_c(\mathbf{x}) =&\phi_c(\mathbf{x})\left(-\frac{1}{4}\rho(\mathbf{x})^{-2}(\vec{\nabla}\rho(\mathbf{x}))^2 + \frac{1}{2}\rho(\mathbf{x})^{-1}\nabla^2\rho(\mathbf{x}) - (\vec{\nabla}\theta(\mathbf{x}))^2 + i\rho(\mathbf{x})^{-1}\vec{\nabla}\rho(\mathbf{x})\cdot\vec{\nabla}\theta(\mathbf{x}) + i\nabla^2\theta(\mathbf{x})\right)\\ \equiv&\phi_c(\mathbf{x})D_2[\rho,\theta], \qquad (2.32b)\end{aligned}$$

and (2.29) for the complex field ϕ_c becomes a set of coupled equations for the time evolution of the condensate density and phase, ρ, θ:

$$\begin{aligned}\frac{1}{2}\rho(\mathbf{x})^{-1}\partial_t\rho(\mathbf{x}) =& -K_c\,\Im\{D_2[\rho,\theta]\} - K_d\,\Re\{D_2[\rho,\theta]\} - r_d - u_d\rho(\mathbf{x})\\ &+\sqrt{\gamma}\rho(\mathbf{x})^{-1/2}\left(-\sin(\theta(\mathbf{x}))\Re\{\xi(\mathbf{x})\} + \cos(\theta(\mathbf{x}))\Im\{\xi(\mathbf{x})\}\right) \qquad (2.33a)\\ \partial_t\theta(\mathbf{x}) =&K_c\,\Re\{D_2[\rho,\theta]\} - K_d\,\Im\{D_2[\rho,\theta]\} - r_c - u_c\rho(\mathbf{x})\\ &-\sqrt{\gamma}\rho(\mathbf{x})^{-1/2}\left(\cos(\theta(\mathbf{x}))\Re\{\xi(\mathbf{x})\} + \sin(\theta(\mathbf{x}))\Im\{\xi(\mathbf{x})\}\right). \qquad (2.33b)\end{aligned}$$

We can look at the dynamics of the fluctuations of the phase around the steady-state solution $\rho_0 = -r_c/u_c = -r_d/u_d, \theta_0 = 0$. We thus assume that the density fluctuations are small and smooth, *i.e.* we keep only linear terms in the fluctuations of the density $\delta\rho(\mathbf{x})$ and neglect its temporal and spatial derivatives. Hence we get

$$\begin{aligned}\delta\rho(\mathbf{x}) =& -\frac{K_c}{u_d}\nabla^2\theta(\mathbf{x}) + \frac{K_d}{u_d}(\vec{\nabla}\theta(\mathbf{x}))^2 + \frac{\sqrt{\gamma}}{u_d}\rho_0^{-1/2}\left(-\sin(\theta(\mathbf{x}))\Re\{\xi(\mathbf{x})\} + \cos(\theta(\mathbf{x}))\Im\{\xi(\mathbf{x})\}\right) \qquad (2.34a)\\ \partial_t\theta(\mathbf{x}) =& -K_c\left(\frac{K_d}{K_c} - \frac{u_c}{u_d}\right)\nabla^2\theta(\mathbf{x}) - K_c\left(1 + \frac{u_cK_d}{u_dK_c}\right)(\vec{\nabla}\theta(\mathbf{x}))^2\\ &-\sqrt{\gamma}\rho_0^{-1/2}\left[\left(\cos(\theta(\mathbf{x}))\Re\{\xi(\mathbf{x})\} + \sin(\theta(\mathbf{x}))\Im\{\xi(\mathbf{x})\}\right) + \frac{u_c}{u_d}\left(-\sin(\theta(\mathbf{x}))\Re\{\xi(\mathbf{x})\} + \cos(\theta(\mathbf{x}))\Im\{\xi(\mathbf{x})\}\right)\right]\\ \equiv&\nu\nabla^2\theta(\mathbf{x}) + \frac{\lambda}{2}(\vec{\nabla}\theta(\mathbf{x}))^2 + \sqrt{D}\eta(\mathbf{x}). \qquad (2.34b)\end{aligned}$$

We see that (2.34b) is the analogue of the KPZ equation (1.13) for the phase variable $\theta(\mathbf{x})$, with

$$\nu \hat{=} K_c \left(\frac{u_c}{u_d} - \frac{K_d}{K_c} \right) , \; \lambda \hat{=} -2K_c \left(1 + \frac{u_c}{u_d} \frac{K_d}{K_c} \right) , \; D \hat{=} \frac{\gamma}{2\rho_0} \left(1 + \frac{u_c^2}{u_d^2} \right) , \tag{2.35}$$

where we used

$$\begin{aligned} \langle \eta(\mathbf{x}) \eta(\mathbf{x}') \rangle =& \gamma \rho_0^{-1} \left\{ \langle \Re\{\xi(\mathbf{x})\} \Re\{\xi(\mathbf{x}')\} \rangle \left[\cos(\theta(\mathbf{x}) \cos(\theta(\mathbf{x}')) - \frac{u_c}{u_d} \left(\cos(\theta(\mathbf{x})) \sin(\theta(\mathbf{x}')) + \sin(\theta(\mathbf{x})) \cos(\theta(\mathbf{x}')) \right) \right. \right. \\ & \left. \left. + \frac{u_c^2}{u_d^2} \sin(\theta(\mathbf{x})) \sin(\theta(\mathbf{x}')) \right] + \langle \Im\{\xi(\mathbf{x})\} \Im\{\xi(\mathbf{x}')\} \rangle \left[\sin(\theta(\mathbf{x}) \sin(\theta(\mathbf{x}')) - \frac{u_c}{u_d} \left(\cos(\theta(\mathbf{x})) \sin(\theta(\mathbf{x}')) \right) \right. \right. \\ =& \gamma \rho_0^{-1} \left(1 + \frac{u_c^2}{u_d^2} \right) \delta(\mathbf{x} - \mathbf{x}') \end{aligned} \tag{2.36}$$

and the fact that the real and imaginary parts of ξ are uncorrelated, $\langle \Re\{\xi(\mathbf{x})\} \Im\{\xi(\mathbf{x}')\} \rangle = \langle \Re\{\xi(\mathbf{x})\} \rangle \langle \Im\{\xi(\mathbf{x}')\} \rangle$, and that $\langle \Re\{\xi(\mathbf{x})\} \rangle = \langle \Im\{\xi(\mathbf{x})\} \rangle = 0$, $\langle \Re\{\xi(\mathbf{x})\} \Re\{\xi(\mathbf{x}')\} \rangle = \langle \Im\{\xi(\mathbf{x})\} \Im\{\xi(\mathbf{x}')\} \rangle = \delta(\mathbf{x} - \mathbf{x}')$. From (2.35) we note that for having a well-defined equilibrium limit, $\lambda = 0$, we need $(K_c u_c / u_d - K_d) > 0$. This is due to the fact that in equilibrium the coefficient ν/D is linked to the temperature of the system through the Einstein's relation. In the case in which we can focus on the quadratic part of the polariton dispersion (*i.e.* $K_d = 0$), we thus need $K_c u_c > 0$, due to the fact that $u_d > 0$ for a non-zero condensate (see (2.2.3)). This implies that the polariton-polariton interaction must be repulsive for positive effective mass and attractive for negative effective mass. This is indeed the case in the usual experimental setup (*e.g.* [85]).

2.4.2 Dynamics of the Phase in the non-adiabatic limit

We now extend the results reviewed in the last section to the non adiabatic case. We show that the dynamics of the phase of the condensate is still described by the KPZ equation in this case, which was not known. Starting from the dimensionless version of (2.6) and switching to a modulo-phase representation we obtain a set of coupled equations for the time evolution of the dimensionless quantities ρ, θ, n_R,

$$\frac{1}{2} \rho(\mathbf{x})^{-1} \partial_t \rho(\mathbf{x}) = -\operatorname{sgn}(m_{LP}) \Im\{D_2[\rho, \theta]\} + \frac{1}{2}(n_R(\mathbf{x}) - 1) + \rho(\mathbf{x})^{-1/2} \left[\cos(\theta(\mathbf{x})) \Im\{\hat{F}\} - \sin(\theta(\mathbf{x})) \Re\{\hat{F}\} \right] \tag{2.37a}$$

$$\partial_t \theta(\mathbf{x}) = \operatorname{sgn}(m_{LP}) \Re\{D_2[\rho, \theta]\} - 2 r_c n_R(\mathbf{x}) - u_c (p-1) \rho(\mathbf{x}) - \rho(\mathbf{x})^{-1/2} \left[\cos(\theta(\mathbf{x})) \Re\{\hat{F}\} + \sin(\theta(\mathbf{x})) \Im\{\hat{F}\} \right] \tag{2.37b}$$

$$\partial_t n_R(\mathbf{x}) = \tilde{\gamma} \left\{ p - [1 + (p-1)\rho(\mathbf{x})] \, n_R(\mathbf{x}) \right\} . \tag{2.37c}$$

We can look at the dynamics of fluctuations of the phase around the steady-state solution

$$\rho_0 = -\frac{2}{\tilde{g} \tilde{\gamma} (p-1)} = \left(\frac{1}{\tilde{\gamma}} - 1 \right) \frac{1}{p-1}, \quad \theta_0 = 0, \quad n_{R,0} = 1 , \tag{2.38}$$

with

$$\tilde{\gamma} = \frac{\gamma_R}{\gamma}, \quad \tilde{g} = \frac{g}{g_R}, \quad r_c = \frac{g_R}{\hbar R}, \quad u_c = \tilde{g} \tilde{\gamma} r_c . \tag{2.39}$$

If we keep only linear terms in the fluctuations of the densities $\delta\rho(\mathbf{x})$, $\delta n_R(\mathbf{x})$ and neglect their temporal and spatial derivatives, as well as their role in the noise part, we get

$$\delta\rho(\mathbf{x}) = -\frac{1}{\tilde{\gamma}}\frac{1}{p-1}\delta n_R(\mathbf{x}) \tag{2.40a}$$

$$\delta n_R(\mathbf{x}) = 2\,\mathrm{sgn}(m_{LP})\nabla^2\theta(\mathbf{x}) - 2\rho_0^{-1/2}\left[\cos(\theta(\mathbf{x}))\Im\{\hat{F}\} - \sin(\theta(\mathbf{x}))\Re\{\hat{F}\}\right] \tag{2.40b}$$

$$\partial_t\theta(\mathbf{x}) = -\,\mathrm{sgn}(m_{LP})(\vec{\nabla}\theta(\mathbf{x}))^2 - u_c(p-1)\delta\rho(\mathbf{x}) \; - 2r_c\delta n_R - \rho_0^{-1/2}\left[\cos(\theta(\mathbf{x}))\Re\{\hat{F}\} + \sin(\theta(\mathbf{x}))\Im\{\hat{F}\}\right] \tag{2.40c}$$

which leads to the following effective dynamics of the phase,

$$\partial_t\theta(\mathbf{x}) = 2\,\mathrm{sgn}(m_{LP})r_c(\tilde{g}-2)\nabla^2\theta(\mathbf{x}) - \,\mathrm{sgn}(m_{LP})(\vec{\nabla}\theta(\mathbf{x}))^2 + \eta(\mathbf{x}) \tag{2.41}$$

with

$$\langle\eta(\mathbf{x})\eta(\mathbf{x}')\rangle = \rho_0^{-1}\left[4r_c^2(\tilde{g}-2)^2+1\right]\delta(\mathbf{x}-\mathbf{x}') \tag{2.42}$$

and where, as in the adiabatic case, we used the fact that $\Re\{\hat{F}\}$ and $\Im\{\hat{F}\}$ are $i.i.d$ random variables, $i.e.$ $\langle\Re\{\hat{F}(\mathbf{x})\}\Im\{\hat{F}(\mathbf{x}')\}\rangle = 0$. Hence we obtain a KPZ equation with

$$\nu = 2\,\mathrm{sgn}(m_{LP})r_c(\tilde{g}-2), \quad \lambda = -2\,\mathrm{sgn}(m_{LP}), \quad D = \frac{1}{2\rho_0}\left[4r_c^2(\tilde{g}-2)^2+1\right]. \tag{2.43}$$

It is interesting to make some remarks. The additivity of the noise is due to the fact that we took a complex noise $\hat{F}$. With $\Im\{\hat{F}\} = 0$ the noise becomes multiplicative, because we cannot to get rid of the sinus and cosinus terms in that case. Furthermore, to have a positive steady-state density in (2.38), we need a negative $\tilde{g}$, which implies either g or g_R to be negative. Finally, the mapping holds only if fluctuations δn_R of the reservoir density are allowed. Indeed the equation for δn_R allows to get $\delta\rho$, which is needed in order to know the dynamics of θ. Finally, we see that for the same argument used in the section above we need $\mathrm{sgn}(m_{LP})r_c(\tilde{g}-2) > 0$. Interestingly this is the case in real experiments for non-adiabatic EP, where $\tilde{g} < 2, r_c > 0$ but the effective polaritonic mass is negative [83].

2.4.3 Density-Phase Representation of the Keldysh Action

In this part we show that the Keldysh action itself (2.28) can be mapped to the KPZ action (1.37), in the same regime considered previously. Dealing with a microscopic action instead of a full quantum master equation is convenient to exploit the symmetries of the system and thus extract large-scale and universal behaviours. For this purpose the crucial point is that the classical-phase-rotation $\phi_{c,q} \to e^{i\alpha}\phi_{c,q}$ is a symmetry for (2.28) while the quantum-phase-rotation $\{\phi_c \to e^{i\alpha}\phi_c,\ \phi_q \to e^{i\beta}\phi_q\}$ is not; one can show that the breaking of the classical-phase-rotation symmetry is enough to ensure the existence of a Goldstone mode [84]. This describes fluctuations in the phase of the order parameter and will heavily influence the long-range properties of such systems in low dimensionality. Hence it is natural to derive the action for the condensate phase θ, which is the Goldstone boson, switching to a density-phase representation of classical and quantum fields:

$$\phi_c = \sqrt{\rho}e^{i\theta},\ \phi_q = \sqrt{\zeta}e^{i\theta} \tag{2.44}$$

where ρ, ζ are respectively a real and complex fields. To study the physics of the Goldstone boson θ we will perform a mean-field approximation over the densities justified by the fact that in the broken

phase, where θ is more important, the density fluctuations are massive and thus expected to be small compared to the ones associated to θ; this approximation consists in a saddle-point over ρ and ζ:

$$\left.\frac{\delta S}{\delta \rho}\right|_{\rho_{MF},\zeta_{MF}} = 0, \quad \left.\frac{\delta S}{\delta \zeta}\right|_{\rho_{MF},\zeta_{MF}} = 0 \tag{2.45}$$

Due to the fact that the action is at least linear in the quantum field ϕ_c, we can always take as a solution of (2.45)

$$(\rho_{MF}, \zeta_{MF}) = (\rho_0, 0) \tag{2.46}$$

By considering fluctuations up to second order around the mean-field solution for $\zeta = \zeta_1 + i\zeta_2$ and $\rho = \rho_0 + \pi$ and taking the stationary, long-wavelength limit $(\omega, q) \to (0, 0)$ we get that the resulting action for the phase-field θ and its conjugated variable $\tilde{\theta} \hat{=} 2i\rho_0^{\frac{1}{2}}\zeta_1$ is [84]

$$S[\theta, \tilde{\theta}] \hat{=} \int_{\mathbf{x}} \tilde{\theta}\left[\partial_t \theta - \nu\nabla^2\theta - \frac{\lambda}{2}(\nabla\theta)^2 - D\tilde{\theta}\right] \tag{2.47}$$

with the same relations reported in (2.35) and ρ_0 being the mean-field solution of (2.45). Equation (2.47), *i.e.* the Keldysh action reduced to the variables θ and $\tilde{\theta}$, is identical to the KPZ action (1.37) obtained from the MSRJD formalism.

3 Semi-classical dynamics of Exciton-Polaritons and the Mapping to KPZ Beyond the Homogeneous Case

In typical experiments with EP the system is far from being homogeneous. Many physical effects are present which could in principle play an important role in the long-time and large-distance behaviour and thus affect the mapping to the KPZ equation. The Keldysh field-theoretical description is a good starting point to understand how inhomogeneities in the quantum picture translate into the effective phase dynamics. In this chapter we will show that the mapping to KPZ equation still holds when static confinement, random disorder and thermally activated phonons are taken into account. We will present and perform the analytical calculations in order to extend the homogeneous case, discussed in the previous chapter and already known in the literature, to the presence of inhomogeneities. For the case of thermally activated phonons we will also study their effects on the semi-classical dynamics of the condensate, which was never treated before starting from a field-theoretical framework. In what follow we will focus on the one-dimensional case, but the generalization to higher dimensions is straightforward.

3.1 Confinement and Disorder

In several experimental conditions EP are subjected to a one-body external potential whose effect onto the dynamics of the EP can be taken into account via the Hamiltonian

$$\mathcal{H}_{ext} = \int_x \Big[\psi^\dagger(x) V(x) \psi(x)\Big] \,. \tag{3.1}$$

In addition to a confining potential, in-homogeneities in the sample usually lead to an effective multi-well potential which differs between different experimental realisations; this effect can be mimicked by a static one-body random potential. This random potential enters in the microscopic dynamics of the EP under the same form as the confining potential introduced above,

$$\mathcal{H}_{dis} = \int_x \Big[\psi^\dagger(x) V_{dis}(x) \psi(x)\Big] \,. \tag{3.2}$$

with

$$V_{dis}(x) = |\mathcal{F}^{-1}[\tilde{V}_{dis}(k)](x)|, \qquad \tilde{V}_{dis}(k) = V_0 e^{i\varphi} e^{-k^2 \ell_d^2} \tag{3.3}$$

where φ is a uniformly distributed random variable in the range $[0, 2\pi]$, ℓ_d is the disorder correlation length and V_0 is fixed in such a way that the average value of $V(x)$ is of the same order as the thermal noise already present in gGPE. The main difference with respect to the deterministic external potential is that in the case of a random disorder, physically relevant quantities and observables are obtained as averages over many realizations of the disorder. In our case we take a Gaussian distributed disorder V_{dis},

$$P\big[V_{dis}\big] = \exp\left\{ -\frac{1}{2} \int_{\mathbf{x},\mathbf{x}'} V_{dis}(\mathbf{x}) G^{-1}(\mathbf{x}-\mathbf{x}') V_{dis}(\mathbf{x}') \right\}. \tag{3.4}$$

Taking into account the one-body potentials (3.1), (3.2) in the quantum dynamics, and assuming a purely classical potential (i.e. a potential that is the same on both forward and backward Keldysh contours [84]), we end up with a term in the Keldysh action (2.28) of the type (see App. C)

$$S_{ext,dis} = -\int_{\mathbf{x}} V_{ext,dis}(x)\left[\phi_q^*\phi_c + \phi_c^*\phi_q\right] . \tag{3.5}$$

In both cases the presence of the potential results in a modification of the semiclassical limit (2.29), that is now an inhomogeneous Partial Differential Equation (PDE),

$$i\partial_t\phi_c = \left[-(K_c + iK_d)\partial_x^2 + r_c + V_{ext,dis} - ir_d + (u_c - iu_d)|\phi_c|^2\right]\phi_c + \xi\,. \tag{3.6}$$

In the case in which the potential is random and Gaussian distributed, as the one which will be considered in the following, we can collect the effects of V_{dis} and ξ in a single term, *i.e.* an effective multiplicative Gaussian noise ζ with correlations

$$\left\langle \zeta(\mathbf{x})\zeta^*(\mathbf{x}')\right\rangle = \gamma\delta(\mathbf{x}-\mathbf{x}') + \phi_c(\mathbf{x})G(\mathbf{x},\mathbf{x}')\phi_c^*(\mathbf{x}') \tag{3.7}$$

where, as we discussed in the previous chapter, we neglected the multiplicative contribution coming from quantum fluctuations in one-dimension. Interesting effects coming from one-body deterministic and random potential are present in the dynamics of the phase. We will discuss them in the following. For the deterministic case we will directly start from the contribution (3.5), while for the random potential we will average over different realizations of the disorder to study its effect on the phase dynamics.

3.1.1 EP Under Confinement: Analytical Study

In the density-phase representation

$$\phi_c = \sqrt{\rho}e^{i\theta},\ \phi_q = \sqrt{\zeta}e^{i\theta}, \tag{3.8}$$

Eq. (3.5) becomes

$$S_{ext} = -2\int_{\mathbf{x}} V_{ext}(x)\rho^{\frac{1}{2}}\Re(\zeta), \tag{3.9}$$

where $\Re(\zeta)$ stands for the real part of ζ. If we now perform the mean-field approximation (2.45) over the densities ρ and ζ (see App. C.1.1 for the technical details), the uniformity assumption does not apply anymore and we have to consider an inhomogeneous mean-field solution $(\theta,\rho) \equiv (\theta_0(x),\rho_0(x))$. By doing so we obtain

$$\left(iK_c\rho_0^{-\frac{1}{2}}\nabla\rho_0\cdot\nabla\theta_0 - \frac{K_c}{4}\rho_0^{-\frac{3}{2}}(\nabla\rho_0)^2 + \frac{K_c}{2}\rho_0^{-\frac{1}{2}}\nabla^2\rho_0 - K_c\rho_0^{\frac{1}{2}}(\nabla\theta_0)^2 + iK_c\rho_0^{\frac{1}{2}}\nabla^2\theta_0 - r_c\rho_0^{\frac{1}{2}} + \rho_0^{\frac{1}{2}}\right)$$
$$-(u_c - iu_d)\rho_0^{\frac{3}{2}} - V_{ext}\rho_0^{\frac{1}{2}} = 0. \tag{3.10}$$

We assume that the spatial variations of the mean-field density $\nabla\rho_0$ are small compared to the homogeneous mean-field density times the typical length-scale introduced by the interaction potential, i.e.

$$\nabla\rho_0(x)\frac{u_d\lambda_{V_{ext}}^{-1}}{r_d} = O(\epsilon), \qquad \epsilon \ll 1\,. \tag{3.11}$$

This means that spatial fluctuations in the density are negligible when either the uniform density is large or the external potential is very smooth. Using this approximation we obtain

$$\rho_0(x) = -\frac{r_d + K_c\nabla^2\theta_0(x) - K_d(\nabla\theta_0(x))^2}{u_d} \tag{3.12a}$$

$$\rho_0(x) = \frac{-V_{ext}(x) - r_c - K_c(\nabla\theta_0(x))^2 - K_d\nabla^2\theta_0(x)}{u_c}. \tag{3.12b}$$

In the limit where the spatial variation of the phase also plays no role (as in the equilibrium situation) (3.12) reduces to the well-known Thomas-Fermi approximation where r_c plays the role of the chemical potential. It is interesting to notice that in the presence of a confinement the mean-field phase θ_0 must depend at least quadratically on x in order for (3.12) to be both satisfied. We now look at fluctuations around this mean-field solution and study the dynamics of the phase in the stationary, long-wavelength regime as we did in Chap. 2.4.3; in the case of a deterministic potential we obtain (see C.1.1 for calculations)

$$S' = \int_{\mathbf{x}} i\tilde{\theta}\left\{\left[\partial_t\theta + (K_d - \tilde{u}K_c)\nabla^2\theta + (K_c + \tilde{u}K_d)(\nabla\theta)^2\right] - \frac{\gamma + 2u_d\rho_0}{2\rho_0}\left(1+\tilde{u}^2\right)\tilde{\theta}\right\} \tag{3.13}$$

with $Z = \int \mathscr{D}[\theta,\tilde{\theta}]e^{iS'}$ and

$$\tilde{u}(x)\hat{=}\frac{2(r_c + V_{ext}(x)) + 3K_d\nabla^2\theta_0(x) + 3K_c(\nabla\theta_0(x))^2}{2r_d + 3K_c\nabla^2\theta_0(x) - 3K_d(\theta_0)^2}. \tag{3.14}$$

Thus, in the presence of an external potential, one can identify an action which is similar to (2.34b) but with spatially dependent coefficients,

$$\nu\hat{=}K_c\left(\tilde{u}(x) - \frac{K_d}{K_c}\right),\ \lambda\hat{=}-2K_c\left(1+\tilde{u}(x)\frac{K_d}{K_c}\right),\ D\hat{=}\frac{\gamma + 2u_d\rho_0(x)}{2\rho_0(x)}\left(1+\tilde{u}(x)^2\right). \tag{3.15}$$

One can check that in the $V_{ext}(\mathbf{x}) \to 0$ limit, which also implies $\theta_0(x) \equiv \theta_0$, (B.40) is recovered. In the presence of a non zero $V_{ext}(x)$ we end up with a highly inhomogeneous KPZ equation in which all the coefficients are spatially dependent. The effective non-linearity of the KPZ equation, defined as

$$g = \lambda\sqrt{\frac{D}{2\nu^3}} \tag{3.16}$$

becomes $g \equiv g(V_{ext}) \sim V_{ext}^{1/2}$ and thus in principle increases as the strength of the confining potential is increased. This implies that the boundaries, where usually the potential is stronger, will feel a much higher non-linearity than the bulk of the system. Recalling that the coefficient λ is linked to the asymptotic velocity of the front in the KPZ equation, v_∞, we see that we will also have an effect of the confining potential on the average propagation velocity of the phase front. If the difference in the strength of the potential between the boundary and the bulk of the EP condensate is strong enough, this difference of propagation speed could lead to interesting effects such as cusps in the phase front, as we will see in the next chapter.

3.1.2 EP with Disorder: an Analytical Study

Even if the usual experimental condition is the one in which the disorder is a static spatially-correlated random potential, it is interesting to also investigate the case in which the potential has some time correlation

$$\left\langle V_{dis}(\mathbf{x})V_{dis}(\mathbf{x}')\right\rangle = G(\mathbf{x},\mathbf{x}')\,, \tag{3.17}$$

where we recall that $\mathbf{x} = (\vec{x}, t)$. After averaging over the distribution (3.4), we obtain an effective contribution of the disorder in the Keldysh action (2.28) of the type

$$S_{dis,eff} = \frac{i}{2}\int_{\mathbf{x},\mathbf{x}'}\left[\left(\phi_q^*(\mathbf{x})\phi_c(\mathbf{x}) + \phi_c^*(\mathbf{x})\phi_q(\mathbf{x})\right)G(\mathbf{x},\mathbf{x}')\left(\phi_q^*(\mathbf{x}')\phi_c(\mathbf{x}') + \phi_c^*(\mathbf{x}')\phi_q(\mathbf{x}')\right)\right]. \tag{3.18}$$

When transforming to a density-phase representation, the term (3.18) does not affect the mean-field equations for the densities, (3.12), because it is quadratic in ϕ_q; in terms of fluctuations over the mean-field solution up to second order, we get

$$S_{dis,eff} = 2i\rho_0\int_{\mathbf{x},\mathbf{x}'}\zeta_1(\mathbf{x})G(\mathbf{x},\mathbf{x}')\zeta_1(\mathbf{x}')\,. \tag{3.19}$$

It is important to stress that depending on the long-time and large-distance properties of $G(\mathbf{x},\mathbf{x}')$ this contribution could turn out to be irrelevant for the KPZ mapping according to the argument used in Chap. 2.4.3. Supposing a smooth behaviour of $G(\mathbf{x},\mathbf{x}')$ and introducing the response field $\tilde{\theta}(\mathbf{x}) = 2i\rho_0^{\frac{1}{2}}\zeta_1(\mathbf{x})$ we get

$$S_{dis,eff} = -\frac{i}{2}\int_{\mathbf{x}}\tilde{\theta}(\mathbf{x})\int_{\mathbf{x}'}G(\mathbf{x},\mathbf{x}')\tilde{\theta}(\mathbf{x}') \tag{3.20}$$

which implies a modification of the white noise in the KPZ mapping (2.35) of the type

$$D_{dis}\tilde{\theta}(\mathbf{x}) = D\tilde{\theta}(\mathbf{x}) + \frac{1}{2}\int_{\mathbf{x}'}G(\mathbf{x},\mathbf{x}')\tilde{\theta}(\mathbf{x}')\,. \tag{3.21}$$

As we can see, a non-delta correlation $G(\mathbf{x}-\mathbf{x}')$ will introduce a memory-kernel in the noise source. A particular case often present in experimental setups is a purely static disorder,

$$\left\langle V_{dis}(\mathbf{x})V_{dis}(\mathbf{x}')\right\rangle = \tau\Gamma(x-x')\delta(t-t') \tag{3.22}$$

for which we get

$$D_{dis}\tilde{\theta}(\mathbf{x}) = D\tilde{\theta}(\mathbf{x}) + \frac{1}{2}\int_{x'}G(x-x')\tilde{\theta}(x',t)\,. \tag{3.23}$$

Depending on the long-distance properties of the correlation G, a new length-scale ℓ_d appears in the system; due to the self-critical nature of the KPZ equation we expect the emergence of a new time scale related to ℓ_d,

$$t^* \sim \ell_d^z \tag{3.24}$$

where z is the dynamical exponent introduced in Chap. 1.2. It has been shown that the KPZ equation with spatial correlation in the microscopic noise over a finite length remains in the KPZ universality class [86, 87]. We then expect z to be the KPZ one, *i.e.* $z = 3/2$. We will not consider for the EP the case of a disorder with non zero time correlations. This will be investigated for a KPZ interface in Chapter 5.

3.2 EP and Phonons: an Analytical Study

The condensation of EP can be experimentally realized at temperature ranging up to room temperature; under such conditions the effect of thermal fluctuations in the semiconductor material becomes important and needs to be taken into account. The most important of such effects is the interaction with the phonons of the surrounding solid-state environment. In a low-energy picture we are mainly interested in the acoustic phonons; a well known model describing such phonons is the Frölich Hamiltonian [88]:

$$H_{ph} = \sum_{\mathbf{q}} \left\{ \omega_{\mathbf{q}} \hat{b}^\dagger_{\mathbf{q}} \hat{b}_{\mathbf{q}} + \int_k \left[G_{\mathbf{q}} \hat{b}_{\mathbf{q}} \hat{a}^\dagger(k+q_x)\hat{a}(k) + G^*_{\mathbf{q}} \hat{b}^\dagger_{\mathbf{q}} \hat{a}(k+q_x)\hat{a}^\dagger(k) \right] \right\} \tag{3.25}$$

with $\hat{a}^{(\dagger)}(k) = \int_x \hat{\psi}^{(\dagger)}(x) e^{-ikx}$ field operators for the one-dimensional Exciton-Polariton system; here $\hat{b}^{(\dagger)}_{\mathbf{q}}$ is the annihilation (creation) field operator in momentum space for the phonon-bath (assumed to be three-dimensional). The effective contribution coming from (3.25) to (2.28) reads (see App. C.2)

$$S_{ph} = S_l + S_b \tag{3.26}$$

with

$$\begin{aligned} S_l =& \frac{i}{4} \sum_{\vec{q}} |G_{\vec{q}}|^2 \int_{\mathbf{x},\mathbf{x}'} \left(\phi^*_q(\mathbf{x})\phi_c(\mathbf{x})\phi^*_c(\mathbf{x}')\phi_c(\mathbf{x}') + \phi_q(\mathbf{x})\phi^*_c(\mathbf{x})\phi_c(\mathbf{x}')\phi^*_c(\mathbf{x}') \right) \left[e^{iq_x(x-x')-i\omega_{\vec{q}}(t'-t)} e^{-iq_x(x-x')+i\omega_{\vec{q}}(t'-t)} \right] \\ & \times \left[\theta(t-t') - \theta(t'-t) + 1 \right] \end{aligned} \tag{3.27a}$$

$$S_b = i \sum_{\vec{q}} |G_{\vec{q}}|^2 \left(2n(\omega_{\vec{q}}) + 1 \right) \int_{\mathbf{x}} \phi^*_q(\mathbf{x})\phi_q(\mathbf{x}) \int_{\mathbf{x}'} \cos\left(q_x(x-x') - \omega_{\vec{q}}(t-t') \right) \phi^*_c(\mathbf{x}')\phi_c(\mathbf{x}') \tag{3.27b}$$

where $n(\omega_{\vec{q}})$ is the phononic occupation number in mode $\vec{q}$. Thermal activated phonons usually represent an incoherent reservoir, with randomly varying phase [89, 90]. This is the analogous of the Markovian approximation within usual Langevin approach. In this case, (3.26) simplifies to

$$S_{ph,mk} = S_{l,mk} + S_{b,mk} \tag{3.28}$$

with

$$S_{l,mk} = \frac{i}{2} \nu(\omega_0) |G(\omega_0)|^2 \int_{\mathbf{x},x'} \left[\phi^*_q(\mathbf{x})\phi_c(\mathbf{x})\phi^*_c(x',t)\phi_c(x',t) + \phi_q(\mathbf{x})\phi^*_c(\mathbf{x})\phi_c(x',t)\phi^*_c(x',t) \right] \sin\left(\frac{\omega_0}{u}(x-x') \right) \tag{3.29a}$$

$$S_{b,mk} = i\nu(\omega_0)|G(\omega_0)|^2 \left(2n(\omega_0)+1\right) \int_{x,t,x'} \phi^*_q(x,t)\phi_q(x,t)\phi^*_c(x',t)\phi_c(x',t) \cos\left(\frac{\omega_0}{u}(x-x') \right) \tag{3.29b}$$

where ω_0 is the typical frequency of the Markovian phonons bath. Taking the semi-classical limit of this action as we did in the homogeneous case (see Chap. 2.3), we obtain two different contributions in the resulting EP dynamics. The first contribution, coming from S_l gives rise to a non conservative deterministic contribution and takes into account spontaneous emission of phonons by the thermally excited EP condensate. The second term above, coming from S_b, translates into an external stochastic potential in space and time, or equivalently a multiplicative-noise term ξ in the gGPE equation (2.29)

of the form

$$\mathcal{P}[\xi] = \exp\left\{-\frac{1}{2}\int_{x,t,x',t'} \xi^*(x,t)M^{-1}(x-x',t-t')\xi(x',t')\right\} \tag{3.30}$$

$$\left\langle \xi_q^*(x,t)\xi_q(x',t')\right\rangle = 2\nu(\omega_0)|G(\omega_0)|^2(2n(\omega_0)+1)\int_{x''}\cos\left(\frac{\omega_0}{u}(x-x'')\right)\phi_c^*(x'',t)\phi_c(x'',t)\delta(x-x')\delta(t-t') \tag{3.31}$$

with $M^{-1}(x-x',t-t')M(x-x',t-t') = \delta(x-x')\delta(t-t')$ and $M(x-x',t-t') = 2\nu(\omega_0)|G(\omega_0)|^2(2n(\omega_0)+1)$ $\times \int_{x''}\cos\left(\frac{\omega_0}{u}(x-x'')\right)\phi_c^*(x'',t)\phi_c(x'',t)\delta(x-x')\delta(t-t')$. This thermal noise, which is coupled to the condensate density, adds up to the noise coming from the pure driven-dissipative dynamics of the system, whose coupling to the density can be in general neglected as we discussed in Chap. 2.3. These results are in agreement with the description given in [90] in which however the condensate field is treated as completely classical and thus the quantum contribution to the phononic occupation number n is missing, *i.e.* one can set $(2n+1) \simeq 2n$.

3.2.1 Mapping to KPZ equation

In order to get insights into the effects of the interaction with phonons onto the mapping to KPZ equation we switch to modulo-phase representation for the classical and quantum fields. Due to the fact that the term in the Keldysh action coming from the effective contribution of the phonons, (3.26), is at least linear in the Keldysh quantum field, ϕ_q, $\zeta_{MF} = 0$ is still a solution for the mean field equations; as in Chap. 3.1.1 $\rho_M F$ should be space-dependent to reflect the spatial inhomogeneity of S_l, S_b; we will here suppose that the effect of the phonons will not affect the mean field behaviour of the system and take a homogeneous mean-field solution $(\rho_{MF}, \zeta_{MF}) = (\rho_0, 0)$. By looking at second-order fluctuations around such solutions we get

$$S_l = i\int_{\mathbf{x}}\sum_{\mathbf{q}}|G_{\mathbf{q}}|^2\rho_0^{3/2}\zeta_1(\mathbf{x})A_{\mathbf{q}}(\mathbf{x}) \tag{3.32a}$$

$$S_b = i\int_{\mathbf{x}}\sum_{\mathbf{q}}|G_{\mathbf{q}}|^2\left(2n(\omega_{\mathbf{q}})+1\right)|\zeta(\mathbf{x})|^2B_{\mathbf{q}}(\mathbf{x})\,. \tag{3.32b}$$

Taking into account that usually $|G_{\mathbf{q}}|^2 \sim \omega_q$ [90] the bi-linear terms will not affect, for acoustic phonons, the long-time and large-distance limit introduced in Chap. 2.4.3. It is easy to show that the same is valid for the linear term; indeed even if it is just linear in the density fluctuations, it becomes irrelevant due to the behaviour of $|G_{\mathbf{q}}|^2$ and $A_{\mathbf{q}}(\mathbf{x})$ as $\mathbf{x} \to \mathbf{0}$. We hence expect acoustic phonons not to play a key role in the KPZ dynamics of the EP system. For the optical phonons the situation is more subtle. Indeed using the usual Einstein representation for the optical phonon dispersion $E(\omega) \propto \delta(\omega-\omega_0)$, we have that the long-time limit $\omega \to 0$ is not well defined, which physically means that a gapped spectrum cannot affect the low-energy, small k dynamics.

4 Scaling and Distributions of the Phase in Exciton-Polaritons Systems

In this chapter we will discuss the results coming from a numerical simulation of the exciton-polaritons dynamics in one dimension. We will numerically integrate the semi-classical limit of the Keldysh action, i.e. the associated gGPE, in different conditions using the interaction-picture approach to Stochastic Partial Differential Equation (SPDE) [91, 92]. From these simulations we will either directly extract the phase of the condensate, after checking the absence of phase-slips in the system, or work at the level of wave-function correlations, which can be recast into phase-phase correlations via a cumulant-expansion (see App. D). We will focus mainly on the homogeneous case, for which we will first show that the general scaling behaviour for experimentally accessible parameters corresponds to the KPZ universality class. Then we will study the distribution of the phase of the condensate to deduce the type of KPZ geometrical sub-class to which the EP phase belongs.

4.1 Numerical Simulations and Parameters

The parameters in the gGPE depend on the material. We use values typical for CdTe, used *e.g.* in Grenoble experiments in the group of Maxime Richard

$$m_{LP} = 4\times10^{-5}m_e,\ \gamma_l = 0.5\text{ps}^{-1},\ g = 7.59\,10^2\text{ms}^{-1},\ \gamma_r = 0.02\text{ps}^{-1},\ R = 400\text{ms}^{-1},$$
$$p = 1.6,\ K_d = 0.45,\ K_c^{(2)} = 2.5\times10^{-3}. \tag{4.1}$$

Using this set of parameters we numerically solve the gGPE

$$i\partial_t\phi = \left[-(1+iK_d)\nabla^2 + K_c^{(2)}\nabla^4 + r_c - ir_d + (u_c - iu_d)|\phi|^2\right]\phi + \sqrt{\sigma}\xi \tag{4.2}$$

with

$$r_d = \frac{p-1}{2},\quad u_d = \frac{p-1}{2},\quad u_c = \frac{\gamma_r g}{R\gamma_l}\frac{p-1}{p},\quad \sigma = \frac{1}{2\hat{x}}\frac{R}{\gamma_r}\frac{p(p+1)}{p-1},\quad r_c = \frac{r_d u_c}{u_d} \tag{4.3}$$

and $\langle\xi(x,t)\xi^*(x',t')=2\delta(x-x')\delta(t-t')\rangle$. The parameters K_d and $K_c^{(2)}$ are not well determined in experiments and in our simulations we choose $K_d = 0.45$ and $K_c^{(2)} = 2.5\times10^{-3}$. The space, time and condensate wavefunction are dimensionless, rescaled from their physical counterparts according to the choice reported in Chap. 2.2.3. In each simulation, we determine the wavefunction $\phi(t,x)$, and extract its phase $\theta(t,x)$. We work in the low-noise regime, where we checked that the density fluctuations are negligible. In this regime, topological defects, *i.e.* phase slips in 1D associated with solitonic solutions, are absent. Hence the phase can be uniquely unwinded to obtain $\theta\in(-\infty,\infty)$. This is a crucial point as can be inferred from (1.48); indeed both elementary scaling properties and the advanced geometrical sub-classes linked to the rescaled variable $\tilde{h}$ rely on the non-compact nature of the height field. A clear example comes from the behaviour of the roughness w^2 which according to KPZ equation (1.13) saturates to a value L^χ, which in general does not lie inside $[0,2\pi)$.

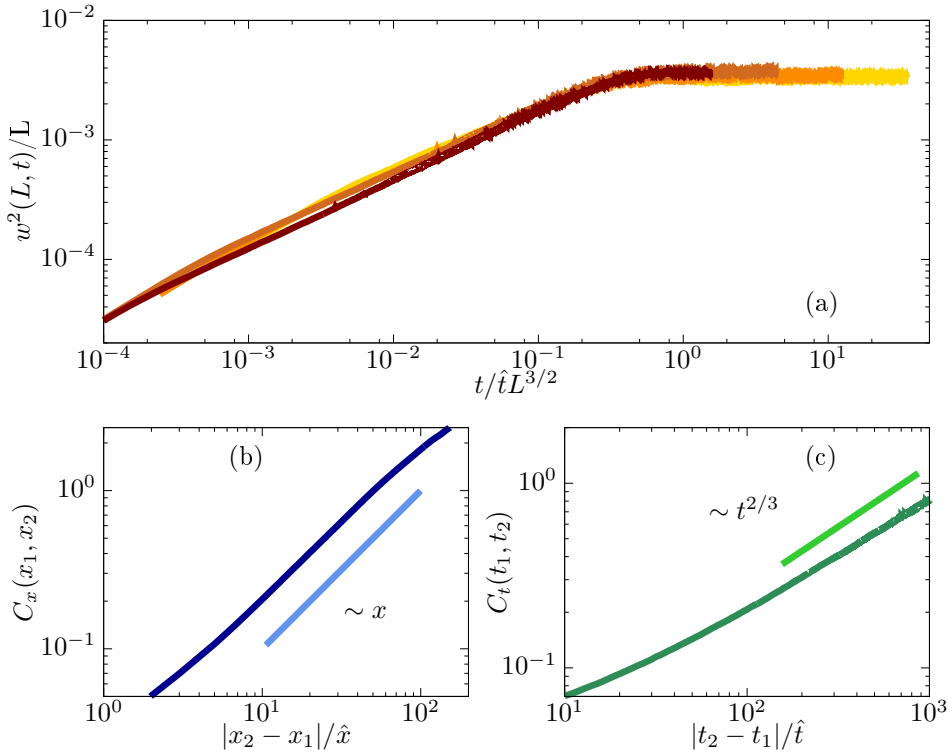

Figure 4.1: (a) Collapse of the roughness $w(L,t)$ with KPZ scaling $\chi = 1/2$, $z = 3/2$ for different system sizes $L/\bar{x} = 2^7, 2^8, 2^9, 2^{10}$ (size growing from lighter- to darker-color). Two-point (b) spatial and (c) temporal correlation together with the KPZ theoretical behaviour, corresponding to a (stretched) exponential in $\rho_1(x_1,t,x_2,t) = e^{-C_x(x_1,x_2)}$ and $\rho_1(x,t_1,x,t_2) = e^{-C_t(t_1,t_2)}$

4.1.1 Numerical Integration Prescription

The numerical integration is performed using the interaction picture method (IP) for solving non-linear stochastic partial differential equations (SPDE) [91, 92]. This integration scheme relies on a similar idea as the interaction picture formalism in quantum mechanics: first, the linear part is solved in Fourier space, then it is transformed back to real-space and evolved via the non-linear part of the equation using semi-implicit Runge-Kutta method.

4.2 Homogeneous Case

4.2.1 KPZ scaling

We have computed the roughness function $w^2(L,t)$ for the unwinded phase θ of EP,

$$w^2(L,t) = \left\langle \frac{1}{L}\int_x \theta^2(x,t) - \left(\frac{1}{L}\int_x \theta(x,t)\right)^2 \right\rangle . \tag{4.4}$$

Our results are reported in Fig. 4.1, and show that using the KPZ exponents, one obtains for the roughness a perfect collapse onto the expected Family-Vicsek scaling form (1.17). This shows that the findings of [25] obtained for suitably chosen parameters can also be achieved for realistic experimental conditions. Let us stress that the inclusion of a momentum-dependent damping rate is crucial since it

stabilizes the solution for our choice of experimental parameters, which corresponds to a larger KPZ effective non-linearity parameter $|g| \equiv |\lambda|(D/2\nu^3)^{1/2} \simeq 0.48$ than that used in [25]. This difference in parameters has an important effect, since we obtain KPZ scaling not only in the long-time saturation regime $t > T_s$, where the roughness function reaches a constant in time, but also in the growth regime. If the KPZ nonlinearity is too weak, only the initial Edward-Wilkinson (EW) scaling (with $\chi = 1/2$ and $z = 2$) is visible, and the crossover to the KPZ one cannot occur before t reaches T_s. The KPZ scaling exponents can equivalently be determined directly from the condensate wavefunction, through the first-order correlation function, $\rho_1(\mathbf{x}, \mathbf{x}') = \langle \phi^*(\mathbf{x})\phi(\mathbf{x}')\rangle$ (see App. D). Focusing on purely spatial or purely temporal correlations, we define

$$C_x(x_1, x_2)|_t = -\log|\rho_1(x_1, t; x_2, t)|, \quad C_t(t_1, t_2)|_x = -\log|\rho_1(x, t_1; x, t_2)|. \tag{4.5}$$

At large distances, the main contribution to the correlation functions comes from the phase-phase correlations, that according to KPZ scaling is predicted to behave as

$$\langle \theta(x_1, t)\theta(x_2, t)\rangle \sim |x_2 - x_1|^{2\chi} \tag{4.6}$$

and

$$\langle \theta(x, t_1)\theta(x, t_2)\rangle \sim |t_2 - t_1|^{2\beta} \tag{4.7}$$

respectively. Our results for the correlation functions in the saturated regime $t > T_s$, obtained from the numerical solution of the gGPE, are shown in the lower panels of Fig. 4.1. For both time and space correlations, we obtain $\chi \simeq 0.49$ and $\beta \simeq 0.31$ for a system size $L/\bar{x} = 2^{10}$ in close agreement with the KPZ exponents $\chi = 1/2$ and $\beta = 1/3$, which confirms our result from the roughness. These features are observable down to system size of about 50μm, as will be shown in the following. This is remarkable since critical behaviours are generically expected in the limit of infinite system size. It is also important to stress that the time-correlation is mandatory to discriminate between the KPZ and EW scalings, since only the β exponent differs between the two in 1D. Let us emphasize that, whereas the measure of the roughness function may be difficult in EP systems since it requires to resolve the phase in time since the beginning of the phase unwinding, both space and time correlations are routinely experimentally accessible (see *e.g.* [85]), and suffice for the determination of the critical exponents.

4.3 Beyond scaling: Tracy-Widom statistics

As emphasized in Chap. 1.4, unprecedented theoretical advances have yielded the exact probability distribution of the fluctuations of the 1D KPZ interface for sharp-wedge, flat, and stationary initial conditions. To further assess KPZ universality in EP systems, we thus study the fluctuations of the unwinded phase $\delta\theta = (\theta - \langle\theta\rangle_{\xi,x})$ of the condensate (which subtracts the $v_\infty t$ term in (1.48)). In practice, we use the gGPE simulations to determine the distribution of the random variable $\tilde{\theta}(\mathbf{x}) = \delta\theta/(\Gamma t)^{1/3}$.

To extract the parameter Γ from the numerical data, we use the relation

$$|\Gamma| = \lim_{t\to\infty} \left(\langle \delta\theta^2(x, t)\rangle / \mathrm{Var}_\chi\right)^{3/2} / t \tag{4.8}$$

with $\langle\delta\theta^2\rangle = \langle(\theta - \langle\theta\rangle_{\xi,x})^2\rangle_{\xi,x}$ and where Var_χ is the theoretical value of the variance of the distribution. It is important to note that from the variance we only have access to the absolute value of Γ, which being proportional to λ (see (1.49)), can be negative for exciton-polariton systems (see (2.35)). In our simulation, where the effective mass is positive and the polariton-polariton interaction is repulsive, this is the case and hence all the odd moments of $\tilde{\theta}$ will be the opposite of the standard KPZ ones. This implies that

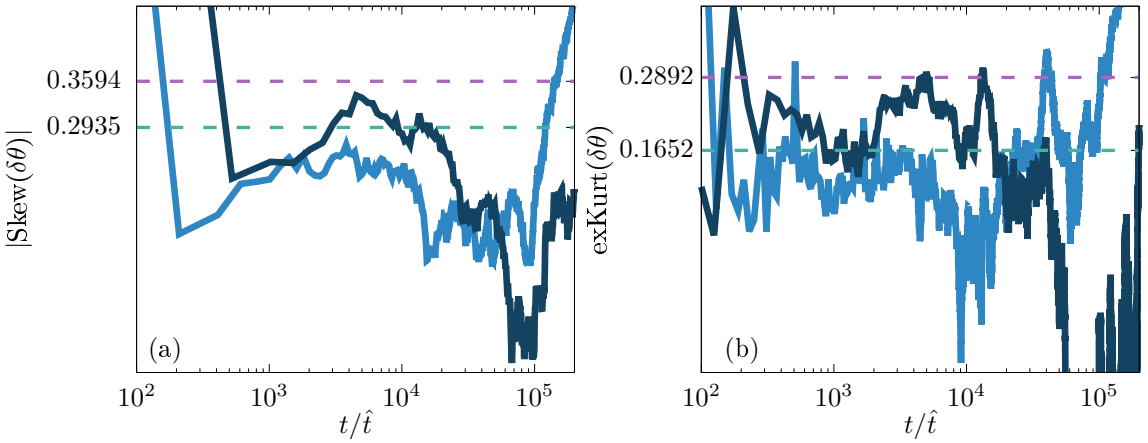

Figure 4.2: (a) The absolute value of the Skewness and (b)the excess Kurtosis (lower panel) of the phase-field in the condensate for $L/\bar{x} = 2^9, 2^{10}$, together with the theoretical values for TW-GOE and BR statistics (green and purple dashed-line respectively). TW-GOE values are reached on a plateau around times $t/\bar{t} \simeq 10^4$. We see that we cannot clearly discriminate between the two.

the distribution of $\tilde{\theta}$ will be the reflection with respect to the zero value of the distributions introduced in Chap. 1.4. The determination of Γ requires to identify which distribution is realized. For this, we first compute universal ratios of cumulants of $\delta\theta$, which do not depend on Γ, namely the skewness and the excess kurtosis, defined in (1.51), that in our case read

$$\mathrm{Skew}(\delta\theta) = \langle \delta\theta^3 \rangle / \langle \delta\theta^2 \rangle^{3/2} \tag{4.9}$$

and

$$\mathrm{eKurt}(\delta\theta) = \langle \delta\theta^4 \rangle / \langle \delta\theta^2 \rangle^2 - 3 \tag{4.10}$$

respectively, with $\langle \delta\theta^n \rangle = \langle (\theta - \langle \theta \rangle_{\xi,x})^n \rangle_{\xi,x}$. These quantities are exactly zero for a Gaussian distribution and are reported in Table 1.1 for the distributions associated with the 1D KPZ equation. We find that they reach stationary values on plateaus depending on the system size but roughly extending between

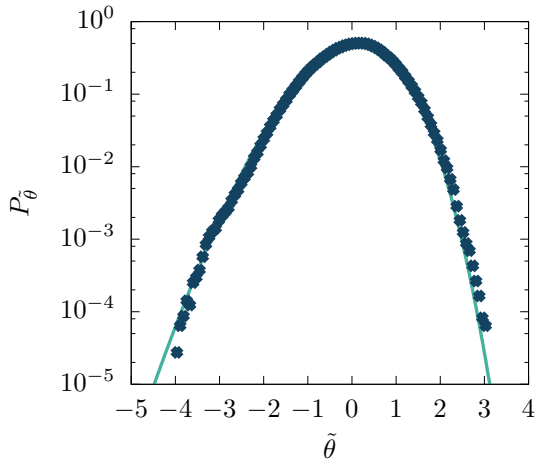

Figure 4.3: (a) Distribution of $\tilde{\theta}$ for $L/\bar{x} = 2^{10}$, together with the theoretical centred GOE-TW distribution.

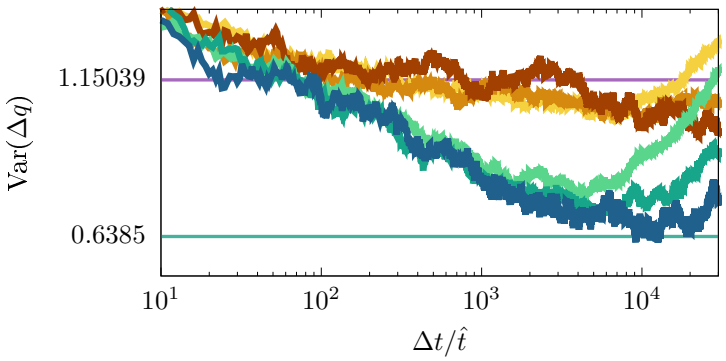

Figure 4.4: Numerical and theoretical values of Var(Δq) for different initial times $t_0/\bar{t} = 10^2, 2 \times 10^4$ (blue and brown color-scale respectively) and sizes $L/\bar{x} = 2^8, 2^9, 2^{10}$ (increasing from lighter to darker). The lower plateau is the one associated to TW-GOE statistics, reached for very large Δt. One can see that a higher plateau for small Δt appears increasing t_0 in large systems; This is consistent with the crossover to the stationary BR class, which is further supported by the value of the ratio between the two plateaus, which is $\simeq 1.781$, close to the theoretical value $\mathrm{Var}_{BR}/\mathrm{Var}_{TW-GOE} = 1.803$.

$t = 10^3$ and 10^4 in units of $\bar{t}$. The values of these plateaus are compatible with both TW-GOE and BR distributions introduced in Chap. 1.4 (see Fig. 4.2). However, as discussed in Chap. 1.4.1, in principle we expect either TW-GUE or TW-GOE to appear before BR statistics, which is associated to fluctuations of the size of the sample. We thus used the exact value of $\mathrm{Var}_{\mathrm{TW-GOE}}$ to extract Γ, and recorded the probability distribution of $\tilde{\theta}$ accumulated during the plateaus, which is represented in Fig. 4.3. We find that it is in excellent agreement with the TW-GOE distribution, thus providing a convincing confirmation that KPZ dynamics is relevant in EP systems. It is interesting to notice that the TW-GOE distribution is associated with a flat (*i.e.* spatially constant) initial condition for the KPZ height field, whereas in EP systems, the initial phase of the condensate is essentially random, and not controllable, and moreover KPZ behaviour sets in after a non-universal transient dynamics of the condensate.

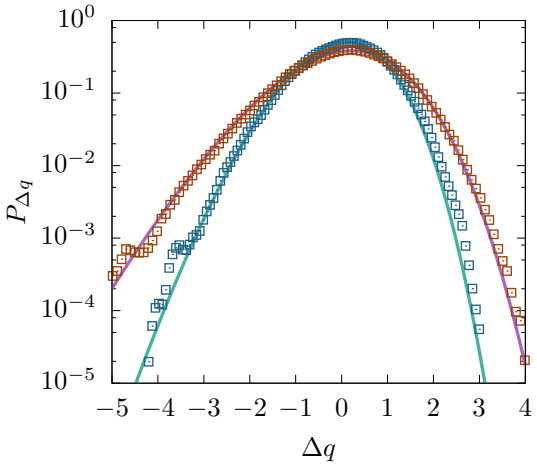

Figure 4.5: Distribution of $\Delta q(x, t_0, \Delta t)$ for $\Delta t/t_0 = 10^3$ (light-green symbols) and $\Delta t/t_0 = 5 \times 10^{-3}$ (purple symbols) for $L/\bar{x} = 2^{10}$, together with the theoretical centred TW-GOE (green solid line) and BR (purple solid line) distributions.

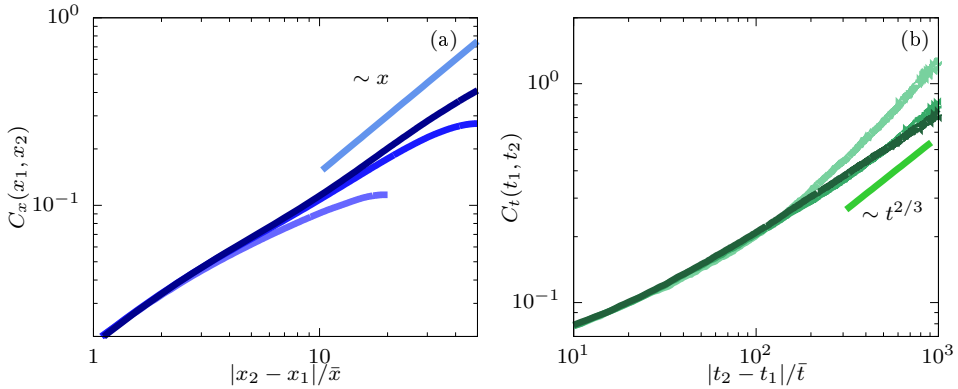

Figure 4.6: First-order (a) spatial and (b) temporal correlation function of the phase, for different system sizes $L = 20, 50, 100$ μm (growing from lighter to darker colors), together with the KPZ theoretical power-law behaviour (reference straight lines). These power-laws are visible on about a decade for system sizes down to 50 μm, but not below.

4.3.1 Beyond scaling: Baik-Rains statistics

The TW distribution is associated to the growth regime of KPZ dynamics. As introduced in Chap. 1.4.1, in a finite-size system, a crossover to the stationary KPZ regime, characterized by the Baik-Rains distribution, is expected at sufficiently long times, but before finite-size effects dominate [52]. Indications of a change of regime are manifest in Fig. 4.2 since the skewness and excess Kurtosis depart from the plateaus at large times. However, this change is hindered by the noise and finite-size effects, which become more and more relevant as the correlation length becomes comparable with the system size. In order to reduce finite-size effects and study this crossover, we follow Takeuchi [52] and introduce a new variable

$$\Delta q(x, t_0, \Delta t) = \frac{\delta\theta(x, t_0 + \Delta t) - \delta\theta(x, t_0)}{(\Gamma t)^{1/3}}. \tag{4.11}$$

Since this variable involves a phase difference, it does not require to know the absolute phase, and is hence accessible in EP experiments. This variable is expected to display a TW-GOE distribution for $t_0 \to 0, \Delta t \to \infty$ and a BR distribution for $t_0 \to \infty, \Delta t \to 0$, with this precise ordering of the limits. The distribution of Δq is plotted in Fig. 4.5 for different ratios $\Delta t/t_0$. Both TW and BR distributions are clearly identified. Our analysis hence shows that the homogeneous EP condensate is an ideal playground to observe non-trivial out-of-equilibrium behaviour associated with KPZ universality sub-classes.

4.4 Finite Size Effects in the EP-KPZ Mapping

In the previous section, we demonstrated that exciton polariton systems display advanced KPZ properties: *i.e.* not only the scaling of first-order correlation function of the phase, but also the full phase distributions reproduce the ones expected for KPZ dynamics. The results are mainly illustrated for a system of size $L/\bar{x} = 2^{10}$, which for our choice of parameters corresponds to samples of about 1 mm, in order to have a clear picture, in particular of the crossover phenomenon in the phase distributions. Although such sizes can be found in current EP experiments (e.g. in [76], which actually work with a sample of a few millimetres spot size), it is quite large compared to typical set-ups. In this section, we report the results for the first-order correlation and for the phase distribution obtained for systems of size $L \simeq 20, 50, 100\,\mu$m, which are relevant experimental values, to show how these results depend on the system size.

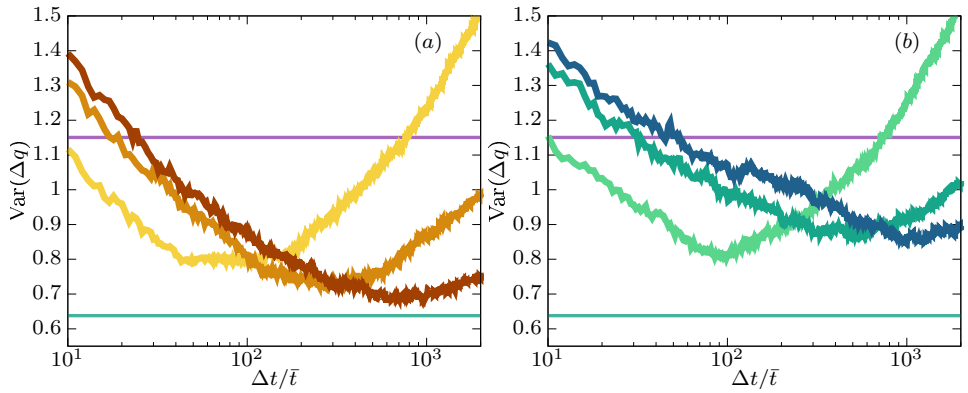

Figure 4.7: (Color online) Variance of Δq for different system sizes $L = 20, 50, 100$ μm (growing from lighter to darker colors), together with the TW-GOE and BR theoretical predictions (green and purple solid lines respectively). (*a*) For $t_0/\bar{t} = 10$, a clear approach to the TW-GOE value is visible as the system size and Δt are increased, as expected in the $\Delta t/t_0 \to \infty$ limit. (*b*) For $t_0/\bar{t} = 100, 500, 1000$ respectively for $L = 20, 50, 100$ μm, a plateau is emerging as the system size is increased, which approaches towards the BR value, although it is not attained for such small sizes. This indicates that only the beginning of the crossover towards BR is observable for small systems.

4.4.1 First Order Correlation Function

For each system size, we determine the stationary first-order correlation functions $C_x(x_1, x_2)$ and $C_t(t_1, t_2)$ defined in (4.5). The results are shown on Fig. 4.6. We find that the correlation functions still exhibit a regime of power-law behaviour, extending on a little more than one decade, even in relatively small samples, down to about $L = 50$ μm. The associated critical exponents are $\chi \simeq 0.43$ and $\beta \simeq 0.28$ for $L = 100$ μm. These values are in qualitative agreement with the KPZ values $\chi = 0.5$ and $\beta = 0.33$, although one cannot really discriminate from the EW value $\beta = 0.25$ on these data.

4.4.2 Probability distribution

For each system size, we determine the full distribution of the variable Δq defined in the previous section. For this, we first need to study the variance of Δq in order to check whether the KPZ distributions are realized, and to extract the parameter Γ. This variance is shown for both large and small $\Delta t/\bar{t}$ on Fig. 4.7(a) and 4.7(b) respectively. For small $\Delta t/\bar{t}$, we find that the variance exhibits a plateau whose value tends to the TW-GOE one as the system size is increased. It is not attained for the smallest system size considered, *i.e.* 20μm. The full distribution of Δq for a value of $\Delta t/\bar{t}$ belonging to the corresponding plateau is shown in Fig. 4.8(a). It confirms that the TW-GOE distribution is observable, and qualitatively well reproduced, for small systems down to about 50μm. For the smallest system, noticeable discrepancies are visible, in particular in the right tail. However, let us emphasize that these distributions clearly deviate from Gaussians, which allow ones to exclude EW universality class, and is thus more conclusive than the mere critical exponents. This shows that, thanks to the relatively high effective non-linearity, the KPZ regime can still occur for small systems.

For large $\Delta t/\bar{t}$, we find indications of a crossover towards BR statistics. Indeed, one observes that the variance, shown in Fig. 4.7(b), exhibits a plateau, whose value departs from the TW-GOE one and crosses over towards the BR value, although the latter is not attained. In accordance with this, the full distribution of Δq, recorded on the corresponding plateaus and plotted in Fig. 4.8(b), confirms that the crossover occurs, but is not fully achieved because finite size effects set in, even for the system of 100μm.

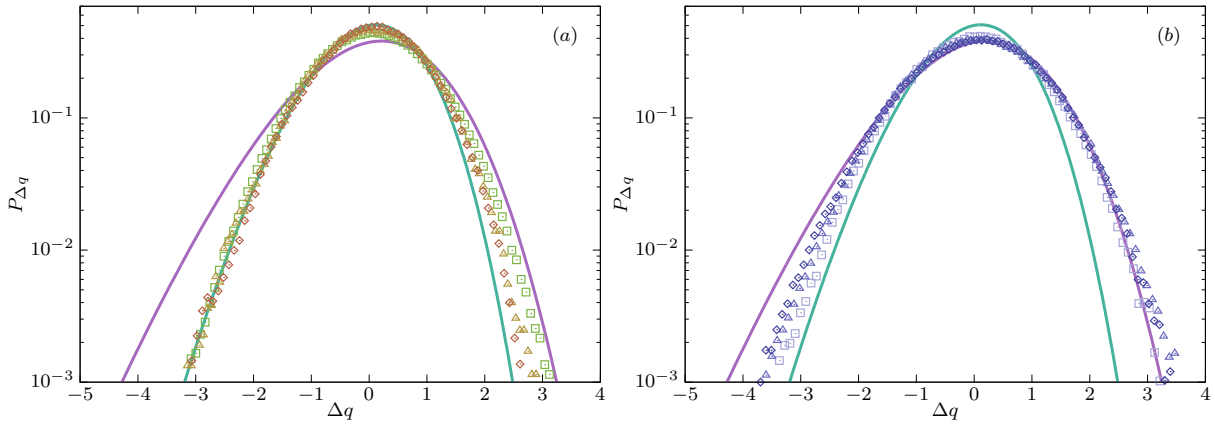

Figure 4.8: (Color online) Full distribution of Δq for different sample sizes $L = 20, 50, 100$ μm (squares, triangles and rhombi respectively). Panel (a) corresponds to large $\Delta t/t_0$, where TW-GOE distribution is expected. The value of $\Delta t/t_0$ for each system size is $10, 50, 100$ respectively, chosen such that it belongs to the corresponding plateau on Fig. 4.7. The TW-GOE distribution is qualitatively well reproduced down to sizes of about 50μm. Panel (b) corresponds to small $\Delta t/t_0$, where the BR distribution is expected. The value of $\Delta t/t_0$ for each system size is $0.5, 0.2, 0.1$ respectively, again chosen on the corresponding plateaus in Fig. 4.7. A departure from the TW-GOE distribution and a crossover towards the BR one is observable down to 50 μm, although the latter is not attained. In these small systems, the finite size effects take over before the full transition to the stationary KPZ distribution is established.

To fully study this crossover, a larger system, of size about 1 mm is required.

4.4.3 Conclusions About Finite Size Effects

We find that advanced KPZ properties can still be observed in exciton-polaritons down to systems of size of the order of 50 μm. Clear signatures of KPZ physics are still observable in such small samples. We find that both the critical exponents, and the phase distribution of EP belong to KPZ universality class. The crossover to the BR distribution still occurs, but it is not fully realized in systems smaller than typically 1 mm, hindered by finite size effects.

4.5 Beyond Homogeneity

We here report some numerical results about the EP-KPZ mapping for the non homogeneous case analytically studied in Chapter 3.

4.5.1 EP Under Confinement

To well describe the confinement in the EP system we choose a smooth box, defined by a potential of the type $V(x) = |\mathcal{F}^{-1}[V(k)](x)|$ with $V_d(k) = V_0 e^{-p^2\ell^2}$. By changing ℓ this functional form interpolates between a flat potential ($\ell \to \infty$ limit) and hard-wall potential ($\ell \to 0$ limit), as we can see in Fig. 4.9. In Chap. 3.1.1 we discussed how the inclusion of a generic external potential $V(x)$ in the microscopic description of EP modifies the associated KPZ equation for the phase field. In the smooth box case the theoretical results for the inhomogeneous KPZ coefficients (3.15) indicate that the non-linearity is increased on the boundary. Quite interestingly the velocity of the propagation of the front is also proportional to the coefficient λ in the KPZ equation (2.34b): it thus increases at the boundary if ℓ is

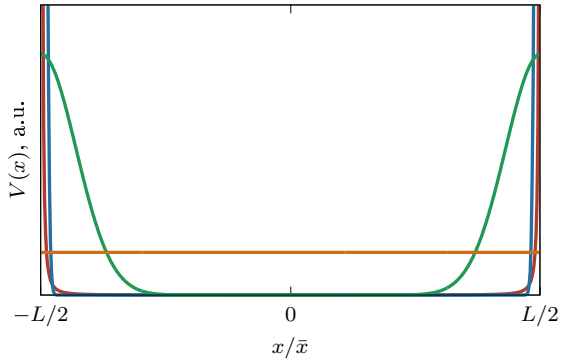

Figure 4.9: Different shapes of the potential $V(x)$ for different $\ell = 10^{-2}, 10^{-1}, 1, 10$ growing from steeper to flatter shape. We can see how this form of the external potential interpolates between a flat and a hard-wall potential; this change in the shape has non-trivial consequences for the phase-front dynamics.

decreased. This is exactly the scenario coming out from the numerical simulations: indeed, we see in Fig. 4.10 that in the case of a hard-wall potential the boundaries of the systems propagate much faster than the bulk.

Even if in the density the effect is confined at the boundaries and the bulk does not feel any effect of the confinement, in the phase dynamics, the fact that boundaries move much faster translates into an effective drag that eventually reaches also the bulk. If the confinement is steep enough, cusps appear in the phase front, leading to interesting physical behaviours; in the case of smooth confinement potential the front remains smooth even if the boundaries move faster than the bulk (see Fig. 4.10). The appearance or not of the cusps in the front leads to different dynamics. In order to get insights into the effects of the shape of the potential we look at the variance of the phase

$$\mathrm{Var}(\theta) = \langle \left(\theta - \langle\theta\rangle_\eta\right)^2 \rangle_\eta \,. \tag{4.12}$$

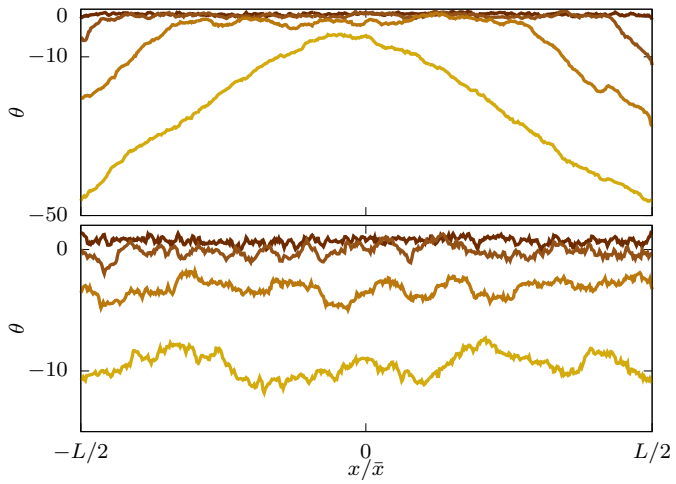

Figure 4.10: Evolution of the phase-front for different $\ell = 10^{-2}, 10$(upper and lower panel respectively) and different times $t/\bar{t} = 10, 100, 400, 1000$ (growing from top to bottom in each panel). We can see how the presence of a hard-wall potential influences the dynamics of the front by an effective drag on the boundary. It is worth noting the cusp in the upper panel propagating from the boundary to the bulk.

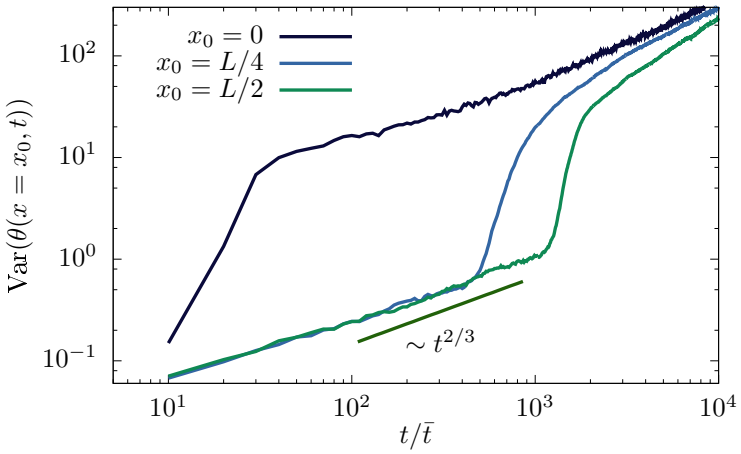

Figure 4.11: Variance of $\theta(x = x_0, t)$ for $L/\bar{x} = 2^9$ and different $x_0 = 0, L/4, L/2$ together with the theoretical prediction for KPZ behaviour. We see that the existence of KPZ scaling strongly depends on the distance from the wall at $x = 0$. Indeed the variance at $x_0 = 0$ never shows KPZ scaling because it suddenly feels the drag we can observe in Fig. 4.10. On the contrary the variance at the two different points $x_0 = L/4, L/2$ follows the KPZ scaling up to the time in which the cusp which develops in the front reaches the point under analysis. After this time the scaling differs from the KPZ one.

It is important to stress that due to spatial inhomogeneity we do not perform the average over space, but only over the stochastic noise η. The variance of the phase is expected to behave as $\mathrm{Var}(\theta) \sim t^{2/3}$ if the dynamics follows the KPZ one (see (1.48)). In Fig. 4.11 we focus on the hard wall case and look at how the variance behaves as we change the point in the front. When the cusp reaches the chosen point in the front, the variance suddenly deviates from the KPZ behaviour. In figure 4.12 we see that the system shows this power-law behaviour for a typical time-scale t^*, related to the typical length scale ℓ of the confining potential, which decreases by decreasing ℓ. This departure from KPZ

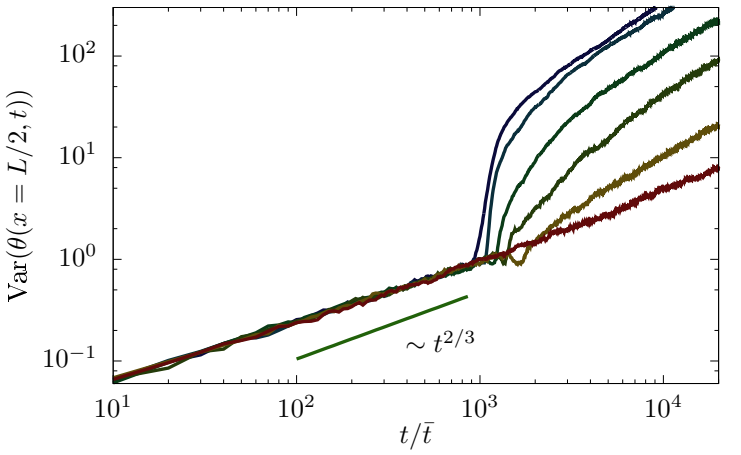

Figure 4.12: Variance of $\theta(x = L/2)$ for $L/\bar{x} = 2^9$ and different $\ell = 0.2, 0.5, 0.7, 1, 2, 10$ (growing from blue to red) together with the theoretical prediction for KPZ behaviour. We see that KPZ physics persists even under a confinement potential for a time-scale t^* which depends on the typical length-scale ℓ.

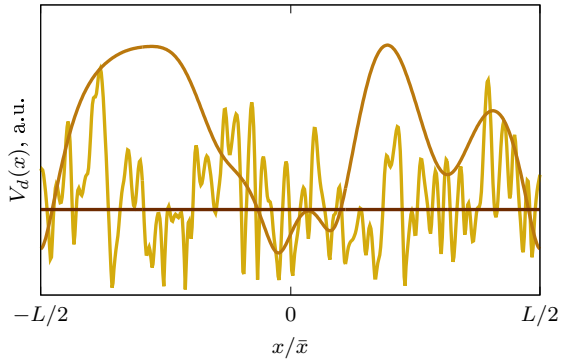

Figure 4.13: Different shape of the disorder for $\ell_d\hat{x} = 10^{-1}, 1, 10$ (increasing from lighter to darker); we can see how this form of the disorder interpolates between a white noise and a constant potential.

behaviour coincides indeed with the arrival of the cusp at the chosen space-point (here $x = 0$). After t^* we have a non-universal behaviour which resembles the typical departure from KPZ behaviour that we have observed in the homogeneous case, and that are linked to finite-size effects.

4.5.2 EP with Disorder

We finally perform a study of the effects of a smooth static disorder with correlation length ℓ_d. A choice for the functional form of the disorder potential which is relevant for experiments is to take $V_d(x) = |\mathcal{F}^{-1}[V_d(k)](x)|$ with $\langle V_d(x)V_d(x')\rangle = G(x - x')$, $V_d(k) = V_0 e^{i\varphi} e^{-p^2\ell_d^2}$ and φ a uniformly distributed random variable in the range $[0, 2\pi)$; V_0 here is chosen such that the strength of the disorder is smaller or comparable with the other energy scales in the gGPE. By changing the correlation length, this

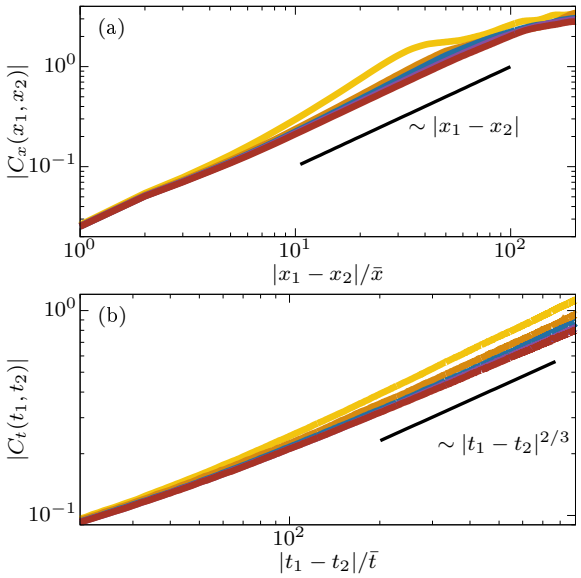

Figure 4.14: Power-law behaviour of the (*a*) space- and (*b*) time-correlation functions for $L = 2^9$ and different $\ell_d\hat{x} = 10^{-1}, 1, 2, 2.5, 3$ (increasing from lighter to darker). Both correlations are close to the theoretical predictions for KPZ dynamics (solid-black lines).

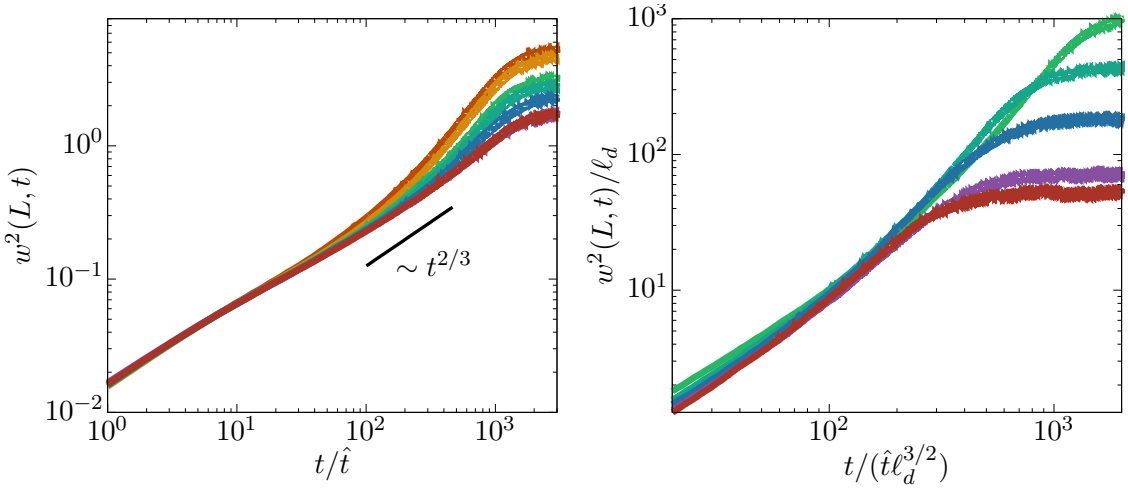

Figure 4.15: (Left) behaviour of the roughness w^2 for $L = 2^9$ and different $\ell_d = 0.1, 0.5, 1, 1.5, 2, 2.5, 3$ (growing from lighter to darker). We see a departure from KPZ scaling happening on a time-scale t^* which depends on ℓ_d. (Right) Collapse of the roughness under re-scaling using KPZ exponents; we clearly see that $t^* \sim \ell_d^{3/2}$. This is a further indication of KPZ dynamics in the system at $t < t^*$.

describes any intermediate condition between a uniform potential for $\ell_d \to \infty$ to a white-noise disorder in the $\ell_d \to 0$ limit; for a finite $\ell_d \simeq L/10$, with L the system size, we obtain a shape close to the real disorder present in experiments (see Fig. 4.13). As discussed in Chap. 3.1.2 such a disorder should result in a non-local shift in the KPZ noise related to the correlation of the disorder itself. We chose a disorder with spatial correlation of finite typical length ℓ_d. In this case Galilean invariance is not broken and we expect the main features of KPZ universality to be preserved with some interesting effects due to the presence of a new length scale in the system. This prediction is confirmed by numerical simulations. Both the roughness and the space- and time-correlation follow the KPZ scaling as we can see in Fig. 4.14, 4.15; the flatter is the potential the better is the agreement with KPZ predictions. Interestingly, we have a further confirmation of the underlying KPZ physics by looking in more detail at the roughness function, which is quite sensitive to the different length-scale present in the system. As shown in Fig. 4.15, we can find the KPZ power-law behaviour on a typical time-scale which depends on the correlation

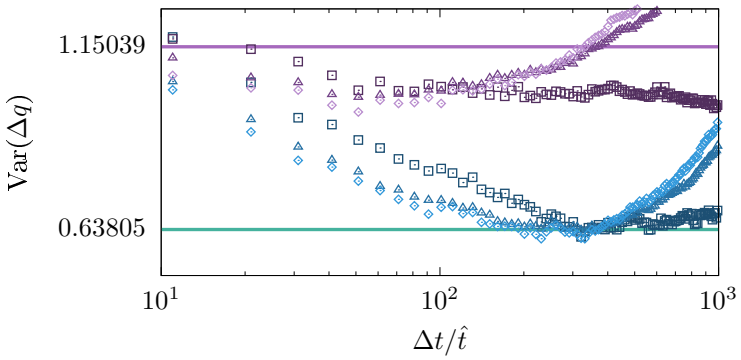

Figure 4.16: Numerical and theoretical values for $\mathrm{Var}(\Delta q)$ for different disorder correlation lengths $\ell_d/L = 0.02, 0.07, 0.15$ (from lighter to darker) for $\Delta t/t_0 \simeq 10^2$ (blue symbols) and $\Delta t/t_0 \simeq 10^{-1}$ (purple symbols), with $L/\bar{x} = 2^{10}$. The solid lines correspond to TW-GOE (cyan) and BR (violet) theoretical prediction.

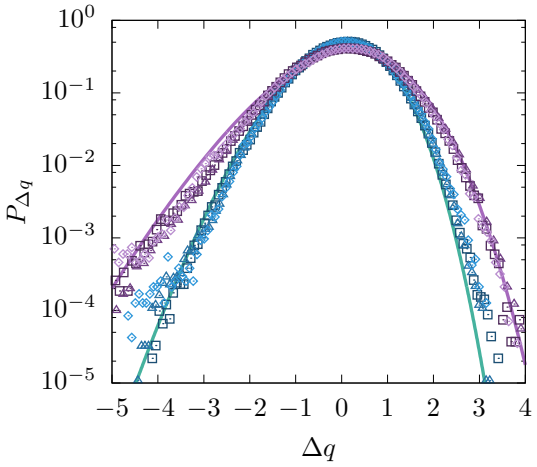

Figure 4.17: Distribution of $\Delta q(x, t_0, \Delta t)$ for different disorder correlation lengths $\ell_d/L = 0.02, 0.07, 0.15$ (from lighter to darker) for $\Delta t/t_0 \simeq 10^2$ (blue symbols) and $\Delta t/t_0 \simeq 10^{-1}$ (purple symbols), with $L/\bar{x} = 2^{10}$. The solid lines correspond to centred TW-GOE (cyan) and BR (violet) theoretical distributions.

length of the disorder. This is expected in a self-critical system out-of-equilibrium, where the presence of a length scale implies the existence of an associated time-scale; the relation between the two is *via* the dynamical exponent z. If KPZ physics is present in the system we expect this relation to be $t^* \sim \ell_d^z$ with $z = 3/2$; this is indeed the case, as we can see in the right panel of Fig. 4.15. We hence expect that for $t < t_d$, KPZ physics is still observable, while for $t > t_d$ the features of the disorder become dominant. Furthermore we expect the departure point to collapse if the time is rescaled by t^*. As we can see in Fig. 4.15 this is indeed the case. Besides the scaling of the correlations, we determined the distribution of the variable Δq, in both regimes of large and small $\Delta t/t_0$. The results, presented in Fig. 4.16 and 4.17, show that for large $\Delta t/t_0$, the TW-GOE distribution is still accurately reproduced. Increasing t_0, the approach to the BR distribution is also clearly visible, even if it cannot be fully attained, since t_0 is limited to t_d by the presence of the disorder.

4.6 Conclusions

In this chapter we showed that the phase dynamics of an out-of-equilibrium condensate of EP under experimental realistic conditions shows advanced properties of the KPZ equation. In the intermediate-time regime, the probability distribution of the rescaled phase follows the TW-GOE distribution, that is the one for KPZ height field with flat initial conditions. When the size of the correlations becomes comparable with the size of the system, the TW-GOE distribution changes into the BR distribution, that is the one for KPZ height field with stationary initial condition. This cross-over is in analogy with the results found in turbulent liquid-crystal experiments [51]. We then analysed the influence of finite-size effects and we found that a good agreement with KPZ scaling persists down to system sizes around 50μm. The KPZ properties are robust with respect to the presence of inhomogeneities in the system, such as an external potential, disorder and thermally activated phonons. For the first two cases we showed numerically that the temporal and spatial correlations still follow the KPZ scaling, notwithstanding the appearance of non-trivial effects. In the presence of random disorder we also showed that both the TW-GOE distribution for the rescaled phase and the TW-GOE to BR crossover when stationarity is approached, are preserved when averaging over the disorder.

5 Kardar-Parisi-Zhang Equation with Temporally Correlated Noise

In this chapter we investigate the universal behaviour of the Kardar-Parisi-Zhang equation with temporally correlated noise. The presence of time correlations in the microscopic noise breaks the statistical tilt symmetry, or Galilean invariance, of the original KPZ equation with delta-correlated noise (denoted SR-KPZ), and conflicting results exist concerning whether the KPZ universality class is preserved even in the limit of short-range time correlations. Using NPRG techniques, we study the influence of two types of temporal noise correlator: a short range one with a typical time-scale τ, and a power-law one with a varying exponent θ in both $d = 1$ and $d = 2$ dimensions. While the results in $d = 1$ can be compared to previous estimates, no other prediction was available in $d = 2$ dimension.

5.1 KPZ Equation with non-delta Correlation in the Noise

The noise η in the original KPZ equation (1.13) discussed in Chap. 1 is usually taken as delta correlated in both time and space,

$$\left\langle \eta(\mathbf{x})\eta(\mathbf{x}')\right\rangle = \delta(\mathbf{x}-\mathbf{x}'). \tag{5.1}$$

Such delta correlations of the noise are an idealization, as it is not likely to be realized in real physical systems. This raises the natural question of the robustness of the KPZ properties with respect to the presence of some microscopic correlations in the stochastic process driving the growth. This question was first investigated by Medina *et al.* [93], who considered the more general form of noise correlator

$$\langle \eta(t,\vec{x})\eta(t',\vec{x}')\rangle = 2D(|\vec{x}-\vec{x}'|, t-t') \tag{5.2}$$

with long-range (LR) power-law correlations, defined in the Fourier space as

$$D_\infty(\omega,\vec{q}) = D_0 + D_\theta q^{-2\rho}\omega^{-2\theta}\,. \tag{5.3}$$

In this chapter we also consider short range (SR) temporal correlations of the form

$$D_\tau(\omega,\vec{q}) = e^{-\frac{1}{2}\omega^2\tau^2}\,. \tag{5.4}$$

These modifications of the noise structure break the integrability of the original KPZ equation with delta correlation, which will be referred to as SR-KPZ. The effect of spatially correlated noise has been thoroughly investigated, both analytically and numerically [94, 95, 96, 97, 98, 99, 100, 101, 102, 103, 104, 105, 106, 107, 86]. It was shown that for a SR enough noise, *i.e.* $\rho < \rho_c$, the standard SR-KPZ properties are preserved, while beyond ρ_c, a LR phase with ρ-dependent critical exponents emerges. For a noise with some finite correlation length ξ, it was shown for one-dimensional interface that the time-reversal symmetry, which is broken by such correlations, is restored at large distance, and thus one also finds SR-KPZ physics [87]. In contrast, temporally correlated noise has received much less attention. The few existing analytical [93, 108, 109, 53, 110] and numerical [111, 112] studies yield conflicting results, summarized below. One of the reasons is that, as discussed in Chap. 1.3.1, the presence of temporal

correlations is much more severe, in that it breaks the Galilean symmetry (1.40). Thus it is not clear a priori whether even an infinitesimal amount of time-correlation destroys or not KPZ physics, and both answers have been given. Let us summarize these results.

5.1.1 Temporally correlated noise: state of the art

The problem of temporal correlation of the noise was first investigated using dynamical RG by Medina *et al.*, focusing on $d = 1$ [93]. They found that the SR-KPZ fixed point is stable up to a threshold value $\theta_c = 1/6$, and thus for $\theta \leq \theta_c$, the critical exponents are the standard SR ones $z_{\rm SR} = 3/2$ and $\chi_{\rm SR} = 1/2$ in $d = 1$. Above the threshold, they determined from the one-loop flow equations an approximate expression of the critical exponents

$$\chi_{\rm LR} = \frac{1+4\theta}{3+2\theta} \quad , \qquad z_{\rm LR} = 2 - \chi_{\rm LR} \, , \tag{5.5}$$

obtained by neglecting the corrections to the effective non-linearity induced by the violations of Galilean invariance related to the temporal correlations. This expression is thus only valid for small θ close to the threshold. Indeed, the exact relation $\chi_{\rm SR} + z_{\rm SR} = 2$ stemming from Galilean invariance only holds at the SR fixed point, and is replaced at the LR fixed point by the exact relation

$$z_{\rm LR}(1+2\theta) - 2\chi_{\rm LR} - 1 = 0 \, , \tag{5.6}$$

which is violated by the estimate (5.5). The authors then solved numerically a truncated system of flow equations which led to critical exponents, that could be fitted by

$$\chi_{\rm LR} = 1.69\theta + 0.22 \quad , \qquad z_{\rm LR} = \frac{2\chi_{\rm LR}+1}{1+2\theta} \, . \tag{5.7}$$

At variance with this scenario, Ma and Ma [108] advocated on the basis of a Flory-type scaling argument a smooth variation of the critical exponents as functions of θ, with no threshold, following

$$\chi_{\rm LR} = \frac{2+4\theta}{2\theta+d+3} \quad , \qquad z_{\rm LR} = \frac{2d+4}{d+3+2\theta} \, , \tag{5.8}$$

such that the SR-KPZ exponents are only preserved at $\theta = 0$. This alternative scenario was supported by a Self-Consistent Expansion (SCE) developed by Katzav and Schwartz [109]. The authors found within the SCE two strong-coupling solutions, one which coincides with the one-loop DRG result, and the other, considered as dominant, which leads to a smooth dependence on θ with no threshold, but with a decreasing $z_{\rm LR}(\theta)$, whereas the solution (5.7) is increasing. The problem was re-visited using perturbative Functional Renormalization Group (FRG) within the framework of elastic manifolds in correlated disorder [53]. In this context, a crossover from a SR behaviour to a LR one beyond a certain threshold was confirmed. The two-loop LR exponents were calculated in a perturbative expansion in $\epsilon = 4 - d$ where d is the dimension of the elastic manifold. However, the KPZ interface is equivalent to a $d = 1$ directed polymer, which implies $\epsilon = 3$, and the extrapolation to such a large value is not reliable. Notwithstanding this limitation, the two-loop results indicate a decreasing $z_{\rm LR}$ for small θ, at variance with (5.7). Based on a stability criterion, the author also derives bounds for the value of $z_{\rm LR}$ as

$$\frac{5}{3+2\theta} \leq z_{\rm LR} \leq \frac{3}{2} \tag{5.9}$$

where the lower bound coincides with the one-loop result (5.5). This bound rules out both the second SCE solution and the scaling solution. On the analytical side, the situation is thus unclear. Moreover,

the very few existing numerical simulations can not convincingly discriminate between the two scenarii (presence or absence of a threshold) nor on the sense of variation of $z_{\rm LR}$ [111]. They essentially find a very weak dependence at small θ and are too scattered to settle whether $z_{\rm LR}$ is decreasing or increasing. Note that the effect of temporal correlation is also crucial in the context of turbulence. In particular, field theoretical approaches are constructed from Navier-Stokes equation with a stochastic forcing, which is delta-correlated in time to preserve Galilean invariance. The presence of temporal correlation in the forcing correlator was investigated in [113], and support the robustness of the SR properties below a threshold value.

5.2 NPRG approach to KPZ equation

In the following, we analyse the effect of temporal correlation of the noise in the framework of the Non-Perturbative Renormalization Group (NPRG). Indeed, this method has turned out to be successful to describe KPZ interfaces since the NPRG flow equations embed the strong-coupling fixed point in any dimensions [114], whereas the latter cannot be reached at any order from perturbative expansions [39]. Moreover, a controlled approximation scheme, based on symmetries, can be devised in this framework [23, 115]. It was shown that it reproduces with extreme accuracy the exact results in $d = 1$ for the scaling function [23]. It yielded predictions for dimensionless ratios for $d = 2$ and 3 [115] which were later accurately confirmed by large-scale numerical simulations [116, 117]. This framework was extended to study anisotropy [118], and also spatial correlations in the noise, following a power-law [86] or with a finite length-scale [87].

5.2.1 Non-Perturbative Renormalization Group formalism

We here give a basic introduction to NPRG in order to understand the results we will derive in the main part of the chapter. A more technical introduction is given in App. E. Integrating out microscopic fluctuations is the key ingredient to understand the long-distance universal properties of a physical system. The NPRG is a modern implementation of Wilson's original idea of the RG [6], conceived to efficiently average over fluctuations, even when they develop at all scales, as in standard critical phenomena [119]. The progressive integration of fluctuation modes is achieved by introducing in the KPZ action a scale-dependent quadratic term

$$\Delta\mathcal{S}_\kappa = \frac{1}{2}\int_{\omega,\vec{q}} \phi_i(\omega,\vec{q})[R_\kappa(\omega,\vec{q})]_{i,j}\phi_j(-\omega,-\vec{q}) \tag{5.10}$$

where κ is a momentum scale, and $\phi_1 \equiv h$, $\phi_2 \equiv \tilde{h}$. The matrix elements of R_κ are proportional to a cutoff function $r(q^2/\kappa^2)$, with $q = |\vec{q}|$, which ensures the selection of fluctuation modes: $r(x)$ is required to be large for $x \lesssim 1$ such that the fluctuation modes $\phi_i(q \lesssim \kappa)$ are essentially frozen and do not contribute in the path integral, and to be negligible for $x \gtrsim 1$ such that the other modes ($\phi_i(q \gtrsim \kappa)$) are not affected. $\Delta\mathcal{S}_\kappa$ must preserve the symmetries of the original action and causality properties. For the KPZ field theory, a suitable form is [114]

$$R_\kappa(\omega,\vec{q}) \equiv R_\kappa(\vec{q}) = r\left(\frac{q^2}{\kappa^2}\right)\begin{pmatrix} 0 & \nu_\kappa q^2 \\ \nu_\kappa q^2 & -2D_\kappa \end{pmatrix}, \tag{5.11}$$

where the running coefficients ν_κ and D_κ are defined later. Here we work with the cutoff function

$$r(x) = \alpha/(\exp(x) - 1), \tag{5.12}$$

where α is a free parameter whose rôle is discussed in E. We emphasize that the regulator (5.11) does not depend on frequency. Whereas it would be desirable to also regulate in frequency, it is much simpler not to, and it is the actual choice made in most applications to non-equilibrium systems [120, 23]. It turns out that for most applications, regularizing in momentum is enough to ensure the analyticity of the Effective Average Action (EAA). The implementation of a frequency regularization was studied in [121] on the example of Model A, where it was shown that it does improve the results. However, the difficulty lies in formulating a regulator which respects both causality and all the symmetries of the model. For KPZ, the Galilean invariance precludes from having a (manageable) frequency-dependent regulator. This has implications for the study of the power-law correlator D_∞ in (5.3), since it brings non-analyticities in ω which would be cured (as they should) by a frequency regularization, whereas with only a momentum regulator they will survive and have be dealt with. The inclusion of $\Delta\mathcal{S}_\kappa$ in (1.37) leads to a scale-dependent generating functional $\mathcal{Z}_\kappa$. Field expectation values in the presence of the external sources j and $\tilde{j}$ are obtained from the functional $\mathcal{W}_\kappa = \log \mathcal{Z}_\kappa$ as

$$\psi(\mathbf{x}) = \langle h(\mathbf{x})\rangle = \frac{\delta \mathcal{W}_\kappa}{\delta j(\mathbf{x})} \ , \ \tilde{\psi}(\mathbf{x}) = \langle \tilde{h}(\mathbf{x})\rangle = \frac{\delta \mathcal{W}_\kappa}{\delta \tilde{j}(\mathbf{x})}. \tag{5.13}$$

The EAA is defined as the modified Legendre transform of $\mathcal{W}_\kappa$ as

$$\Gamma_\kappa[\psi,\tilde{\psi}] + \mathcal{W}_\kappa[j,\tilde{j}] = \int j_i \varphi_i - \frac{1}{2}\int \varphi_i \,[R_\kappa]_{ij}\, \varphi_j. \tag{5.14}$$

where j_i are the sources associated with the fields φ_i, with $\varphi_1 = \psi$, $\varphi_2 = \tilde{\psi}$. The scale-dependent EAA obeys an exact flow equation, usually referred to as Wetterich equation [20] (see App. E for the derivation):

$$\partial_s \Gamma_\kappa = \frac{1}{2}\mathrm{Tr}\left\{\partial_s R_\kappa \left[\Gamma_\kappa^{(2)} + R_\kappa\right]^{-1}\right\} \tag{5.15}$$

where

$$[\Gamma_\kappa^{(2)}]_{i,j} = \frac{\delta^2 \Gamma_\kappa[\{\varphi\}]}{\delta\varphi_i\, \delta\varphi_j} \tag{5.16}$$

and $\mathrm{Tr}\{\cdot\}$ is the trace over all the internal degrees of freedom. Even though the equation (5.15) is exact, it cannot be solved exactly because of its non-linear functional integro-differential structure. One has to employ some approximation scheme [122]. The key advantage of this approach is that these approximations do not have to be perturbative in the couplings or in the dimensions, but they are rather based on some controlled truncation of the functional space. The most common approximation scheme within the NPRG framework is the Derivative Expansion (DE), which consists in expanding the EAA in powers of the gradients and time derivatives of the fields. However, due to the derivative nature of the KPZ interaction, this approximation is not enough to obtain quantitative results, as we show in Chap. 5.2.3. The approximation scheme appropriate for the KPZ equation is inspired by another common approximated scheme called Blaizot-Mendez-Wschebor scheme [123], but adapted to preserve the KPZ symmetry. Its rationale is expounded in details in [23, 115]. It can be implemented using an Ansatz for the EAA, which is presented in the following.

5.2.2 The Local Potential Approximation

Let us first present the simplest possible approximation scheme for the EAA, which is the lowest order of the DE, that is called Local Potential Approximation (LPA). This approximation is already very useful

to study many equilibrium problems, as well as in some non-equilibrium ones such as reaction-diffusion systems, where focusing on the zero momentum and frequency sector is enough to obtain satisfactory results [119]. In the well-known case of the Ising model, this approximation reads

$$\Gamma_{k,LPA}[M] = \int_{\vec{x}} \left(U_k(M) + (\vec{\nabla} M)^2 \right) , \tag{5.17}$$

where $M \equiv M(\vec{x})$ is the magnetization field and U_k is the effective potential. It contains only $\mathbb{Z}_2$ invariant terms, *i.e.* in principle all the even power of the magnetization. If we expand this effective potential at quartic order,

$$U_k(M) = g_{2,k} M^2 + g_{4,k} M^4 , \tag{5.18}$$

the Wetterich equation becomes just a set of ordinary differential equation for the couplings kept in the ansatz,

$$\partial_s g_{n,k} = \beta_{n,k}(\{g_{m,k}\}) . \tag{5.19}$$

A more refined approximation, referred to as LPA', also includes the field renormalization, Z_k

$$\Gamma_{k,LPA'}[M] = \int_{\vec{x}} \left(U_k(M) + Z_k(M)(\vec{\nabla} M)^2 \right) . \tag{5.20}$$

The LPA can be generalized by including higher order terms in the DE. This procedure has been systematically implemented for the Ising model up to the sixth order, yielding extremely accurate results compatible with the conformal bootstrap ones [124]. Furthermore, in the same paper, it was shown that the DE has a finite radius of convergence and hence it is a controlled approximation scheme.

5.2.3 LPA Aprroximation for the KPZ Equation

After a brief introduction to the LPA scheme, it is instructive to derive the results one can get for the KPZ equation using such an approximation in the NPRG ansatz. At LPA level, the simplest ansatz for the KPZ EAA reads

$$\begin{aligned} \Gamma_{k,LPA}[\varphi, \tilde{\varphi}] &= \int_{\mathbf{q}} \tilde{\varphi} \left(\partial_t \varphi - \nu_k \nabla^2 \varphi - \lambda_k |\vec{\nabla} \varphi|^2 \right) - D_k \tilde{\varphi}^2 \\ &= \int_{\mathbf{q}} \tilde{\varphi} \left(\partial_t \varphi - \nabla^2 \varphi - \sqrt{g_k} |\vec{\nabla} \varphi|^2 \right) - \tilde{\varphi}^2 , \end{aligned} \tag{5.21}$$

where we introduced the usual effective non linearity $g_k = \lambda_k^2 D_k / \nu_k^3$ and we expanded the renormalization functions to lowest orders in the fields. Recalling (E.17) and (5.11), we end up with a propagator of the form

$$G_k(q) = \begin{pmatrix} \frac{2D_k(r(y)+1)}{q^4 \nu_k^2 (r(y)+1)^2 + \omega^2} & \frac{1}{q^2 \nu_k (r(y)+1) - i\omega} \\ \frac{1}{q^2 \nu_k (r(y)+1) + i\omega} & 0 \end{pmatrix} \tag{5.22}$$

with $y = \frac{q^2}{k^2}$. The flows of the couplings can be extracted from the 2- and 3-point functions, indeed

$$\Gamma_k^{(1,1)}(\mathbf{p}) = i\omega + \nu_k p^2, \quad \Gamma_k^{(0,2)}(\mathbf{p}) = -2D_k, \quad \Gamma_k^{(2,1)}(\mathbf{p}_1, \mathbf{p}_2) = \lambda_k \vec{p}_1 \cdot \vec{p}_2 \tag{5.23}$$

leading to

$$\kappa\partial_\kappa \nu_\kappa = \frac{1}{2p^2}\left[\kappa\partial_\kappa \Gamma_\kappa^{(1,1)}(\mathbf{p}) + \kappa\partial_\kappa \Gamma_\kappa^{(1,1)}(-\mathbf{p})\right]_{RP} \tag{5.24a}$$

$$\kappa\partial_\kappa D_\kappa = -2\kappa\partial_\kappa \Gamma_\kappa^{(0,2)}(\mathbf{p})\Big|_{RP} \tag{5.24b}$$

$$\kappa\partial_\kappa \lambda_\kappa = \frac{1}{p^2}\kappa\partial_\kappa \Gamma_\kappa^{(2,1)}(\mathbf{p},\mathbf{p})\Big|_{RP} \tag{5.24c}$$

where $RP = (0,0)$ in what follows. By explicitly computing (E.21), (E.22) using the ansatz (5.21) we get

$$\begin{aligned}\frac{\kappa\partial_\kappa \nu_\kappa}{\nu_\kappa} =& -2g_\kappa \int_{\mathbf{q}} \frac{y}{\kappa^4 \nu_\kappa P(\hat\omega^2, y)^3}\left\{\partial_y r_\kappa^D(y)\cos^2(\psi)\left(\ell(y)\left(P(\hat\omega^2,y) - 4\hat\omega^2\right) + 2y^2 r'(y) X(\hat\omega^2, y)\right)\right.\\ &\left. -\partial_y r_\kappa^\nu(y)\left(\ell(y)\left(\sin^2(\psi)P(\hat\omega^2,y) - 2\hat\omega^2\right) + 2y^2\cos^2(\psi) r'(y) X(\hat\omega^2,y)\right)\right\}\end{aligned} \tag{5.25a}$$

$$\frac{\kappa\partial_\kappa D_\kappa}{D_\kappa} = 2g_\kappa \int_{\mathbf{q}} \frac{y\,\ell(y)}{\kappa^4 \nu_\kappa P(\hat\omega^2,y)^3}\left[\partial_y r_\kappa^D(y) P(\hat\omega^2,y) - 2\partial_y r_\kappa^\nu(y)\ell(y)^2\right] \tag{5.25b}$$

$$\begin{aligned}\frac{\kappa\partial_\kappa \lambda_\kappa}{\lambda_\kappa} =& -2g_\kappa \int_{\mathbf{q}} \frac{y^2}{k^4 \nu_\kappa P(\hat\omega^2,y)^4}\cos^2(\psi)\left\{\partial_y r_\kappa^D(y) P(\hat\omega^2,y)\left[P(\hat\omega^2,y) - 4\hat\omega^2\right]\right.\\ &\left. -4\partial_y r_\kappa^\nu(y)\ell(y)^2\left[P(\hat\omega^2,y) - 6\hat\omega^2\right]\right\}\end{aligned} \tag{5.25c}$$

with $\ell(y) = y(1 + r(y))$, $X(\hat\omega^2, y) = -\hat\omega^2 + \ell(y)^2$ and $P(\hat\omega^2, y) = \hat\omega^2 + \ell(y)^2$. Because of the polynomial behaviour in ω of the integrand, all the integrals above can be calculated analytically in the frequency sectors. Using (5.60) and (5.62), we get

$$\frac{\kappa\partial_\kappa \nu_\kappa}{\nu_\kappa} = \frac{K_d}{8d} g_\kappa \kappa^{d-2}\int_0^\infty \frac{y^{\frac{d}{2}}}{\ell(y)^3}\left\{\partial_y r_\kappa^\nu(y)\left[(d-2)\ell(y) + 2y^2 r'(y)\right] - 2y^2\partial_y r_\kappa^D(y) r'(y)\right\} \tag{5.26a}$$

$$\frac{\kappa\partial_\kappa D_\kappa}{D_\kappa} = \frac{K_d}{8} g_\kappa k^{d-2}\int_0^\infty \mathrm{d}y\,\frac{y^{d/2}}{\ell(y)^2}\left[2\partial_y r_\kappa^D(y) - 3\partial_y r_\kappa^\nu(y)\right] \tag{5.26b}$$

$$\frac{\kappa\partial_\kappa \lambda_\kappa}{\lambda_\kappa} = 0 \tag{5.26c}$$

Recalling that $\hat g_\kappa = \kappa^{d-2} g_\kappa = \kappa^{d-2}\lambda_\kappa^2 D_\kappa/\nu_\kappa^3$ we obtain a flow for the dimensionless coupling $\hat g_\kappa$ of the type

$$\frac{\kappa\partial_\kappa \hat g\kappa}{\hat g_\kappa} = d - 2 + \frac{K_d}{4d} g_\kappa k^{d-2}\int_0^\infty \mathrm{d}y\,\frac{y^{d/2}}{\ell(y)^3}\left\{\partial_y r_\kappa^D(y)\left[d\,\ell(y) + 3y^2 r'(y)\right] - 3\partial_y r_\kappa^\nu(y)\left[(d-1)\ell(y) + y^2 r'(y)\right]\right\} \tag{5.27}$$

It is interesting to explicit $\partial_y r_\kappa^X(y)$,

$$\partial_y r_\kappa^X(y) = -\left(\eta_\kappa^X + 2y\partial_y r(y)\right), \tag{5.28}$$

where $\eta_\kappa^X = -\partial_s \ln X_\kappa$ is the running scaling dimension of X_κ. This quantity measures the difference between the full and the canonical (or engineering) dimension of X_κ at a given fixed point, and is zero

at the non-interacting fixed point (see App. E.2.2 for the relation between η_κ^X and the critical exponent). We thus have

$$\begin{aligned}\frac{\kappa\partial_\kappa\hat{g}_\kappa}{\hat{g}_\kappa} =& d-2+K_d\hat{g}_\kappa\frac{2d-3}{2d}\int_0^\infty \mathrm{d}y\, y^{\frac{d}{2}-1}\frac{r'(y)}{(r(y)+1)^2}\\ &-\frac{\hat{g}_\kappa}{4d}\int_0^\infty \mathrm{d}y\,\frac{y^{\frac{d}{2}-2}r(y)}{(r(y)+1)^3}\left\{\eta_\kappa^D\left[dr(y)+d+3yr'(y)\right]-3\eta_\kappa^\nu\left[(d-1)(r(y)+1)+yr'(y)\right]\right\}.\end{aligned} \tag{5.29}$$

We see that thanks to the presence of η_κ^X, this equation not only is non-linear in $\hat{g}_\kappa$ but in principle recursively contains all its powers. Equations (5.26), (5.29) cannot be solved analytically for a generic $r(y)$; however there are particular choices which allow one to overcome this difficulty. In the following we will see two cases in which such equations can be solved analytically. First we will set $\eta_\kappa^X=0$; by doing so the flow of $\hat{g}$ becomes integrable in the proximity of $d=2$ for any form of the regulator. This procedure however, destroys the non-perturbative nature of the flow equations (5.26), (5.29) because the contributions of higher order terms in λ embodied in the η_κ^X is not present anymore. The second approach we will investigate is to keep the anomalous dimensions different from zero and to choose a particular form of the regulator $r(y)$.

Exact Integration around $d=2$

We see that after setting $\eta_\kappa^X=0$, Eq. (5.29) becomes integrable around $d=2$, that is the lower critical dimension of the model. Indeed we have

$$\frac{\kappa\partial_\kappa\hat{g}_\kappa}{\hat{g}_\kappa} = d-2+K_d\hat{g}_\kappa\frac{2d-3}{2d}\int_0^\infty \mathrm{d}y\,\frac{r'(y)}{(r(y)+1)^2} \tag{5.30}$$

Using (E.2) we get

$$\frac{\kappa\partial_\kappa\hat{g}_\kappa}{\hat{g}_\kappa} = d-2+\hat{g}_\kappa K_d\frac{3-2d}{2d} \tag{5.31}$$

which is exactly (1.34) obtained via DRG, recalling that the NPRG scale κ goes from Λ to 0, while the DRG scale ℓ goes from Λ to ∞, leading to an overall relative minus sign in the flows. As in the case presented in the main text, this flow suffer from divergences which prevent from reaching the strong-coupling KPZ fixed point.

Litim Regulator

As we saw in the previous section, around the lower critical dimension and setting the anomalous dimensions to zero, we can perform the analytical integration for any form of the regulator. However these calculations are possible only in $d=2$ and furthermore they are perturbative in λ. To overcome such restriction we can choose a particular form of the regulator and explore different dimensions, keeping the anomalous dimensions. Of course the results depend on the choice of the regulator once approximations are performed. A convenient choice is the Litim regulator, which allows to perform analytically the momentum integrals [125]. This regulator is,

$$R_{lit,\kappa} = q^2 r_{lit}(y) = (\kappa^2-q^2)\,\theta(q^2-\kappa^2) \tag{5.32}$$

with $r_{lit}(y)=(y^{-1}-1)\,\theta(1-y)$. Its usefulness in our model relies on the fact that one can extend the analytical calculations to any dimensions while keeping the anomalous dimensions, which ensures the

flow to be non-perturbative in the non-linearity. Using this form of the regulator in (5.26) and noting that

$$\partial_y r^X_{lit,\kappa}(y) = \frac{\partial_y X_\kappa r_{lit}(y)}{X_\kappa} = -\left[\eta^X_\kappa (y^{-1}-1) + 2y^{-2}\right]\theta(1-y) \tag{5.33}$$

we get

$$\frac{\kappa\partial_\kappa \nu_\kappa}{\nu_\kappa} = \hat{g}_\kappa K_d \left\{\frac{(d-2)}{2d^2} - \frac{1}{d^2(d+2)}\eta^D_\kappa - \frac{(d-4)}{2d^2(d+2)}\eta^\nu_\kappa\right\} \tag{5.34a}$$

$$\frac{\kappa\partial_\kappa D_\kappa}{D_\kappa} = -\hat{g}_\kappa K_d \left\{\frac{1}{2d} + \frac{1}{d(d+2)}\eta^D_\kappa - \frac{3}{2d(d+2)}\eta^\nu_\kappa\right\} \tag{5.34b}$$

$$\frac{\kappa\partial_\kappa \lambda_\kappa}{\lambda_\kappa} = 0 \tag{5.34c}$$

which give

$$\frac{\kappa\partial_\kappa \hat{g}_\kappa}{\hat{g}_\kappa} = d - 2 + \hat{g}_\kappa K_d \left\{\frac{(3-2d)}{d^2} - \frac{d-3}{d^2(d+2)}\eta^D_\kappa + \frac{3(d-2)}{d^2(d+2)}\eta^\nu_\kappa\right\} \tag{5.35}$$

We see that this form is more general than (5.31), which is recovered by setting $\eta^X_\kappa = 0$ in $d = 2$.

The Importance of Being Non-Perturbative

We can now compare the two approaches and see how being non perturbative is fundamental already at this level of approximation in the ansatz (5.21). As we briefly mentioned in the section above, the presence of the anomalous dimensions in the flow is very important in (5.34). Indeed η^D_κ, η^ν_κ are defined from the flow of D_κ and ν_κ respectively which themselves depend on η^X_κ and are linear in the coupling $\hat{g}_\kappa$. This recursive relation renders (5.34), (5.35) not analytically solvable but ensures that all the orders of $\hat{g}_\kappa$ to be taken into account, *i.e.* makes (5.34), (5.35) non-perturbative in the effective non-linearity. To see the effects of this non-perturbative nature of the flow , we can integrate numerically (5.34), (5.35) and compare the results with the perturbative ones $\eta^X_\kappa = 0$. The results are reported in Fig. 5.1. As we see, already with the Litim regulator we are able to discriminate between the non-interacting Gaussian fixed point and the strong-coupling KPZ fixed point in any dimension. We recall that at one-loop perturbative level, no strong-coupling fixed point is accessible. Even if the qualitative behaviour and the phase diagram are well reproduced within the LPA approximation, this scheme fails to give a quantitative reliable prediction of the critical exponents in $d \geq 2$ [126]. This is due to the derivative nature of the non-linearity, which asks for a full functional treatment of the momentum sector of the theory. In the following section we will see how this task can be accomplished with a field, rather than momentum, truncation.

5.2.4 Effective Average Action for the KPZ Equation: SO and NLO Schemes

In the original KPZ equation, a general ansatz for the EAA can be constructed using invariants under the symmetries listed in Chap. 1.3.1. In particular, for the Galilean symmetry, one can define a function $f(t,\vec{x})$ as a scalar density if its infinitesimal transform under (1.40) is $\delta f(t,\vec{x}) = \lambda\vec{v}(t)\cdot\vec{\nabla}f$, which implies that $\int d^d\vec{x} f$ is invariant under Galilean transformation. One can check that with this definition, he elementary Galilean scalar densities are $\tilde{\varphi}$, $\partial_i\partial_j\varphi$, and

$$D_t\varphi \equiv \partial_t\varphi - \frac{\lambda}{2}(\vec{\nabla}\varphi)^2\,, \tag{5.36}$$

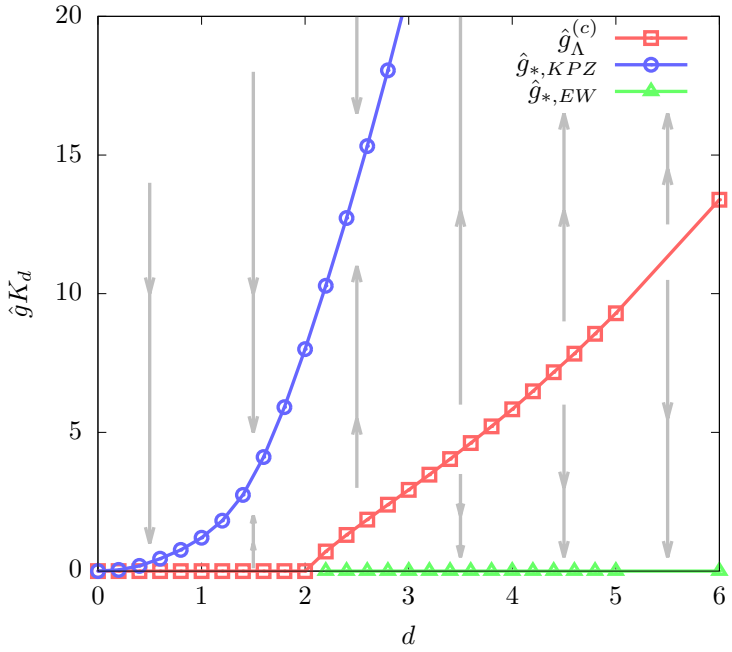

Figure 5.1: The phase diagram of KPZ equation at the level of LPA using Litim regulator. For $d > 2$ the basin of attraction of the strong-coupling KPZ fixed point $\hat{g}_* \neq 0$ (blue line with circles) is separated from the one of the EW fixed point $\hat{g}_* = 0$ (green line with triangles) by a line of critical values for the initial non-linearity $\hat{g}_\Lambda$ (red line with cubes). For $d \leq 2$ only the KPZ fixed point is present.

but not $\partial_t \varphi$ alone. The scalar property is preserved by the operator ∇ and by the covariant time derivative

$$\tilde{D}_t = \partial_t - \lambda \vec{\nabla}\varphi \cdot \vec{\nabla}\,, \tag{5.37}$$

but not the simple time derivative ∂_t. Using these building blocks, one can construct an ansatz which explicitly preserves Galilean symmetry. At quadratic order in the response field, the most general ansatz obtained this way, called SO, was first proposed in [127] and reads (see App. E.2.3 for a discussion on the relation between different approximations scheme for the KPZ ansatz):

$$\Gamma_\kappa[\varphi,\tilde{\varphi}] = \int_x \left\{ \tilde{\varphi} f_\kappa^\lambda(-\tilde{D}_t^2,-\nabla^2) D_t\varphi - \tilde{\varphi} f_\kappa^D(-\tilde{D}_t^2,-\nabla^2)\tilde{\varphi} - \frac{1}{2}\Big[\nabla^2\varphi f_\kappa^\nu(-\tilde{D}_t^2,-\nabla^2)\tilde{\varphi} + \tilde{\varphi} f_\kappa^\nu(-\tilde{D}_t^2,-\nabla^2)\nabla^2\varphi\Big]\right\} \tag{5.38}$$

with f^X analytic functions of their arguments defined as

$$f^X(-\tilde{D}_t^2,-\nabla^2) = \sum_{m,n=0}^{\infty} a_{mn}^X (-\tilde{D}_t^2)^m (-\nabla^2)^n \tag{5.39}$$

The microscopic KPZ action corresponds to the initial condition $f_\Lambda^\nu(\omega^2,p^2) = \nu$, $f_\Lambda^\lambda(\omega^2,p^2) = 1$ and $f_\Lambda^D(\omega^2,p^2) = D$. The constraints stemming from Galilean invariance are two-fold: first λ is not renormalized, which implies that the term proportional to $D_t\varphi$ renormalizes as a whole, with a unique function f_κ^λ in (5.38). The second constraint is that time derivatives only enter via the covariant time derivatives $\tilde{D}_t$. This constraint can be expressed on the vertices $\Gamma_\kappa^{(n)}$, under the form of exact Ward identities, which

relate a $\Gamma^{(n+1)}$ vertex with one vanishing momentum on a φ leg to a lower order vertex $\Gamma^{(n)}$ [23] (see App E). Furthermore, additional constraints stem from the other symmetries. The time-gauged shift symmetry (1.3.1) imposes that $f_\kappa^\lambda(\omega^2, p^2 = 0) = 1$ at all scale κ. In $d = 1$, the time-reversal symmetry further imposes that $f_\kappa^D = f_\kappa^\nu$, and $f_\kappa^\lambda = 1$, such that there is a single independent function in one dimension. The ansatz (5.38) truncates the functional dependence in $\tilde{\varphi}$ at quadratic order, but it remains functional in φ through the operators $\tilde{D}_t$. This ansatz provides a non-trivial frequency and momentum dependence for all vertices $\Gamma_\kappa^{(n)}$. This dependence is the most general one for the two point functions, but it is not for higher order vertices. It was shown in [23] that this ansatz yields very accurate results. It reproduces in particular to a very high precision level the exact result available in $d = 1$ for the scaling function associated with the two-point correlation function. However, solving the flow equations at SO represents quite a heavy numerical task in $d > 1$. Thus, a simplification was proposed in [115], which consists in neglecting the frequency dependence of the functions f_κ^X, in the integrands of the flow equation. This approximation, named NLO, allows one to explore higher spatial dimensions in a reasonable computational time. Indeed, at NLO, all the $n-$point functions $\Gamma_\kappa^{(n)}$, with $n > 2$, vanish except the bare one $\Gamma_\kappa^{(2,1)}$ (see App. E). The NLO approximation leads to reliable estimates for the exponents, and it enables one to determine non-trivial properties of the rough phase in $d > 1$, such as scaling functions, and associated universal amplitude ratio. This prediction was accurately confirmed by subsequent numerical simulations. Note that this approximation turns out to deteriorate when the dimension grows, and it becomes unreliable above $d \gtrsim 3.5$. Therefore it cannot be used for instance to probe the existence or not of an upper critical dimension, for which the full SO order should be implemented. In the following, we use the NLO approximation, extended to take into account possible breaking of both Galilean invariance and time reversal symmetry.

5.3 Effective average action with broken Galilean invariance: NLO$_\omega$ scheme

Introducing a non-trivial frequency dependence in the noise correlator breaks Galilean invariance at the microscopic level. This means that the constraints associated with this symmetry no longer apply. In particular, the non-linear coupling acquires a non-trivial RG flow $\lambda \equiv \lambda_k$. As a consequence, the two terms of $D_t\varphi$ are renormalized independently, such that one is led to introduce two independent functions as follows

$$f_\kappa^\lambda \, D_t\varphi \to f_\kappa^t \, \partial_t\varphi - \frac{\lambda}{2} f_\kappa^\lambda \, (\vec{\nabla}\varphi)^2 \, . \tag{5.40}$$

On the other hand, to take into account analytical temporal correlations in the noise, such as the SR case (5.4), at the microscopic level, we need to implement a time-dependence in the initial conditions for f^D. Keeping the full dependence on the covariant time derivative, as prescribed by the SO approximation, would lead to flow equations which, at the moment, are not treatable in a reasonable amount of time at the numerical level. To overcome this difficulty we replace the covariant time derivative by a simple time derivative in the argument of the running functions f_κ^X:

$$f_\kappa^X(-\tilde{D}_t^2, -\nabla^2) \to f_\kappa^X(-\partial_t^2, -\nabla^2) \, . \tag{5.41}$$

This in turn implies that the functions f_κ^X no longer depend on the field φ, which results in a truncation at quadratic order in φ also (see App. F for more technical details). On the other hand, in order to take into account the temporal correlation of the noise, one has to treat the full time-dependence of the functions f_κ^X, preserving it in the right-hand side of the flow equations as well, contrarily to the NLO approximation. It is important to note that this approximation scheme, termed NLO$_\omega$, does not preserve

the Galilean Invariance. Indeed, differently from the $\tilde{D}_t$ operator, the simple time derivative ∂_t does not generate scalars under Galilean transformation. We will see in the next section how this spurious breaking of GI affects the flow of the running non-linearity λ_κ. The NLO$_\omega$ ansatz reads

$$\Gamma_\kappa[\varphi,\tilde{\varphi}] = \int_{\mathbf{x}} \left\{ \tilde{\varphi} f_\kappa^t \partial_t \varphi - \frac{\lambda_\kappa}{2} \tilde{\varphi} f_\kappa^\lambda (\vec{\nabla}\varphi)^2 - \tilde{\varphi} f_\kappa^D \tilde{\varphi} - \frac{1}{2}\left[\nabla^2 \varphi f_\kappa^\nu \tilde{\varphi} + \tilde{\varphi} f_\kappa^\nu \nabla^2 \varphi \right] \right\} , \tag{5.42}$$

where all the functions f_κ^X depend on $(-\partial_t^2, -\vec{\nabla}^2)$. With this ansatz, the two-point functions are given by

$$\begin{aligned} \Gamma_\kappa^{(1,1)}(\omega,\vec{p}) &= i\omega f_\kappa^t(\omega^2,p^2) + p^2 f_\kappa^\nu(\omega^2,p^2) \\ \Gamma_\kappa^{(0,2)}(\omega,\vec{p}) &= -2 f_\kappa^D(\omega^2,p^2) \\ \Gamma_\kappa^{(2,0)}(\omega,\vec{p}) &= 0\,. \end{aligned} \tag{5.43}$$

As with the NLO ansatz, the only non-zero vertex function is the 3-point one $\Gamma_\kappa^{(2,1)}$, which reads

$$\Gamma_\kappa^{(2,1)}(\omega_1,\vec{p}_1,\omega_2,\vec{p}_2) = \lambda_\kappa \vec{p}_1\cdot\vec{p}_2 f_\kappa^\lambda((\omega_1+\omega_2)^2, |\vec{p}_1+\vec{p}_2|^2). \tag{5.44}$$

5.4 Flow equations and running anomalous dimensions

The flow equations for the running functions f_κ^ν, f_κ^t, respectively f_κ^D can be deduced from the flow equation of the two-point function $\Gamma_\kappa^{(1,1)}$, respectively $\Gamma_\kappa^{(0,2)}$. The calculations and the results are similar to those reported in [115]. We obtain

$$\partial_s f_\kappa^D(\bar{\omega}^2,p^2) = 2g f_\kappa^\lambda(\bar{\omega}^2,p^2)^2 \int_{\mathbf{q}} \frac{(\vec{q}\cdot\vec{Q})^2 k_\kappa(\Omega^2,Q^2)}{P_\kappa\left(\omega^2,q^2\right)^2 P_\kappa\left(\Omega^2,Q^2\right)} \left[\partial_s S_\kappa^D(q^2) P_\kappa(\omega^2,q^2) - 2q^2 \partial_s S_\kappa^\nu(q^2) k_\kappa(\omega^2,q^2)\ell_\kappa(\omega^2,q^2) \right] \tag{5.45a}$$

$$\begin{aligned} \partial_s f_\kappa^\nu(\bar{\omega}^2,p^2) =& 2g f_\kappa^\lambda(\bar{\omega}^2,p^2) \int_{\mathbf{q}} \frac{\vec{q}\cdot\vec{Q}}{p^2 P_\kappa(\omega^2,q^2)^2 P_\kappa(\Omega^2,Q^2)} \Big\{ \vec{q}\cdot\vec{p}\,\partial_s S_\kappa^D(q^2)\ell_\kappa(\Omega^2,Q^2) P_\kappa(\omega^2,q^2) f_\kappa^\lambda(\Omega^2,Q^2) \\ &+ q^2\,\partial_s S_\kappa^\nu(q^2)\Big[\vec{p}\cdot\vec{Q}\,k_\kappa(\Omega^2,Q^2) X_\kappa(\omega^2,q^2,\omega^2,q^2) f_\kappa^\lambda(\omega^2,q^2) \\ &- 2\,\vec{q}\cdot\vec{p}\,k_\kappa(\omega^2,q^2)\ell_\kappa(\omega^2,q^2)\ell_\kappa(\Omega^2,Q^2) f_\kappa^\lambda(\Omega^2,Q^2)\Big]\Big\} \end{aligned} \tag{5.45b}$$

$$\begin{aligned} \partial_s f_\kappa^t(\bar{\omega}^2,p^2) =& 2g f_\kappa^\lambda(\bar{\omega}^2,p^2) \int_{\mathbf{q}} \frac{\vec{q}\cdot\vec{Q}}{\omega P_\kappa(\omega^2,q^2)^2 P_\kappa(\Omega^2,Q^2)} \Big\{ -\Omega\,\vec{q}\cdot\vec{p}\,\partial_s S_\kappa^D(q^2) P_\kappa(\omega^2,q^2) f_\kappa^\lambda(\Omega^2,Q^2) f_\kappa^t(\Omega^2,Q^2) \\ &+ 2q^2 \partial_s S_\kappa^\nu(q^2)\ell_\kappa(\omega^2,q^2)\Big[\Omega\,\vec{q}\cdot\vec{p}\,k_\kappa(\omega^2,q^2) f_\kappa^\lambda(\Omega^2,Q^2) f_\kappa^t(\Omega^2,Q^2) \\ &+ \omega\,\vec{p}\cdot\vec{Q}\,k_\kappa(\Omega^2,Q^2) f_\kappa^\lambda(\omega^2,q^2) f_\kappa^t(\omega^2,q^2)\Big]\Big\} , \end{aligned} \tag{5.45c}$$

with

$$\ell_\kappa(\omega^2, q^2) = q^2\big[f^\nu_\kappa(\omega^2, q^2) + \nu_\kappa\, r(q^{\,2}/\kappa^2)\big], \tag{5.46a}$$
$$k_\kappa(\omega^2, q^2) = f^D_\kappa(\omega^2, q^2) + D_\kappa r(q^2/\kappa^2), \tag{5.46b}$$
$$P_\kappa(\omega^2, q^2) = \omega^2\, f^t_\kappa(\omega^2, q^2)^2 + \ell_\kappa(\omega^2, q^2)^2, \tag{5.46c}$$
$$X_\kappa(\bar\omega, p^2, \omega, q^2) = \ell_\kappa(\bar\omega^2, p^2)\ell_\kappa(\omega^2, q^2) - \bar\omega\omega f^t_\kappa(\bar\omega^2, p^2) f^t_\kappa(\omega^2, q^2), \tag{5.46d}$$
$$S^X_\kappa(q^2) = X_\kappa r(y)\ ,\ \ y = q^2/\kappa^2\ ,\ \ X \in \{D, \nu\}, \tag{5.46e}$$
$$\partial_s S^X_\kappa(y) = -X_\kappa\,(\eta^X_\kappa r(y) + 2y\,\partial_y r(y)) \tag{5.46f}$$

The additional running function $f^\lambda_\kappa(\bar\omega^2, p^2)$ can be defined from the 3-point vertex $\Gamma^{(2,1)}_\kappa$ as

$$f^\lambda_\kappa(\bar\omega^2, p^2) = \frac{4}{\lambda p^2}\Gamma^{(2,1)}_\kappa\left(\frac{\bar\omega}{2}, \frac{\vec p}{2}, \frac{\omega}{2}, \frac{\vec p}{2}\right)\ . \tag{5.47}$$

One introduces two scale-dependent coefficient ν_κ and D_κ, defined as

$$D_\kappa \equiv f^D_\kappa(0,0)\ , \qquad \nu_\kappa \equiv f^\nu_\kappa(0,0)\,, \tag{5.48}$$

which encompass the renormalization of the fields and the anomalous scaling between space and time. One defines two running anomalous dimensions associated with these coefficients

$$\eta^D_\kappa = -\kappa\partial_\kappa \ln D_\kappa\ , \qquad \eta^\nu_\kappa = -\kappa\partial_\kappa \ln \nu_\kappa\ . \tag{5.49}$$

Working with rescaled running functions and units,

$$\hat f^X_\kappa = \frac{f^X_\kappa}{X_\kappa}, \quad \hat p = \frac{p}{\kappa}, \quad \hat\omega = \frac{\bar\omega}{\nu_\kappa\kappa^2}\,, \tag{5.50}$$

the dimensionless flow equations take the form

$$\partial_s \hat f^X_\kappa(\hat{\bar\omega}^2, \hat p^2) = \left(\eta^X_\kappa + (2-\eta^\nu_\kappa)\hat\omega\partial_{\hat\omega} + \hat p\,\partial_{\hat p}\right)\hat f^X_\kappa(\hat{\bar\omega}^2, \hat p^2) + \hat I^X_\kappa(\hat{\bar\omega}^2, \hat p^2)\,, \tag{5.51}$$

with

$$\hat I^X_\kappa(\hat{\bar\omega}^2, \hat p^2) = \frac{1}{X_\kappa}\partial_s f^X_\kappa(\bar\omega^2, p^2). \tag{5.52}$$

One can show that the critical exponents can be expressed in terms of the fixed point values of the anomalous exponents (5.49) as (see App. E.2.2)

$$z = 2 - \eta^\nu_*\ , \qquad \chi = (2 - d + \eta^D_* - \eta^\nu_*)/2\,. \tag{5.53}$$

The shift-gauged symmetry is still valid in the presence of temporal correlations and imposes that $f^t_\kappa(0,0) = 1$. On the other hand, one can define a running non-linear coupling by fixing

$$f^\lambda_\kappa(0,0) = 1. \tag{5.54}$$

Let us denote its flow as

$$\kappa\partial_\kappa \ln\lambda_\kappa = -\eta^\lambda_\kappa. \tag{5.55}$$

One obtains that the flow of the dimensionless coupling $\hat{g}_\kappa$ is given by

$$\partial_s \hat{g}_k = \hat{g}_k \left(d - 2 - 2\eta_\kappa^\lambda + 3\eta_\kappa^\nu - \eta_\kappa^D \right) . \tag{5.56}$$

At a non-zero fixed point, this fixes

$$z + \chi - 2 = \eta_*^\lambda . \tag{5.57}$$

If Galilean symmetry is present, then $\eta_*^\lambda = 0$ and one recovers the standard relation $z + \chi = 2$. A non-zero η_*^λ quantifies the violation of Galilean invariance.

5.5 Flow of λ_κ in the NLO$_\omega$ scheme

As we discussed above, the NLO$_\omega$ scheme allows one to keep the full time dependence in the running functions at the price of an additional breaking of Galilean invariance. The effect of such a violation of the Galilean symmetry can be seen directly in the flow of the running non-linearity λ_κ. In a Galilean invariant system indeed we expect $\partial_s \lambda_\kappa = 0$, because it is the structure constant of the Galilean transformation. At NLO$_\omega$ level the flow of λ_κ, defined as

$$\partial_s \lambda_\kappa = \frac{4}{\lambda p^2} \partial_s \Gamma_\kappa^{(2,1)} \left(\frac{\omega}{2}, \frac{\vec{p}}{2}, \frac{\omega}{2}, \frac{\vec{p}}{2} \right) \Big|_{\omega=0, p=0} , \tag{5.58}$$

reads (see App. F for derivation)

$$\begin{aligned} \partial_s \lambda_\kappa = & - S_d \frac{2 g_\kappa}{d} \int_0^\infty \frac{\mathrm{d}q}{(2\pi)^d} \int_{-\infty}^\infty \frac{\mathrm{d}\omega}{2\pi} \frac{q^{d+3} f_\kappa^\lambda(\omega^2, q^2)^2}{P_\kappa(\omega^2, q^2)^4} \Big\{ \partial_s S_\kappa^D(q^2) P_\kappa(\omega^2, q^2) \\ & \times \left[P_\kappa(\omega^2, q^2) - 4\omega^2 f_\kappa^t(\omega^2, q^2)^2 \right] - 4q^2 \partial_s S_\kappa^\nu(q^2) k_\kappa(\omega^2, q^2) \ell_\kappa(\omega^2, q^2) \left[P_\kappa(\omega^2, q^2) - 6\omega^2 f_\kappa^t(\omega^2, q^2)^2 \right] \Big\} , \end{aligned} \tag{5.59}$$

where we used $\vec{p} \cdot \vec{q} = \cos\psi$ in (5.58), together with the fact that

$$S_{d-1} \int_0^\pi \mathrm{d}\psi \sin(\psi)^{d-2} \cos(\psi)^2 = \frac{S_d}{d} , \tag{5.60}$$

where $S_d = 2\pi^{d/2}/\Gamma(d/2)$ is the d-dimensional solid angle. Equation (5.59) is in general non-zero, but it vanishes in the NLO limit when $f_\kappa^X(\omega^2, q^2) \to f_\kappa^X(q^2)$. Indeed at NLO the flow equation for λ_κ reads

$$\begin{aligned} \partial_s \lambda_\kappa = & - S_d \frac{2 g_\kappa}{d} \int_0^\infty \frac{\mathrm{d}q}{(2\pi)^d} q^{d+3} f_\kappa^\lambda(q^2)^2 \int_{-\infty}^\infty \frac{\mathrm{d}\omega}{2\pi} \frac{1}{P_\kappa(\omega^2, q^2)^4} \Big\{ \partial_s S_\kappa^D(q^2) P_\kappa(\omega^2, q^2) \\ & \times \left[P_\kappa(\omega^2, q^2) - 4\omega^2 f_\kappa^t(q^2)^2 \right] - 4q^2 \partial_s S_\kappa^\nu(q^2) k_\kappa(q^2) \ell_\kappa(q^2) \left[P_\kappa(\omega^2, q^2) - 6\omega^2 f_\kappa^t(q^2)^2 \right] \Big\} \end{aligned} \tag{5.61}$$

and the integral over the frequency ω can be performed analytically. Noting that

$$\int_{-\infty}^\infty \frac{\mathrm{d}\omega}{2\pi} \frac{P_\kappa(\omega^2, q^2) - a\omega^2 f_\kappa^t(q^2)^2}{P_\kappa(\omega^2, q^2)^b} = (2b - a - 2) \frac{\Gamma\left(b - \frac{3}{2}\right) l_\kappa(q^2)^{3-2b}}{4\sqrt{\pi}\Gamma(b) f_\kappa^t(q^2)}, \qquad b > \frac{3}{2} , \tag{5.62}$$

one obtains that (5.61) is exactly zero. This is expected because the NLO approximation scheme preserves the Galilean Invariance. With the non-trivial frequency dependence of the NLO$_\omega$ scheme, (5.59) is in general not vanishing and leads to an artificial breaking of Galilean invariance. We will show in Chap. 5.6.2 that this violation of Galilean invariance remains small. .

5.5.1 Power-law noise correlator

With a non-zero D_θ in (5.3), one introduces another coupling, related to the non-analytic part. The function f_κ^D is now composed of two parts

$$f_\kappa^D \to \tilde{f_\kappa^D}(\omega^2, q^2) = f_\kappa^D(\omega^2, q^2) + w_\kappa^\theta \omega^{2\theta}\,, \tag{5.63}$$

and the function $k_\kappa(\omega^2, q^2)$ in (5.46) changes accordingly. In principle, the NPRG flow is analytic, such that no non-analytic contribution can arise to renormalize the coupling w_κ^θ. The situation is more subtle here since the frequency sector is not regularized, see discussion in F.2, but the non-renormalization of w_κ^θ is preserved. Defining the dimensionless running coupling $\hat{w}_\kappa^\theta$ as

$$\hat{w}_\kappa^\theta = \kappa^{-4\theta} w_\kappa^\theta \frac{1}{D_\kappa \nu_\kappa^{2\theta}} \tag{5.64}$$

one deduces its flow as

$$\partial_s \hat{w}_\kappa^\theta = \hat{w}_\kappa^\theta \left(-4\theta + \eta_\kappa^D + 2\theta \eta_\kappa^\nu\right) \tag{5.65}$$

For any fixed point solution for which $\hat{w}_*^\theta \neq 0$, one deduces that

$$\eta_*^D = 4\theta - 2\theta \eta_*^\nu \tag{5.66}$$

which yields if $\hat{g}_* \neq 0$

$$\eta_*^\lambda = \frac{1}{2}(2 - d + 4\theta - (3 + 2\theta)\eta_*^\nu), \tag{5.67}$$

which is non-zero. Hence, if a LR fixed point with $\hat{w}_*^\theta \neq 0$ exists and is stable, it leads to a violation of Galilean symmetry. Assuming that the two fixed points, the LR and the SR ones, compete then the transition from one to the other occurs when the corresponding exponents are equal, that is for $z_{\mathrm{LR}} = z_{\mathrm{SR}}$ and thus $\eta_\lambda^* = 0$. One deduces from (5.67) that the corresponding critical θ_c is given by

$$\theta_c(d) = \frac{1}{2(\eta_\nu^* - 2)}(2 - d - 3\eta_\nu^*)\,. \tag{5.68}$$

Hence, if two competing fixed points are found, one expects a transition from a SR to a LR dominated phase with exponents:

$$\begin{array}{lll} \mathrm{SR}: & z + \chi = 2, & \theta < \theta_c \\ \mathrm{LR}: & z + \chi = 2 - \eta_\lambda^*(\theta), & \theta > \theta_c \end{array}$$

5.6 Results

In this section we report the results coming from the numerical integration of the flow equations, using the scheme reported in App. F.3. We first focus on the case in which the correlation has a finite time scale τ. After that we focus on the case of power-law correlations, in both one and two dimension. We will discuss our results and compare them with the different scenarii present in the literature.

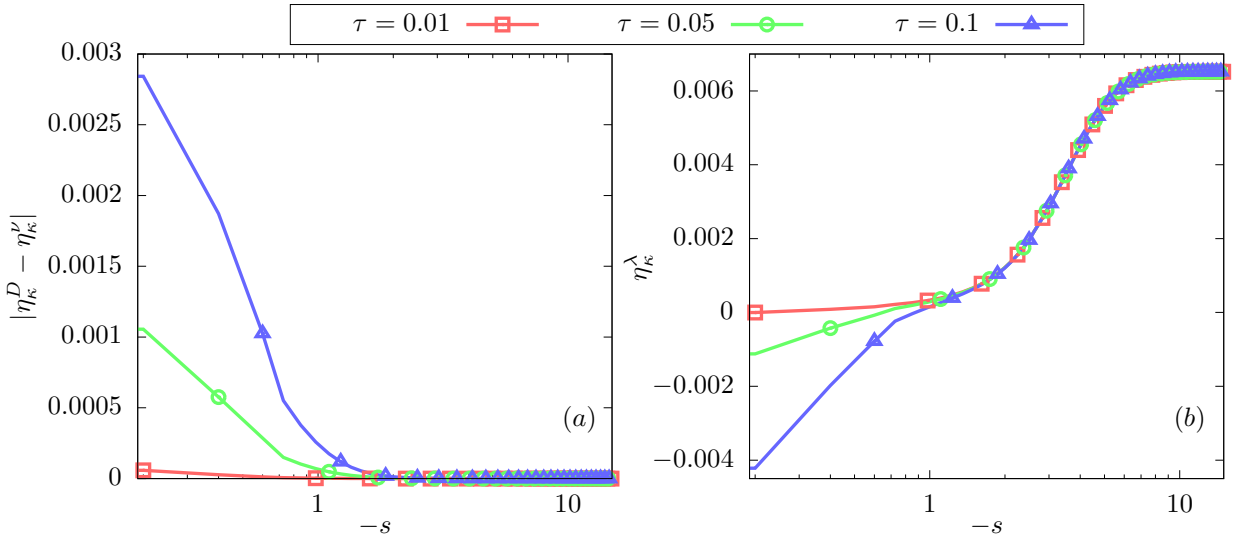

Figure 5.2: (a) η_κ^λ and (b) $|\eta_\kappa^D - \eta_\kappa^\nu|$ for different values of $\tau = 0.01, 0.05, 0.1$, as $s = \log(\kappa)$ decreases from $s = 0$ to $s = -15$. We see that the time-reversal symmetry is always restored, *i.e.* $\eta_*^D = \eta_*^\nu$, which implies that the roughness exponent is exactly the SR-KPZ one $\chi = (1 - \eta_*^D + \eta_*^\nu)/2 = 1/2$. The Galilean symmetry is also restored dynamically for all τ, although only approximately at the NLO$_\omega$ level of approximation ($\eta_*^\lambda \simeq 0.006$). By increasing τ, no LR fixed-point seems to appear, and the flow always reach the SR-KPZ fixed point with a dynamical exponent $z = 2 - \chi - \eta_*^\lambda$ which is slightly different from the theoretical prediction for KPZ $z = 2 - \chi = 3/2$ (less then 0.5%).

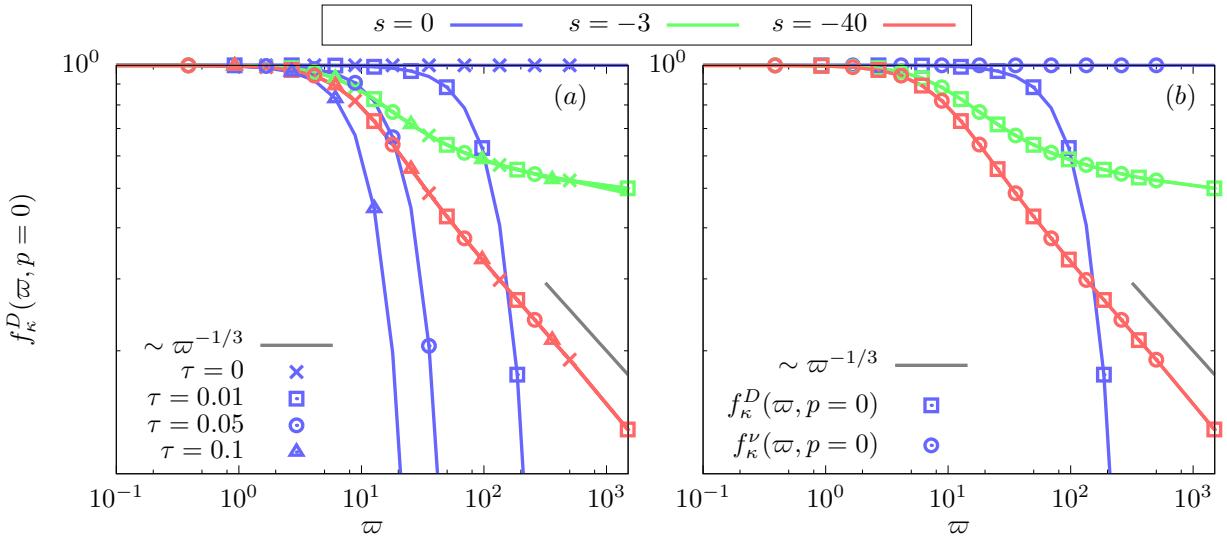

Figure 5.3: (a) The running function $f_\kappa^D(\omega, 0)$ for different values of $\tau = 0.01, 0.05, 0.1$ and $-\log(\kappa/\Lambda) = 0, 3, 40$. For any microscopic value of τ, f_κ^D reaches a power-law behaviour at the fixed point of the type $f_{*,\tau}^D(\omega, 0) \sim \omega^{\eta_*^D/z}$, with $z = 2 - \chi - \eta_*^\lambda$, very close to the pure KPZ case $f_{*,\tau=0}^D(\omega, 0) \sim \omega^{1/3}$ (purple line). (b) The running functions $f_\kappa^D(\omega, 0)$, $f_\kappa^\nu(\omega, 0)$ for $\tau = 0.01$ and different values of $-\log(\kappa/\Lambda) = 0, 3, 40$. Even if the initial conditions break the time-reversal symmetry, *i.e.* $f_\Lambda^D(\omega, p) \neq f_\Lambda^\nu(\omega, p)$, this symmetry is restored at the fixed point, $f_*^D(\omega, p) = f_*^\nu(\omega, p)$. This implies that the exponent χ is exactly the same as in the pure KPZ case (see Fig. 5.2).

5.6.1 Temporal correlations with a finite correlation time

In this section, we study the effect in $d = 1$ of a microscopic noise with short-range correlation of the form (5.4). This is simply implemented by specifying the initial condition at scale Λ:

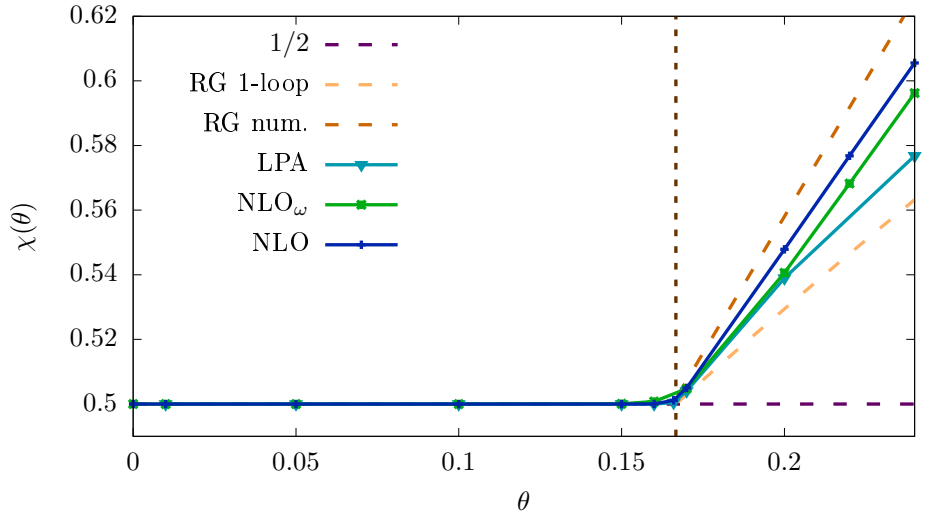

Figure 5.4: The roughness exponent $\chi(\theta)$ in one dimension for different approximation schemes, as θ varies from $\theta = 0$ to $\theta = 0.24$. The exponent follows the KPZ prediction $\chi = 1/2$ up to a critical value very close to the theoretical prediction $\theta_c = 1/6$ (dashed green line). After this value, $\chi(\theta)$ varies continuously with θ. The LPA results (light-blue solid line) improves the analytical result at one-loop given in (5.5) (dashed orange line), where we recall the authors set $\eta^\lambda_\kappa = 0$, but still are far from the NLO results (dark-blue solid line). At NLO we find an almost linear behaviour of $\chi(\theta) \simeq 1.43\theta + 0.26$, close to numerical estimation (5.7) (yellow dashed line).

$$f^D_{\kappa=\Lambda}(\mathbf{p}) = D_\tau(\mathbf{p}) = e^{-\frac{1}{2}\omega^2\tau^2} \,. \tag{5.69}$$

Since we work in $d = 1$, we keep $f^t_\kappa = f^\lambda_\kappa = 1$ not to induce a supplementary breaking of time reversal symmetry [23]. Under these assumptions we have that the contribution coming from $\partial_s S^D_\kappa$ in the flow of λ_k, (5.59), vanishes and we are thus left with the flow

$$\partial_s \lambda_\kappa = S_d \frac{8 g_\kappa}{d} \int_0^\infty \frac{\mathrm{d}q}{(2\pi)^d} q^{d+5} \int_{-\infty}^\infty \frac{\mathrm{d}\omega}{2\pi} \frac{1}{P_\kappa(\omega^2, q^2)^4} \partial_s S^\nu_\kappa(q^2) k_\kappa(\omega^2, q^2) \ell_\kappa(\omega^2, q^2) \left[P_\kappa(\omega^2, q^2) - 6\omega^2 \right] , \tag{5.70}$$

which corresponds to the effective artificial breaking of the Galilean invariance due to the NLO$_\omega$ approximation scheme. The SR noise is characterized by a typical time-scale τ; in the long-time physics one thus expects such microscopic correlation to be washed out by fluctuations. For all values of τ, we observed that the flow reaches a fixed-point, with stationarity in κ for all quantities. The coupling g_κ tends to a fixed-point value g_*. At the same time, the renormalization functions f^D_κ and f^ν_κ smoothly evolve to endow a fixed-point form, which does not depend on the value of τ, as illustrated for f^D_κ in Fig. 5.3 (a). This means that the large distance physics is universal, *i.e.* independent of the microscopic details, and it corresponds to the SR-KPZ universality class (the same fixed-point is attained as for $\tau = 0$). Furthermore, although they start with very different shapes, the two functions f^D_κ and f^ν_κ become equal at the fixed point $f^D_*(\omega, p) \equiv f^\nu_*(\omega, p)$, as illustrated in Fig. 5.3 (b). This means that the time-reversal symmetry is dynamically restored at large distances. This is further illustrated in Fig. 5.2 (a), which shows that the difference $|\eta^\nu_\kappa - \eta^D_\kappa|$ vanishes at the fixed point for all τ. According to Eq. (5.53), this implies that the χ exponent is exactly the KPZ one $\chi = 1/2$. Moreover, the Galilean symmetry is also restored at the fixed point, although only approximately. This can be assessed by the value of η^*_λ, which is represented in Fig. 5.2 (b). One observes that it reaches a constant value, which is not strictly zero but a small number

of order 0.0065. As explained before, this reflects the spurious violation of Galilean invariance induced by the NLO$_\omega$ ansatz , (5.70). This value is the same as for the pure KPZ case (for $\tau = 0$) and yields an error of less than 0.5% on the exponent z. Furthermore, we observe that for any finite τ, the function f^D_* decays at large frequency as a power law $f^D_{*,\tau}(\bar{\omega}, 0) \sim \bar{\omega}^{\eta^D_*/z}$, with $z = 2 - \chi - \eta^\lambda_*$, very close to the pure KPZ case $f^D_{*,\tau=0}(\bar{\omega}, 0) \sim \bar{\omega}^{1/3}$. Hence one can conclude that for all τ, the universal properties of the interface are the standard SR-KPZ ones. To summarize on the temporally SR-correlated noise, we found in $d = 1$ that its presence does not change the large-distance properties of the interface, which is still characterized by the SR-KPZ universality class. Hence, although both the Galilean and time-reversal symmetries are broken at the microscopic level, these symmetries are restored dynamically along the flow. This is the first analysis of the effect of SR time-correlations in the KPZ equation, which is here rendered possible by the both functional and non-perturbative formalism we use.

Comments about the two-dimensional case

In $d = 2$ we did not manage to access the strong-coupling fixed point within the NLO$_\omega$ scheme, even for the pure KPZ case. This is probably due to the fact that the artificial breaking of Galilean invariance in NLO$_\omega$ is too severe in two dimensions where, differently from the one-dimensional case, no additional symmetry (such as the time-reversal one in $d = 1$) is present to constraint the RG flow. On the other hand, the NLO scheme, which was proven to find very good results in $d = 1$ and $d = 2$ for the KPZ equation, is not enough to implement initial conditions of the flows involving frequency-dependent f^D_Λ. The study of the two dimensional KPZ equation with short-range temporal correlation would then require the use of the full SO ansatz, which does not break the Galilean invariance and allows for temporal dependence of the running functions f^X_κ. This is beyond the scope of the present thesis.

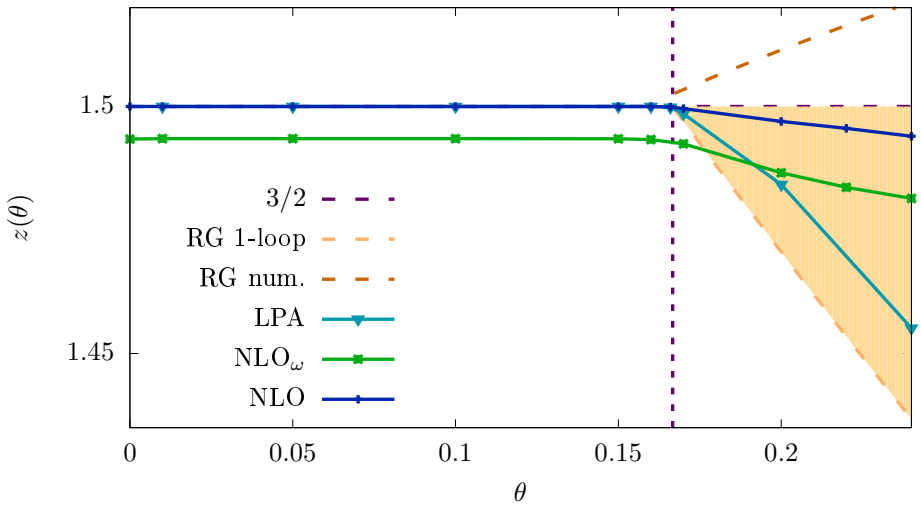

Figure 5.5: The dynamical exponent $z(\theta)$ in one dimension for different approximation schemes, as θ varies from $\theta = 0$ to $\theta = 0.24$. The exponent, as in the case for the roughness χ, follows the KPZ prediction $z = 3/2$ up to a critical value very close to the theoretical prediction $\theta_c = 1/6$ (dashed green line). After this value, $z(\theta)$ varies continuously with θ. Both LPA and NLO (light- and dark-blue solid lines respectively), differently from the numerical prediction (5.7) (orange solid line), are in agreement with the bounds given in (5.9) (yellow region).

5.6.2 Power-law temporal correlations

We now study temporal correlations with no typical length-scale, *i.e.* a power-law. Such a microscopic behaviour could in principle modify the universal properties of the system and is the one usually studied in the literature. To analyse how this LR correlation modifies the flow we initialize it at $\kappa = \Lambda$ as

$$f^{D}_{\kappa=\Lambda}(\mathbf{p}) = D_{\infty}(\mathbf{p}) = D_0 + D_\theta \omega^{-2\theta} \,. \tag{5.71}$$

As discussed in the previous sections this term introduces a new coupling constant w^θ_κ in the RG flow which can lead to two different scenarii: a SR fixed point with $w^\theta_* = 0$ or a LR fixed point with $w^\theta_* \neq 0$, retaining memories of the initial microscopic correlations. Such a fixed point is associated to a violation of GI, $z + \chi \neq 2$. In what follows we always work at the NLO level of approximation. Indeed in the LR case it is not necessary to retain the full time-dependence in the running functions, because the temporal dependence of the noise correlator is linked to the new coupling w^θ_κ. Going to NLO we also remove the artificial breaking of GI present at NLO$_\omega$ level (5.59). By doing so, the violation of GI comes only from the coupling w^θ_κ,

$$\partial_s \lambda_\kappa = S_d \frac{8 g_\kappa w^\theta_\kappa}{d} \int_0^\infty \frac{\mathrm{d}q}{(2\pi)^d} q^{d+5} f^\lambda_\kappa(q^2)^2 \partial_s S^\nu_\kappa(q^2) \ell_\kappa(q^2) \int_{-\infty}^{\infty} \frac{\mathrm{d}\omega}{2\pi} \frac{\omega^{-2\theta}}{P_\kappa(\omega^2, q^2)^4} \left[P_\kappa(\omega^2, q^2) - 6\omega^2 f^t_\kappa(q^2)^2 \right] \tag{5.72}$$

Furthermore we keep $f^\lambda_\kappa = f^t_\kappa$, in order to be able to recover the correct SR limit when $w^\theta_* = 0$.

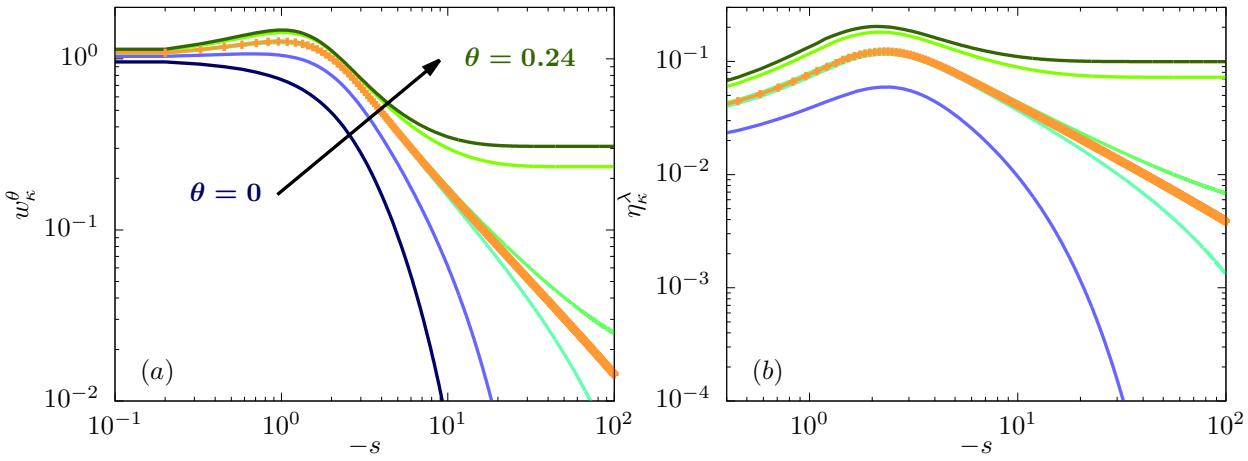

Figure 5.6: (a) The LR coupling w^θ_κ and (b) η^λ_κ, for different values of $\theta = 0, 0.1, 0.16, 0.17, 0.22, 0.24$ (from blueish to greenish) and $\theta = 0.166$ (orange) as the scale s varies from $s = 0$ to $s = -100$, in one dimension. We see that for $\theta < \theta_c$ the flow reaches the SR-GI KPZ fixed-point where $w^\theta_* = 0, \eta^\lambda_* = 0$, while for $\theta > \theta_c$ a new LR non-GI fixed point with $w^\theta_* \neq 0, \eta^\lambda_* \neq 0$ is reached. The critical value $\theta_c = 0.166$ corresponds to the theoretical prediction $\theta_c = 1/6$. Interestingly we can see that for the critical value of θ, the fixed point is reached in an algebraic RG-time s (linear in the log − log scale). The accuracy in the estimation of the critical θ is due to the fact that η^λ_κ is going to zero as the FP is approached for $\theta < \theta_c$; this implies that the stability criterion leading to (5.68) holds in an exact way. It is important to stress that this is not the case for the NLO$_\omega$ approximation scheme. There indeed, GI is never restored exactly, even at the SR fixed-point $w^\theta_* = 0$; we hence expect the critical value of θ to be slightly shifted due to a non-zero η^λ_* in the SR regime.

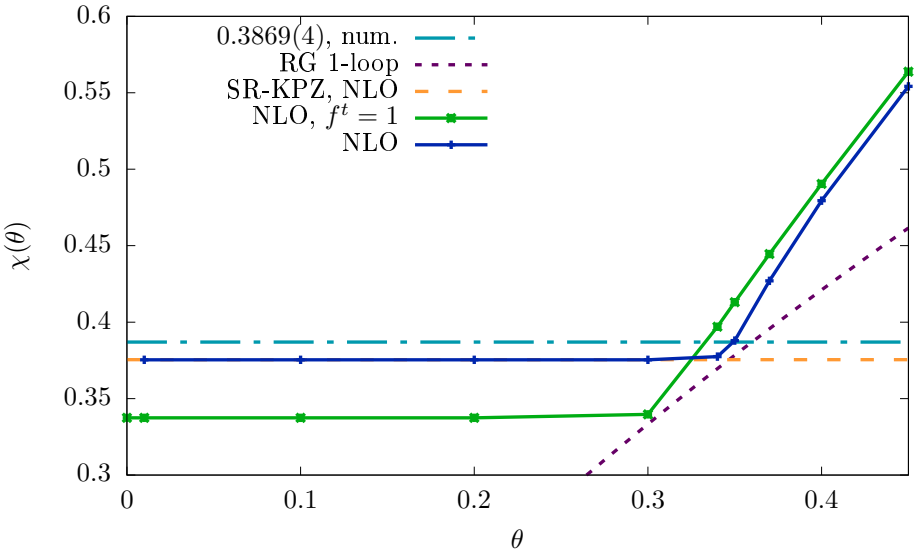

Figure 5.7: (The roughness exponent $\chi(\theta)$ in two dimensions for different approximation schemes, as θ varies from $\theta = 0$ to $\theta = 0.45$. The NLO results are compared with both the numerical estimation for the pure KPZ case [128] and the one-loop analytical result (5.5). The exponent follows the NLO result for the pure KPZ, $\chi = 0.375$, up to a critical value $\theta_c \simeq 0.346$. The same conclusions as in one dimension (see Fig. 5.6) about the accuracy in the determination of θ_c hold.

One dimension

We first study the one-dimensional case. In this case we keep $f_\kappa^t = f_\kappa^\lambda = 1$ in order to recover the time-reversal symmetry at the SR $w_*^\theta = 0$ fixed point. These conditions lead to the following NLO ansatz,

$$\Gamma_\kappa[\varphi,\tilde{\varphi}] = \int_x \left\{ \tilde{\varphi} D_{t,\kappa}\varphi - \tilde{\varphi} f_\kappa^D(-\tilde{D}_t^2,-\nabla^2)\tilde{\varphi} - \frac{1}{2}\left[\nabla^2\varphi f_\kappa^\nu(-\tilde{D}_t^2,-\nabla^2)\tilde{\varphi} + \tilde{\varphi} f_\kappa^\nu(-\tilde{D}_t^2,-\nabla^2)\nabla^2\varphi\right]\right\} \tag{5.73}$$

with $D_{t,k}\varphi = \partial_t\varphi - \lambda_k/2(\partial_x\varphi)^2$. The results for the roughness exponent χ are reported in Fig. 5.4. We can clearly notice the existence of a critical value θ_c below which the SR KPZ fixed-point is retrieved. Above this value of the temporal correlation exponent, we find a line of LR fixed-point with $\chi \equiv \chi(\theta)$. This is in agreement with the results presented in [93, 53], and rules out the appearance of a line of LR fixed-point for any non-vanishing θ. As expected at NLO, GI is dynamically restored exactly at the SR fixed-point (see Fig. 5.6), differently from the NLO$_\omega$ we discussed in Chap. 5.6.1 where a residual $\eta_*^\lambda \neq 0$ remains at the SR fixed-point. In the LR regime $\theta > \theta_c$ the NLO results are in good agreement with the numerical estimation (5.7). It is interesting to note that the transition is found already at the LPA level with the regulator (5.12), where $\chi(\theta)$ is close to the one-loop result (5.5); on the contrary, at LPA level with the Litim regulator $R_k(q^2) = (\kappa^2 - q^2)\theta(q^2 - \kappa^2)$ only the SR fixed-point is accessible, which shows that this regulator is not adapted to study KPZ problems. For the dynamical exponent z the results are reported in Fig. 5.5. At both the LPA and NLO level, $z(\theta)$ in the LR regime falls inside the bounds given by (5.9), ruling out the numerical estimation (5.7). It is also interesting to note that at the critical value of θ, both w_κ^θ and η_κ^λ go to zero algebraically as the fixed-point $k \to 0$ is approached (see Fig. 5.6).

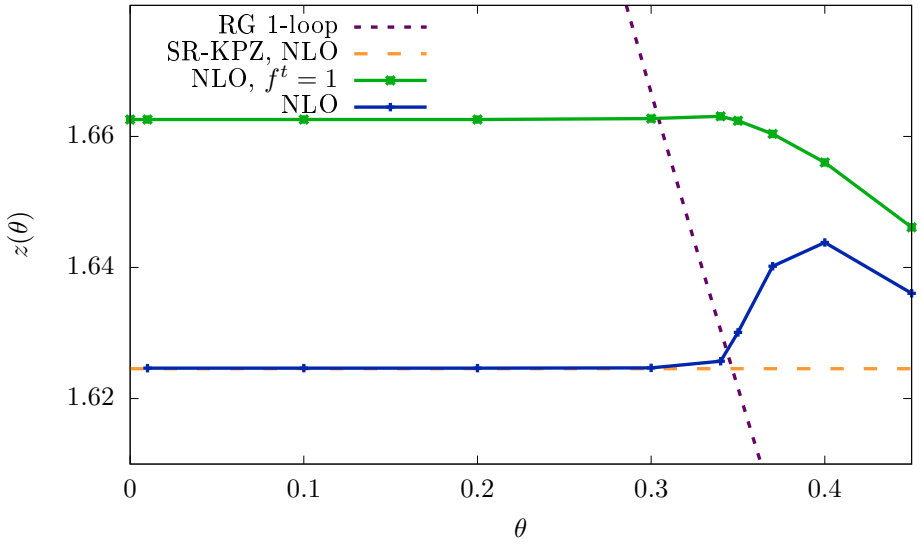

Figure 5.8: The dynamical exponent $\chi(\theta)$ in two dimensions for different approximation schemes, as θ varies from $\theta = 0$ to $\theta = 0.45$. The NLO results are compared with the one-loop analytical result (5.5). The exponent follows the NLO result for the pure KPZ, $\chi = 0.375$, up to a critical value $\theta_c \simeq 0.346$. The same conclusions as in one dimension (see Fig. 5.6) about the accuracy in the determination of θ_c hold. We can see that the one-loop estimation is far from the NLO result; this is expected because (5.5) holds for small θ and $\eta^\lambda_* = 0$, *i.e.* close to the θ_c.

Two dimensions

The study of the two-dimensional case is more difficult than the one-dimensional one. By looking at the analytical formula for θ_c , (5.68), and substituting the NLO estimation for the η^ν_* anomalous dimension for the two-dimensional pure KPZ $\eta^\nu_* = 0.375$, we find a theoretical critical value for the correlator exponent $\theta_c = 0.346$. As was already noted in [93], a non-physical divergence in the flow equations appears at $\theta = 1/4$. At the NLO and NLO$_\omega$ level we see that this non-physical divergence comes from a $(\omega + \bar{\omega})^{-4\theta}$ contribution in the argument of the flow equation for $\kappa\partial_\kappa f^D_\kappa$, which diverges for $\theta \geq 1/4$ if the external frequency $\bar{\omega}$ vanishes. In practice we can avoid this non-physical divergence by taking a different renormalization point $RP = (\bar{\omega}, p = 0)$. By doing so, at NLO the flow equation of λ_κ, (5.72) is modified in a non-trivial way. The associated flow equation is reported in App. F. The results for the roughness exponent using $RP = (0.01, p = 0)$ are given in Fig. 5.7. As in $d = 1$, we find a transition from a SR phase with KPZ exponents where Galilean symmetry is restored, and a LR dominated phase with $\theta-$dependent exponents and no Galilean symmetry.

5.7 Conclusions

In this chapter we studied the KPZ equation with temporal correlation in the microscopic noise, using a NPRG approach. For the case of a short-range correlation in the noise over a time-scale τ, we showed that these microscopic correlations are washed out at large scales for any value of τ in one dimension. We thus recover a KPZ fixed point where both time-reversal and Galilean symmetries are recovered, although only approximately for the Galilean one within the level of approximation used, the NLO$_\omega$ scheme. In two dimensions we did not manage to find a good fixed-point at NLO$_\omega$ level, for $f^t_\kappa = f^\lambda_\kappa \neq 1$. This is probably due to the artificial breaking of Galilean invariance that is intrinsic to the approximation

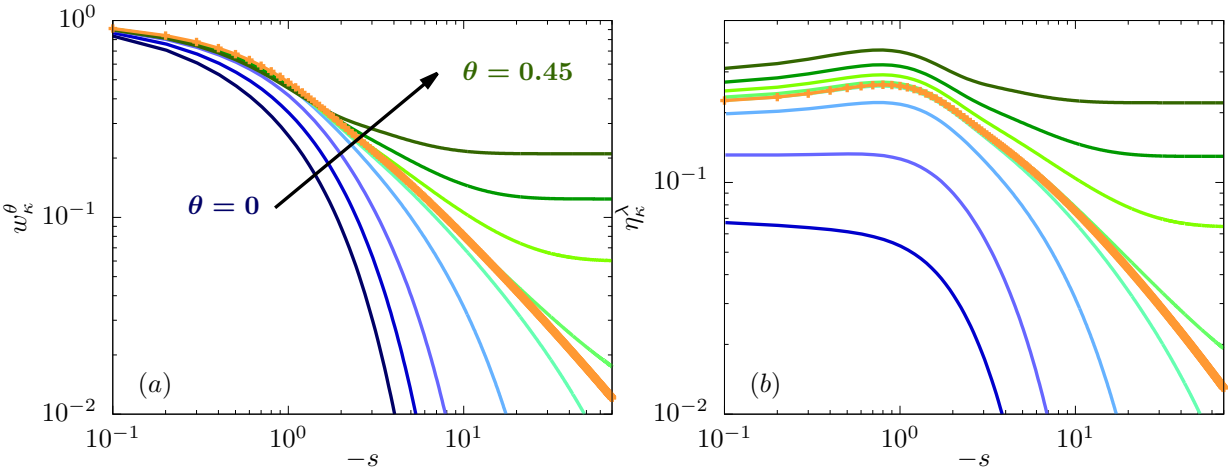

Figure 5.9: (a) The LR coupling w_κ^θ and (b) η_κ^λ, for different values of $\theta = 0, 0.1, 0.2, 0.3, 0.34, 0.35, 0.4, 0.45$ (from blueish to greenish) and $\theta = 0.346$ (orange line) as the scale s varies from $s = 0$ to $s = -100$, in two dimensions. We can draw the same conclusions as in the one-dimensional case. It is interesting to note that also in two dimensions w_κ^θ and η_κ^λ approach zero algebraically at $\theta_c = 0.346$.

scheme. In the case with the power-law correlation we find results that are in good agreement with the numerical RG estimations given by Medina *et al.* in [93] and with the analytical bounds given by Fedorenko in [53]. Our results thus confirm the presence of a critical value of the exponent, θ_c, below which SR-KPZ is recovered. The same scenario appears in two dimensions, with $\theta_c \simeq 0.346$. In $d = 2$ no prediction exists in the literature, apart from the one-loop perturbative result given in [93] for which the critical value of θ vanishes in $d = 2$. These perturbative results however are valid for small θ and do not take into account the renormalization of the non-linearity λ.

Conclusions and Perspectives

In this thesis we studied two out-of-equilibrium physical problems related to the KPZ equation.

The first is a driven-dissipative quantum system of exciton-polaritons, which displays Bose-Einstein condensation. For homogeneous systems, we showed that the phase of a one-dimensional condensate in its steady state displays KPZ scaling for an experimental accessible set of parameters, in the long time regime. The KPZ scaling persists down to sample size of about 50μm. When this power-law behaviour in the correlations is present, we found that the full distribution of the phase of the condensate is the TW-GOE distribution, which is characteristic of KPZ equation with flat initial conditions. As the size of the correlations grows, we observed a crossover from the TW-GOE distribution to the BR one, typical of KPZ equation with stationary initial conditions. This is in agreement with the recent experimental results found in turbulent liquid crystals [51]. Using Keldysh field-theoretical approach we showed that the mapping from EP to KPZ, which was demonstrated theoretically only for homogeneous systems, is robust with respect to the inclusion of inhomogeneities typical of experimental setups, such as confinement, disorder and thermically activated phonons. In the presence of a confining potential we found that the associated coefficients in the KPZ equation become inhomogeneous in space. In particular, the velocity of propagation of the front becomes strongly space dependent. This prediction was verified by the numerical simulation of strongly confined EP, where we observed that the boundaries of the phase front are much faster than the center. This provokes cusps propagating from the boundary to the bulk. A point in the phase front then follows KPZ dynamics up to the moment at which it is reached by cusps. In the case of space-time correlated disorder, the associated KPZ equation acquires a memory kernel in the noise correlator, linked to the correlator of the disorder. For KPZ it was showed that in the presence of a static and not too long ranged disorder, the large distance universal KPZ behaviour is unchanged [86, 87]. For EP, we checked numerically that in the case of a static disorder of typical lengthscale ℓ_d^*, the time correlations follow the KPZ scaling up to a typical time t^* which scales as $\ell_d^{2/3}$ as predicted by KPZ equation. When this scaling is present, we found both the TW-GOE distribution for the full phase and the TW-BR crossover as stationarity is approached. Concerning the effects of thermally activated phonons, we first computed the resulting semi-classical dynamics of the EP condensate starting from the full Keldysh action, finding agreement with the results coming from a purely classical treatment of the phonons [90]. Then, we focused on the mapping to the KPZ equation of EP interacting with thermally activated phonons. We found that the coefficients of the mapping are not affected by neither acoustic nor optical phonons.
This interesting phenomena ask for experimental realizations. Definitely demonstrating the KPZ scaling of the EP phase would indeed shed a light on the purely out-of-equilibrium nature of the EP condensate. In this direction, an accurate measurement of the first order correlation functions in EP would be enough to assess at least the KPZ scaling of the correlations. For the more advanced properties, such as the full phase distribution, a proper protocol to extract the phase in real time is needed. Furthermore the extension of the numerical simulation to two dimensional systems would be important for both KPZ and EP communities. For KPZ equation indeed, no exact prediction for the phase distribution in $d > 1$ exists, and

no experimental realization with a high-precision level has been devised in $d = 2$. Going to two dimensional systems would also introduce relevant topological defects in the EP condensate, rendering more subtle the extraction and the unwinding of the phase, and making a possible KPZ behaviour competing with the Kosterlitz-Thouless physics [129]. On the other hand, on the experimental side, two dimensional EP systems already exist, and thus they would be an ideal playground for investigating 2D KPZ physics.

The second model investigated in the manuscript is the KPZ equation with finite time correlation in the noise, which breaks the Galilean invariance at the microscopic level. This equation was first studied in the late eighties and, since then, a lot of controversial results about the dynamical restoration or not of the Galilean invariance at large scale exist in the literature. To shed a light on this fundamental question we used a NPRG approach, which already proved to be successful in tackling the pure KPZ case [114, 23, 115]. In the case of short range correlations we extended the already existing NLO scheme in order to have an ansatz taking into account the full time dependence of the running functions at the microscopic level, the NLO$_\omega$ scheme. This approximation has a residual breaking of Galilean invariance due to the truncation in the functional dependence on the field φ. Using this scheme we found that for any short range microscopic correlation, the pure KPZ fixed point is recovered in $d = 1$, with an exact restoration of the time-reversal symmetry and an almost exact restoration of the Galilean one. For the two-dimensional case the NLO$_\omega$ scheme seems not sufficient to find the expected SR fixed point. This difference with respect to the one dimensional case is probably due to the presence of the additional time reversal symmetry in $d = 1$. To our knowledge, this is the first analysis of KPZ equation with SR time correlation in the noise. When the noise is long-range correlated, *i.e.* via a power-law, the NLO scheme is sufficient and a new coupling w_κ^θ is responsible for the LR nature of the physics. In one dimension we found that below a critical value θ_c of the power-law correlation exponent θ, the pure KPZ fixed point with $w_*^\theta = 0$ is recovered, with both time-reversal symmetry and Galilean symmetry that are dynamically restored. Above θ_c, a line of θ—dependent fixed point with $w_*^\theta \neq 0$ appears. There, neither time-reversal nor Galilean symmetry are restored. In the two dimensional case, where no previous results existed in the literature, we found a similar picture. This confirms the existence of a critical value for the power-law exponents below which the pure KPZ physics is recovered in the large distance limit.
As a future direction, the implementation of the full SO scheme for the KPZ ansatz, introduced in [23], would be desirable in order to extend the analysis of the SR correlation in $d > 1$. This scheme indeed, differently from the NLO$_\omega$ one, introduces a full frequency dependence in the running functions while preserving the Galilean invariance. Furthermore the SO scheme would probably help in clarifying the long lasting debate on the existence of an upper critical dimension for the KPZ equation. The investigation of the geometrical subclasses of KPZ equation, found in $d = 1$, via the NPRG technique is also an appealing topic for future studies. The dependence on the initial conditions can be seen either as a boundary NPRG problem, or as a geometrical dependent NPRG. In the first case one should include the effects of the boundaries in the Wetterich equation. In the second case, the geometry dependence would imply the field theoretical analysis of the KPZ equation generalized to an arbitrary manifold [130].

A Field-theory formulation of Langevin dynamics

Field-theoretical formalism is the natural framework to develop suitable perturbation theories and investigate responses and correlations. We here review the standard response-field formalism for Langevin dynamics. Suppose to have m ϕ_α slow fields describing some coarse-grained dynamics of a physical system where the effects of fast-varying fields are embodied in m Gaussian distributed noise fields ξ_α

$$\partial_t \phi_\alpha(\mathbf{x}) = F_\alpha[\Phi] + \xi_\alpha(\mathbf{x}) \tag{A.1}$$

with $\langle \xi_\alpha(\mathbf{x})\xi_\beta(\mathbf{x}')\rangle = G_{\alpha\beta}(\mathbf{x}-\mathbf{x}')$ and $\Phi = \{\phi_\alpha\}_{\alpha=1}^m$; it is easy to generalize (A.1) to the case in which the number of slowing fields and noise fields differs.

A.1 Onsager-Machlup Functional

In a stochastic process we are interested in computing the expectation value of some observable O over different noise realizations,

$$\langle O\rangle = \int \mathcal{D}[\xi]\, O[\xi]\mathcal{P}[\xi] = \int \mathcal{D}[\xi]\, O[\xi] e^{-\frac{1}{2}\int \xi_\alpha G^{-1}_{\alpha\beta}\,\xi_\beta} \tag{A.2}$$

The most natural thing to do is to look at the noise field as a functional of the fields ϕ_α,

$$\xi[\Phi] = \partial_t\phi_\alpha - F_\alpha[\Phi]. \tag{A.3}$$

By doing so we end up with

$$\langle O\rangle = \int \mathcal{D}[\Phi]\, J[\Phi]\, O[\Phi]\, e^{-S_{OM}[\Phi]} \tag{A.4}$$

where $S_{OM}[\Phi] = \int_{\mathbf{x}} \left(\partial_t\phi_\alpha - F_\alpha[\Phi]\right) G^{-1}_{\alpha\beta} \left(\partial_t\phi_\beta - F_\beta[\Phi]\right)$ is known as Onsager-Machlup(OM) functional [131], and J is the Jacobian of the change of variables from ξ to ϕ,

$$J[\Phi] = \left\| \det\left(\delta_{\alpha,\beta}\partial_t\delta(\mathbf{x}-\mathbf{x}') - \frac{\delta F_\alpha[\Phi]}{\delta\phi_\beta}\delta(\mathbf{x}-\mathbf{x}')\right)\right\|. \tag{A.5}$$

We see that we have our first field-theoretical formulation of Langevin dynamics described by (A.1). However this formulation has some inconveniences. First of all we see that it implies the inverse of the noise-correlator, which is a divergent quantity for $\mathbf{q}\to\mathbf{0}$ for standard conserved dynamics, in which $G_{\alpha\beta} = \vec{\nabla}^2\delta(\mathbf{x}-\mathbf{x}')$. Another weakness is the fact that S_{OM} increases the degree of non-linearity of the original dynamics due to the multiplication between $F_{\alpha,\beta}[\Phi]$.

A.2 Martin-Siggia-Rose-Janssen-De Dominicis Functional

A proper way to solve the first problem is to introduce a set of auxiliary Hubbard-Stratonovich field $\bar{\Phi}$ in order to make $G_{\alpha\beta}$ appear instead of $G^{-1}_{\alpha\beta}$:

$$\langle O\rangle = \int \mathcal{D}[\xi]\mathcal{D}[\bar{\Phi}]\, O[\xi] e^{-\frac{1}{2}\int \bar{\phi}_\alpha G_{\alpha\beta}\,\bar{\phi}_\beta + \int \bar{\phi}_\alpha \xi_\alpha}. \tag{A.6}$$

This procedure also cures the second pathology of the OM functional, *i.e.* the increasing degree of non-linearity. Indeed now the exponential is linear in the noise field ξ and if we now pass from the integration over the noise to the integration over the slow field ϕ, we get

$$\langle O\rangle = \int \mathcal{D}[\Phi]\, J[\Phi]\mathcal{D}[\bar{\Phi}]\, O[\Phi] e^{-S[\Phi,\bar{\Phi}]} \tag{A.7}$$

with the action

$$S[\Phi,\bar{\Phi}] = \frac{1}{2}\int \bar{\phi}_\alpha G_{\alpha\beta}\,\bar{\phi}_\beta - \int \bar{\phi}_\alpha\left(\partial_t\phi_\alpha - F_\alpha[\Phi]\right) \tag{A.8}$$

and the Jacobian (A.5). The action (A.8) is usually referred to as Martin-Siggia-Rose-Janssen-De Dominicis(MSR) functional [14, 15, 16], with the auxiliary field $\tilde{\phi}_\alpha$ known as response-field, because of its direct relation to the response propagator of the theory [36]. From the MSR action we can compute expectation values of field-momenta by introducing the currents $j, \tilde{j}$ in the partition function Z,

$$Z[j,\tilde{j}] = \int \mathcal{D}[\Phi, i\tilde{\Phi}] \exp\left\{-S[\Phi,\tilde{\Phi}] + \int_{t,\vec{x}}\left(j\Phi + \tilde{j}\tilde{\Phi}\right)\right\}. \tag{A.9}$$

Indeed we have that any n-point correlation can be derived via

$$\left\langle \prod_{ik} \phi_{\alpha_i}(\mathbf{x}_i)\tilde{\phi}_{\alpha_k}(\mathbf{x}_k)\right\rangle = \prod_{ik}\frac{\delta}{\delta j_{\alpha_i}(\mathbf{x}_i)}\frac{\delta}{\delta \tilde{j}_{\alpha_k}(\mathbf{x}_k)} Z[j,\tilde{j}]_{j,\tilde{j}=0} \tag{A.10}$$

A.3 Discretization Prescriptions

It is instructive to explicitly compute the Jacobian (A.5):

$$\begin{aligned} J[\Phi] = \left\| \det\left(\delta_{\alpha,\beta}\partial_t\delta(\mathbf{x}-\mathbf{x}') - \frac{\delta F_\alpha[\Phi]}{\delta\phi_\beta}\delta(\mathbf{x}-\mathbf{x}')\right)\right\| &= \left\|\det(\partial_t)\det\left(\delta_{\alpha,\beta}\delta(\mathbf{x}-\mathbf{x}')\right.\right. \\ \left.\left. -\frac{\delta F_\alpha[\Phi]}{\delta\phi_\beta}\theta(t-t')\delta(\vec{x}-\vec{x}')\right)\right\| &= \left\|\det(\partial_t) e^{\mathrm{Tr}\,\ln\left(\delta_{\alpha,\beta}\delta(\mathbf{x}-\mathbf{x}') - \frac{\delta F_\alpha[\Phi]}{\delta\phi_\beta}\theta(t-t')\delta(\vec{x}-\vec{x}')\right)}\right\| \end{aligned} \tag{A.11}$$

where we used $\det \mathsf{AB} = \det \mathsf{A}\det\mathsf{B}$ and $\det \mathsf{A} = e^{\mathrm{Tr}\,\ln \mathsf{A}}$. We can now expand the logarithm in the exponent and explicitly compute the trace,

$$\begin{aligned} \mathrm{Tr}\,\ln\left(\delta_{\alpha,\beta}\delta(\mathbf{x}-\mathbf{x}') - \frac{\delta F_\alpha[\Phi]}{\delta\phi_\beta}\theta(t-t')\delta(\vec{x}-\vec{x}')\right) &= -\,\theta_t(0)\,\mathrm{Tr}\int_{\mathbf{y}}\frac{\delta F_\alpha[\Phi]}{\delta\phi_\beta}(\mathbf{y}) \\ &\quad + \frac{1}{2}\,\mathrm{Tr}\int_{\mathbf{y},\mathbf{y}'}\theta(\mathbf{y}-\mathbf{y}')\theta(\mathbf{y}'-\mathbf{y})\frac{\delta F_\alpha[\Phi]}{\delta\phi_\beta}\frac{\delta F_\gamma[\Phi]}{\delta\phi_\delta} + \dots \end{aligned} \tag{A.12}$$

We see that all the higher order terms disappear due to the multiplication of theta functions. We thus have

$$J[\Phi] = \left\| \det(\partial_t) e^{-\theta_t(0)\,\mathrm{Tr}\,\frac{\delta F_\alpha[\Phi]}{\delta \phi_\beta}} \right\| \tag{A.13}$$

where now the trace also includes the integration over internal degrees of freedom. In the Jacobian thus appears the ill-defined quantity $\theta_t(0)$ which depends on the discretization scheme: in the Itô prescription $\theta_t(0) = 0$ and the Jacobian is independent of the field, while in the Stratonovich prescription $\theta_t(0) = 1/2$ and we have an additional term in the action. One can show [132, 36] that in the case of additive noise, Feynman diagrams of closed response loops exactly cancel this contribution coming from the Jacobian. A convenient choice is thus to take the Itô prescription omitting closed response loops directly from the beginning.

B Schwinger-Keldysh Formalism and Homogeneous Driven-Dissipative Systems

We here review the details of the calculations which lead to the results reported in the main text, for homogeneous EP. The first part is a short introduction to the Schwinger-Keldysh field-theoretical formalism. This approach has been extensively studied in the literature and several reviews exist [133, 134]. In the last part we will focus on the application of this formalism to driven-dissipative EP, mostly following the review [84]. This last part will be useful in the next chapter, where we will derive new results for the case in which different inhomogeneities are present.

B.1 Keldysh representation of the Markovian Master Equation

Suppose to have a bosonic open quantum system described by a density matrix ρ whose dynamics follows the Markovian master equation

$$\partial_t \rho = -i[H_{LP}, \rho] + \mathcal{L}\rho \hat{=} \mathscr{L}\rho \tag{B.1}$$

where

$$\begin{aligned} H_{LP} &= \int \mathrm{d}\vec{x} \left[\psi^\dagger(\vec{x}) \left(\omega^0_{LP} - \frac{\nabla^2}{2m_{LP}} \right) \psi(\vec{x}) + u_c \psi^\dagger(\vec{x})^2 \psi(\vec{x})^2 \right] \\ &= \int \mathrm{d}\vec{x}\, h_{LP}(\vec{x}) \end{aligned} \tag{B.2}$$

describes the unitary dynamics and

$$\mathcal{L}\rho = \int d\vec{x} \left(\gamma_p \mathcal{D}[\psi(\vec{x})^\dagger]\rho + \gamma_l \mathcal{D}[\psi(\vec{x})]\rho + 2u_d \mathcal{D}[\psi(\vec{x})^2]\rho \right) \tag{B.3}$$

takes into account the incoherent single-particle pumping and losses as well as the two-body losses. Here the superoperator $\mathcal{D}[\cdot]\rho$ acts in the Lindbladian way

$$\mathcal{D}[L]\rho = L\rho L^\dagger - \frac{1}{2}\{L^\dagger L, \rho\} \tag{B.4}$$

and the non-linear loss-term ensures the saturation of the pumping.
This is an effective description for the dynamics of a $driven-dissipative$ bosonic system.
The formal solution to (B.1) is given by

$$\rho(t) = e^{(t-t_0)\mathscr{L}}\rho(t_0) = \lim_{N\to\infty} (\mathbb{I} + \delta_t \mathscr{L})^N \rho(t_0) \tag{B.5}$$

with $\delta_t = (t-t_0)/N$. The last equality suggests that joining a Trotter decomposition could lead us toward a field-theoretical description of the Markovian master equation, with the same spirit as Feynman's

path-integral representation in quantum mechanics. Here, however, the picture is somewhat more subtle. Indeed, a general mixed-state density matrix evolves according to $\rho(t) = G(t, t_0)\rho(t_0)G(t, t_0)^\dagger$ where $G(t, t_0)$ is some general evolution operator that does not have to be unitary; this implies that the evolution occurs on both sides of the density matrix and in both time directions. This leads to a doubling of the degrees of freedom with respect to Feynman's path integral where the evolving quantity is a vector and thus only the forward time-direction is needed. Furthermore, we are interested in the partition function of the system to get some physical information in analogy with standard statistical mechanics. In order to find such a quantity one has to trace out all the degrees of freedom in the system, that in this case amounts to identifying the two extremes of the time-evolution path. This gives rise to a closed contour. We thus define two different sets of fields, one for the upper part of the contour and one for the lower, or in an open-contour picture, one at the right-side of $\rho(t)$ and one at the left-side.
Before going into the details of the calculations, it is useful to recall the definition of coherent states and some of their properties.
A coherent state $|\psi\rangle$ is an eigenstate of the annihilation operator a, $a|\psi\rangle = \psi|\psi\rangle$, with $|\psi\rangle = e^{\psi^\dagger a}|0\rangle$ and $|0\rangle$ the vacuum in the Fock space; clearly, $\langle\psi| a^\dagger = \langle\psi|\psi^*$. Coherent states satisfy two fundamental properties:

$$\langle\psi|\phi\rangle = e^{\psi^*\phi} \tag{B.6a}$$

$$\mathbb{I} = \int \frac{\mathrm{d}\psi\mathrm{d}\psi^*}{\pi} e^{-\psi^*\psi} |\psi\rangle\langle\psi| \tag{B.6b}$$

We now try to tackle the Trotter decomposition for the dynamics of ρ.
Eq. (B.5) tells us that the evolution in a time interval $\Delta = t - t_f$ is made by infinitesimal time steps $\delta_t = \Delta/N$ in which the action of $\mathscr{L}$ on ρ is linear. If we take the $n-$th step,

$$\rho_{n+1} = e^{\delta_t}\rho_n = (\mathbb{I} + \delta_t\mathscr{L})\rho_n + O(\delta_t^2) \tag{B.7}$$

together with the representation of ρ_n on the coherent states will read

$$\rho_n = \int \frac{\mathrm{d}\psi_{+,n}\mathrm{d}\psi^*_{+,n}}{\pi}\frac{d\psi_{-,n}d\psi^*_{-,n}}{\pi} e^{-\psi^*_{+,n}\psi_{+,n}-\psi^*_{-,n}\psi_{-,n}} \langle\psi_{+,n}|\rho_n|\psi_{-,n}\rangle |\psi_{+,n}\rangle\langle\psi_{-,n}| \ , \tag{B.8}$$

where ψ_+ and ψ_- are the coherent states on the forward and backward contour respectively. We can thus find the matrix element $\langle\psi_{+,n+1}|\rho_{n+1}|\psi_{-,n+1}\rangle$ by evaluating $\langle\psi_{+,n+1}|\mathscr{L}\left(|\psi_{+,n}\rangle\langle\psi_{-,n}|\right)|\psi_{-,n+1}\rangle$ recalling the definition of $\mathscr{L}$ given by (B.1), (B.2) and (B.3) (we neglect spatial degrees of freedom for the sake of compactness in the notation):

$$\begin{aligned}\langle\psi_{+,n+1}\mathscr{L}\left(|\psi_{+,n}\rangle\langle\psi_{-,n}|\right)|\psi_{-,n+1}\rangle = &-i\left(\langle\psi_{+,n+1}|h_{LP}|\psi_{+,n}\rangle\langle\psi_{-,n}|\psi_{-,n+1}\rangle\right.\\ &\left.-\langle\psi_{+,n+1}|\psi_{+,n}\rangle\langle\psi_{-,n}|h_{LP}|\psi_{-,n+1}\rangle\right)\\ &+\sum_{\alpha=1,2,3}\gamma_\alpha\left[\langle\psi_{+,n+1}|L_\alpha|\psi_{+,n}\rangle\left\langle\psi_{-,n}|L_\alpha^\dagger|\psi_{-,n+1}\right\rangle\right.\\ &\left.-\frac{1}{2}\left(\left\langle\psi_{+,n+1}|L_\alpha^\dagger L_\alpha|\psi_{+,n}\right\rangle\left\langle\psi_{-,n}|L_\alpha^\dagger L_\alpha|\psi_{-,n+1}\right\rangle\right)\right]\end{aligned} \tag{B.9}$$

with $\boldsymbol{\gamma} = (\gamma_p, \gamma_l, 2u_d)$ and $\mathsf{L} = (\psi^*, \psi, \psi^2)$. We now require all the operators appearing in the above equation to be normal-ordered with respect to the annihilation and creation operators; while this makes

no loss of generality for the Hamiltonian, it is a bit more subtle for the Lindblad operators. As far as they are linear in a, $a^\dagger$ normal ordering does not affect them while when they are a general quasi-local polynomial one should pay attention because of ambiguities coming from the Markovian approximation; we will go deeper into that in next section. Normal ordering implies that any $\left\langle \psi|\hat{O}|\phi \right\rangle$ can be directly substituted with $O(\psi^*, \phi)$:

$$\left\langle \psi_{+,n+1}|\mathscr{L}\left(|\psi_{+,n}\rangle\langle\psi_{-,n}|\right)|\psi_{-,n+1}\right\rangle = e^{\psi^*_{+,n+1}\psi_{+,n}+\psi^*_{-,n}\psi_{-,n+1}}\mathscr{L}\left(\psi^*_{+,n+1},\psi_{+,n},\psi_{-,n+1},\psi^*_n\right) \tag{B.10}$$

Thus,

$$\begin{aligned}\langle\psi_{+,n+1}|\rho_{n+1}|\psi_{-,n+1}\rangle &= \int \frac{\mathrm{d}\psi_{+,n}\mathrm{d}\psi^*_{+,n}}{\pi}\frac{d\psi_{-,n}d\psi^*_{-,n}}{\pi}e^{\psi_{+,n}(\psi^*_{+,n+1}-\psi^*_{+,n})+\psi^*_{-,n}(\psi_{-,n+1}-\psi_{-,n})}\\ &\times\left(1+\delta_t\mathscr{L}\left(\psi^*_{+,n+1},\psi_{+,n},\psi_{-,n+1},\psi^*_n\right)\right)\langle\psi_{+,n}|\rho_n|\psi_{-,n}\rangle+O(\delta_t^2)\\ &\simeq \int \frac{\mathrm{d}\psi_{+,n}\mathrm{d}\psi^*_{+,n}}{\pi}\frac{d\psi_{-,n}d\psi^*_{-,n}}{\pi}\langle\psi_{+,n}|\rho_n|\psi_{-,n}\rangle\\ &\quad e^{i\delta_t\left[-i\psi_{+,n}\frac{\psi^*_{+,n+1}-\psi^*_{+,n}}{\delta_t}-i\psi^*_{-,n}\frac{\psi_{-,n+1}-\psi_{-,n}}{\delta_t}-i\mathscr{L}\left(\psi^*_{+,n+1},\psi_{+,n},\psi_{-,n+1},\psi^*_n\right)\right]}\\ &= \int \frac{\mathrm{d}\psi_{+,n}\mathrm{d}\psi^*_{+,n}}{\pi}\frac{d\psi_{-,n}d\psi^*_{-,n}}{\pi}\langle\psi_{+,n}|\rho_n|\psi_{-,n}\rangle e^{iS_n}\end{aligned} \tag{B.11}$$

with $S_n = \delta_t\left[-i\psi_{+,n}\frac{\psi^*_{+,n+1}-\psi^*_{+,n}}{\delta_t}-i\psi^*_{-,n}\frac{\psi_{-,n+1}-\psi_{-,n}}{\delta_t}-i\mathscr{L}\left(\psi^*_{+,n+1},\psi_{+,n},\psi_{-,n+1},\psi^*_n\right)\right]$. Iterating this procedure from t_0 to t (i.e. spanning the whole closed contour) and then integrating also over $\frac{d\psi_{+,N}d\psi^*_{+,N}}{\pi}\frac{d\psi_{-,N}d\psi^*_{-,N}}{\pi}$ one traces out all degrees of freedom and obtains the partition function for this system:

$$Z_{t,t_0} = \int\prod_{n=0}^{N}\frac{d\psi_{+,n}d\psi^*_{+,n}}{\pi}\frac{d\psi_{-,n}d\psi^*_{-,n}}{\pi}e^{iS_n}\langle\psi_{+,0}|\rho_0|\psi_{-,0}\rangle+O(\delta_t^2) \tag{B.12}$$

where ρ_0 is the density matrix for the initial system.
We now take the $N\to\infty$, $\delta_t\to 0$ $N\delta_t = cst$ limit and look for stationary properties of the system, i.e. $t_0\to-\infty$, $t\to\infty$ limit; under this assumption (B.12) becomes

$$Z = \int\mathscr{D}[\psi_+,\psi^*_+,\psi_-,\psi^*_-]e^{iS} \tag{B.13}$$

with

$$S = \int\mathrm{d}\vec{x}\int_{-\infty}^{+\infty}\mathrm{d}t(\psi^*_+i\partial_t\psi_+-\psi^*_-i\partial_t\psi_--i\mathcal{L}(\psi_+,\psi^*_+,\psi_-,\psi^*_-)) \tag{B.14a}$$

$$\mathscr{D}[\psi_+,\psi^*_+,\psi_-,\psi^*_-] = \lim_{n\to\infty}\prod_{n=0}^{N}\frac{d\psi_{+,n}d\psi^*_{+,n}}{\pi}\frac{d\psi_{-,n}d\psi^*_{-,n}}{\pi} \tag{B.14b}$$

where in the first derivative term in (B.14a) we collected $\psi^*_{+,n}$ instead of $\psi_{+,n}$ as in (B.11), and $\mathcal{L}$ is given in (B.16) below. In writing (B.13) we assumed a complete loss of memory of the initial state, which is a reasonable assumption for stationary states and introduced back the spatial degrees of freedom. A key feature of Keldysh partition function is that

$$Z = \int \mathscr{D}[\psi_+, \psi_+^*, \psi_-, \psi_-^*] e^{iS} = 1 \tag{B.15}$$

by construction in the absence of external sources; this is a heavy simplification with respect to equilibrium situation where one has always to pay attention to normalization factor. Furthermore it is time independent, which ensures the conservation of probability. Looking at the quantity

$$\mathcal{L}(\psi_+^*, \psi_+, \psi_-^*, \psi_-) = -i(h_{LP,+} - h_{LP,-}) + \sum_{\alpha=1,2,3} \gamma_\alpha \left[L_{\alpha,+} L_{\alpha,-}^* - \frac{1}{2} \left(L_{\alpha,+} L_{\alpha,+}^* + L_{\alpha,-}^* L_{\alpha,-} \right) \right] \tag{B.16}$$

we see that the mapping between Markovian master equation and Keldysh formalism can be done in a very direct way by noting that all the operators acting on the left(right) of the density matrix will be translated into fields residing onto the forward(backward) Keldysh contour. Indeed $h_{LP,\pm} = h_{LP}(\psi_\pm^*, \psi_\pm)$ as well as $L_{\alpha,\pm}^{(*)}$ contain fields only on the $\pm$ contour respectively. A more physical representation is achieved by performing the Keldysh-rotation,

$$\phi_c = \frac{1}{\sqrt{2}}(\psi_+ + \psi_-), \; \phi_q = \frac{1}{\sqrt{2}}(\psi_+ - \psi_-) \tag{B.17}$$

with $c(q)$ standing for classical(quantum); this terminology reflects the fact that classical fields can acquire a field expectation value while quantum fields cannot.

B.2 Keldysh field-theory for homogeneous Exciton-Polaritons

In this section we will review the application of the formalism introduced in the previous section to a homogeneous condensate of EP. Plugging (B.2) and (B.3) inside (B.16) and performing the Keldysh rotation, one gets the Schwinger-Keldysh action associated to (B.1):

$$\begin{aligned} S = \int_{\mathbf{x}} \{ & \phi_q^*(i\partial_t + K_c\nabla^2 - r_c + ir_d)\phi_c + c.c. - \Big[(u_c - iu_d)(\phi_q^*\phi_c^*\phi_c^2 + \phi_q^*\phi_c^*\phi_q^2) \\ & + c.c.\Big] + i2(\gamma + 2u_d\phi_c^*\phi_c)\phi_q^*\phi_q \} \end{aligned} \tag{B.18}$$

where $K_c \hat{=} \frac{1}{2m_{LP}}$, $r_c \hat{=} \omega_{LP}^0$, γ is the *noise* level $\gamma \hat{=} \frac{\gamma_l + \gamma_p}{2}$ and r_d is the gap from saturation $r_d \hat{=} \frac{\gamma_l - \gamma_p}{2}$. Notice that here we have not modelled the effect of a momentum dependent loss rate, used in Chap. 2. This amounts to take $K_d = 0$, *i.e.* no complex-diffusion term. The formalism and the approximations used are easily extensible to the $K_d \neq 0$ case.

B.2.1 Semiclassical limit of Keldysh Action

Sometimes it is interesting to look at how the system behaves at scales which are greater than the microscopic one at which the Markovian master equation pertains; we could refer to it as a semi-classical limit in which quantum fluctuations do not necessarily vanish. Keldysh formalism is particularly useful in that direction.
Intuitively, thinking at large-scale behaviour suggests to apply some coarse-graining procedure on the system's microscopic quantities; we could exploit this procedure by means of a Renormalization Group (RG) approach. We would thus keep in the Keldysh action only the terms that are relevant in the RG sense. The roughest way for discriminating relevant quantities from irrelevant ones is to look at

their canonical dimension $\Delta_i = [\lambda_i]$ (where the λ_i are the quantities under investigation) classifying as irrelevant the ones with $\Delta_i < 0$; this approach holds in the vicinity of criticality where the correlation functions show scaling behaviour and neglect possible anomalous dimensions, which are supposed to be small corrections to the canonical scaling. For the physical model under investigation the scaling regime will be in the vicinity of the saturation threshold $r_d = 0$ where a condensation of exciton-polariton can occur.
Having two different fields in the system we need two conditions for fixing their canonical dimensions and thus understand the canonical scaling of the parameters associated to any combination of these fields. The first constraint is the adimensionality of (B.18); by definition of canonical dimensions, $[\nabla^2] = 2$ and thus the integration measure has dimension $[\mathrm{d}\vec{x}\mathrm{d}t] = -d-2$. The second constraint is that the coupling associated to the noise vertex γ (we will see in what follows the reasons of this nomenclature), which is the non-equilibrium analogue of the equilibrium temperature, remains constant through the coarse-graining procedure; this assumption leads to $2[\phi_q] = d+2$ and thus to $[\phi_q] = \frac{d+2}{2}$. Now we can fix also the canonical dimension of the classical field, which is $[\phi_c] = \frac{d-2}{2}$. Let us now take a generic vertex $u_{i,k}$ coupled to i classical and k quantum fields; its canonical dimension is then $[u_{i,k}] = \frac{d}{2}(2-k-i)+(2+i-k)$.

Three-dimensional case

If we focus on the case of three spatial dimensions, using the above estimate for the scaling dimensions, we see that any quartic vertex with more than one quantum field is irrelevant and can thus be neglected in our semiclassical picture; the noise vertex is marginal and is kept in the analysis.
This leads to the semiclassical Keldysh action:

$$S = \int_{\mathrm{x}} \{\phi_q^*(i\partial_t + K_c\nabla^2 - r_c + ir_d)\phi_c + c.c. - \left[(u_c - iu_d)\phi_q^*\phi_c^*\phi_c^2 + c.c.\right] + i2\gamma\phi_q^*\phi_q\} \tag{B.19}$$

This action is now at most quadratic in the quantum fields; the semiclassical partition function is thus

$$Z = \int \mathcal{D}[\phi_c, \phi_c^*, \phi_q, \phi_q^*] e^{i\int_{\mathrm{x}}\{\phi_q^*(i\partial_t + K_c\nabla^2 - r_c + ir_d)\phi_c + c.c. - \left[(u_c - iu_d)\phi_q^*\phi_c^*\phi_c^2 + c.c.\right] + i2\gamma\phi_q^*\phi_q\}}. \tag{B.20}$$

We see that performing a Hubbard-Stratonovich transformation we could switch to an action linear in $\phi_q^{(*)}$ and then totally get rid of the quantum field thank to a Dirac-delta:

$$\begin{aligned}
Z &= \int \mathcal{D}[\phi_c, \phi_c^*, \phi_q, \phi_q^*] e^{i\int_{\mathrm{x}}\{\phi_q^*(i\partial_t + K_c\nabla^2 - r_c + ir_d)\phi_c + c.c. - \left[(u_c - iu_d)\phi_q^*\phi_c^*\phi_c^2 + c.c.\right] + i2\gamma\phi_q^*\phi_q\}} \\
&= \int \mathcal{D}[\phi_c, \phi_c^*, \phi_q, \phi_q^*, \xi, \xi^*] e^{i\int_{\mathrm{x}}\{\phi_q^*(i\partial_t + K_c\nabla^2 - r_c + ir_d)\phi_c + c.c. - \left[(u_c - iu_d)\phi_q^*\phi_c^*\phi_c^2 + c.c.\right] + i\frac{1}{2\gamma}\xi^*\xi - (\phi_q^*\xi + \xi^*\phi_q)\}} \\
&= \int \mathcal{D}[\phi_c, \phi_c^*, \xi, \xi^*] e^{-\frac{1}{2\gamma}\int_{\mathrm{x}}\xi^*\xi} \delta\left(\left[i\partial_t + K_c\nabla^2 - r_c + ir_d - (u_c - iu_d)|\phi_c|^2\right]\phi_c - \xi\right) \\
&\quad \times \delta\left(\left[-i\partial_t + K_c\nabla^2 - r_c - ir_d - (u_c + iu_d)|\phi_c|^2\right]\phi_c^* - \xi^*\right).
\end{aligned} \tag{B.21}$$

The last line has a clear physical interpretation; given one realization of the auxiliary pair of Gaussian variables (ξ, ξ^*) the integral will select the pair of classical fields (ϕ_c, ϕ_c^*) that satisfies the two delta functions. The physical content of (B.19) is exactly the same as the following Langevin equation for ϕ_c (the same holds for the c.c.)

$$i\partial_t\phi_c = \left[-K_c\nabla^2 + r_c - ir_d + (u_c - iu_d)|\phi_c|^2\right]\phi_c + \xi \tag{B.22}$$

where ξ is a Gaussian noise of strength 2γ. We can now also understand the definition of the noise vertex given above.
Equation (B.22) is the usual Stochastic Gross-Pitaevskii equation for driven-dissipative systems, with an additive effective noise. From this derivation we can see that is an effective long-wavelength description of the microscopic system described by (B.1).

One-dimensional case

In one spatial dimension, there is one more quartic term surviving in the long-scale regime, namely the one with two quantum and two classical fields whose vertex has canonical scaling dimension $[\lambda] = 1$. In this case the mapping to a Langevin equation is more subtle because the coefficient of the bilinear term $\phi_q\phi_q^*$ is now dependent on the classical field; in order to decouple this term and be able to use Dirac-delta properties we thus need a more involved Hubbard-Stratonovich transformation with respect to the one used in previous section.
Let us introduce the identity

$$1 = \int \mathcal{D}[\xi, \xi^*] \exp\left\{ -\int_x \frac{1}{2}\xi\xi^* \right\} \tag{B.23}$$

and do the shift

$$\xi \to \xi + 2i\sqrt{\gamma + 2u_d|\phi_c|^2}\phi_q, \qquad \xi^* \to \xi^* + 2i\sqrt{\gamma + 2u_d|\phi_c|^2}\phi_q^* \tag{B.24}$$

which leads to

$$1 = \int \mathcal{D}[\xi, \xi^*] \exp\left\{ -\frac{1}{2}\int_x \left[\xi\xi^* + \left(2i\xi\sqrt{\gamma + 2u_d|\phi_c|^2}\phi_q^* - c.c \right) - 4\left(\gamma + 2u_d|\phi_c|^2\right)\phi_q\phi_q^* \right] \right\} \tag{B.25}$$

We can see that inserting this identity in the partition function cancels out the quadratic vertex $\phi_q\phi_q^*$ leading to a Keldysh action

$$S \to S - \int_x \sqrt{\gamma + 2u_d|\phi_c|^2}\left(\xi\phi_q^* + \xi^*\phi_q\right) \tag{B.26}$$

Resulting in a partition function of the type

$$\begin{aligned} Z = \int \mathcal{D}[\phi_c, \phi_c^*, \xi, \xi^*] e^{-\frac{1}{2}\int_x \xi^*\xi} \delta\left(\left[i\partial_t + K_c\nabla^2 - r_c + ir_d - (u_c - iu_d)|\phi_c|^2 \right]\phi_c - \sqrt{\gamma + 2u_d|\phi_c|^2}\xi \right) \\ \times \delta\left(\left[-i\partial_t + K_c\nabla^2 - r_c - ir_d - (u_c + iu_d)|\phi_c|^2 \right]\phi_c^* - \sqrt{\gamma + 2u_d|\phi_c|^2}\xi^* \right) \end{aligned} \tag{B.27}$$

We hence recover equation (2.29).

B.2.2 Density-phase representation of Keldysh Action and mapping to KPZ

Dealing with a microscopic action instead of a full quantum master equation, one can more easily exploit symmetries of the system and thus study the large-scale and universal behaviours. For this purpose the crucial point is that the classical phase rotation $\phi_{c,q} \to e^{i\alpha}\phi_{c,q}$ is a symmetry for (B.18) while the quantum phase rotation $\{\phi_c \to e^{i\alpha}\phi_c,\ \phi_q \to e^{i\beta}\phi_q\}$ is not; one can show that breaking of classical phase rotation symmetry is enough to ensure the existence of a Goldstone mode [84]. The latter describes fluctuations in the phase of the order parameter and heavily influences the long-distance properties of

such systems in low dimensionality. Hence it is natural to derive the action for the Goldstone boson θ switching to a density-phase representation of classical and quantum fields:

$$\phi_c = \sqrt{\rho}e^{i\theta},\ \phi_q = \zeta e^{i\theta} \tag{B.28}$$

where ρ, ζ are respectively a real and a complex variable. Noting that

$$\nabla^2\phi_c = e^{i\theta}\left[-\frac{1}{4}\rho^{-\frac{3}{2}}(\nabla\rho)^2 + i\rho^{-\frac{1}{2}}\nabla\rho\cdot\nabla\theta + \frac{1}{2}\rho^{-\frac{1}{2}}\nabla^2\rho - \rho^{\frac{1}{2}}(\nabla\theta)^2 + i\rho^{\frac{1}{2}}\nabla^2\theta\right] \tag{B.29}$$

the Keldysh action for the new variables becomes

$$\begin{aligned} S = \int_x \Bigg\{ & \zeta^* \left(\frac{i}{2}\rho^{-\frac{1}{2}}\partial_t\rho - \rho^{\frac{1}{2}}\partial_t\theta + iK_c\rho^{-\frac{1}{2}}\nabla\rho\cdot\nabla\theta - \frac{K_c}{4}\rho^{-\frac{3}{2}}(\nabla\rho)^2 \right. \\ & \left. + \frac{K_c}{2}\rho^{-\frac{1}{2}}\nabla^2\rho - K_c\rho^{\frac{1}{2}}(\nabla\theta)^2 + iK_c\rho^{\frac{1}{2}}\nabla^2\theta - r_c\rho^{\frac{1}{2}} + ir_d\rho^{\frac{1}{2}} \right) + c.c. \\ & - \left[(u_c - iu_d)(\zeta^*\rho^{\frac{3}{2}} + \zeta|\zeta|^2\rho^{\frac{1}{2}}) + c.c.\right] + i2(\gamma + 2u_d\rho)|\zeta|^2 \Bigg\}\ . \end{aligned} \tag{B.30}$$

To study the physics of the Goldstone boson θ we perform a mean-field approximation over the densities. This is justified by the fact that in the broken phase, where θ is more important, the density fluctuations are massive and thus expected to be small compared to the ones associated to the phase. In this case we perform a saddle-point expansion over ρ and ζ:

$$\left.\frac{\delta S}{\delta\rho}\right|_{\rho_0,\zeta_0} = 0,\ \left.\frac{\delta S}{\delta\zeta}\right|_{\rho_0,\zeta_0} = 0\,. \tag{B.31}$$

Since (B.30) is at least linear in ζ, the first equation in (B.31) is satisfied $\forall\,(\rho_0, 0)$; under this assumption the second equation yields

$$\left.\frac{\delta S}{\delta\zeta}\right|_{\rho_0,0} = -r_c - ir_d - (u_c + iu_d)\rho_0 = 0 \tag{B.32}$$

that is satisfied when

$$\rho_0 = -\frac{r_c}{u_c} = -\frac{r_d}{u_d}\,. \tag{B.33}$$

We now go one step further and consider fluctuations up to second order around the mean-field solution for $\zeta = \zeta_1 + i\zeta_2$ and $\rho = \rho_0 + \pi$. Recalling that $(x+\delta)^\alpha = x^\alpha + \alpha x^{\alpha-1}\delta + O(\delta^2)$ one gets

$$\begin{aligned} S \simeq \int_x \Bigg\{ & \zeta_2\rho^{-\frac{1}{2}}\partial_t\pi - 2\zeta_1\rho_0^{\frac{1}{2}}\partial_t\theta - \zeta_1\rho_0^{-\frac{1}{2}}\pi\partial_t\theta + 2\zeta_2K_c\rho_0^{-\frac{1}{2}}\nabla\pi\cdot\nabla\theta \\ & + \zeta_1K_c\rho_0^{-\frac{1}{2}}\nabla^2\pi - 2\zeta_1K_c\rho_0^{\frac{1}{2}}(\nabla\theta)^2 - \zeta_1K_c\rho_0^{-\frac{1}{2}}\pi(\nabla\theta)^2 + 2\zeta_2K_c\rho_0^{\frac{1}{2}}\nabla^2\theta \\ & + \zeta_2K_c\rho_0^{-\frac{1}{2}}\pi\nabla^2\theta - 2\zeta_1r_c\rho_0^{\frac{1}{2}} - \zeta_1r_c\pi^{-\frac{1}{2}} + 2\zeta_2r_d\rho^{\frac{1}{2}} - \Big[2u_c\zeta_1\rho_0^{\frac{3}{2}} \\ & + 3u_c\zeta_1\pi\rho_0^{\frac{1}{2}} - 2u_d\zeta_2\rho_0^{\frac{3}{2}} - 3\zeta_2\pi u_d\rho_0^{\frac{1}{2}}\Big] + i2(\gamma + 2u_d\rho_0)|\zeta|^2 \Bigg\} \end{aligned} \tag{B.34}$$

Thanks to (B.33), we then obtain

$$\begin{aligned} S \simeq \int_{\mathbf{x}} \Big\{ & \zeta_2 \rho^{-\frac{1}{2}} \partial_t \pi - 2\zeta_1 \rho_0^{\frac{1}{2}} \partial_t \theta - \zeta_1 \rho_0^{-\frac{1}{2}} \pi \partial_t \theta + 2\zeta_2 K_c \rho_0^{-\frac{1}{2}} \nabla \pi \cdot \nabla \theta \\ & + \zeta_1 K_c \rho_0^{-\frac{1}{2}} \nabla^2 \pi - 2\zeta_1 K_c \rho_0^{\frac{1}{2}} (\nabla \theta)^2 - \zeta_1 K_c \rho_0^{-\frac{1}{2}} \pi (\nabla \theta)^2 + 2\zeta_2 K_c \rho_0^{\frac{1}{2}} \nabla^2 \theta \\ & + \zeta_2 K_c \rho_0^{-\frac{1}{2}} \pi \nabla^2 \theta + 2(u_c \zeta_1 - u d \zeta_2) \pi \rho_0^{\frac{1}{2}} + i2(\gamma + 2u_d \rho_0) |\zeta|^2 \Big\} \end{aligned} \tag{B.35}$$

We now consider the long distance and long time properties, and thus neglect all the linear and quadratic terms in the perturbation containing derivatives because they are negligible in the $(\omega, q) \to (0,0)$ limit, where ω and $\vec{q} = q\hat{\mathbf{u}}_{\vec{q}}$ are respectively the variable conjugated to t and $\vec{x}$; this correspond to the stationary, long-wavelength limit. Under this assumptions,

$$S \simeq 2 \int_{\mathbf{x}} \left\{ \rho_0^{\frac{1}{2}} \left[-\zeta_1 \left(\partial_t \theta + K_c (\nabla \theta)^2 \right) + \zeta_2 K_c \nabla^2 \theta - (u_c \zeta_1 - u_d \zeta_2) \pi \right] + i(\gamma + 2u_d \rho_0) |\zeta|^2 \right\} \hat{=} S' \tag{B.36}$$

leading to a partition function

$$Z = \int \mathscr{D}[\pi, \theta, \zeta_1, \zeta_2] e^{S'} = \int \mathscr{D}[\theta, \zeta_1, \zeta_2] \delta[u_c \zeta_1 - u_d \zeta_2] e^{iS''} = \int \mathscr{D}[\theta, \zeta_1] e^{iS'''} \tag{B.37}$$

with

$$\begin{aligned} S''' =& 2 \int_{\mathbf{x}} \left\{ \rho_0^{\frac{1}{2}} \left[-\zeta_1 \left(\partial_t \theta + K_c (\nabla \theta)^2 \right) + \frac{u_c K_c}{u_d} \zeta_1 \nabla^2 \theta \right] + i(\gamma + 2u_d \rho_0) \left(1 + \frac{u_c^2}{u_d^2} \right) \zeta_1^2 \right\} \\ =& \int_{\mathbf{x}} i\tilde{\theta} \left[\partial_t \theta + K_c (\nabla \theta)^2 - \frac{u_c K_c}{u_d} \nabla^2 \theta - \frac{\gamma + 2u_d \rho_0}{2\rho_0} \left(1 + \frac{u_c^2}{u_d^2} \right) \tilde{\theta} \right] \\ =& i S_{KPZ} \end{aligned} \tag{B.38}$$

where the response-field $\tilde{\theta} \doteq 2i\rho_0^{\frac{1}{2}} \zeta_1$ has been introduced and we identify the KPZ action for the phase field,

$$S_{KPZ}[\theta, \tilde{\theta}] \hat{=} \int_{\mathbf{x}} \tilde{\theta} \left[\partial_t \theta - D \nabla^2 \theta - \frac{\lambda}{2} (\nabla \theta)^2 - \Delta \tilde{\theta} \right] \tag{B.39}$$

with

$$\nu \hat{=} \frac{u_c K_c}{u_d}, \quad \lambda \hat{=} -2K_c, \quad D \hat{=} \frac{\gamma + 2u_d \rho_0}{2\rho_0} \left(1 + \frac{u_c^2}{u_d^2} \right) . \tag{B.40}$$

C Schwinger-Keldysh Field Theory for Inhomogeneous Exciton-Polaritons

In this appendix we extend the results presented in App. B to inhomogeneous EP. These inhomogeneities correspond to realistic effects present in actual experiments, such as confinement, disorder and thermal effects. For any of these cases, we will also analyse how the long-time and -distance mapping to KPZ equation is modified. We will recall some of the results already presented in the main text and detail the analytical calculations to get them. For the sake of simplicity we focus on the case $K_d = 0$. The extension to the case $K_d \neq 0$ presented in the main text is straightforward.

C.1 Exciton-Polariton under an External Potential

The first extension beyond the homogeneous case is the description of a one-body external potential. We start with the deterministic case, *i.e.* confinement or trapping, and then move to the random one, *i.e.* consider a disordered system.
As discussed in the main text in Chap. 3.1.1, in both cases the Hamiltonian of the problem is modified by the additional term

$$\mathcal{H}_{ext,dis} = \int \mathrm{d}\vec{x} \left[\psi^\dagger(\vec{x}) V_{ext,dis}(\vec{x}) \psi(\vec{x}) \right] \tag{C.1}$$

that corresponds to a term in the Keldysh action on the contour of the type

$$S_{ext,dis} = -\int \mathrm{d}\vec{x} \int_{-\infty}^{\infty} \mathrm{d}t \left[\psi_+^*(\mathbf{x}) V_{ext,dis,+}(\vec{x}) \psi_+(\mathbf{x}) - \psi_-^*(\mathbf{x}) V_{ext,dis,-}(\vec{x}) \psi_-(\mathbf{x}) \right] . \tag{C.2}$$

Doing the usual Keldysh rotation (B.17) and assuming a purely classical potential (i.e. a potential that is the same on both forward and backward contour) we obtain

$$S_{ext,dis} = -\int_{\mathbf{x}} V_{ext,dis} \left[\phi_q^* \phi_c + \phi_c^* \phi_q \right] . \tag{C.3}$$

C.1.1 KPZ mapping in the Deterministic Case

As introduced in the main text, a confinement potential results in a modification of the semiclassical limit (2.29), that is now an inhomogeneous PDE with an additive noise:

$$i\partial_t \phi_c(\mathbf{x}) = \left[-K_c \nabla^2 + r_c + V_{ext}(\vec{x}) + -r_d + (u_c - i u_d) |\phi_c|^2 \right] \phi_c(\mathbf{x}) + \xi(\mathbf{x}) . \tag{C.4}$$

For the mapping to KPZ equation the effects are more subtle. In the density-phase representation, (C.3) becomes $S_{int} = -2 \int_{\mathbf{x}} V_{ext}(\vec{x}) \rho^{\frac{1}{2}} \Re(\zeta)$, where $\Re(\zeta)$ stands for the real part of ζ. If we now perform a mean-field approximation over the densities, the assumption of a uniform density is not anymore a solution and (B.32) turns into (assuming $(\theta, \rho) \equiv (\theta_0(\vec{x}), \rho_0(\vec{x}))$)

$$\left(iK_c\rho_0^{-\frac{1}{2}}\nabla\rho_0\cdot\nabla\theta_0-\frac{K_c}{4}\rho_0^{-\frac{3}{2}}(\nabla\rho_0)^2+\frac{K_c}{2}\rho_0^{-\frac{1}{2}}\nabla^2\rho_0-K_c\rho_0^{\frac{1}{2}}(\nabla\theta_0)^2+iK_c\rho_0^{\frac{1}{2}}\nabla^2\theta_0-r_c\rho_0^{\frac{1}{2}}+ir_d\rho_0^{\frac{1}{2}}\right)$$
$$-(u_c-iu_d)\rho_0^{\frac{3}{2}}-V_{ext}\rho_0^{\frac{1}{2}}=0\,. \tag{C.5}$$

We now assume the spatial variation of the mean-field density, $\nabla\rho_0$, to be small compared to the homogeneous mean-field density (B.33) times the typical length-scale introduced by the external potential, i.e.

$$\nabla\rho_0(\vec{x})\frac{u_d\lambda_{V_{ext}}^{-1}}{r_d}=O(\epsilon),\qquad \epsilon\ll 1 \tag{C.6}$$

corresponding to the physical assumption that spatial fluctuations in the density are negligible when either the uniform density is large or the external potential is very smooth. Under this assumption (C.5) becomes algebraic for ρ_0, leading to

$$\left(-K_c(\nabla\theta_0)^2+iK_c\nabla^2\theta_0-r_c+ir_d\right)-(u_c-iu_d)\rho_0^{\frac{1}{2}}-V_{ext}=0\,. \tag{C.7}$$

Requiring both real and imaginary parts to vanish and assuming no cortex cores in the system (i.e. points where the density vanishes) we obtain

$$\rho_0(\vec{x})=-\frac{r_d+K_c\nabla^2\theta_0(\vec{x})}{u_d} \tag{C.8a}$$
$$\rho_0(\vec{x})=\frac{-V_{ext}(\vec{x})-r_c-K_c(\nabla\theta_0(\vec{x}))^2}{u_c} \tag{C.8b}$$

that is satisfied when

$$\frac{r_d+K_c\nabla^2\theta_0(\vec{x})}{u_d}=\frac{V_{ext}(\vec{x})+r_c+K_c(\nabla\theta_0(\vec{x}))^2}{u_c}\,. \tag{C.9}$$

Notice that in the limit in which the spatial variation of the phase plays no role (as in the equilibrium situation) (C.8) reduces to the well-known Thomas-Fermi approximation where r_c plays the role of the chemical potential. However, in the nonequilibrium case $\theta_0(x)$ must depend at least quadratically on x (otherwise (C.8) is never satisfied).
We now look at fluctuations of the densities around the mean-field solution and allow the phase to gain temporal dependence thanks to these fluctuations:

$$\zeta(\mathbf{x})=\zeta_1(\mathbf{x})+i\zeta_2(\mathbf{x}),\quad \rho(\mathbf{x})=\rho_0(\vec{x})+\pi(\mathbf{x}),\quad \theta(\mathbf{x})=\theta_0(\vec{x})+\theta_1(\mathbf{x}). \tag{C.10}$$

To quadratic order, upon forcing the mean-field solutions (C.8), the Keldysh action reads

$$\begin{aligned}S=\int_{\mathbf{x}}\Big\{&\zeta_2\rho_0^{-\frac{1}{2}}\partial_t\pi-2\zeta_1\rho_0^{\frac{1}{2}}\partial_t\theta_1-\zeta_1\rho_0^{-\frac{1}{2}}\pi\partial_t\theta_1+2\zeta_2K_c\rho_0^{-\frac{1}{2}}\nabla\rho_0\cdot\nabla\theta+\zeta_1K_c\rho_0^{-\frac{1}{2}}\nabla^2\rho_0-\zeta_1K_c\rho_0^{-\frac{1}{2}}\pi(\nabla\theta)^2\\&+\zeta_2K_c\rho_0^{-\frac{1}{2}}\pi\nabla^2\theta-\zeta_1V_{ext}\pi\rho_0^{-\frac{1}{2}}-3u_c\zeta_1\pi\rho_0^{\frac{1}{2}}+3\zeta_2\pi u_d\rho_0^{\frac{1}{2}}+\zeta_1r_c\pi\rho_0^{\frac{1}{2}}\frac{u_c}{r_c+V_{ext}+K_c(\nabla\theta_0)^2}\\&-\zeta_2\pi\rho_0^{\frac{1}{2}}\frac{r_du_d}{r_d+K_c\nabla^2\theta_0}+i2(\gamma+2u_d\rho_0)|\zeta|^2\Big\}\end{aligned} \tag{C.11}$$

In the stationary, long-wavelength limit introduced in Section B.2.2 the action reduces to

$$S = 2\int_{\mathbf{x}} \left\{ \rho_0^{\frac{1}{2}} \left[-\zeta_1 \partial_t \theta_1 - \frac{V_{ext}}{2}\rho_0^{-1}\zeta_1\pi - \frac{u_c\zeta_1\pi}{2}\left(3 - \frac{r_c}{r_c+V_{ext}}\right) + \zeta_2 K_c \nabla^2\theta_1 - \zeta_1 K_c(\nabla\theta_1)^2 + u_d\zeta_2\pi \right] + i(\gamma + 2u_d\rho_0)|\zeta|^2 \right\} \tag{C.12}$$

where

$$\frac{u_c}{r_c + V_{ext} + K_c(\nabla\theta)^2} \simeq \frac{u_c}{r_c+V_{ext}}\left(1 - \frac{K_c}{r_c+V_{ext}}(\nabla\theta)^2\right), \qquad \frac{u_d}{r_d + K_c\nabla^2\theta} \simeq \frac{u_d}{r_d}\left(1 - \frac{K_c}{r_d}\nabla^2\theta\right) \tag{C.13}$$

have been used. In the partition function the integration over π results in a Dirac-delta function relating ζ_1 and ζ_2. Using this, we end up with a partition function $Z = \int \mathscr{D}[\theta_1, \zeta_1] e^{iS'}$, with

$$\begin{aligned} S' = 2\int_{\mathbf{x}} \Bigg\{ & \rho_0^{\frac{1}{2}} \left[-\zeta_1\partial_t\theta_1 + \frac{K_c\zeta_1}{u_d}\left(\frac{V_{ext}}{2}\rho_0^{-1} + \frac{u_c}{2}\left(3 - \frac{r_c}{r_c+V_{ext}}\right)\right)\nabla^2\theta_1 - \zeta_1 K_c(\nabla\theta_1)^2 \right] \\ & + i(\gamma + 2u_d\rho_0)\zeta_1^2\left(1 + \frac{1}{u_d^2}\left(\frac{V_{ext}}{2}\rho_0^{-1} + \frac{u_c}{2}\left(3 - \frac{r_c}{r_c+V_{ext}}\right)\right)^2\right)\Bigg\}. \end{aligned} \tag{C.14}$$

If we now introduce the response field $\tilde{\theta} = \hat{=} 2i\rho_0^{\frac{1}{2}}\zeta_1$ and let $\theta_1 \to \theta$ we obtain

$$\begin{aligned} S' = \int_{\mathbf{x}} i\tilde{\theta}\Bigg\{ & \left[\partial_t\theta - \frac{K_c}{u_d}\left(\frac{V_{ext}}{2}\rho_0^{-1} + \frac{u_c}{2}\left(3 - \frac{r_c}{r_c+V_{ext}}\right)\right)\nabla^2\theta + K_c(\nabla\theta)^2\right] \\ & - \frac{\gamma + 2u_d\rho_0}{2\rho_0}\left(1 + \frac{1}{u_d^2}\left(\frac{V_{ext}}{2}\rho_0^{-1} + \frac{u_c}{2}\left(3 - \frac{r_c}{r_c+V_{ext}}\right)\right)^2\right)\tilde{\theta}\Bigg\} = iS_{KPZ} \end{aligned} \tag{C.15}$$

Using the definition (B.39) we can identify the KPZ coefficients in the case of an external spatial-dependent potential,

$$D(\vec{x}) \hat{=} \frac{K_c}{u_d}u_c(\vec{x}), \quad \lambda \hat{=} -2K_c, \quad \Delta(\vec{x}) \hat{=} \frac{\gamma + 2u_d\rho_0}{2\rho_0}\left(1 + \frac{1}{u_d^2}u_c^2(\vec{x})\right) \tag{C.16}$$

with

$$u_c(\vec{x}) = \frac{V_{ext}(\vec{x})}{2}\rho_0^{-1} + \frac{u_c}{2}\left(3 - \frac{r_c}{r_c + V_{ext}(\vec{x})}\right). \tag{C.17}$$

We see that in the $V_{ext}(\vec{x}) \to 0$ limit we recover (B.40). The same argument could be used with a generic $V_{ext}(\mathbf{x})$ adiabatically switched on and off as $t \to \pm\infty$ respectively.

C.1.2 Random Potential

We now consider the case in which the potential is random with zero mean and a Gaussian distribution,

$$P[V_{dis}] = \exp\left\{-\frac{1}{2}\int_{\mathbf{x},\mathbf{x}'} V_{dis}(\mathbf{x})G^{-1}(\mathbf{x}-\mathbf{x}')V_{dis}(\mathbf{x}')\right\}. \tag{C.18}$$

The explicit form of G depends on the choice of the second momentum of V_{dis}; we analyse different cases in the following. The physical observables are obtained by averaging over all the possible realizations of the disorder,

$$\left\langle \overline{O} \right\rangle = \int \mathcal{D}[\phi_c, \phi_c^*, \phi_q, \phi_q^*, V_{dis}] O(\phi_c, \phi_c^*, \phi_q, \phi_q^*) P[V_{dis}] e^{iS[V_{dis}]} . \tag{C.19}$$

In the following we focus on the implications the random potential has on the KPZ mapping. The effects of such a potential on the semi-classical limit will also be discussed.

KPZ mapping in presence of a random potential: delta-correlation in time and space

The easiest example of random potential is a delta-correlated one in both time and space,

$$\left\langle V_{dis}(\mathbf{x}) V_{dis}(\mathbf{x}') \right\rangle = \Gamma \delta(\mathbf{x} - \mathbf{x}') \tag{C.20}$$

Its contribution to the averaged partition function is thus

$$\begin{aligned} \overline{e^{iS_{dis}}} &= \int \mathcal{D}[V_{dis}] \exp\left\{ - \int_{\mathbf{x}} \left[\frac{V_{dis}^2(\mathbf{x})}{2\Gamma\tau} - i V_{dis}(\mathbf{x}) \left(\phi_q^*(\mathbf{x})\phi_c(\mathbf{x}) + \phi_c^*(\mathbf{x})\phi_q(\mathbf{x}) \right) \right] \right\} \\ &= \exp\left\{ -\frac{\Gamma\tau}{2} \int_{\mathbf{x}} \left(\phi_q^*(\mathbf{x})\phi_c(\mathbf{x}) + \phi_c^*(\mathbf{x})\phi_q(\mathbf{x}) \right)^2 \right\} \\ &= e^{iS_{dis,eff}} \end{aligned} \tag{C.21}$$

with

$$S_{dis,eff} = i\frac{\Gamma\tau}{2} \int_{\mathbf{x}} \left[\phi_q^{*2}(\mathbf{x})\phi_c^2(\mathbf{x}) + \phi_c^{*2}(\mathbf{x})\phi_q^2(\mathbf{x}) + 2\phi_q^*(\mathbf{x})\phi_c(\mathbf{x})\phi_c^*(\mathbf{x})\phi_q(\mathbf{x}) \right] . \tag{C.22}$$

When passing to a density-phase representation and performing a mean field approximation over densities (mean field equations are the same because terms introduced by disorder are at least linear in the quantum field) we obtain, for the fluctuations around the mean-field solution of the density (B.33)

$$S_{dis,eff} = i\frac{\Gamma\tau}{2} \int_{\mathbf{x}} \left[\left(\zeta_1^2 - 2i\zeta_1\zeta 2 - \zeta_2^2 \right) (\rho_0 + \pi) + c.c. + 2 \left(\zeta_1^2 + \zeta_2^2 \right) (\rho_0 + \pi) \right] = 2i\gamma\tau \int_{\mathbf{x}} (\rho_0 + \pi) \zeta_1^2 . \tag{C.23}$$

Keeping only terms up to second order,

$$S_{dis,eff} = 2i\gamma\tau \int_{\mathbf{x}} \rho_0 \zeta_1^2 \tag{C.24}$$

The delta-delta correlated random potential thus turns into a modification of the white noise in the KPZ mapping (B.40),

$$D \to D_{dis} = D + \frac{\gamma\tau}{2} . \tag{C.25}$$

We see that in the case in which the disorder is delta correlated, the effect on the KPZ mapping is just a shift in the noise correlator. The model should still fall in the KPZ universality class.

KPZ mapping in the presence of a random potential: general space-time correlation

We now relax the delta conditions on the correlations,

$$\left\langle V_{dis}(\mathbf{x}) V_{dis}(\mathbf{x}') \right\rangle = G(\mathbf{x}, \mathbf{x}') \tag{C.26}$$

which implies

$$\begin{aligned}\overline{e^{iS_{dis}}} &= \int \mathcal{D}[V_{dis}] \exp\left\{\int_{\mathbf{x},\mathbf{x}'}\left[V_{dis}(\mathbf{x})G^{-1}(\mathbf{x},\mathbf{x}')V_{dis}(\mathbf{x}') - iV_{dis}(\mathbf{x}')\left(\phi_q^*(\mathbf{x}')\phi_c(\mathbf{x}') + \phi_c^*(\mathbf{x}')\phi_q(\mathbf{x}')\right)\delta(\mathbf{x}-\mathbf{x}')\right]\right\} \\ &= \exp\left\{-\frac{1}{2}\int_{\mathbf{x},\mathbf{x}'}\left[\left(\phi_q^*(\mathbf{x})\phi_c(\mathbf{x}) + \phi_c^*(\mathbf{x})\phi_q(\mathbf{x})\right)G(\mathbf{x},\mathbf{x}')\left(\phi_q^*(\mathbf{x}')\phi_c(\mathbf{x}') + \phi_c^*(\mathbf{x}')\phi_q(\mathbf{x}')\right)\right]\right\} \\ &= e^{iS_{dis,eff}} \end{aligned} \tag{C.27}$$

with

$$S_{dis,eff} = \frac{i}{2}\int_{\mathbf{x},\mathbf{x}'}\left[\left(\phi_q^*(\mathbf{x})\phi_c(\mathbf{x}) + \phi_c^*(\mathbf{x})\phi_q(\mathbf{x})\right)G(\mathbf{x},\mathbf{x}')\left(\phi_q^*(\mathbf{x}')\phi_c(\mathbf{x}') + \phi_c^*(\mathbf{x}')\phi_q(\mathbf{x}')\right)\right]. \tag{C.28}$$

When passing to a density-phase representation this new term does not affect the mean-field equations for the densities, because is again at least linear in ϕ_q; in terms of fluctuations over the mean-field solution up to second order, we'll have

$$\begin{aligned} S_{dis,eff} =& i\rho_0\int_{\mathbf{x},\mathbf{x}'}G(\mathbf{x},\mathbf{x}')\left\{\left[\zeta_1(\mathbf{x}) + i\zeta_2(\mathbf{x})\right]\left[\zeta_1(\mathbf{x}') - i\zeta_2(\mathbf{x}')\right] + \frac{1}{2}\left[\left(\zeta_1(\mathbf{x}) + i\zeta_2(\mathbf{x})\right)\left(\zeta_1(\mathbf{x}') + i\zeta_2(\mathbf{x}')\right)\right]\right. \\ &\left. + \left(\zeta_1(\mathbf{x}) - i\zeta_2(\mathbf{x})\right)\left(\zeta_1(\mathbf{x}') - i\zeta_2(\mathbf{x}')\right)\right\} \\ =& 2i\rho_0\int_{\mathbf{x},\mathbf{x}'}\zeta_1(\mathbf{x})G(\mathbf{x},\mathbf{x}')\zeta_1(\mathbf{x}'). \end{aligned} \tag{C.29}$$

Introducing the response-field $\tilde{\theta}(\mathbf{x}) = 2i\rho_0^{\frac{1}{2}}\zeta_1(\mathbf{x})$, this can be rewritten as

$$S_{dis,eff} = -\frac{i}{2}\int_{\mathbf{x}}\tilde{\theta}(\mathbf{x})\int_{\mathbf{x}'}G(\mathbf{x},\mathbf{x}')\tilde{\theta}(\mathbf{x}') \tag{C.30}$$

which implies a modification of the white noise in the KPZ mapping (B.40) of the type

$$D\tilde{\theta}(\mathbf{x}) \to D_{dis}\tilde{\theta}(\mathbf{x}) = D\tilde{\theta}(\mathbf{x}) + \frac{1}{2}\int_{\mathbf{x}'}G(\mathbf{x},\mathbf{x}')\tilde{\theta}(\mathbf{x}') \tag{C.31}$$

A non-delta correlation in the disorder potential thus introduces a memory-kernel in the noise. This memory kernel, as discussed in the main text, could in principle affect the universal properties of the system. Indeed, while for short range enough spatial correlation the model still fall in the KPZ universality class [86, 87], this is no longer the case for long range spatial correlations.

Semi-classical limit in the presence of a random potential

The more interesting case for the semi-classical limit in an external random potential is the one-dimensional case where the quartic vertices arising in the disorder averaged Keldysh action are relevant in the long distance regime (see App. B). We will treat this contribution separately from the existing one and then merge the two.
It is interesting and useful to treat the very general case, with finite correlations in both time and space:

$$\left\langle V_{dis}(\mathbf{x})V_{dis}(\mathbf{x}')\right\rangle = G(\mathbf{x},\mathbf{x}') \tag{C.32}$$

which leads to a disorder-averaged contribution to the partition function of the type

$$\overline{e^{iS_{dis}}} = \exp\left\{-\int_{\mathbf{x},\mathbf{x}'} \frac{1}{2}\left[\left(\phi_q^*(\mathbf{x})\phi_c(\mathbf{x}) + \phi_c^*(\mathbf{x})\phi_q(\mathbf{x})\right) G(\mathbf{x},\mathbf{x}')\left(\phi_q^*(\mathbf{x}')\phi_c(\mathbf{x}') + \phi_c^*(\mathbf{x}')\phi_q(\mathbf{x}')\right)\right]\right\}$$
$$\hat{=} \exp\left\{-\int_{\mathbf{x},\mathbf{x}'} \frac{1}{2}\rho(\mathbf{x})G(\mathbf{x},\mathbf{x}')\rho(\mathbf{x}')\right\} \tag{C.33}$$

with $\rho(\mathbf{x})\hat{=}\phi_q^*(\mathbf{x})\phi_c(\mathbf{x}) + \phi_c^*(\mathbf{x})\phi_q(\mathbf{x})$. We now introduce the identity

$$1 = \int \mathcal{D}[\chi] \exp\left\{-\int_{\mathbf{x},\mathbf{x}'} \frac{1}{2}\chi(\mathbf{x})G^{-1}(\mathbf{x},\mathbf{x}')\chi(\mathbf{x}')\right\} \tag{C.34}$$

where $\int dy d\tau\, G^{-1}(x,y,t,\tau)G(y,x',\tau,t') = \delta(\mathbf{x}-\mathbf{x}')\ \forall t$ and $G^{-1}(\mathbf{x},\mathbf{x}')$ has a positive real part; after doing the shift

$$\chi(\mathbf{x}) \to \chi(\mathbf{x}) + i\int_{y,\tau} G(x,y,t,\tau)\rho(y,\tau) \tag{C.35}$$

and plugging the unity inside (C.33) we get

$$\overline{e^{iS_{dis}}} = \int \mathcal{D}[\chi] \exp\left\{-\int_{\mathbf{x},\mathbf{x}'} \frac{1}{2}\chi(\mathbf{x})G^{-1}(\mathbf{x},\mathbf{x}')\chi(\mathbf{x}') - i\int_{\mathbf{x}} \rho(\mathbf{x})\chi(\mathbf{x})\right\}$$
$$= \int \mathcal{D}[\chi] \exp\left\{-\int_{\mathbf{x},\mathbf{x}'} \frac{1}{2}\chi(\mathbf{x})G^{-1}(\mathbf{x},\mathbf{x}')\chi(\mathbf{x}') - i\int_{\mathbf{x}} \chi(\mathbf{x})\left[\phi_q^*(\mathbf{x})\phi_c(\mathbf{x}) + \phi_c^*(\mathbf{x})\phi_q(\mathbf{x})\right]\right\} \tag{C.36}$$

where we required $G(\mathbf{x},\mathbf{x}') = G(\mathbf{x}',\mathbf{x})$. Integrating out the quantum fields in the partition function and using the usual properties of Dirac's delta, the Langevin equation for the real part of ϕ_c(the one for the imaginary part comes straightforwardly) under this conditions reads

$$i\partial_t\phi_c = \left[-K_c\nabla^2 + r_c - ir_d + (u_c - iu_d)|\phi_c|^2 + \chi\right]\phi_c + \xi \tag{C.37}$$

where ξ and χ are normally distributed random variables with correlations

$$\left\langle \xi(\mathbf{x})\xi^*(\mathbf{x}')\right\rangle = (\gamma + 2u_d|\phi_c|^2)\delta(\mathbf{x}-\mathbf{x}'), \qquad \left\langle \chi(\mathbf{x})\chi(\mathbf{x}')\right\rangle = G(\mathbf{x},\mathbf{x}') \tag{C.38}$$

where we used the fact that if X is a random-variable with normal distribution $\mathcal{N}(0,\sigma^2)$ than aX is again a normally distributed random variable with distribution $\mathcal{N}(0,a^2\sigma^2)$. We now introduce $\zeta = \xi + \chi'$ with $\chi'(\mathbf{x}) = \phi_c(\mathbf{x})\chi(\mathbf{x})$ and

$$\left\langle \chi'(\mathbf{x})\chi'^*(\mathbf{x}')\right\rangle = \phi_c(\mathbf{x})\left\langle \chi(\mathbf{x})\chi(\mathbf{x}')\right\rangle \phi_c^*(\mathbf{x}') = \phi_c(\mathbf{x})G(\mathbf{x},\mathbf{x}')\phi_c^*(\mathbf{x}')\,. \tag{C.39}$$

The distribution of ζ is then $\mathcal{N}(0, Var(\xi) + Var(\chi'))$ thanks to properties of Gaussian random variables. Equation (C.37) becomes

$$i\partial_t\phi_c = \left[-K_c\nabla^2 + r_c - ir_d + (u_c - iu_d)|\phi_c|^2\right]\phi_c + \zeta \tag{C.40}$$

with $\left\langle \zeta(\mathbf{x})\zeta^*(\mathbf{x}')\right\rangle = \gamma\delta(\mathbf{x}-\mathbf{x}') + \phi_c(\mathbf{x})\left[2u_d\delta(\mathbf{x}-\mathbf{x}') + G(\mathbf{x},\mathbf{x}')\right]\phi_c^*(\mathbf{x}')$. We see that the Hubbard-Stratonovich field χ takes exactly the place V_{dis} would have taken if we had treated it as a deterministic potential, *i.e.* without averaging over its distribution. Indeed we still have in principle to take the average over the distribution of χ in the partition function, (C.36). This is because after averaging, a non-linear term

arises, which has to be made linear again via the introduction of the Hubbard-Stratonovich field in order to be able to take the semi-classical limit as we did in Chap. B. Hence we are not able to include the effect of the disorder in the semi-classical picture in a non-trivial way using this formalism. It would be interesting to formalize the semi-classical limit in a different way in order not to be forced to have a linear action in the fields $\phi_q^{(*)}$. Due to the triviality of this results we did not reported it in the main text.

C.2 Adding the phonon's contribution

In order to describe experimental setups it is important to include thermal fluctuations and thus thermally activated phonons pf the bulk of the semiconductor material. We will restrict the procedure to acoustic phonons. To model their interaction with the EP system we will use the Frölich Hamiltonian:

$$H_{ph} = \sum_{\vec{q}} \left\{ \omega_{\vec{q}} \hat{b}^\dagger_{\vec{q}} \hat{b}_{\vec{q}} + \int_k \left[G_{\vec{q}} \hat{b}_{\vec{q}} \hat{a}^\dagger(k+q_x)\hat{a}(k) + G^*_{\vec{q}} \hat{b}^\dagger_{\vec{q}} \hat{a}(k+q_x)\hat{a}^\dagger(k) \right] \right\} \tag{C.41}$$

with $\hat{a}^{(\dagger)}(k) = \int_x \hat{\psi}^{(\dagger)}(x) e^{-ikx}$ field operators in the one-dimensional EP system; here $\hat{b}^{(\dagger)}_{\vec{q}}$ is the annihilation (creation) field operator in momentum space for the phonon bath (assumed three-dimensional). For our purpose, it is better to switch to real space for the EP fields and to normal-order the resulting Hamiltonian, leading to

$$H_{ph} = \sum_{\vec{q}} \left\{ \omega_{\vec{q}} \hat{b}^\dagger_{\vec{q}} \hat{b}_{\vec{q}} + \int_x \left[G_{-q_x,q_y,q_z} \hat{b}_{-q_x,q_y,q_z} + G^*_{\vec{q}} \hat{b}^\dagger_{\vec{q}} \right] e^{-iq_x x} \hat{\psi}^\dagger(x)\hat{\psi}(x) \right\} + cst \tag{C.42}$$

where the constant term arises from the normal ordering procedure and will be neglected. Switching to a coherent state representation we obtain

$$H_{ph} = \sum_{\vec{q}} \left\{ \omega_{\vec{q}} b^*_{\vec{q}} b_{\vec{q}} + \int_x \left[G_{-q_x,q_y,q_z} b_{-q_x,q_y,q_z} + G^*_{\vec{q}} b^*_{\vec{q}} \right] e^{-iq_x x} \psi^*(x)\psi(x) \right\} . \tag{C.43}$$

If we now go to the Keldysh contour, we get an action of the type

$$\begin{aligned}
S_{ph} =& \sum_{\vec{q}} \Bigg\{ \int_{t,t'} \left(b^*_{\vec{q},+}(t), b^*_{\vec{q},-}(t) \right) \begin{pmatrix} \Gamma^{++}_{\vec{q}}(t,t') & \Gamma^{+-}_{\vec{q}}(t,t') \\ \Gamma^{-+}_{\vec{q}}(t,t') & \Gamma^{--}_{\vec{q}}(t,t') \end{pmatrix}^{-1} \begin{pmatrix} b_{\vec{q},+}(t) \\ b_{\vec{q},-}(t) \end{pmatrix} \\
&+ \int_{\mathbf{x}} b_{\vec{q},+}(t) \left[G_{\vec{q}} e^{iq_x x} \psi^*_+(\mathbf{x}) \psi_+(\mathbf{x}) \right] + b^*_{\vec{q},+}(t) \left[G^*_{\vec{q}} e^{-iq_x x} \psi^*_+(\mathbf{x}) \psi_+(\mathbf{x}) \right] \\
&- (\text{"-" contour}) \Bigg\} \\
=& \sum_{\vec{q}} \Bigg\{ \int_{t,t'} \left(b^*_{\vec{q},+}(t), b^*_{\vec{q},-}(t) \right) \begin{pmatrix} \Gamma^{++}_{\vec{q}}(t,t') & \Gamma^{+-}_{\vec{q}}(t,t') \\ \Gamma^{-+}_{\vec{q}}(t,t') & \Gamma^{--}_{\vec{q}}(t,t') \end{pmatrix}^{-1} \begin{pmatrix} b_{\vec{q},+}(t) \\ b_{\vec{q},-}(t) \end{pmatrix} \\
&+ \int_{\mathbf{x}} \Bigg[\left(b^*_{\vec{q},+}(t), b^*_{\vec{q},-}(t) \right) \begin{pmatrix} G^*_{\vec{q}} e^{-iq_x x} \psi^*_+(\mathbf{x}) \psi_+(\mathbf{x}) \\ -G^*_{\vec{q}} e^{-iq_x x} \psi^*_-(\mathbf{x}) \psi_-(\mathbf{x}) \end{pmatrix} \\
&+ \begin{pmatrix} b_{\vec{q},+}(t) \\ b_{\vec{q},-}(t) \end{pmatrix} \left(G_{\vec{q}} e^{iq_x x} \psi^*_+(\mathbf{x}) \psi_+(\mathbf{x}), -G_{\vec{q}} e^{iq_x x} \psi^*_-(\mathbf{x}) \psi_-(\mathbf{x}) \right) \Bigg] \Bigg\} \\
\hat{=}& \sum_{\vec{q}} \Bigg\{ \int_{t,t'} \left(b^*_{\vec{q},+}(t), b^*_{\vec{q},-}(t) \right) \begin{pmatrix} \Gamma^{++}_{\vec{q}}(t,t') & \Gamma^{+-}_{\vec{q}}(t,t') \\ \Gamma^{-+}_{\vec{q}}(t,t') & \Gamma^{--}_{\vec{q}}(t,t') \end{pmatrix}^{-1} \begin{pmatrix} b_{\vec{q},+}(t) \\ b_{\vec{q},-}(t) \end{pmatrix} \\
&+ \int_{\mathbf{x}} \left[G^*_{\vec{q}} e^{-iq_x x} \left(b^*_{\vec{q},+}(t), b^*_{\vec{q},-}(t) \right) \begin{pmatrix} \Phi_+(\mathbf{x}) \\ -\Phi_-(\mathbf{x}) \end{pmatrix} + G_{\vec{q}} e^{iq_x x} \begin{pmatrix} b_{\vec{q},+}(t) \\ b_{\vec{q},-}(t) \end{pmatrix} (\Phi_+(\mathbf{x}), -\Phi_-(\mathbf{x})) \right] \Bigg\}, \qquad \text{(C.44)}
\end{aligned}$$

where [133, 134, 84]

$$\begin{aligned}
\Gamma^{+-}_{\vec{q}}(t,t') =& -in(\omega_{\vec{q}}) e^{-i\omega_{\vec{q}}(t-t')}, & \Gamma^{-+}_{\vec{q}}(t,t') =& -i\left(n(\omega_{\vec{q}})+1\right) e^{-i\omega_{\vec{q}}(t-t')} \\
\Gamma^{++}_{\vec{q}}(t,t') =& \theta(t-t')\Gamma^{-+}_{\vec{q}}(t,t') + \theta(t'-t)\Gamma^{+-}_{\vec{q}}(t,t'), & \Gamma^{--}_{\vec{q}}(t,t') =& \theta(t'-t)\Gamma^{-+}_{\vec{q}}(t,t') + \theta(t-t')\Gamma^{+-}_{\vec{q}}(t,t')
\end{aligned} \qquad \text{(C.45)}$$

with $n(\omega_{\vec{q}})$ the average occupation number for the phononic mode $\vec{q}$ in the bath assumed at thermal equilibrium as $t \to -\infty$, and we defined $\Phi(\mathbf{x}) = \psi^*(\mathbf{x})\psi(\mathbf{x})$. This action is quadratic in the phonon-bath fields and we can integrate them out in the partition function, leading to an effective action looking like

$$\begin{aligned}
S_{ph,eff} =& -\sum_{\vec{q}} |G_{\vec{q}}|^2 \int_{\mathbf{x},\mathbf{x}'} e^{iq_x(x-x')} (\Phi_+(\mathbf{x}), -\Phi_-(\mathbf{x})) \begin{pmatrix} \Gamma^{++}_{\vec{q}}(t,t') & \Gamma^{+-}_{\vec{q}}(t,t') \\ \Gamma^{-+}_{\vec{q}}(t,t') & \Gamma^{--}_{\vec{q}}(t,t') \end{pmatrix} \begin{pmatrix} \Phi_+(\mathbf{x}') \\ -\Phi_-(\mathbf{x}') \end{pmatrix} \\
=& -\sum_{\vec{q}} |G_{\vec{q}}|^2 \int_{\mathbf{x},\mathbf{x}'} e^{iq_x(x-x')} \hat{\Phi}^t(\mathbf{x}) \hat{\Gamma}_{\vec{q}}(t,t') \hat{\Phi}(\mathbf{x}'), \qquad \text{(C.46)}
\end{aligned}$$

with

$$\hat{\Phi}(\mathbf{x}) = \begin{pmatrix} \Phi_+(\mathbf{x}) \\ -\Phi_-(\mathbf{x}) \end{pmatrix}, \qquad \hat{\Gamma}_{\vec{q}}(t,t') = \begin{pmatrix} \Gamma^{++}_{\vec{q}}(t,t') & \Gamma^{+-}_{\vec{q}}(t,t') \\ \Gamma^{-+}_{\vec{q}}(t,t') & \Gamma^{--}_{\vec{q}}(t,t') \end{pmatrix}. \qquad \text{(C.47)}$$

This action is in principle quartic in the classical and quantum Keldysh fields ϕ_c, ϕ_q. In order to treat its semi-classical limit we are interested in getting rid of all the non-linear terms in ϕ_q.

C.2.1 Full time dependence

We now try to directly decouple the effective quartic interactions stemming out from (C.46); before doing that it is important to understand the physical role of each of the term. To do so we perform Keldysh rotation

$$\Phi_+(\mathbf{x}) = \frac{1}{2}\left(\phi_c^* + \phi_q^*\right)\left(\phi_c + \phi_q\right), \qquad \Phi_-(\mathbf{x}) = \frac{1}{2}\left(\phi_c^* - \phi_q^*\right)\left(\phi_c - \phi_q\right). \tag{C.48}$$

We see that four kind of vertices arise from (C.46):

- Quartic and cubic terms in ϕ_q: we neglect them because they are irrelevant in the semi-classical limit for both three and one dimensional systems.
- Quadratic terms in ϕ_q: we keep them and try to decouple them in order to easily get an associated Langevin-like equation for ϕ_c in the semi-classical limit.
- Linear terms in ϕ_q: we keep them and they give a coherent contribution to the Keldysh action.
- 0-th order terms in ϕ_q: we should keep them in the semi-classical limit according to a power-counting argument but we expect them to vanish because of the probability-conservation constraint $S(\phi_c, 0) = 0$; indeed this is the case because $\Gamma^{++} + \Gamma^{--} - \Gamma^{-+} - \Gamma^{+-} = 0$, as one could easily check from the discrete formulation of (C.45).

For the linear part we get, after some simple algebra,

$$\begin{aligned} S_l =& \frac{1}{4}\sum_{\vec{q}} |G_{\vec{q}}|^2 \int_{\mathbf{x},\mathbf{x}'} \left(\phi_q^*(\mathbf{x})\phi_c(\mathbf{x})\phi_c^*(\mathbf{x}')\phi_c(\mathbf{x}') + \phi_q(\mathbf{x})\phi_c^*(\mathbf{x})\phi_c(\mathbf{x}')\phi_c^*(\mathbf{x}')\right) \Big\{ e^{iq_x(x-x')}\Big[\Gamma_{\vec{q}}^{++}(t,t') \\ &+\Gamma_{\vec{q}}^{-+}(t,t') - \Gamma_{\vec{q}}^{+-}(t,t') - \Gamma_{\vec{q}}^{--}(t,t')\Big] + e^{-iq_x(x-x')}\Big[\Gamma_{\vec{q}}^{++}(t',t) - \Gamma_{\vec{q}}^{-+}(t',t) + \Gamma_{\vec{q}}^{+-}(t',t) - \Gamma_{\vec{q}}^{--}(t',t)\Big]\Big\}. \end{aligned} \tag{C.49}$$

Using the definitions (C.45), Eq. (C.49) reduces to

$$\begin{aligned} S_l =& \frac{i}{4}\sum_{\vec{q}} |G_{\vec{q}}|^2 \int_{\mathbf{x},\mathbf{x}'} \left(\phi_q^*(\mathbf{x})\phi_c(\mathbf{x})\phi_c^*(\mathbf{x}')\phi_c(\mathbf{x}') + \phi_q(\mathbf{x})\phi_c^*(\mathbf{x})\phi_c(\mathbf{x}')\phi_c^*(\mathbf{x}')\right)\Big[e^{iq_x(x-x')-i\omega_{\vec{q}}(t'-t)} \\ &-e^{-iq_x(x-x')+i\omega_{\vec{q}}(t'-t)}\Big]\left[\theta(t-t') - \theta(t'-t) + 1\right]. \end{aligned} \tag{C.50}$$

For the quadratic terms in ϕ_q, ϕ_q^* we get a more involved contribution,

$$\begin{aligned} S_b =& -\frac{1}{4}\sum_{\vec{q}} |G_{\vec{q}}|^2 \int_{\mathbf{x},\mathbf{x}'} \phi_q^*(\mathbf{x})\phi_q(\mathbf{x}) \Big\{ e^{iq_x(x-x')}\Big[\Gamma_{\vec{q}}^{++}(t,t') + \Gamma_{\vec{q}}^{--}(t,t') + \Gamma_{\vec{q}}^{+-}(t,t') + \Gamma_{\vec{q}}^{-+}(t,t')\Big] \\ &+ e^{-iq_x(x-x')}\Big[\Gamma_{\vec{q}}^{++}(t',t) + \Gamma_{\vec{q}}^{--}(t',t) + \Gamma_{\vec{q}}^{+-}(t',t) + \Gamma_{\vec{q}}^{-+}(t',t)\Big]\Big\}\phi_c^*(\mathbf{x}')\phi_c(\mathbf{x}') + e^{iq_x(x-x')}\Big[\Gamma_{\vec{q}}^{++}(t,t') \\ &+\Gamma_{\vec{q}}^{--}(t,t') - \Gamma_{\vec{q}}^{+-}(t,t') - \Gamma_{\vec{q}}^{-+}(t,t')\Big]\left(\phi_q^*(\mathbf{x})\phi_c(\mathbf{x}),\ \phi_c^*(\mathbf{x})\phi_q(\mathbf{x})\right)\begin{pmatrix}1 & 1\\ 1 & 1\end{pmatrix}\begin{pmatrix}\phi_q^*(\mathbf{x}')\phi_c(\mathbf{x}')\\ \phi_c^*(\mathbf{x}')\phi_q(\mathbf{x}')\end{pmatrix} \\ =& i\sum_{\vec{q}} |G_{\vec{q}}|^2 \left(2n(\omega_{\vec{q}}) + 1\right)\int_{\mathbf{x}} \phi_q^*(\mathbf{x})\phi_q(\mathbf{x}) \int_{\mathbf{x}'} \cos\left(q_x(x-x') - \omega_{\vec{q}}(t-t')\right)\phi_c^*(\mathbf{x}')\phi_c(\mathbf{x}'). \end{aligned} \tag{C.51}$$

Using a simple Hubbard-Stratonovich transformation, one can see that this term gives rise to a multiplicative Gaussian noise of the type

$$\mathcal{P}[\xi] = \exp\left\{-\frac{1}{2}\int_{\mathbf{x},\mathbf{x}'} \xi^*(\mathbf{x}) M^{-1}(\mathbf{x}-\mathbf{x}')\xi(\mathbf{x}')\right\} \tag{C.52}$$

$$\left\langle \xi^*(\mathbf{x})\xi(\mathbf{x}')\right\rangle = 2\sum_{\vec{q}} |G_{\vec{q}}|^2 \left(2n(\omega_{\vec{q}})+1\right) \int_{x'',t''} \cos\left(q_x(x-x'') - \omega_{\vec{q}}(t-t'')\right) \phi_c^*(x'',t'')\phi_c(x'',t'')\delta(\mathbf{x}-\mathbf{x}') \tag{C.53}$$

with

$$M^{-1}(\mathbf{x}-\mathbf{x}')M(\mathbf{x}-\mathbf{x}') = \delta(\mathbf{x}-\mathbf{x}') \tag{C.54}$$

and

$$M(\mathbf{x}-\mathbf{x}') = 2\sum_{\vec{q}} |G_{\vec{q}}|^2 \left(2n(\omega_{\vec{q}})+1\right) \int_{x'',t''} \cos\left(q_x(x-x'') - \omega_{\vec{q}}(t-t'')\right) \phi_c^*(x'',t'')\phi_c(x'',t'')\delta(\mathbf{x}-\mathbf{x}')\,. \tag{C.55}$$

The same type of noise was derived by Savenko et al. [90]. This result holds for a general bath in thermal equilibrium. In the following we focus on the case in which the time-scales of the bath and of the systems are decoupled, and no back-action of the system on the bath is present.

C.2.2 Markovian approximation

We now take the limit of densely lying phononic modes centred around some typical frequency ω_0 with a bandwidth θ and then switch to a continuum notation; for the sake of simplicity we assume the phonon bath to be 1D and acoustic,

$$\sum_{q_x} |G_{q_x}|^2 e^{iq_x(x-x')} \to \int_{\omega_0-\theta}^{\omega_0+\theta} \frac{1}{2\pi}\nu(\omega)|G(\omega)|^2 e^{i\frac{\omega}{u}(x-x')} \tag{C.56}$$

where $\nu(\omega)$ is the phononic density of state and u is the sound velocity inside the bath; generalization to higher dimensional baths with more complicated dispersion relation can be done. We furthermore take advantages of the form of the bosonic propagator $\Gamma(t,t') \equiv \Gamma(t-t')$ and assume that the evolution in the system is much slower than both the evolution in the bath and its autocorrelation, i.e. $\omega_{sys} \ll \omega_0, \theta$. This assumption is the analogue of a Markov approximation and leads to an effective action local in time. In the evaluation of tadpole graph however this locality can produce some ambiguities and thus we should keep in mind the real nature of the non-local action [84]. For this purpose we indicate $t' = t \pm \tau$ as $t \pm \delta$. We then focus on each of the four terms in Γ separately:

- Γ^{+-}

$$-i\int_{\mathbf{x},x',\tau} \Phi_+(\mathbf{x})\Phi_-(x',t-\delta) \int_{\omega_0-\theta}^{\omega_0+\theta} \frac{1}{2\pi}\nu(\omega)|G(\omega)|^2 n(\omega) e^{i\frac{\omega}{u}(x-x')} e^{-i\omega\tau} = -i\int_{\mathbf{x},x'} \Phi_+(\mathbf{x})\Phi_-(x',t-\delta)$$
$$\times \int_{\omega_0-\theta}^{\omega_0+\theta} \frac{1}{2\pi}\nu(\omega)|G(\omega)|^2 n(\omega) e^{i\frac{\omega}{u}(x-x')}\delta(\omega) \simeq -i\nu(\omega_0)n(\omega_0)|G(\omega_0)|^2 \int_{\mathbf{x},x'} e^{i\frac{\omega_0}{u}(x-x')}\Phi_+(\mathbf{x})\Phi_-(x',t-\delta) \tag{C.57}$$

  where in the last passage we took the $\theta \to \infty$ limit.

- Γ^{-+}
  Using a similar argument for Γ^{-+},

$$
\begin{aligned}
&- i \int_{\mathbf{x},x',\tau} \Phi_-(\mathbf{x})\Phi_+(x',t-\delta) \int_{\omega_0-\theta}^{\omega_0+\theta} \frac{1}{2\pi} \nu(\omega) |G(\omega)|^2 [n(\omega)+1]\, e^{i\frac{\omega}{u}(x-x')} e^{-i\omega\tau} \\
&\simeq -i\nu(\omega_0)[n(\omega_0)+1]|G(\omega_0)|^2 \int_{\mathbf{x},x'} e^{i\frac{\omega_0}{u}(x-x')} \Phi_-(\mathbf{x})\Phi_+(x',t-\delta)
\end{aligned} \tag{C.58}
$$

- Γ^{++}

$$
i \int_{\mathbf{x},x',\tau} \Phi_+(\mathbf{x})\Phi_+(x',t-\delta) \int_{\omega_0-\theta}^{\omega_0+\theta} \frac{1}{2\pi} \nu(\omega) |G(\omega)|^2 e^{i\frac{\omega}{u}(x-x')} \left\{\theta(\tau)[n(\omega)+1] + \theta(-\tau) n(\omega)\right\} e^{-i\omega\tau} \tag{C.59}
$$

  Now,

$$
\begin{aligned}
&\int_\tau \theta(\tau) \int_{\omega_0-\theta}^{\omega_0+\theta} \frac{1}{2\pi}[n(\omega)+1]\, e^{-i\omega\tau} = \lim_{\epsilon\to 0} \int_{\omega_0-\theta}^{\omega_0+\theta} \frac{1}{2\pi}[n(\omega)+1] \int_0^\infty d\tau\, e^{-\epsilon\tau} e^{-i\omega\tau} \\
&= \lim_{\epsilon\to 0} \int_{\omega_0-\theta}^{\omega_0+\theta} \frac{1}{2\pi}[n(\omega)+1] \left\{ \frac{\epsilon}{\epsilon^2+\omega} - i\frac{\omega}{\epsilon^2+\omega} \right\} = \int_{\omega_0-\theta}^{\omega_0+\theta} \frac{1}{2\pi}[n(\omega)+1] \left\{ \pi\delta(\omega) - i\mathcal{P}\frac{1}{\omega} \right\}
\end{aligned} \tag{C.60}
$$

  where we used the definition

$$
\theta(x) = \begin{cases} \lim_{\epsilon\to 0} e^{-\epsilon x} & \text{if } x \geq 0 \\ 0 & \text{if } x < 0 \end{cases} . \tag{C.61}
$$

  A similar result comes from the $\theta(-\tau)$ term apart from $\Phi_+(x',t-\delta) \to \Phi_+(x',t+\delta)$ due to the presence of $-\tau$ in the Heaviside's theta function. Hence, taking the $\theta \to \infty$ limit, (C.59) becomes

$$
\simeq \frac{i}{2}\nu(\omega_0)|G(\omega_0)|^2 \int_{\mathbf{x},x'} e^{i\frac{\omega}{u}(x-x')} \Phi_+(\mathbf{x}) \left\{ [n(\omega_0)+1]\Phi_+(x',t-\delta) + n(\omega_0)\Phi_+(x',t+\delta) \right\}, \tag{C.62}
$$

  where we neglected the principal values. This term, usually referred to as "Lamb shift", gives a contribution to the coherent dynamics of the system of the same physical nature as the dissipative one but it typically renormalizes the Hamiltonian coefficients in a sub-dominant way [84].

- Γ^{--}
  Using a similar argument for Γ^{--},

$$
\begin{aligned}
&i \int_{\mathbf{x},x',\tau} \Phi_-(\mathbf{x})\Phi_-(x',t-\delta) \int_{\omega_0-\theta}^{\omega_0+\theta} \frac{1}{2\pi} \nu(\omega) |G(\omega)|^2 e^{i\frac{\omega}{u}(x-x')} \left\{\theta(-\tau)[n(\omega)+1] + \theta(\tau) n(\omega)\right\} e^{-i\omega\tau} \\
&\simeq \frac{i}{2}\nu(\omega_0)|G(\omega_0)|^2 \int_{\mathbf{x},x'} e^{i\frac{\omega_0}{u}(x-x')} \Phi_+(\mathbf{x}) \left\{ [n(\omega_0)+1]\Phi_+(x',t+\delta) + n(\omega_0)\Phi_+(x',t-\delta) \right\} .
\end{aligned} \tag{C.63}
$$

Putting all the terms together and neglecting the regularization prescription $\pm\delta$ we get

$$\begin{aligned}S_{ph,eff} =& -i\nu(\omega_0)|G(\omega_0)|^2\int_{\mathbf{x},x'} e^{i\frac{\omega_0}{u}(x-x')}\Big\{(n(\omega_0)+1)\Big[\Phi_-(\mathbf{x})\Phi_+(x',t)-\frac{1}{2}\left(\Phi_+(\mathbf{x})\Phi_+(x',t)\right.\\ &\left.+\Phi_-(\mathbf{x})\Phi_-(x',t)\right)\Big]+n(\omega_0)\left[\Phi_+(\mathbf{x})\Phi_-(x',t)-\frac{1}{2}\left(\Phi_+(\mathbf{x})\Phi_+(x',t)+\Phi_-(\mathbf{x})\Phi_-(x',t)\right)\right]\Big\}\\ =& i\nu(\omega_0)|G(\omega_0)|^2\int_{\mathbf{x},x'} e^{i\frac{\omega_0}{u}(x-x')}\left(\Phi_+(\mathbf{x}),-\Phi_-(\mathbf{x})\right)\begin{pmatrix}n(\omega_0)+\frac{1}{2} & n(\omega_0)\\ n(\omega_0)+1 & n(\omega_0)+\frac{1}{2}\end{pmatrix}\begin{pmatrix}\Phi_+(x',t)\\ -\Phi_-(x',t)\end{pmatrix}.\end{aligned} \tag{C.64}$$

We now perform the usual Keldysh rotation and, following the same argument as in Chap. C.2.1, we treat separately the linear and quadratic contributions in ϕ_q, and neglect higher order vertices. For the linear part we get, after substituting the set of Markovian Γs in (C.49),

$$\begin{aligned}S_{l,mk} =& \frac{i}{4}\nu(\omega_0)|G(\omega_0)|^2\int_{\mathbf{x},x'}\left[\phi_q^*(\mathbf{x})\phi_c(\mathbf{x})\phi_c^*(x',t)\phi_c(x',t)+\phi_q(\mathbf{x})\phi_c^*(\mathbf{x})\phi_c(x',t)\phi_c^*(x',t)\right]\\ &\times\left(e^{i\frac{\omega_0}{u}(x-x')}-e^{-i\frac{\omega_0}{u}(x-x')}\right)\\ =& \frac{i}{2}\nu(\omega_0)|G(\omega_0)|^2\int_{\mathbf{x},x'}\left[\phi_q^*(\mathbf{x})\phi_c(\mathbf{x})\phi_c^*(x',t)\phi_c(x',t)+\phi_q(\mathbf{x})\phi_c^*(\mathbf{x})\phi_c(x',t)\phi_c^*(x',t)\right]\sin\left(\frac{\omega_0}{u}(x-x')\right).\end{aligned} \tag{C.65}$$

We do the same for the quadratic term (C.51), getting

$$\begin{aligned}S_{b,mk} =& \frac{i}{2}\nu(\omega_0)|G(\omega_0)|^2(2n(\omega_0)+1)\int_{\mathbf{x},x'}\phi_q^*(\mathbf{x})\phi_q(\mathbf{x})\phi_c^*(x',t)\phi_c(x',t)\left(e^{i\frac{\omega_0}{u}(x-x')}+e^{-i\frac{\omega_0}{u}(x-x')}\right)\\ =& i\nu(\omega_0)|G(\omega_0)|^2(2n(\omega_0)+1)\int_{\mathbf{x},x'}\phi_q^*(\mathbf{x})\phi_q(\mathbf{x})\phi_c^*(x',t)\phi_c(x',t)\cos\left(\frac{\omega_0}{u}(x-x')\right).\end{aligned} \tag{C.66}$$

Decoupling this term, gives rise to a multiplicative white noise of the type

$$\mathcal{P}[\xi]=\exp\left\{-\frac{1}{2}\int_{\mathbf{x},\mathbf{x}'}\xi^*(\mathbf{x})M^{-1}(\mathbf{x}-\mathbf{x}')\xi(\mathbf{x}')\right\} \tag{C.67}$$

$$\left\langle\xi_q^*(\mathbf{x})\xi_q(\mathbf{x}')\right\rangle=2\nu(\omega_0)|G(\omega_0)|^2(2n(\omega_0)+1)\int_{x''}\cos\left(\frac{\omega_0}{u}(x-x'')\right)\phi_c^*(x'',t)\phi_c(x'',t)\delta(\mathbf{x}-\mathbf{x}') \tag{C.68}$$

with

$$M^{-1}(\mathbf{x}-\mathbf{x}')M(\mathbf{x}-\mathbf{x}')=\delta(\mathbf{x}-\mathbf{x}') \tag{C.69}$$

and

$$M(\mathbf{x}-\mathbf{x}')=2\nu(\omega_0)|G(\omega_0)|^2(2n(\omega_0)+1)\int_{x''}\cos\left(\frac{\omega_0}{u}(x-x'')\right)\phi_c^*(x'',t)\phi_c(x'',t)\delta(\mathbf{x}-\mathbf{x}'). \tag{C.70}$$

The effective contribution to the EP dynamics coming from the Markovian phonon bath is thus

$$S_{mk}=S_{l,mk}+S_{b,mk}, \tag{C.71}$$

as presented in the main text.

D About Cumulant Expansions and Complex Exponentials

The purpose of this appendix is to write a cumulant expansion for the exponential of the phase-phase correlators at different space and times. The usual method to extract momenta of a random variable χ starting from its moment-generating function $\langle e^{t\chi}\rangle$ id to write

$$\begin{aligned}\langle e^{t\chi}\rangle &= 1 + t\langle\chi\rangle + \frac{t^2}{2}\langle\chi^2\rangle + O(\langle\chi^3\rangle) \simeq e^{t\langle\chi\rangle + \frac{t^2}{2}\langle\chi^2\rangle} \\ &\to \log\left(\langle e^{\chi}\rangle\right) \simeq t\langle\chi\rangle + \frac{t^2}{2}\langle\chi^2\rangle\,. \end{aligned} \tag{D.1}$$

This method turns out to be difficult to use in our case. The first problem is the complex nature of the argument, which implies that any general ratio of $g_1(x,t) = \langle\psi^*(0,0)\psi(x,t)\rangle \simeq \rho_0\langle\exp\left(i\Delta\theta(x,t)\right)\rangle = \rho_0\tilde{g}_1(x,t)$ is in principle a complex function. The logarithm of such ratios cannot be taken naively as we do in the real case. The other difficulty comes from the fact that the random variable $\Delta\theta$ is not centred. It is value is indeed expected to behave as

$$\Delta\theta(x,t) \simeq v_\infty t + (\Gamma t)^\beta\chi \tag{D.2}$$

with $\beta < 1$. Extracting the v_∞ parameter can be done by noting that

$$\langle\Delta\theta(x,t)\rangle = \arg\left(\tilde{g}_1(x,t)\right) \to \lim_{t\to\infty}\frac{\arg\left(\tilde{g}_1(x,t)\right)}{t} = v_\infty \tag{D.3}$$

Another useful quantity out of $\tilde{g}_1$ is its squared modulus. Indeed

$$\begin{aligned}|g_1(x,t)|^2 &= \left(\sum_{k=0}^{\infty}\frac{i^k}{k!}\langle\Delta\theta(x,t)^k\rangle\right)\left(\sum_{\ell=0}^{\infty}\frac{(-1)^\ell i^\ell}{\ell!}\langle\Delta\theta(x,t)^\ell\rangle\right) = \sum_{k=0}^{\infty}\sum_{\ell=0}^{k}\frac{(-1)^{k-\ell}}{\ell!(k-\ell)!}i^k\langle\Delta\theta(x,t)^\ell\rangle\langle\Delta\theta(x,t)^{k-\ell}\rangle \\ &= 1 - \langle\Delta\theta(x,t)^2\rangle + \langle\Delta\theta(x,t)\rangle^2 + \frac{1}{12}\langle\Delta\theta(x,t)^4\rangle - \frac{1}{3}\langle\Delta\theta(x,t)\rangle\langle\Delta\theta(x,t)^3\rangle + \frac{1}{4}\langle\Delta\theta(x,t)^2\rangle^2 \\ &\quad - \frac{1}{360}\langle\Delta\theta(x,t)^6\rangle + \frac{1}{60}\langle\Delta\theta(x,t)\rangle\langle\Delta\theta(x,t)^5\rangle - \frac{1}{24}\langle\Delta\theta(x,t)^2\rangle\langle\Delta\theta(x,t)^4\rangle + \frac{1}{36}\langle\Delta\theta(x,t)^3\rangle^2 \\ &\quad + O(\langle\Delta\theta(x,t)^8\rangle) \\ &\simeq \exp(-\langle\Delta\theta(x,t)^2\rangle + \langle\Delta\theta(x,t)\rangle^2) = \exp(-\mathrm{Var}\Delta\theta(x,t)) \sim \exp(-(\Gamma t)^{2\beta}\mathrm{Var}(\chi)) \end{aligned} \tag{D.4}$$

where $\sum_{i=0}^{\infty}a_i\cdot\sum_{k=0}^{\infty}b_k = \sum_{n=0}^{\infty}\sum_{m=0}^{\infty}a_m b_{n-m}$ has been used. We then expect

$$-\log(|g_1(x,t)|^2) \sim (\Gamma t)^{2\beta}\mathrm{Var}(\chi) \tag{D.5}$$

This quantity is the one we determined in numerical simulations. Such observable could be in principle a good starting point for getting the variance of χ, which is a known quantity. Indeed,

$$-\lim_{t\to\infty}\frac{\log(|g_1(x,t)|^2)}{(\Gamma t)^{2\beta}} = \mathrm{Var}(\chi) \tag{D.6}$$

The microscopic parameter Γ can thus in principle be extracted from the fit of the re-scaled function $\tilde{g}_1$ with the theoretical scaling function $g(y)$. Accessing higher order momenta starting from just the two-point function $\tilde{g}_1$ is very difficult in practice. The only quantity that seems accessible is the variance of χ.

E Non-Perturbative Renormalization Group and its Application to KPZ Equation

In this Appendix we will introduce the Non Perturbative Renormalization Group (NPRG) technique in a slightly more technical way than in the main text. After a general basic introduction we will see how to apply this formalism to KPZ equation and how to recover perturbative results with a simple ansatz. We will then give some example of NPRG calculations for the pure KPZ equation. These are useful in the next chapter, where new calculations for the broken GI case are performed.

E.1 NPRG as Generalization of Momentum-Shell RG

Non-perturbative Renormalization Group (NPRG) is a smart generalization of the Wilson's momentum-shell RG, in which fluctuations linked to higher momenta are subsequently integrated out in order to obtain the long range effective behaviour of the system (see [135, 136]). In the Wilson's idea however, the momentum shell is finite or equivalently the cut-off of the momentum integration is sharp. The NPRG idea, introduced by Polchinski in [19], consists in introducing a smooth cut-off function which allows to follow the entire RG flow and not just to focus on a finite momentum shell. In order to smoothly integrate out high-energy fluctuations while going towards the infrared, we introduce an effective mass in the theory which has the role of freezing out low-energy modes in the integration:

$$\Delta S_\kappa = \frac{1}{2}\int_{\mathbf{q}} h_i(-\mathbf{q})[R_\kappa(\mathbf{q})]_{ij} h_j(\mathbf{q})\,. \tag{E.1}$$

The quantity κ is the physical momentum scale at which we are looking at the system. The regulator R_κ must satisfy the following limits:

- $q^2 \gg \kappa^2$
  We want the fast modes to be easily integrated by the flow, and thus have no additional mass:

$$R_\kappa(\mathbf{q}) \to 0 \tag{E.2a}$$

- $q^2 \ll \kappa^2$
  We want the slow modes to be frozen, and thus have a large mass:

$$R_\kappa(\mathbf{q}) \to \kappa^2 \tag{E.2b}$$

- $\kappa \to \Lambda^2$
  At the microscopic level we want to recover the mean field (MF) description where no fluctuations have been integrated yet, *i.e.* all the modes are frozen:

$$R_\kappa(\mathbf{q}) \to \infty \tag{E.2c}$$

- $\kappa \to 0$ The more we integrate out fluctuations, the more we want the regulator to play no role such that the true effective action of the model is recovered:

$$R_\kappa(\mathbf{q}) \to 0 \tag{E.2d}$$

Note that (E.2a) and (E.2b) ensure the fast and slow modes of the theory to be decoupled during the NPRG flow. It is important for the matrix R_κ to respect the symmetries of the problem, especially once approximations are performed. With such a regulator the generating functional of the correlation function, Z, becomes scale dependent,

$$Z_\kappa[j,\tilde{j}] \equiv e^{W_\kappa[j,\tilde{j}]} = \int \mathcal{D}[h,i\tilde{h}] \exp\left\{-S[h,\tilde{h}] - \Delta S_\kappa + \int_{\mathbf{x}} \left(jh + \tilde{j}\tilde{h}\right)\right\} . \tag{E.3}$$

Taking the derivative with respect to the scale, we get that the of Z_κ with respect to k is given by

$$\partial_\kappa e^{W_\kappa[j,\tilde{j}]} = -\partial_\kappa \langle \Delta S_\kappa[h,\tilde{h}]\rangle = -\frac{1}{2}\int_{\mathbf{q}} \partial_\kappa [R_\kappa(\mathbf{q})]_{ij} \langle h_i(-\mathbf{q}) h_j(\mathbf{q})\rangle \tag{E.4}$$

where we used the explicit form of the regulator (E.1); here

$$\langle h_1 \dots h_n \tilde{h}_{n+1} \tilde{h}_{n+m}\rangle = \frac{\delta^{n+m} Z_\kappa}{\delta j_1 \dots \delta j_n \delta \tilde{j}_{n+1} \delta \tilde{j}_{n+m}} = \frac{\delta^{n+m} e^{W_\kappa}}{\delta j_1 \dots \delta j_n \delta \tilde{j}_{n+1} \delta \tilde{j}_{n+m}} \tag{E.5}$$

with the argument of the $k-$th field being $(\mathbf{x}_k)$. Thus

$$\partial_\kappa e^{W_k[j,\tilde{j}]} = -\frac{1}{2}\int_{\mathbf{q}} \partial_\kappa [R_\kappa]_{ij} \frac{\delta}{\delta J_i}\frac{\delta}{\delta J_j} e^{W_\kappa[j,\tilde{j}]} = -\frac{1}{2}\int_{\mathbf{q}} \partial_\kappa [R_\kappa]_{ij} e^{W_\kappa[j,\tilde{j}]} \left[\frac{\delta^2}{\delta J_i \delta J_j} W_\kappa[j,\tilde{j}] + \frac{\delta}{\delta J_i} W_\kappa[j,\tilde{j}] \frac{\delta}{\delta J_j} W_\kappa[j,\tilde{j}]\right] \tag{E.6}$$

with $J^t = (j,\tilde{j})$. Recalling that $\partial_\kappa e^{W_\kappa[j,\tilde{j}]} = (\partial_\kappa W_\kappa[j,\tilde{j}]) e^{W_\kappa[j,\tilde{j}]}$ we thus obtain for the evolution equation for W_κ

$$\begin{aligned}\partial_\kappa W_\kappa[j,\tilde{j}] &= -\frac{1}{2}\int_{\mathbf{q}} \partial_\kappa [R_\kappa]_{ij} \left[\frac{\delta^2}{\delta J_i \delta J_j} W_\kappa[j,\tilde{j}] + \frac{\delta}{\delta J_i} W_\kappa[j,\tilde{j}] \frac{\delta}{\delta J_j} W_\kappa[j,\tilde{j}]\right] \\ &= -\frac{1}{2}\int_{\mathbf{q}} \partial_\kappa [R_\kappa]_{ij} \left[[W_\kappa^{(2)}]_{ij} + \varphi_i \varphi_j\right]\end{aligned} \tag{E.7}$$

with

$$[W_\kappa^{(2)}]_{ij} = \frac{\delta^2 W_\kappa}{\delta J_i \delta J_j}, \qquad \varphi_i = \frac{\delta W_\kappa}{\delta J_i} . \tag{E.8}$$

E.1.1 Effective average action and the Wetterich equation

We now perform a Legendre transform in order to switch to the description of the system in terms of the average fields φ rather than the sources J_i,

$$\Gamma_k[\varphi,\tilde{\varphi}] + \mathcal{W}_k[j,\tilde{j}] = \int_{\mathbf{x}} j_i \varphi_i - \frac{1}{2}\int_{\mathbf{x}} \varphi_i [R_k]_{ij} \varphi_j . \tag{E.9}$$

The regulator term is added to the Legendre transform in order to recover (E.2c) and (E.2d),

$$\Gamma_\kappa \overset{\kappa\to\Lambda}{\to} S\,, \quad \Gamma_\kappa \overset{\kappa\to 0}{\to} \Gamma\,. \tag{E.10}$$

Equation (E.9) implies

$$J_l(\mathbf{q}_1) = \frac{\delta\Gamma_\kappa}{\delta\varphi_l(\mathbf{q}_1)} + \frac{1}{2}\left([R_\kappa(\mathbf{q}_1)]_{lj}\varphi_j(-\mathbf{q}_1) + \varphi_i(\mathbf{q}_1)[R_\kappa(\mathbf{q}_1)]_{il}\right)\,. \tag{E.11}$$

Taking the k-derivative of (E.9) we get

$$\partial_\kappa\Gamma_\kappa[\varphi,\tilde{\varphi}] + \partial_\kappa\mathcal{W}_\kappa[j,\tilde{j}] = \int_{\mathbf{q}} j_i\partial_\kappa\varphi_i - \frac{1}{2}\int_{\mathbf{q}}\varphi_i\varphi_j\partial_\kappa[R_\kappa]_{ij} - \int_{\mathbf{q}}[R_\kappa]_{ij}\varphi_j\partial_\kappa\varphi_i \tag{E.12}$$

recalling that everything is taken at constant J. Using (E.7),

$$\begin{aligned}\partial_\kappa\Gamma_\kappa[\varphi,\tilde{\varphi}] =& \frac{1}{2}\int_{\mathbf{q}}\partial_\kappa[R_\kappa]_{ij}\left[[W_\kappa^{(2)}]_{ij} + \varphi_i\varphi_j\right] + \int_{\mathbf{q}} j_i\partial_\kappa\varphi_i - \frac{1}{2}\int_{\mathbf{q}}\varphi_i\varphi_j\partial_\kappa[R_\kappa]_{ij} - \int_{\mathbf{q}}[R_\kappa]_{ij}\varphi_j\partial_\kappa\varphi_i \\ =& \frac{1}{2}\int_{\mathbf{q}}\partial_\kappa[R_\kappa]_{ij}[W_\kappa^{(2)}]_{ij} + \int_{\mathbf{q}} j_i\partial_\kappa\varphi_i - \int_{\mathbf{q}}[R_\kappa]_{ij}\varphi_j\partial_\kappa\varphi_i\,.\end{aligned} \tag{E.13}$$

All the previous derivatives evaluated at constant-source will now be evaluated at constant-field:

$$\partial_\kappa\circ|_J = \partial_\kappa\circ|_{\varphi_i} + \int\partial_\kappa\varphi_i|_J\frac{\delta}{\delta\varphi_i}\circ\,. \tag{E.14}$$

This leads to

$$\begin{aligned}\partial_\kappa\Gamma_\kappa[\varphi,\tilde{\varphi}] =& \frac{1}{2}\int_{\mathbf{q}}\partial_\kappa[R_\kappa]_{ij}[W_\kappa^{(2)}]_{ij} + \int_{\mathbf{q}} j_i\partial_\kappa\varphi_i - \int_{\mathbf{q}}[R_\kappa]_{ij}\varphi_j\partial_\kappa\varphi_i - \int_{\mathbf{q}}\partial_\kappa\varphi_i|_J\frac{\delta}{\delta\varphi_i}\Gamma_\kappa[\varphi,\tilde{\varphi}] \\ =& \frac{1}{2}\int_{\mathbf{q}}\partial_\kappa[R_\kappa]_{ij}[W_\kappa^{(2)}]_{ij}\end{aligned} \tag{E.15}$$

where in the last passage we used (E.11). It is interesting to express $[W_\kappa^{(2)}]_{ij}$ in terms of $[\Gamma_\kappa^{(2)}]_{ij}$ in order to get a closed expression for the evolution of Γ. To do so we exploit the properties of functional delta. From (E.9) we can see indeed that

$$\begin{aligned}\delta(\mathbf{x}-\mathbf{x}_1) =& \frac{\delta^2 W_\kappa}{\delta J_i(\mathbf{x})\delta\varphi_i(\mathbf{x}_1)} = \int_{\mathbf{x}_2}\frac{\delta^2 W_\kappa}{\delta J_i(\mathbf{x})\delta J_l(\mathbf{x}_2)}\frac{\delta J_l(\mathbf{x}_2)}{\delta\varphi_i(\mathbf{x}_1)} \\ =& \int_{\mathbf{x}_2}\frac{\delta^2 W_\kappa}{\delta J_i(\mathbf{x})\delta J_l(\mathbf{x}_2)}\left[\frac{\delta^2\Gamma}{\delta\varphi_i(\mathbf{x}_1)\delta\varphi_l(\mathbf{x}_2)} + [R_\kappa(\mathbf{x}_1-\mathbf{x}_2)]_{il}\right].\end{aligned} \tag{E.16}$$

We conclude that, in an operatorial way,

$$W_\kappa^{(2)} \equiv G_\kappa = \left(\Gamma_\kappa^{(2)} + R_\kappa\right)^{-1}. \tag{E.17}$$

This relation leads to the evolution equation for Γ_κ,

$$\partial_\kappa \Gamma_\kappa[\varphi,\tilde{\varphi}] = \frac{1}{2}\int_{\mathbf{q}} \partial_\kappa [R_\kappa]_{ij} \left([\Gamma_\kappa^{(2)}] + [R_\kappa] \right)^{-1}_{ij} = \frac{1}{2}\mathrm{Tr}\left[\partial_\kappa R_\kappa \left(\Gamma_\kappa^{(2)} + R_\kappa \right)^{-1} \right] \tag{E.18}$$

where the trace is over both indices and internal variables. We thus have

$$\partial_\kappa \Gamma_\kappa = \frac{1}{2}\mathrm{Tr}\int_{\mathbf{q}} (\partial_\kappa R_\kappa)\, G_\kappa \tag{E.19a}$$

$\partial_\kappa \Gamma_\kappa =$ 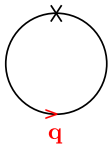 (E.19b)

which is the Wetterich's equation [20]. Equation (E.19b) is the diagrammatic representation of the Wetterich equation, which will be useful in the next chapter. The cross element is the κ-derivative of the regulator, $\partial_\kappa R_\kappa$. For the following, it is important to compute the flow of the two and three point functions by iteratively differentiating (E.19) with respect to the desired combination of $\varphi, \tilde{\varphi}$. Recalling that

$$\frac{\delta G_\kappa[\varphi(\mathbf{q})]}{\delta\varphi(\mathbf{q}_1)} = \frac{\delta}{\delta\varphi(\mathbf{q}_1)} \left(\Gamma_\kappa^{(2)}(\mathbf{q}) + R_\kappa(\mathbf{q}) \right)^{-1} = -\int_{\mathbf{q}_2,\mathbf{q}_3} W_\kappa^{(2)}(\mathbf{q}_3) \left(\frac{\delta\Gamma_\kappa^{(2)}(\mathbf{q}_2)}{\delta\varphi(\mathbf{q}_1)} \right) W_\kappa^{(2)}(\mathbf{q}) \,, \tag{E.20}$$

we obtain

$$\partial_\kappa [\Gamma_\kappa^{(2)}]_{i,j}(\mathbf{p}) = \frac{1}{2}\mathrm{Tr}\left\{ \partial_\kappa R_\kappa(\mathbf{q}) G_\kappa(\mathbf{q}) \left[-\Gamma^{(4)}_{\kappa,ij}(\mathbf{p},-\mathbf{p},\mathbf{q}) + \Gamma^{(3)}_{\kappa,i}(\mathbf{p},\mathbf{q}) G_\kappa(\mathbf{p}+\mathbf{q}) \Gamma^{(3)}_{\kappa,j}(-\mathbf{p},\mathbf{p}+\mathbf{q}) \right] G_\kappa(\mathbf{q}) \right\} \tag{E.21a}$$

$\partial_\kappa [\Gamma_\kappa^{(2)}]_{i,j}(\mathbf{p}) = -\frac{1}{2}$ 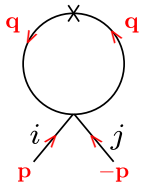 $+\frac{1}{2}\sum_{(i,j)\in P_2}$ 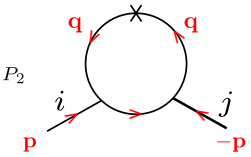 (E.21b)

and

$$\begin{aligned}\partial_\kappa [\Gamma_\kappa^{(3)}]_{i,j,k}(\mathbf{p}_1,\mathbf{p}_2) = \frac{1}{2}\mathrm{Tr}\Big\{ & \partial_\kappa R_\kappa(\mathbf{q}) G_\kappa(\mathbf{q}) \Big[-\Gamma^{(5)}_{\kappa,ijk}(\mathbf{p}_1,\mathbf{p}_2,-\mathbf{p}_1-\mathbf{p}_2,\mathbf{q}) \\ & + \Gamma^{(4)}_{\kappa,ij}(\mathbf{p}_1,\mathbf{p}_2,\mathbf{q}) G_\kappa(\mathbf{p}_1+\mathbf{p}_2+\mathbf{q}) \Gamma^{(3)}_{\kappa,k}(-\mathbf{p}_1-\mathbf{p}_2,\mathbf{p}_1+\mathbf{p}_2+\mathbf{q}) \\ & - \Gamma^{(3)}_{\kappa,i}(\mathbf{p}_1,\mathbf{q}) G_\kappa(\mathbf{p}_1+\mathbf{q}) \Gamma^{(3)}_{\kappa,j}(\mathbf{p}_2,\mathbf{p}_1+\mathbf{q}) G_\kappa(\mathbf{p}_1+\mathbf{p}_2+\mathbf{q}) \Gamma^{(3)}_{\kappa,k}(-\mathbf{p}_1-\mathbf{p}_2,\mathbf{p}_1+\mathbf{p}_2+\mathbf{q}) \Big] G_\kappa(\mathbf{q}) \Big\}\end{aligned} \tag{E.22a}$$

$\partial_\kappa [\Gamma_\kappa^{(3)}]_{i,j,k}(\mathbf{p}_1,\mathbf{p}_2) = -\frac{1}{2}$ 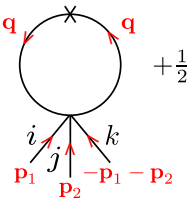 $+\frac{1}{2}\sum_{(i,j,k)\in P_3}$ 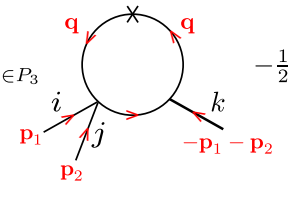 $-\frac{1}{2}\sum_{(i,j,k)\in P_3}$ 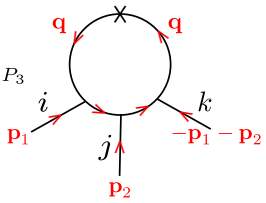 (E.22b)

with

$$\Gamma^{(n+2)}_{\kappa,1\dots n}(\mathbf{q},\mathbf{p}_1,\dots,\mathbf{p}_n)=\frac{\delta^n\Gamma^{(2)}(\mathbf{q})}{\delta\varphi_1(\mathbf{p}_1)\dots\delta\varphi_n(\mathbf{p}_n)}\,, \tag{E.23}$$

for the two and three point functions respectively. Here and henceforth the trace operation also includes all non-trivial permutations of the external momenta and frequencies. As a general property, we see that (E.19),(E.21) and (E.22) link the RG evolution of $\Gamma^{(n)}_\kappa$ to $\Gamma^{(n+2)}_\kappa$. At the analytical level a lot of effort has been spent in the last years in order to find controlled approximation schemes able to close this hierarchy. One of such schemes is the BMW method, proposed in the early 2000s by Blaizot, Mendez-Galain and Wschebor [123]. As discussed in the main text, the ansatz we will use for KPZ equation is related to the BMW scheme.

E.2 NPRG and KPZ

After a brief introduction to the method of NPRG we can apply it to the main topic of this thesis, that is KPZ equation. As we have seen in the main text a perturbative approach to KPZ fails to describe the properties of the strong coupling fixed point. A non-perturbative approach is then the natural way to explore such universal physics.

E.2.1 NPRG Ansatz for KPZ Equation

A first approach to KPZ using NPRG technique involved a derivative expansion of the action 1.37. However, due to the derivative nature of the non linearity, a truncation in the derivative of the field, *i.e.* a restriction in the momentum sector of the theory, fails to give quantitatively accurate results, even though enables one to get the strong-coupling fixed point (see Chap. 5.2.3) [126]. As we saw in Chap. 1.3.1, the two main symmetries of KPZ equation are the Galilean invariance and the time-reversal symmetry in $d=1$. A way to keep the full-momentum dependence of the theory and have a RG flow preserving the symmetries of the theory is to devise an ansatz which contains only operators which generate scalars of the symmetries of the system [114, 127]. In the case of KPZ the main symmetry in any dimension is, as discussed in Chap. 1.3.1, the Galilean one; we thus construct the ansatz by using scalars under Galilean transformation. A function $f(\mathbf{x})$ is defined as a scalar under Galilean transformation it transforms as

$$f\to f+\delta f\,,\qquad \delta f(\mathbf{x})=t\lambda\vec{v}\cdot\vec{\nabla}f(\mathbf{x}). \tag{E.24}$$

We see from (1.40) that $\tilde{h}$ is a scalar while h itself is not. Similarly the temporal derivative of a scalar is not itself a scalar. Furthermore, if $f(\mathbf{x})$ is a scalar function the quantities $\tilde{D}_t f\equiv\partial_t f-\lambda\vec{\nabla}h\cdot\vec{\nabla}f$ and $\partial_i\partial_j f$ are scalars; in the following we will take $i=j$ because of translational invariance. Foe field itself, one can construct scalars as $\partial_i\partial_j h$ and $D_t h\equiv\partial_t h-\lambda/2(\vec{\nabla}h)^2$, with a 1/2 factor in this case. Hence we can create scalars quantities by acting with $\tilde{D}_t$ ans ∇^2 onto $\tilde{h}$, $D_t h$ and $\nabla^2 h$. Together with these constraints the effective action must be at least linear in the response field $\tilde{h}$ for the conservation of probability and causality; furthermore in the following we keep only quadratic vertices in $\tilde{h}$. This level of approximation is usually referred to as SO approximation scheme. We end up with an ansatz of the form [127]

$$\begin{aligned}\Gamma[\varphi,\varphi]=\int_{\mathbf{x}}\Big\{&\tilde{\varphi}(\mathbf{x})f_k^{\lambda}(-\tilde{D}_t^2,-\nabla^2)D_t\varphi(\mathbf{x})-\frac{\nu}{2D}\Big[\nabla^2\varphi(\mathbf{x})f_k^{\nu}(-\tilde{D}_t^2,-\nabla^2)\tilde{\varphi}(\mathbf{x})+\tilde{\varphi}(\mathbf{x})f_k^{\nu}(-\tilde{D}_t^2,-\nabla^2)\nabla^2\varphi(\mathbf{x})\Big]\\&-\tilde{\varphi}(\mathbf{x})f_k^{D}(-\tilde{D}_t^2,-\nabla^2)\tilde{\varphi}(\mathbf{x})\Big\}\,.\end{aligned} \tag{E.25}$$

It is important to define the order of the operators in $f_\kappa^X(-\tilde{D}_t^2, -\nabla^2)$ because $\tilde{D}_t^2$ and ∇^2 do not commute; in the following we choose

$$f_k^X(-\tilde{D}_t^2, -\nabla^2) = \sum_{m,n=0}^{\infty} a_{m,n}(-\tilde{D}_t^2)^m(-\nabla^2)^n. \tag{E.26}$$

We stress that thanks to the form of $f_k^X(-\tilde{D}_t^2, -\nabla^2)$ we are keeping an arbitrary dependence on momentum, frequency and the field φ.

E.2.2 Anomalous dimensions and critical exponents

As discussed in the main text in Chap. 5.4, we can associate to each running function a running coupling,

$$X_\kappa = f_\kappa^X(\omega, p)\big|_{RP} \tag{E.27}$$

where RP is the chosen renormalization point. The usual choice is to take $RP = (\omega_{RP}, |\vec{p}_{RP}|) = (0, 0)$ because we are interested in the low energy sector of the theory. As we saw in Chap. 5.6.2 however, one can choose a different RP depending on the specific characteristics of the theory. The running couplings are important because they are associated to a scaling dimension

$$\eta_\kappa^X = -\partial_s \ln X_\kappa \,. \tag{E.28}$$

In the critical region, where η_κ^X attains its fixed point value $\eta_\kappa^X \to \eta_*^X$, we see that the running coefficients X_κ acquire a power-law behaviour,

$$X_\kappa \sim \kappa^{\eta_*^X}. \tag{E.29}$$

Using the fact that high and low energy sectors decouple in the RG flow for the KPZ equation [115], together with (5.51), one can show that these scaling dimensions also describe the scaling of the running functions at the fixed point $\partial_s \hat{f}_\kappa^X = 0$:

$$f_*^X(\hat{\omega}, \hat{p}) = \hat{p}^{-\eta_*^X} \zeta^X(\frac{\hat{\omega}}{\hat{p}^z}) \,. \tag{E.30}$$

Furthermore the scaling dimensions are related to the critical exponents of the theory χ, z. Recalling that the dimension of the frequency in units of the running momentum cut-off κ is $[\omega] = \nu_\kappa k^2$ and that $\omega \sim p^z$, we immediately get

$$z = 2 - \eta_*^\nu \,. \tag{E.31}$$

To find the link between χ and the scaling dimensions η_κ^X, we recall that it is related to

$$C(x, t) = \langle h(x, t)h(0, 0)\rangle_c \sim x^{2\chi} F_C(\frac{t}{x^z}) \,. \tag{E.32}$$

In the NPRG formalism, the two point correlation matrix $W^{(2)}$ is defined as the running propagator G_κ when all the fluctuations have been integrated out [115]

$$W^{(2)}(\mathbf{q}) = \lim_{\kappa\to 0} G_\kappa(\mathbf{q}) = [\Gamma_*^{(2)}(\mathbf{q})]^{-1} = \begin{pmatrix} \Gamma_*^{(2,0)}(\mathbf{q}) & \Gamma_*^{(1,1)}(\mathbf{q}) \\ \Gamma_*^{(1,1)}(-\mathbf{q}) & \Gamma_*^{(0,2)}(\mathbf{q}) \end{pmatrix}^{-1} = \frac{1}{|\Gamma_*^{(1,1)}(\mathbf{q})|^2} \begin{pmatrix} -\Gamma_*^{(0,2)}(\mathbf{q}) & \Gamma_*^{(1,1)}(\mathbf{q}) \\ \Gamma_*^{(1,1)}(-\mathbf{q}) & -\Gamma_*^{(2,0)}(\mathbf{q}) \end{pmatrix}. \tag{E.33}$$

Hence we have for the two-point correlator $C(x,t)$ and the response function $G(x,t) = \langle h(x,t)\tilde{h}(0,0)\rangle_c$,

$$C(\mathbf{q}) = -\frac{\Gamma_*^{(0,2)}(\mathbf{q})}{|\Gamma_*^{(1,1)}(\mathbf{q})|^2}, \quad G(\mathbf{q}) = \frac{\Gamma_*^{(1,1)}(\mathbf{q})}{|\Gamma_*^{(1,1)}(\mathbf{q})|^2}. \tag{E.34}$$

Recalling (5.43), we thus get

$$C(\mathbf{q}) = \frac{f_*^D(\mathbf{q})}{q^4 f_*^\nu(\mathbf{q})^2 + \omega^2 f_*^t(\mathbf{q})^2}, \quad G(\mathbf{q}) = \frac{1}{q^2 f_*^\nu(\mathbf{q}) - i\omega f_*^t(\mathbf{q})}. \tag{E.35}$$

By noting from (E.32) that $C(\mathbf{q}) = \mathcal{F}[C(\mathbf{x})](\mathbf{q}) \sim q^{-d-z-2\chi}$, and using (E.31), we finally get

$$\chi = \frac{1}{2}\left(2 - d + \eta_*^D - \eta_*^\nu\right). \tag{E.36}$$

Usually the quantities η_*^X are referred to as anomalous dimensions, in that it takes into account the non trivial scaling acquired by an operator at an interacting fixed point [135]. Indeed at a non interacting (Gaussian) fixed point, $\eta_*^X = 0$ and the dimension of the operators is the canonical one introduced in Chap. 1.3.

E.2.3 The Hierarchy of Approximations for the KPZ Ansatz: from the SO to the Local Potential Approximation (LPA)

In the previous section we introduced the SO approximation scheme, which is the minimal truncation in the field dependence preserving Galilean invariance and full frequency and momentum dependence in the two-point function. The ansatz (E.25) indeed, is quadratic in the response field $\tilde{\varphi}$ (which is the same dependence we have in the bare action (1.37)) and is linear in the Galilean scalars $D_t\varphi$ and $\nabla^2\varphi$, but keeps the full functional dependence in the field φ through the running functions $f_\kappa^X(-\tilde{D}_t^2, -\nabla^2)$. It is important to stress that truncating the $\tilde{\varphi}$ or φ is not equivalent, because the Galilean invariance constrains the φ dependence of the ansatz. The choice of truncating the field dependence rather then the frequency and momentum one is due to the derivative nature of the non-linear term in the KPZ equation (1.13), which suggests to keep the full functional dependence in the momentum [126, 127]. In the following we will see that we can pass from the SO approximation scheme to the LPA by further simplifications in the ansatz (E.25).

- **NLO Approximation** The first approximation one can perform on the SO ansatz is to neglect the frequency dependence of the running functions f_κ^X appearing in the *r.h.s* of the Wetterich equation (E.19), while keeping the functional dependence in the momentum. Due to a non-constant external frequency, this procedure still ensures a non-trivial frequency dependence of the running functions on the *l.h.s* of (E.19), which can be computed analytically by performing the integration over the internal frequency ω. Such an approximation scheme is usually referred to as NLO scheme. Even if the frequency dependence only comes from the loop integration, this approximation scheme gives a scaling of the two-point function in very good agreement with the exact result in $d = 1$, and can be generalised to $d > 1$ [115, 42].

- **LO Approximation** A stronger assumption is to take a constant external frequency (usually $\bar{\omega} = 0$); this choice completely neglect the frequency dependence of the running functions f_κ^X, which remains functional in the momentum, and corresponds to the LO approximation scheme.

- **LPA Approximation** The last, sharpest approximation is to neglect both the frequency and the momentum dependence of the running functions f_κ^X, which become simple running couplings. Thus one remains with only the $\nabla^2\varphi$ and $(\vec{\nabla}\varphi)^2$ derivative terms in the NPRG ansatz for the EAA: this level of approximation then corresponds to a LPA approximation scheme. As we will see in App. 5.2.3, at the LPA level one can get analytical results for the NPRG flow of the couplings using some particular type of regulator R_κ, and easily recover the one-loop perturbative results. For the KPZ equation, the LPA scheme provides qualitatively good results, being able to find the good non-perturbative strong-coupling fixed point. On the quantitative ground however, in $d \geq 2$ the results are unphysical [126].

E.3 Symmetries and Ward Identities

We now exploit the consequences implied by the invariance under some affine transformation of the fields. Suppose to have only one field φ, with $Z_\kappa = \int \mathcal{D}\varphi \exp\{A[\varphi]\}$ and to do a infinitesimal transformation $\varphi \to \varphi + \delta\varphi$, then

$$Z'_\kappa = \int \mathcal{D}\varphi \exp\{A[\varphi+\delta\varphi]\} \simeq \int \mathcal{D}\varphi \exp\{A[\varphi]+\delta A[\varphi]\} = \int \mathcal{D}\varphi \sum_n \frac{(\delta A)^n}{n!} \exp\{A[\varphi]\} \simeq Z_\kappa + \langle \delta A\rangle \tag{E.37}$$

The value of the functional integral is however invariant under a change in the integrating field, implying $\langle \delta A\rangle = 0$. In the FRG context this condition reads

$$\langle \delta S + \delta\Delta S_\kappa\rangle = \langle \int_{\mathbf{x}} j_i \delta h_i\rangle \tag{E.38}$$

These relations are known in literature as Ward Identities(WI). For an exact symmetry of the action, as the two presented in Chap. 1.3.1, $\delta S = 0$. Using (E.9) and the explicit form of ΔS_κ (assuming $R_{12} = R_{21}$) we get in general that

$$\langle \delta S\rangle = \langle \int_{\mathbf{x}} \frac{\delta\Gamma_\kappa}{\delta\varphi_i}\delta h_i\rangle = \int_{\mathbf{x}} \frac{\delta\Gamma_\kappa}{\delta\varphi_i}\langle\delta h_i\rangle \tag{E.39}$$

We see that there are two interesting cases in which WI will be really useful: the case in which the transformation under analysis is an exact symmetry of the system and the case in which the variation in the action is linear in the fields. In the first case we have a set of WIs $\int_{\mathbf{x}} \frac{\delta\Gamma_\kappa}{\delta\varphi_i}\langle\delta h_i\rangle = 0$; for the second case corresponding to extended symmetries, one can also derive useful identities.

E.3.1 WI for KPZ Equation

In the following we will look at the WI for Galilean transformation (1.40) and its gauged counterpart

$$\begin{aligned} h(t,\vec{x}) \to h'(t,\vec{x}) &= \vec{x}\cdot\partial_t\vec{v}(t) + h(t,\vec{x}+\lambda\vec{v}(t)) = h(t,\vec{x}) + \vec{x}\cdot\partial_t\vec{v}(t) + \lambda\vec{v}(t)\cdot\vec{\nabla}_{\vec{x}}h(t,\vec{x}) + \mathcal{O}(|\vec{v}|^2) \\ \tilde{h}(t,\vec{x}) \to \tilde{h}'(t,\vec{x}) &= \tilde{h}(t,\vec{x}+\lambda\vec{v}(t)) = \tilde{h}(t,\vec{x}) + \lambda\vec{v}(t)\cdot\vec{\nabla}_{\vec{x}}\tilde{h}(t,\vec{x}) + \mathcal{O}(|\vec{v}|^2) \end{aligned} \tag{E.40}$$

where $\vec{v}(t)$ is now an infinitesimal function of time. This is an example of linear variation of the action, together with the constraints they imply on the derivatives of Γ. These calculations show the general procedure to study how symmetries and their extensions constraint the correlations in the systems.

Galilean transformation

The global Galilean transformation corresponds to $\vec{v}(t) = \vec{v}t$. In this case $\delta S = 0$ and (E.39) becomes the functional Ward identity:

$$\begin{aligned} 0 &= \int_{\mathrm{x}} \left[\langle \vec{x}\cdot\vec{v} + \lambda t\vec{v}\cdot\vec{\nabla} h\rangle \frac{\delta\Gamma}{\delta\varphi} + \langle \lambda t\vec{v}\cdot\vec{\nabla}\tilde{h}\rangle \frac{\delta\Gamma}{\delta\tilde{\varphi}} \right] \\ &= \int_{\mathrm{x}} \left[(\vec{x}\cdot\vec{v} + \lambda t\vec{v}\cdot\vec{\nabla}\varphi) \frac{\delta\Gamma}{\delta\varphi} + (\lambda t\vec{v}\cdot\vec{\nabla}\tilde{\varphi}) \frac{\delta\Gamma}{\delta\tilde{\varphi}} \right] \end{aligned} \tag{E.41}$$

We now look at the implications of such relation on one-,two- and three-point functions under uniform fields $\tilde{\varphi}$. From now on, we use the short-hand notation

$$\Gamma^{(m,n)}(\mathrm{x}_1,\ldots,\mathrm{x}_m,\mathrm{x}_{m+1},\ldots,\mathrm{x}_{m+n}) = \frac{\delta\Gamma[\varphi,\tilde{\varphi}]}{\delta\varphi(\mathrm{x}_1)\ldots\delta\varphi(\mathrm{x}_m)\delta\tilde{\varphi}(\mathrm{x}_{m+1})\ldots\delta\tilde{\varphi}(\mathrm{x}_{m+n})} \tag{E.42}$$

Under uniform fields (*i.e.* $\vec{\nabla}^{(\sim)}\varphi = 0$) we thus get

$$\Gamma^{(1,0)} \int_{\mathrm{x}} \vec{x}\cdot\vec{v} = 0,\ \forall\vec{v} \rightarrow \Gamma^{(1,0)} = 0 \tag{E.43}$$

We now perform a functional derivative $\delta/\delta\varphi(\mathrm{x}_1)$ over (E.41) in order to see the implication of the WI on $\Gamma^{(2,0)}$; we obtain

$$\begin{aligned} 0 &= \int_{\mathrm{x}} \left[\vec{x}\cdot\vec{v}\,\Gamma^{(2,0)}(\mathrm{x},\mathrm{x}_1) + \lambda t\varphi\Gamma^{(1,0)}(\mathrm{x})\vec{v}\cdot\vec{\nabla}\delta(\mathrm{x}-\mathrm{x}_1) + \lambda t\vec{v}\cdot\vec{\nabla}\varphi\Gamma^{(2,0)}(\mathrm{x},\mathrm{x}_1) + (\lambda t\vec{v}\cdot\vec{\nabla}\tilde{\varphi})\Gamma^{(1,1)}(\mathrm{x}_1,\mathrm{x}) \right] \\ &\overset{p.p.i.}{=} \int_{\mathrm{x}} \left[\vec{x}\cdot\vec{v}\,\Gamma^{(2,0)}(\mathrm{x},\mathrm{x}_1) - \lambda t\vec{\nabla}\Gamma^{(1,0)}(\mathrm{x})\cdot\vec{v}\,\delta(\mathrm{x}-\mathrm{x}_1) + \lambda t\vec{v}\cdot\vec{\nabla}\varphi\Gamma^{(2,0)}(\mathrm{x},\mathrm{x}_1) + (\lambda t\vec{v}\cdot\vec{\nabla}\tilde{\varphi})\Gamma^{(1,1)}(\mathrm{x}_1,\mathrm{x}) \right] \end{aligned} \tag{E.44}$$

At uniform fields we get

$$\int_{\mathrm{x}} \vec{x}\cdot\vec{v}\,\Gamma^{(2,0)}|_{\varphi=0} = 0 \rightarrow \Gamma^{(2,0)}|_{\varphi=0} = 0 \tag{E.45}$$

A more interesting result comes from the analysis of $\Gamma^{(2,1)}$, *i.e.* by differentiating over $\tilde{\varphi}(\mathrm{x}_2)$ the previous WI,

$$\begin{aligned} 0 &= \int_{\mathrm{x}} \Big[\vec{x}\cdot\vec{v}\,\Gamma^{(2,1)}(\mathrm{x},\mathrm{x}_1,\mathrm{x}_2) - \lambda t\vec{\nabla}\Gamma^{(1,1)}(\mathrm{x},\mathrm{x}_2)\cdot\vec{v}\,\delta(\mathrm{x}-\mathrm{x}_1) + \lambda t\vec{v}\cdot\vec{\nabla}\varphi\Gamma^{(2,1)}(\mathrm{x},\mathrm{x}_1,\mathrm{x}_2) \\ &\quad + \lambda t\Gamma^{(1,1)}(\mathrm{x}_1,\mathrm{x})\vec{v}\cdot\vec{\nabla}\delta(\mathrm{x}-\mathrm{x}_2) + \lambda t\vec{v}\cdot\vec{\nabla}\tilde{\varphi}\Gamma^{(1,2)}(\mathrm{x}_1,\mathrm{x},\mathrm{x}_2) \Big] \\ &\overset{p.p.i.}{=} \int_{\mathrm{x}} \Big[\vec{x}\cdot\vec{v}\,\Gamma^{(2,1)}(\mathrm{x},\mathrm{x}_1,\mathrm{x}_2) - \lambda t\vec{\nabla}\Gamma^{(1,1)}(\mathrm{x},\mathrm{x}_2)\cdot\vec{v}\,\delta(\mathrm{x}-\mathrm{x}_1) + \lambda t\vec{v}\cdot\vec{\nabla}\varphi\Gamma^{(2,1)}(\mathrm{x},\mathrm{x}_1,\mathrm{x}_2) \\ &\quad + -\lambda t\vec{\nabla}\Gamma^{(1,1)}(\mathrm{x}_1,\mathrm{x})\cdot\vec{v}\,\delta(\mathrm{x}-\mathrm{x}_2)\lambda t\vec{v}\cdot\vec{\nabla}\tilde{\varphi}\Gamma^{(1,2)}(\mathrm{x}_1,\mathrm{x},\mathrm{x}_2) \Big] \end{aligned} \tag{E.46}$$

Under a uniform-field configuration this reads

$$0 = \int_{\mathbf{x}} \left[\vec{x} \cdot \vec{v}\, \Gamma^{(2,1)}(\mathbf{x}, \mathbf{x}_1, \mathbf{x}_2) - \lambda t \vec{\nabla} \Gamma^{(1,1)}(\mathbf{x}, \mathbf{x}_2) \cdot \vec{v}\, \delta(\mathbf{x} - \mathbf{x}_1) - \lambda t \vec{\nabla} \Gamma^{(1,1)}(\mathbf{x}_1, \mathbf{x}) \cdot \vec{v}\, \delta(\mathbf{x} - \mathbf{x}_2) \right], \quad \forall \vec{v} \tag{E.47}$$

implying

$$\int_{\mathbf{x}} \vec{x} \Gamma^{(2,1)}(\mathbf{x}, \mathbf{x}_1, \mathbf{x}_2) = \lambda \int_{\mathbf{x}} t \left[\vec{\nabla} \Gamma^{(1,1)}(\mathbf{x}, \mathbf{x}_2) \delta(\mathbf{x} - \mathbf{x}_1) + \vec{\nabla} \Gamma^{(1,1)}(\mathbf{x}_1, \mathbf{x}) \delta(\mathbf{x} - \mathbf{x}_2) \right] \tag{E.48}$$

It is instructive to do once the full calculation for representing (E.48) into Fourier-space,

$$\begin{aligned}
\int_{\mathbf{x},\{\mathbf{p}\}} \vec{x} \tilde{\Gamma}^{(2,1)}(\mathbf{p}, \mathbf{p}_1, \mathbf{p}_2) e^{i \sum_k^2 (\vec{x}_k \cdot \vec{p}_k - \omega_k t_k)} &= \lambda \int_{\mathbf{x},\{\mathbf{p}\}} t \left[\vec{\nabla}_{\vec{x}} \tilde{\Gamma}^{(1,1)}(\mathbf{p}, \mathbf{p}_2) e^{i(\vec{p}_2 \cdot \vec{x}_2 - \omega_2 t_2)} e^{i\vec{p}_1 \cdot (\vec{x} - \vec{x}_1) - i\omega_1 (t - t_1)} \right. \\
&\quad \left. + \vec{\nabla}_{\vec{x}} \tilde{\Gamma}^{(1,1)}(\mathbf{p}_1, \mathbf{p}) e^{i(\vec{p}_1 \cdot \vec{x}_1 - \omega_1 t_1)} e^{i\vec{p}_2 \cdot (\vec{x} - \vec{x}_2) - i\omega_2 (t - t_2)} \right] e^{i(\vec{p} \cdot \vec{x} - \omega t)} \\
i \int_{\mathbf{x},\{\mathbf{p}\}} \vec{\nabla}_{\vec{p}} \tilde{\Gamma}^{(2,1)}(\mathbf{p}, \mathbf{p}_1, \mathbf{p}_2) e^{i \sum_k^2 (\vec{x}_k \cdot \vec{p}_k - \omega_k t_k)} &= i\lambda \int_{\mathbf{x},\{\mathbf{p}\}} t \left[\vec{p}_1 \tilde{\Gamma}^{(1,1)}(\mathbf{p}, \mathbf{p}_2) e^{i(\vec{p}_2 \cdot \vec{x}_2 - \omega_2 t_2)} e^{i\vec{p}_1 \cdot (\vec{x} - \vec{x}_1) - i\omega_1 (t - t_1)} \right. \\
&\quad \left. + \vec{p}_2 \tilde{\Gamma}^{(1,1)}(\mathbf{p}_1, \mathbf{p}) e^{i(\vec{p}_1 \cdot \vec{x}_1 - \omega_1 t_1)} e^{i\vec{p}_2 \cdot (\vec{x} - \vec{x}_2) - i\omega_2 (t - t_2)} \right] e^{i(\vec{p} \cdot \vec{x} - \omega t)}
\end{aligned} \tag{E.49}$$

now let $\omega + \omega_1 \to \omega$, $\mathbf{p}_1 \to -\mathbf{p}_1$ in the first term of rhs and $\omega + \omega_2 \to \omega$, $\mathbf{p}_2 \to -\mathbf{p}_2$ in the second term of rhs,

$$\begin{aligned}
i \int_{\mathbf{x},\{\mathbf{p}\}} \vec{\nabla}_{\vec{p}} \tilde{\Gamma}^{(2,1)}(\mathbf{p}, \mathbf{p}_1, \mathbf{p}_2) e^{i \sum_k^2 (\vec{x}_k \cdot \vec{p}_k - \omega_k t_k)} &= -i\lambda \int_{\mathbf{x},\{\mathbf{p}\}} t \left[\vec{p}_1 \tilde{\Gamma}^{(1,1)}(\omega + \omega_1, \vec{p}, \omega_2, \vec{p}_2) \right. \\
&\quad \left. + \vec{p}_2 \tilde{\Gamma}^{(1,1)}(\omega_1, \vec{p}_1, \omega + \omega_2, \vec{p}) \right] e^{i \sum_k^2 (\vec{x}_k \cdot \vec{p}_k - \omega_k t_k)} \qquad \text{(E.50a)} \\
i \int_{\mathbf{x},\{\mathbf{p}\}} \vec{\nabla}_{\vec{p}} \tilde{\Gamma}^{(2,1)}(\mathbf{p}, \mathbf{p}_1, \mathbf{p}_2) e^{i \sum_k^2 (\vec{x}_k \cdot \vec{p}_k - \omega_k t_k)} &= \lambda \int_{\mathbf{x},\{\mathbf{p}\}} \left[\vec{p}_1 \partial_\omega \tilde{\Gamma}^{(1,1)}(\omega + \omega_1, \vec{p}, \omega_2, \vec{p}_2) \right. \\
&\quad \left. + \vec{p}_2 \partial_\omega \tilde{\Gamma}^{(1,1)}(\omega_1, \vec{p}_1, \omega + \omega_2, \vec{p}) \right] e^{i \sum_k^2 (\vec{x}_k \cdot \vec{p}_k - \omega_k t_k)} \\
\int_{\mathbf{p}_1, \mathbf{p}_2} \vec{\nabla}_{\vec{p}} \tilde{\Gamma}^{(2,1)}(\mathbf{p}, \mathbf{p}_1, \mathbf{p}_2)|_{\mathbf{p}=0} e^{i \sum_{k=1}^2 (\vec{x}_k \cdot \vec{p}_k - \omega_k t_k)} &= \lambda \int_{\mathbf{p}_1, \mathbf{p}_2} \left[\vec{p}_1 \partial_{\omega_1} \tilde{\Gamma}^{(1,1)}(\omega_1, \vec{p}, \omega_2, \vec{p}_2) + \vec{p}_2 \partial_{\omega_2} \tilde{\Gamma}^{(1,1)}(\omega_1, \vec{p}_1, \omega_2, \vec{p}) \right] \\
&\quad \times e^{i \sum_{k=1}^2 (\vec{x}_k \cdot \vec{p}_k - \omega_k t_k)}
\end{aligned} \tag{E.50b}$$

where in the last passage we used the fact that $\partial_x f(x + y)|_{x=0} \equiv f(y)$. We now exploit the fact that frequencies and momenta are conserved in a uniform-field configuration, and extract from the $\tilde{\Gamma}(m, n)$ the delta-functions related to such conservation relations:

$$\tilde{\Gamma}(m, n)(\mathbf{p}_1, \ldots, \mathbf{p}_{m+n}) = (2\pi)^{d+1} \delta(\sum_i \mathbf{p}_i) \Gamma(\mathbf{p}_1, \ldots, \mathbf{p}_{m+n-1}) \,. \tag{E.51}$$

We thus get

$$
\begin{aligned}
i\int_{\mathbf{p}_1,\mathbf{p}_2}\vec{\nabla}_{\vec{p}}\,\Gamma^{(2,1)}(\mathbf{p},\mathbf{p}_1)|_{\mathbf{p}=\mathbf{0}}\delta(\mathbf{p}_1+\mathbf{p}_2)e^{i\sum_{k=1}^{2}(\vec{x}_k\cdot\vec{p}_k-\omega_k t_k)} &= \lambda\int_{\mathbf{p}_1,\mathbf{p}_2}\Big[\vec{p}_1\partial_{\omega_1}\left(\Gamma^{(1,1)}(\omega_1,\vec{p})\delta(\mathbf{p}_1+\mathbf{p}_2)\right)\\
&+\vec{p}_2\partial_{\omega_2}\left(\Gamma^{(1,1)}(\mathbf{p}_1)\delta(\mathbf{p}_1+\mathbf{p}_2)\right)\Big]e^{i\sum_{k=1}^{2}(\vec{x}_k\cdot\vec{p}_k-\omega_k t_k)}\\
&= \lambda\int_{\mathbf{p}_1,\mathbf{p}_2}\Big[\vec{p}_1\delta(\mathbf{p}_1+\mathbf{p}_2)\partial_{\omega_1}\Gamma^{(1,1)}(\omega_1,\vec{p})\\
&+(\vec{p}_1+\vec{p}_2)\Gamma^{(1,1)}(\mathbf{p}_1)\delta'(\mathbf{p}_1+\mathbf{p}_2)\Big]e^{i\sum_{k=1}^{2}(\vec{x}_k\cdot\vec{p}_k-\omega_k t_k)}\\
&= \lambda\int_{\mathbf{p}_1,\mathbf{p}_2}\vec{p}_1\delta(\mathbf{p}_1+\mathbf{p}_2)\partial_{\omega_1}\Gamma^{(1,1)}(\omega_1,\vec{p})e^{i\sum_{k=1}^{2}(\vec{x}_k\cdot\vec{p}_k-\omega_k t_k)}
\end{aligned}
\tag{E.52}
$$

where in the last passage we used the fact that $\int_x x\delta(x)=0$. We thus end up with

$$
i\vec{\nabla}_{\vec{p}}\,\Gamma^{(2,1)}(\mathbf{p},\mathbf{p}_1)|_{\mathbf{p}=\mathbf{0}} = \lambda\vec{p}_1\partial_{\omega_1}\Gamma^{(1,1)}(\omega_1,\vec{p}) \tag{E.53}
$$

Gauged-Galilean transformation

In the gauged case, there is an additional contribution coming from the non-zero variation of the action,

$$
\langle\delta S\rangle = \langle\int_{\mathbf{x}}(\vec{x}\cdot\partial_t^2\vec{v}(t))\tilde{h}(\mathbf{x})\rangle = \int_{\mathbf{x}}(\vec{x}\cdot\partial_t^2\vec{v}(t))\tilde{\varphi}(\mathbf{x}) \tag{E.54}
$$

leading to the functional WI

$$
\begin{aligned}
0 &= \int_{\mathbf{x}}\left[(\vec{x}\cdot\partial_t\vec{v}(t)+\lambda\vec{v}(t)\cdot\vec{\nabla}\varphi)\frac{\delta\Gamma}{\delta\varphi}+(\lambda\vec{v}(t)\cdot\vec{\nabla}\tilde{\varphi})\frac{\delta\Gamma}{\delta\tilde{\varphi}}-(\vec{x}\cdot\partial_t^2\vec{v}(t))\tilde{\varphi}(\mathbf{x})\right]\\
&\overset{p.p.i.}{=} \int_t\vec{v}(t)\cdot\int_{\vec{x}}\left[-\vec{x}\partial_t\frac{\delta\Gamma}{\delta\varphi}+\lambda\vec{\nabla}\varphi\frac{\delta\Gamma}{\delta\varphi}+\lambda\vec{\nabla}\tilde{\varphi}\frac{\delta\Gamma}{\delta\tilde{\varphi}}-\vec{x}\cdot\partial_t^2\tilde{\varphi}(\mathbf{x})\right],\qquad\forall\vec{v}(t)
\end{aligned}
\tag{E.55}
$$

which implies

$$
0 = \int_{\vec{x}}\left[-\vec{x}\partial_t\frac{\delta\Gamma}{\delta\varphi}+\lambda\vec{\nabla}\varphi\frac{\delta\Gamma}{\delta\varphi}+\lambda\vec{\nabla}\tilde{\varphi}\frac{\delta\Gamma}{\delta\tilde{\varphi}}-\vec{x}\cdot\partial_t^2\tilde{\varphi}(\mathbf{x})\right]. \tag{E.56}
$$

Let us emphasize how gauging the transformation changes the WIs for $\Gamma^{(m,n)}$. The main difference between (E.41) and (E.56) is that the latter is integrated in space but is local in time. It is thus more general. As an example let us derive the resulting identity for $\Gamma^{(2,1)}$. To do so we differentiate (E.56) with respect to $\varphi(\mathbf{x}_1)$ and $\tilde{\varphi}(\mathbf{x}_2)$, getting

$$
0 = \int_{\vec{x}}\left[-\vec{x}\partial_t\tilde{\Gamma}^{(2,1)}(\mathbf{x},\mathbf{x}_1,\mathbf{x}_2)-\lambda\vec{\nabla}\tilde{\Gamma}^{(1,1)}(\mathbf{x},\mathbf{x}_2)\delta(\mathbf{x}-\mathbf{x}_1)-\lambda\vec{\nabla}\tilde{\Gamma}^{(1,1)}(\mathbf{x}_1,\mathbf{x})\delta(\mathbf{x}-\mathbf{x}_2)+\lambda\vec{\nabla}\tilde{\varphi}(\mathbf{x})\tilde{\Gamma}^{(1,2)}(\mathbf{x}_1,\mathbf{x},\mathbf{x}_2)\right] \tag{E.57}
$$

In a uniform-field configuration this reads

$$
\begin{aligned}
\partial_t\int_{\vec{x}}\vec{x}\,\tilde{\Gamma}^{(2,1)}(\mathbf{x},\mathbf{x}_1,\mathbf{x}_2) &= -\lambda\int_{\vec{x}}\left[\vec{\nabla}\tilde{\Gamma}^{(1,1)}(\mathbf{x},\mathbf{x}_2)\delta(\mathbf{x}-\mathbf{x}_1)+\vec{\nabla}\tilde{\Gamma}^{(1,1)}(\mathbf{x}_1,\mathbf{x})\delta(\mathbf{x}-\mathbf{x}_2)\right]\\
&= -\lambda\left[\vec{\nabla}_{\vec{x}_1}\tilde{\Gamma}^{(1,1)}(\mathbf{x}_1,\mathbf{x}_2)+\vec{\nabla}_{\vec{x}_2}\tilde{\Gamma}^{(1,1)}(\mathbf{x}_1,\mathbf{x}_2)\right] = -\lambda\left(\vec{\nabla}_{\vec{x}_1}+\vec{\nabla}_{\vec{x}_2}\right)\tilde{\Gamma}^{(1,1)}(\mathbf{x}_1,\mathbf{x}_2)
\end{aligned}
$$

In the Fourier space we get

$$\omega\vec{\nabla}_{\vec{p}}\tilde{\Gamma}^{(2,1)}(\mathbf{p},\mathbf{p}_1,\mathbf{p}_2)|_{\vec{p}=\vec{0}} = -i\lambda\left[\vec{p}_1\tilde{\Gamma}^{(1,1)}(\omega+\omega_1,\vec{p}_1,\omega_2,\vec{p}_2)+\vec{p}_2\tilde{\Gamma}^{(1,1)}(\omega_1,\vec{p}_1,\omega+\omega_2,\vec{p}_2)\right] \tag{E.58}$$

which by exploiting frequency and momentum conservation becomes

$$i\omega\vec{\nabla}_{\vec{p}}\Gamma^{(2,1)}(\mathbf{p},\mathbf{p}_1)|_{\vec{p}=\vec{0}} = \lambda\vec{p}_1\left[\Gamma^{(1,1)}(\omega+\omega_1,\vec{p}_1)-\Gamma^{(1,1)}(\omega_1,\vec{p}_1)\right] \tag{E.59}$$

We thus see that gauging the Galilean transformation yields a much stronger WI because it is valid for any ω and not only $\omega = 0$ as in (E.53). Eq. (E.59) simplifies to (E.53) in the $\omega \to 0$ limit.

E.4 Functional derivative of f_κ^X

Before continuing in the analysis of the WI for KPZ action, we compute a key quantity for the calculation presented in the next sections. To perform all the functional derivatives of the ansatz (E.25) for Γ_κ with respect to the fields, one crucial element is the functional derivative of the running functions with respect to the field φ,

$$\frac{\delta f^X(-\tilde{D}_t^2,-\nabla^2)}{\delta\varphi} = \frac{1}{\delta\varphi}\sum_{m,n=0}^{\infty} a^X_{m,n}(-\tilde{D}_t^2)^m(-\nabla^2)^n. \tag{E.60}$$

Recalling that

$$\frac{\delta\left(-\tilde{D}_t^2\right)^m}{\delta\varphi(\mathbf{x}_1)} = \sum_{l=0}^{m-1}(-\tilde{D}_t^2)^l\frac{\delta(-\tilde{D}_t^2)}{\delta\varphi(\mathbf{x}_1)}(-\tilde{D}_t^2)^{m-l-1} \tag{E.61}$$

we get

$$\frac{\delta f^X(-\tilde{D}_t^2,-\nabla^2)}{\delta\varphi(\mathbf{x}_1)} = \sum_{m=1,n=0}^{\infty} a^X_{m,n}\sum_{l=0}^{m-1}(-\tilde{D}_t^2)^l\frac{\delta(-\tilde{D}_t^2)}{\delta\varphi(\mathbf{x}_1)}(-\tilde{D}_t^2)^{m-l-1}(-\nabla^2)^n. \tag{E.62}$$

In order to compute this quantity we need to find $\delta(-\tilde{D}_t^2)/\delta\varphi$:

$$\begin{aligned}\frac{\delta(-\tilde{D}_t^2)}{\delta\varphi(\mathbf{x}_1)} =& -\frac{\delta}{\delta\varphi(\mathbf{x}_1)}(\partial_t-\lambda\vec{\nabla}\varphi\cdot\vec{\nabla})(\partial_t-\lambda\vec{\nabla}\varphi\cdot\vec{\nabla})\\ =&\lambda\left[\vec{\nabla}\delta(\mathbf{x}-\mathbf{x}_1)\cdot\vec{\nabla}(\partial_t-\lambda\vec{\nabla}\varphi\cdot\vec{\nabla})+(\partial_t-\lambda\vec{\nabla}\varphi\cdot\vec{\nabla})\vec{\nabla}\delta(\mathbf{x}-\mathbf{x}_1)\cdot\vec{\nabla}\right].\end{aligned} \tag{E.63}$$

In the following we omit the terms proportional to $\vec{\nabla}\varphi$, that will vanish in the uniform-field configuration we are interested in. Switching to Fourier space, we obtain

$$\begin{aligned}\frac{\delta(-\tilde{D}_t^2)}{\delta\varphi(\mathbf{x}_1)} =&\lambda\int_{\mathbf{p}_1}\left[\delta(t-t_1)\vec{\nabla}e^{i\vec{p}_1\cdot(\vec{x}-\vec{x}_1)}\cdot\vec{\nabla}\partial_t+\partial_t\left(e^{-i\omega_1(t-t_1)}\vec{\nabla}e^{i\vec{p}_1\cdot(\vec{x}-\vec{x}_1)}\cdot\vec{\nabla}\right)\right]\\ =&\lambda\int_{\mathbf{p}_1}\left[\delta(\mathbf{x}-\mathbf{x}_1)\left(i\vec{p}_1\cdot\vec{\nabla}\partial_t\right)+\delta(\vec{x}-\vec{x}_1)\left(\partial_t e^{-i\omega_1(t-t_1)}+e^{-i\omega_1(t-t_1)}\partial_t\right)\left(i\vec{p_1}\cdot\vec{\nabla}\right)\right]\\ =&\lambda\int_{\mathbf{p}_1}\delta(\mathbf{x}-\mathbf{x}_1)\left[\left(i\vec{p}_1\cdot\vec{\nabla}\partial_t\right)+(-i\omega_1+\partial_t)\left(i\vec{p_1}\cdot\vec{\nabla}\right)\right]\overset{test\,f(\mathbf{x})}{=} i\lambda\int_{\mathbf{p}_1,\mathbf{p}}\delta(\mathbf{x}-\mathbf{x}_1)\vec{p}_1\cdot\vec{p}\,(\omega_1+2\omega)\end{aligned} \tag{E.64}$$

Now, recalling that on the *r.h.s.* we have the phases coming from the whole term in the ansatz and that we want to have the same coefficients in the exponentials in order to use the property of uniqueness of the Fourier transform, we do the change of variables $\mathbf{p}+\mathbf{p}_1 \to \mathbf{p}$, $\mathbf{p}_1 \to -\mathbf{p}_1$. We thus have

$$\mathcal{F}\left[\frac{\delta(-\tilde{D}_t^2)}{\delta\varphi(\mathbf{x}_1)}\right](\mathbf{p},\mathbf{p}_1) = -i\lambda\vec{p}_1\cdot(\vec{p}_1+\vec{p})(\omega_1+2\omega). \tag{E.65}$$

Using the ansatz (E.25) at uniform field, the only non zero contributions from functional derivatives of the running functions are $\left(\delta f_X^k/\delta\varphi(\mathbf{x}_i)\right)\delta(\mathbf{x}-\mathbf{x}_j)$. Using the previous result, this quantity is equal to

$$\frac{\delta f_X^k(-\tilde{D}_t^2,-\nabla^2)}{\delta\varphi(\mathbf{x}_i)}\delta(\mathbf{x}-\mathbf{x}_j) = i\lambda\int_{\mathbf{x},\mathbf{p}_i,\mathbf{p}_j}\delta(\mathbf{x}-\mathbf{x}_i)\delta(\mathbf{x}-\mathbf{x}_j)\frac{\vec{p}_i}{\omega_i}\cdot\vec{p}_j\left[f_X^k\left((\omega_i+\omega_j)^2,\vec{p}_j^{\,2}\right)-f_X^k(\omega_j^2,\vec{p}_j^{\,2})\right], \tag{E.66}$$

where we used the relation

$$\sum_{k=0}^{n-1}\omega_j^{2k}(\omega_i+\omega_j)^{2(n-k-1)} = \frac{(\omega_i+\omega_j)^n-\omega_j^n}{(\omega_i+\omega_j)^2-\omega_j^2}. \tag{E.67}$$

E.5 Recovering WIs from the Ansatz

Once we write down the ansatz for Γ_κ it is important to check that all the WIs previously found are satisfied by such a functional. As an example we show here that the WI for $\Gamma^{(2,1)}$, (E.59), is well reproduced by (E.25). To get $\Gamma^{(2,1)}$ we first differentiate twice with respect to $\varphi(\mathbf{x}_1)$, $\varphi(\mathbf{x}_2)$ and then with respect to $\varphi(\mathbf{x}_3)$ getting, in the homogeneous-field configuration,

$$\begin{aligned}\Gamma_k^{(2,1)}(\mathbf{x}_1,\mathbf{x}_2,\mathbf{x}_3) = \int_{\mathbf{x}}\Bigg\{&\delta(\mathbf{x}-\mathbf{x}_3)\left[f_k^\lambda(-\tilde{D}_t^2,-\nabla^2)\frac{\delta^2 D_t\varphi(\mathbf{x})}{\delta\varphi(\mathbf{x}_1)\delta\varphi(\mathbf{x}_2)}+\frac{\delta f_k^\lambda(-\tilde{D}_t^2,-\nabla^2)}{\delta\varphi(\mathbf{x}_1)}\frac{\delta D_t\varphi(\mathbf{x})}{\delta\varphi(\mathbf{x}_2)}\right.\\
&\left.+\frac{\delta f_k^\lambda(-\tilde{D}_t^2,-\nabla^2)}{\delta\varphi(\mathbf{x}_2)}\frac{\delta D_t\varphi(\mathbf{x})}{\delta\varphi(\mathbf{x}_1)}\right]-\frac{\nu}{2D}\left[\left(\nabla^2\delta(\mathbf{x}-\mathbf{x}_1)\frac{\delta f_k^\lambda(-\tilde{D}_t^2,-\nabla^2)}{\delta\varphi(\mathbf{x}_2)}+\nabla^2\delta(\mathbf{x}-\mathbf{x}_2)\frac{\delta f_k^\lambda(-\tilde{D}_t^2,-\nabla^2)}{\delta\varphi(\mathbf{x}_1)}\right)\right]\\
&\times\delta(\mathbf{x}-\mathbf{x}_3)+\delta(\mathbf{x}-\mathbf{x}_3)\left(\frac{\delta f_k^\lambda(-\tilde{D}_t^2,-\nabla^2)}{\delta\varphi(\mathbf{x}_1)}\nabla^2\delta(\mathbf{x}-\mathbf{x}_2)+\frac{\delta f_k^\lambda(-\tilde{D}_t^2,-\nabla^2)}{\delta\varphi(\mathbf{x}_2)}\nabla^2\delta(\mathbf{x}-\mathbf{x}1)\right)\Bigg\}.\end{aligned} \tag{E.68}$$

As introduced in the previous section, we note that all the non vanishing terms containing functional derivatives of the running functions are applied to delta functions. Using (E.66) we get in Fourier space

$$\begin{aligned}\Gamma_k^{(2,1)}(\mathbf{p}_1,\mathbf{p}_2) = {}&\lambda\vec{p}_1\cdot\vec{p}_2 f_k^\lambda((\omega_1+\omega_2)^2,(\vec{p}_1+\vec{p}_2)^2)+\lambda\frac{\omega_1}{\omega_2}\vec{p}_1\cdot\vec{p}_2\left[f_k^\lambda((\omega_1+\omega_2)^2,\vec{p}_1^{\,2})-f_k^\lambda(\omega_1^2,\vec{p}_1^{\,2})\right]\\
&+\lambda\frac{\omega_2}{\omega_1}\vec{p}_1\cdot\vec{p}_2\left[f_k^\lambda((\omega_1+\omega_2)^2,\vec{p}_2^{\,2})-f_k^\lambda(\omega_2^2,\vec{p}_2^{\,2})\right]+i\frac{\nu}{2D}\left\{\vec{p}_1^{\,2}\frac{\vec{p}_2}{\omega_2}\cdot(\vec{p}_1+\vec{p}_2)\left[f_k^\nu((\omega_1+\omega_2)^2,(\vec{p}_1+\vec{p}_2)^2)\right.\right.\\
&\left.-f_k^\nu(\omega_1^2,(\vec{p}_1+\vec{p}_2)^2)\right]+\vec{p}_2^{\,2}\frac{\vec{p}_1}{\omega_1}\cdot(\vec{p}_1+\vec{p}_2)\left[f_k^\nu((\omega_1+\omega_2)^2,(\vec{p}_1+\vec{p}_2)^2)-f_k^\nu(\omega_2^2,(\vec{p}_1+\vec{p}_2)^2)\right]\\
&+\vec{p}_1^{\,2}\frac{\vec{p}_2}{\omega_2}\cdot\vec{p}_1\left[f_k^\nu((\omega_1+\omega_2)^2,\vec{p}_1^{\,2})-f_k^\nu(\omega_1^2,\vec{p}_1^{\,2})\right]+\vec{p}_2^{\,2}\frac{\vec{p}_1}{\omega_1}\cdot\vec{p}_2\left[f_k^\nu((\omega_1+\omega_2)^2,\vec{p}_2^{\,2})-f_k^\nu(\omega_2^2,\vec{p}_2^{\,2})\right]\Bigg\}.\end{aligned} \tag{E.69}$$

We now take the derivative with respect to $\vec{p}_1$, and evaluate everything at $\vec{p}_1 = \vec{0}$:

$$\begin{aligned}\vec{\nabla}_{\vec{p}_1}\Gamma_k^{(2,1)}(\mathbf{p}_1,\mathbf{p}_2)\big|_{\vec{p}_1=\vec{0}} =& \lambda\vec{p}_2 f_k^\lambda((\omega_1+\omega_2)^2,\vec{p}_2^2) + \lambda\frac{\omega_2}{\omega_1}\vec{p}_2\left[f_k^\lambda((\omega_1+\omega_2)^2,\vec{p}_2^2) - f_k^\lambda(\omega_2^2,\vec{p}_2^2)\right] \\ &+ i\nu\frac{\nu}{D}\vec{p}_2^2\frac{\vec{p}_2}{\omega_1}\left[f_k^\nu((\omega_1+\omega_2)^2,\vec{p}_2^2) - f_k^\nu(\omega_2^2,\vec{p}_2^2)\right] \end{aligned} \tag{E.70}$$

where we used the fact that $f_k^\lambda(\omega_i^2, p_i^2 = 0) = 1$ is constant along the flow due to shift-gauged symmetry [127]. Recalling that [127]

$$\Gamma^{(1,1)}(\omega,\vec{p}) = i\omega f_k^\lambda(\omega^2,\vec{p}^2) + \frac{\nu}{D}\vec{p}^2 f_k^\nu(\omega^2,\vec{p}^2) \tag{E.71}$$

we get

$$i\omega_1\vec{\nabla}_{\vec{p}_1}\Gamma^{(2,1)}(\mathbf{p}_1,\mathbf{p}_2)\big|_{\vec{p}_1=\vec{0}} = \lambda\vec{p}_2\left[\Gamma^{(1,1)}(\omega_1+\omega_2,\vec{p}_2) - \Gamma^{(1,1)}(\omega_2,\vec{p}_2)\right] \tag{E.72}$$

that is exactly (E.59).

F Non-Perturbative RG and its Application to KPZ Equation with Temporally-Correlated Noise

In this appendix we report some technical details about the analytical and numerical tools used to obtain the results presented in Chap. 5. We will first derive the flow equation for f^λ in the NLO$_\omega$ scheme introduced in Chap. 5 and then discuss some subtleties about the latter. We will then focus on some numerical details which are important to properly integrate the NPRG flow.

F.1 Flow equation of f^λ_κ at NLO$_\omega$ level

Recalling the definition (5.47) of f^λ_κ, its flow $\partial_s f^\lambda_\kappa$ can be extracted directly from the flow of the three-point function $\Gamma^{(2,1)}$, (E.22), with $\Gamma^{(2,1)}_\kappa \equiv [\Gamma^{(3)}_\kappa]_{\varphi,\varphi,\tilde\varphi}$. The three different contributions in (E.22) involves up to $\Gamma^{(5)}$, $\Gamma^{(4)}$ and $\Gamma^{(3)}$ respectively. It is easy to check that all the $\Gamma^{(n)}$, $n>3$, calculated from the ansatz (E.25), contain only terms proportional to functional derivative of the running functions in principle up to the $n-1$ order,

$$\frac{\delta f^X}{\delta\varphi_1},\dots,\frac{\delta^{n-1} f^X}{\delta\varphi_1\dots\delta\varphi_{n-1}}, \tag{F.1}$$

applied to some combination of space-time delta functions. As an example we give the result for $\Gamma^{(3,1)}$ and $\Gamma^{(4,1)}$:

$$\begin{aligned}\Gamma^{(3,1)}(\mathbf{p}_k,\mathbf{p}_j,\mathbf{p}_i,\mathbf{p}_4) = \sum_{(i,j,k)\in P_3}\int_{\mathbf{q}}\Bigg\{ &-i\omega_i\mathcal{F}\left\{\delta(\mathbf{x}-\mathbf{x}_4)\frac{\delta^2 f^\lambda_\kappa}{\delta\varphi_j\delta\varphi_k}\delta(\mathbf{x}-\mathbf{x}_i)\right\}\\ &+\lambda_\kappa\vec{p}_j\cdot\vec{p}_k\mathcal{F}\left\{\delta(\mathbf{x}-\mathbf{x}_4)\frac{\delta f^\lambda_\kappa}{\delta\varphi_i}\delta(\mathbf{x}-\mathbf{x}_j)\delta(\mathbf{x}-\mathbf{x}_k)\right\}\\ +\vec{p}_i^{\,2}\frac{\nu_\kappa}{2D_\kappa}\Bigg[\mathcal{F}\left\{\delta(\mathbf{x}-\mathbf{x}_i)\frac{\delta^2 f^\lambda_\kappa}{\delta\varphi_j\delta\varphi_k}\delta(\mathbf{x}-\mathbf{x}_4)\right\}&+\mathcal{F}\left\{\delta(\mathbf{x}-\mathbf{x}_4)\frac{\delta^2 f^\lambda_\kappa}{\delta\varphi_j\delta\varphi_k}\delta(\mathbf{x}-\mathbf{x}_i)\right\}\Bigg]\Bigg\}\end{aligned} \tag{F.2}$$

$$\begin{aligned}\Gamma^{(4,1)}(\mathbf{p}_\ell,\mathbf{p}_k,\mathbf{p}_j,\mathbf{p}_i,\mathbf{p}_5) = \sum_{(i,j,k,\ell)\in P_4}\int_{\mathbf{q}}\Bigg\{ &-i\omega_i\mathcal{F}\left\{\delta(\mathbf{x}-\mathbf{x}_5)\frac{\delta^3 f^\lambda_\kappa}{\delta\varphi_j\delta\varphi_k\delta\varphi_\ell}\delta(\mathbf{x}-\mathbf{x}_i)\right\}\\ &+\lambda_\kappa\vec{p}_\kappa\cdot\vec{p}_\ell\mathcal{F}\left\{\delta(\mathbf{x}-\mathbf{x}_5)\frac{\delta^2 f^\lambda_\kappa}{\delta\varphi_i\delta\varphi_j}\delta(\mathbf{x}-\mathbf{x}_k)\delta(\mathbf{x}-\mathbf{x}_\ell)\right\}\\ +\vec{p}_i^{\,2}\frac{\nu_\kappa}{2D_\kappa}\Bigg[\mathcal{F}\left\{\delta(\mathbf{x}-\mathbf{x}_i)\frac{\delta^3 f^\lambda_\kappa}{\delta\varphi_j\delta\varphi_k\delta\varphi_\ell}\delta(\mathbf{x}-\mathbf{x}_5)\right\}&+\mathcal{F}\left\{\delta(\mathbf{x}-\mathbf{x}_5)\frac{\delta^3 f^\lambda_\kappa}{\delta\varphi_j\delta\varphi_k\delta\varphi_\ell}\delta(\mathbf{x}-\mathbf{x}_i)\right\}\Bigg]\Bigg\}\end{aligned} \tag{F.3}$$

It is interesting to note that $\Gamma^{(n,1)}$ can be calculated in an iterative way. Using the same procedure we used to compute (E.66), we can compute the Fourier transform of the different functional derivatives:

$$\mathcal{F}\left\{\delta(\mathbf{x}-\mathbf{x}_3)\frac{\delta f_\kappa^X}{\delta\varphi_i}\delta(\mathbf{x}-\mathbf{x}_j)\right\} = i\lambda_\kappa\vec{p}_i\cdot\vec{p}_j\left[\frac{f_\kappa^X(\omega_j^2,\vec{p}_j^2)}{\omega_i}-\frac{f_\kappa^X\left((\omega_i+\omega_j)^2,p_j^2\right)}{\omega_i}\right] \tag{F.4}$$

$$\begin{aligned}\mathcal{F}\left\{\delta(\mathbf{x}-\mathbf{x}_4)\frac{\delta^2 f_\kappa^X}{\delta\varphi_i\delta\varphi_j}\delta(\mathbf{x}-\mathbf{x}_k)\right\} &= (i\lambda_\kappa)^2\sum_{(i,j)\in P_2}\vec{p}_i\cdot\vec{p}_k\vec{p}_j\cdot(\vec{p}_i+\vec{p}_k)\\ &\times\left[\frac{f_\kappa^X(\omega_k^2,\vec{p}_k^2)}{\omega_i(\omega_i+\omega_j)}-\frac{f_\kappa^X\left((\omega_i+\omega_k)^2,p_k^2\right)}{\omega_i\omega_j}+\frac{f_\kappa^X\left((\omega_i+\omega_j+\omega_k)^2,\vec{p}_k^2\right)}{\omega_j(\omega_i+\omega_j)}\right]\end{aligned} \tag{F.5}$$

$$\begin{aligned}\mathcal{F}\left\{\delta(\mathbf{x}-\mathbf{x}_5)\frac{\delta^3 f_\kappa^X}{\delta\varphi_i\delta\varphi_j\delta\varphi_k}\delta(\mathbf{x}-\mathbf{x}_\ell)\right\} &= (i\lambda_\kappa)^3\sum_{(i,j,k)\in P_3}\vec{p}_i\cdot\vec{p}_\ell\vec{p}_j\cdot(\vec{p}_i+\vec{p}_\ell)\vec{p}_k\cdot(\vec{p}_i+\vec{p}_j+\vec{p}_\ell)\\ &\times\left[\frac{f_\kappa^X(\omega_\ell^2,\vec{p}_\ell^2)}{\omega_i(\omega_i+\omega_j)(\omega_i+\omega_j+\omega_k)}-\frac{f_\kappa^X\left((\omega_i+\omega_\ell)^2,p_\ell^2\right)}{\omega_i\omega_j(\omega_j+\omega_k)}+\frac{f_\kappa^X\left((\omega_i+\omega_j+\omega_\ell)^2,\vec{p}_\ell^2\right)}{\omega_k\omega_j(\omega_i+\omega_j)}\right.\\ &\left.-\frac{f_\kappa^X\left((\omega_i+\omega_j+\omega_k+\omega_\ell)^2,\vec{p}_\ell^2\right)}{\omega_k(\omega_j+\omega_k)(\omega_i+\omega_j+\omega_k)}\right]\end{aligned} \tag{F.6}$$

As it was for the $\Gamma^{(n,1)}$, we note that we can iteratively find a general $\mathcal{F}\left\{\delta(\mathbf{x}-\mathbf{x}_{n+2})(\delta^n f^X/\delta\varphi_1\cdots\delta\varphi_n)\delta(\mathbf{x}-\mathbf{x}_{n+1})\right\}$. One can check that all these contributions vanish in the NLO limit, in which $f_\kappa^X\equiv f_\kappa^X(p^2)$. Furthermore it is is straightforward to note that they also vanish in the NLO$_\omega$ case, where $f_\kappa^X\equiv f_\kappa^X(p^2,\omega)$ but has no functional dependence on φ, *i.e.* $\delta f^X/\delta\varphi=0$. For the NLO and NLO$_\omega$ case we thus have the same flow equations, in which only $\Gamma^{(n)}$ with $n\leq 3$ are non-vanishing. The flow equation for $\Gamma_\kappa^{(3)}$ then reduces to

$$\begin{aligned}\partial_\kappa[\Gamma_\kappa^{(3)}]_{i,j,k}(\mathbf{p}_1,\mathbf{p}_2) = -\frac{1}{2}\mathrm{Tr}\Big\{&\partial_\kappa R_\kappa(\mathbf{q})G_\kappa(\mathbf{q})\Gamma^{(3)}_{\kappa,i}(\mathbf{p}_1,\mathbf{q})G_\kappa(\mathbf{p}_1+\mathbf{q})\Gamma^{(3)}_{\kappa,j}(\mathbf{p}_2,\mathbf{p}_1+\mathbf{q})G_\kappa(\mathbf{p}_1+\mathbf{p}_2+\mathbf{q})\\ &\times\Gamma^{(3)}_{\kappa,k}(-\mathbf{p}_1-\mathbf{p}_2,\mathbf{p}_1+\mathbf{p}_2+\mathbf{q})G_\kappa(\mathbf{q})\Big\}\end{aligned} \tag{F.7a}$$

$$\partial_\kappa[\Gamma_\kappa^{(3)}]_{i,j,k}(\mathbf{p}_1,\mathbf{p}_2) = -\tfrac{1}{2}\textstyle\sum_{(i,j,k)\in P_3}$$

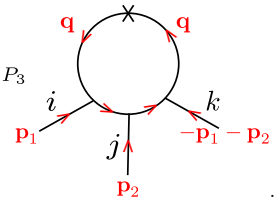

. (F.7b)

It is important to stress that the NLO and NLO$_\omega$ schemes are substantially different approximations even if the resulting flow looks similar. In the NLO approximation we neglect the time-dependence of the flowing functions on the *r.h.s* of the flow equations and hence keep only the explicit frequency dependence coming from the propagator of the theory. This approximation level preserves Galilean invariance because the f^X are functions of $-\nabla^2$ only, which generates scalars of the Galilean transformation. On the contrary, in the NLO$_\omega$ scheme we are able to keep a full dependence on the frequency in the f^X. However it is not the suitable frequency-dependence to preserve Galilean invariance. Indeed, removing the functional dependence on φ in the total time derivative $\tilde{D}_t$, we remove the constraint that Galilean invariance imposes on the relation between time and space. Keeping only the ∂_t dependence in f^X we thus have a full time dependence but the price to pay is a breaking of the Galilean Invariance. Of course, this

does not prevent from describing a Galilean invariant fixed point, but the constraints stemming from this symmetry will be only approximately verified in the NLO$_\omega$ scheme. At NLO$_\omega$ level we then find

$$\begin{aligned}\partial_s f_\kappa^\lambda(\omega^2,\vec{p}^2) =& -2g_\kappa f_\kappa^\lambda(\omega^2,p^2)\int_{\mathbf{q}}\frac{1}{p^2P_\kappa(\varphi^2,\Pi^2)P_\kappa(\varphi_1^2,\Pi_1^2)P_\kappa(\omega^2,q^2)^2P_\kappa(\Omega^2,Q^2)}\\
&\times\Bigg\{\vec{q}\cdot\vec{p}\,\partial_s S_\kappa^D(q^2)P_\kappa(\omega^2,q^2)f_\kappa^\lambda(\varphi^2,\Pi^2)\Bigg[\vec{\Pi}\cdot\vec{\Pi}_1\,\vec{q}\cdot\vec{p}\,P_\kappa(\Omega^2,Q^2)X_\kappa(\varphi,\Pi^2,\varphi_1,\Pi_1^2)f_\kappa^\lambda(\varphi_1^2,\Pi_1^2)\\
&+2\vec{q}\cdot\vec{Q}\vec{p}\cdot\vec{\Pi}P_\kappa(\varphi_1^2,\Pi_1^2)f_\kappa^\lambda(\Omega^2,Q^2)X_\kappa(\Omega,Q^2,\varphi,\Pi^2)\Bigg]\\
&+q^2S_\kappa^\nu(q^2)\Bigg[\vec{\Pi}\cdot\vec{\Pi}_1\,\vec{q}\cdot\vec{p}\,P_\kappa(\Omega^2,Q^2)A_\kappa(\omega,p,\varphi_1,\Pi_1,\varphi,\Pi,\omega,q) \qquad \text{(F.8)}\\
&+2\vec{q}\cdot\vec{Q}\,\vec{p}\cdot\vec{\Pi}P_\kappa(\varphi_1^2,\Pi_1^2)A_\kappa(\omega,p,\Omega,Q,\varphi,\Pi,\omega,q)\Bigg]\Bigg\} \qquad \text{(F.9)}\end{aligned}$$

where $\vec{Q}=\vec{q}+\vec{p}$, $\vec{\Pi}=\vec{p}/2+\vec{q}$, $\vec{\Pi}_1=\vec{p}/2-\vec{q}$ and

$$\begin{aligned}A_\kappa(\omega,p,\varphi_1,\Pi_1,\varphi,p,\omega,q) =& f_\kappa^\lambda(\omega^2,q^2)\Big[\vec{p}\cdot\vec{\Pi}_1\,k_\kappa(\varphi_1^2,\Pi_1^2)f_\kappa^\lambda(\varphi^2,\Pi^2)\ell X_\kappa^{(-)}(\omega,\Pi^2,\omega,q^2)\\
&+\vec{p}\cdot\vec{\Pi}k_\kappa(\varphi^2,\Pi^2)f_\kappa^\lambda(\varphi_1^2,\Pi_1^2)\ell X_\kappa^{(+)}(\varphi_1,\Pi_1^2,\omega,q^2)\Big]\\
&-2\,\vec{q}\cdot\vec{p}\,k_\kappa(\omega^2,q^2)\ell_\kappa(\omega^2,q^2)X_\kappa(\varphi,\Pi^2,\varphi_1,\Pi_1^2)f_\kappa^\lambda(\varphi^2,\Pi^2)f_\kappa^\lambda(\varphi_1^2,\Pi_1^2) \qquad \text{(F.10a)}\\
\ell X_\kappa^{(\pm)}(\varphi_1,\Pi^2,\omega,q^2) =& 2\omega\Omega\ell_\kappa(\omega^2,q^2)f_\kappa^t(\omega^2,q^2)f_\kappa^t(\Omega^2,Q^2)\pm\ell_\kappa(\Omega^2,Q^2)X_\kappa(\omega,q^2,\omega,q^2). \qquad \text{(F.10b)}\end{aligned}$$

In the LR case, the function $k_\kappa(\omega,q^2)$ is different from the pure case $k_\kappa(\omega,q^2)=f_\kappa^D(\omega,q^2)+D_\kappa r(q^2/\kappa^2)$. Indeed we also have the non analytical contribution to f_κ^D coming from the LR correlation. We thus have

$$k_\kappa(\omega^2,q^2)=f_\kappa^D(\omega^2,q^2)+D_\kappa r(q^2/\kappa^2)+\frac{w_\kappa^\theta}{\omega^{2\theta}}. \qquad \text{(F.11)}$$

As discussed in the main text, the flow equation (F.8) is non vanishing for $(\bar{\omega}=0,p=0)$ and $w_\kappa^\theta=0$, and it becomes (5.70). In this limit, one gets the flow equation for λ_κ in the pure KPZ equation, which has to be zero in order for Galilean invariance to hold. This artificial breaking of Galilean invariance comes from the choice of the NLO$_\omega$ scheme. In the NLO limit with $w_\kappa^\theta\neq 0$ one recovers (5.72).

F.2 Non-analycities with power-law correlator

In principles, the presence of the regulator in the NPRG flow ensures the analyticity of all vertex functions $\Gamma_\kappa^{(n)}$ at any finite scale κ. This is always true for the momentum dependence because of the presence of the regulator . However, since we have not included a frequency regulator, this could lead to non-analyticities. The flow of w_κ^θ can be extracted from the flow of $f_\kappa^{\tilde{D}}$ as

$$\partial_s w_\kappa^\theta=\lim_{p,\bar{\omega}\to 0}\omega^{2\theta}\partial_s f_\kappa^{\tilde{D}}(\omega^2,p^2) \qquad \text{(F.12)}$$

with $\tilde{f}_\kappa^D(\omega^2, q^2) = f_\kappa^D(\omega^2, q^2) + f_\kappa^{w^\theta}(\omega^2, p^2)\omega^{2\theta}$ and $w_\kappa^\theta \equiv f_\kappa^{w^\theta}(0,0)$. Within the NLO$_\omega$ scheme, one finds

$$\partial_s w_\kappa^\theta = \lim_{p,\bar{\omega}\to 0} 2\, w_\kappa^\theta f_k^\lambda(\bar{\omega}^2, p^2) \int_{\omega,\vec{q}} \frac{(\vec{q}\cdot\vec{Q})^2}{P(\omega^2,q^2)^2 P(\Omega^2,Q^2)} \frac{\bar{\omega}^{2\theta}}{(\bar{\omega}+\omega)^{2\theta}} \times \left(P(\omega^2,q^2)\partial_s S_k^D(q^2) - 2\vec{q}^2 \ell_\kappa(\omega^2,q^2)\partial_s S_k^\nu(q) \left(\frac{\bar{\omega}}{\omega}\right)^{2\theta} \right) \tag{F.13}$$

For values $\theta < 1/2$, the contribution of the first term in the right hand side always vanishes. The same holds for the second term for $\theta < 1/4$. However, in the range $1/4 \leq \theta < 1/2$, an ambiguity arises in the second term, since this term vanishes only if the limit $\bar{\omega} \to 0$ is taken before integration on ω. This ambiguity arises because the frequency sector is not properly regularized, and would disappear with a frequency-dependent regulator [121]. Since the result should not depend on the choice of the regulator, we simply assume that this term is zero since it should in principle vanish. Under this assumption, the coupling w_κ^θ is indeed not renormalized.

F.3 Numerical Integration

In this part we give some details about the numerical scheme we used to integrate the NPRG flow equations.

F.3.1 Integration scheme

In generic spatial dimension d we have three different integrals to perform: over the modulo of the internal momentum q, the internal frequency ω and the angle ψ between external and internal momentum. We will use quadrature methods for the three of them,

$$\int_0^\pi d\psi \int_0^\infty dq \int_0^\infty d\omega\, f_\kappa^X(\psi, q, \omega) \to \sum_{i,j,k} w_i^{(\psi)} w_j^{(q)} w_k^{(\omega)} f_\kappa^X(\psi_i^*, q_j^*, \omega_k^*) \tag{F.14}$$

where $(\psi_i^*, q_j^*, \omega_k^*)$ are the quadrature grid-points and w_ℓ^X their respective weights. The momentum integral, which in principle lies in the domain $q \in [0,\infty)$, in practice can be performed over a finite domain $q \in [0, q_{max}]$ thanks to the presence of the regulator R_κ which also ensures the absence of divergences. The fact that the frequency sector instead is not regularized has two major consequences: non-analyticities can in principle arise in the flow if they are present at the bare level and the high-frequency sector cannot be neglected in the integration procedure. The former is especially important in the case of long-range correlated noise for which $f_\Lambda^D \sim \omega^{-2\theta}$ and hence is not defined in $\omega = 0$ already at the microscopic scale Λ.

F.3.2 Grid and Interpolation

Due to the presence of non-zero external momentum and frequency $(\vec{p}, \bar{\omega})$ we have to evaluate the flowing functions in $Q = |\vec{p} + \vec{q}|$ and $\Omega = \omega + \bar{\omega}$, that are usually out of the integration grid-points in which we compute the flow; we thus have to build a protocol to have access to $\hat{f}_\kappa^X(Q,\Omega)$. One way to do this is to assume the power-law behaviour of these functions in the neighbours of $(q_{\max}, \omega < \omega_{\max})$ and $(q < q_{\max}, \omega_{\max})$, computing the exponent of such power-law using a log-fit and then extrapolate the value of the function for higher momenta and frequencies [127]. In our work we use a different approach. We define two different grids for the internal and external variables. The internal momentum and frequency,

over which we integrate, correspond to the Gauss-Legendre quadrature roots in the respective integration domains, $q \in (0, q_{max})$ and $\omega \in (0, \omega_{max})$. For the external variables we choose a set of logarithmically distributed points in the range $p \in [0, Q_{max} = p_{max} + q_{max}]$, $\bar{\omega} \in [0, \Omega_{max} = \bar{\omega}_{max} + \omega_{max}]$, with $p_{max} > q_{max}$ and $\bar{\omega}_{max} > \omega_{max}$. We thus have access to the full NPRG flow of $\hat{f}^X_\kappa(\bar{\omega}, p^2)$ up to the point $(\bar{\omega}_{max}, p_{max})$. To compute the flow of the running functions in the point $(\bar{\omega} = \Omega_{max}, p = Q_{max})$ we exploit the fact that high-momentum and -frequency sectors in the flow equations decouple from the low-momentum and -frequency ones as the fixed-point is approached. This implies a vanishing $\hat{l}^X_\kappa(\hat{\bar{\omega}}, \hat{p})$ in (5.51), for sufficiently large external frequency and momentum, leading to a pure dimensional flow in this sector

$$\partial_s \hat{f}^X_\kappa(\hat{\bar{\omega}}^2, \hat{p}^2) = \left(\eta^X_\kappa + (2 - \eta^\nu_\kappa)\hat{\bar{\omega}}\partial_{\hat{\bar{\omega}}} + \hat{p}\,\partial_{\hat{p}}\right)\hat{f}^X_\kappa(\hat{\bar{\omega}}^2, \hat{p}^2). \tag{F.15}$$

For the determination of the values of $\hat{f}^X_\kappa(\Omega^2, Q^2)$ and the derivatives $\partial_q \hat{f}^X_\kappa(\omega^2, q^2)$, $\partial_\omega \hat{f}^X_\kappa(\omega^2, q^2)$ we use a bi-cubic spline interpolation.

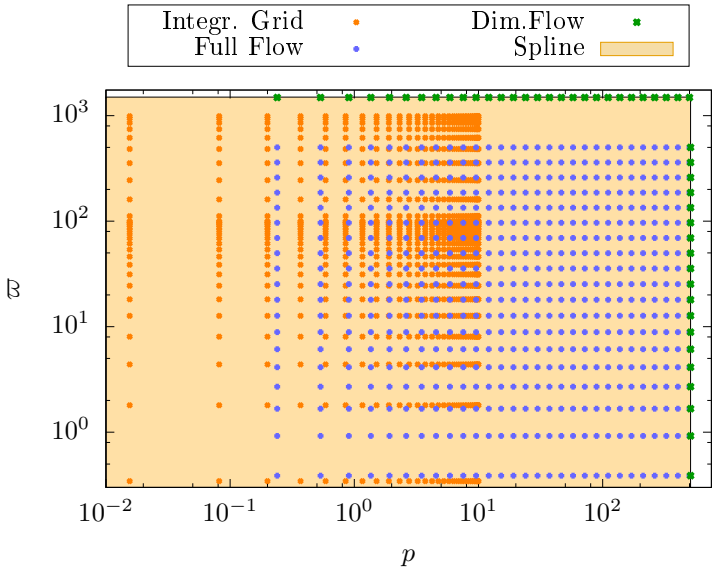

Figure F.1: Sketch of the full momentum-frequency grid used in numerical simulation, at fixed $\psi = \psi_0$.

Bibliography

[1] P. Bak, C. Tang, and K. Wiesenfeld, Phys. Rev. Lett. **59**, 381 (1987).

[2] G. Grinstein, D.-H. Lee, and S. Sachdev, Phys. Rev. Lett. **64**, 1927 (1990).

[3] G. Grinstein, Journal of Applied Physics **69**, 5441 (1991).

[4] L. P. Kadanoff, Physics Physique Fizika **2**, 263 (1966).

[5] K. G. Wilson, Phys. Rev. B **4**, 3174 (1971).

[6] K. G. Wilson, Rev. Mod. Phys. **47**, 773 (1975).

[7] F. J. Dyson, Phys. Rev. **75**, 486 (1949).

[8] E. C. G. Stueckelberg de Breidenbach and A. Petermann, Helv. Phys. Acta **26**, 499 (1953).

[9] M. Gell-Mann and F. E. Low, Phys. Rev. **95**, 1300 (1954).

[10] N. N. Bogolyubov and D. V. Shirkov, Intersci. Monogr. Phys. Astron. **3**, 1 (1959).

[11] C. G. Callan, Phys. Rev. D **2**, 1541 (1970).

[12] K. Symanzik, Communications in Mathematical Physics **18**, 227 (1970).

[13] P. C. Hohenberg and B. I. Halperin, Rev. Mod. Phys. **49**, 435 (1977).

[14] P. C. Martin, E. D. Siggia, and H. A. Rose, Phys. Rev. A **8**, 423 (1973).

[15] H.-K. Janssen, Zeitschrift für Physik B Condensed Matter **23**, 377 (1976).

[16] C. d. Dominicis, C1247 (1976).

[17] J. Schwinger, Journal of Mathematical Physics **2**, 407 (1961).

[18] L. V. Keldysh, Zh. Eksp. Teor. Fiz. **47**, 1515 (1964), [Sov. Phys. JETP20,1018(1965)].

[19] J. Polchinski, Nuclear Physics B **231**, 269 (1984).

[20] C. Wetterich, Physics Letters B **301**, 90 (1993).

[21] U. Ellwanger, Zeitschrift für Physik C Particles and Fields **58**, 619 (1993).

[22] T. R. Morris, International Journal of Modern Physics A **09**, 2411 (1994).

[23] L. Canet, H. Chaté, and B. Delamotte, Journal of Physics A: Mathematical and Theoretical **44**, 495001 (2011).

[24] J. Kasprzak *et al.*, Nature **443**, 409 (2006).

[25] L. He, L. M. Sieberer, E. Altman, and S. Diehl, Phys. Rev. B **92**, 155307 (2015).

[26] T. Halpin-Healy and Y.-C. Zhang, Physics Reports **254**, 215 (1995).

[27] T. Halpin-Healy and K. A. Takeuchi, Journal of Statistical Physics **160**, 794 (2015).

[28] I. Corwin, Random Matrices: Theory and Applications **01**, 1130001 (2012).

[29] J. Krug, Advances in Physics **46**, 139 (1997).

[30] M. Kardar, G. Parisi, and Y.-C. Zhang, Phys. Rev. Lett. **56**, 889 (1986).

[31] J. Maunuksela *et al.*, Phys. Rev. Lett. **79**, 1515 (1997).

[32] J. ichi Wakita, H. Itoh, T. Matsuyama, and M. Matsushita, Journal of the Physical Society of Japan **66**, 67 (1997).

[33] K. A. Takeuchi and M. Sano, Phys. Rev. Lett. **104**, 230601 (2010).

[34] F. Family and T. Vicsek, Journal of Physics A: Mathematical and General **18**, L75 (1985).

[35] S. F. Edwards and D. R. Wilkinson, Proceedings of the Royal Society of London. A. Mathematical and Physical Sciences **381**, 17 (1982).

[36] U. C. Täuber, *Critical dynamics: a field theory approach to equilibrium and non-equilibrium scaling behavior* (Cambridge University Press, Cambridge, 2014).

[37] B. I. Halperin, P. C. Hohenberg, and S.-k. Ma, Phys. Rev. Lett. **29**, 1548 (1972).

[38] S.-k. Ma and G. F. Mazenko, Phys. Rev. B **11**, 4077 (1975).

[39] K. J. Wiese, Phys. Rev. E **56**, 5013 (1997).

[40] J. Krug and P. Meakin, Journal of Physics A: Mathematical and General **23**, L987 (1990).

[41] J. Krug, P. Meakin, and T. Halpin-Healy, Phys. Rev. A **45**, 638 (1992).

[42] M. Prähofer and H. Spohn, Phys. Rev. Lett. **84**, 4882 (2000).

[43] P. Calabrese, P. L. Doussal, and A. Rosso, EPL (Europhysics Letters) **90**, 20002 (2010).

[44] Dotsenko, V., EPL **90**, 20003 (2010).

[45] P. Calabrese and P. Le Doussal, Phys. Rev. Lett. **106**, 250603 (2011).

[46] P. Calabrese and P. Le Doussal, J. Stat. Mech. P06001 (2012).

[47] T. Imamura and T. Sasamoto, Journal of Statistical Physics **150**, 908 (2013).

[48] C. Tracy and H. Widom, Commun. Math. Phys. **159**, 151 (1994).

[49] J. Baik and E. M. Rains, Journal of Statistical Physics **100**, 523 (2000).

[50] C. A. Tracy and H. Widom, in *Calogero—Moser— Sutherland Models*, edited by J. F. van Diejen and L. Vinet (Springer New York, New York, NY, 2000), pp. 461–472.

[51] K. Takeuchi and M. Sano, J. Stat. Phys. **147**, 853 (2012).

[52] K. A. Takeuchi, Phys. Rev. Lett. **110**, 210604 (2013).

[53] A. A. Fedorenko, Phys. Rev. B **77**, 094203 (2008).

[54] J. Burgers, in *A Mathematical Model Illustrating the Theory of Turbulence*, Vol. 1 of *Advances in Applied Mechanics*, edited by R. V. Mises and T. V. Kármán (Elsevier, Amsterdam, 1948), pp. 171 – 199.

[55] J. M. Burgers, in *The Nonlinear Diffusion Equation: Asymptotic Solutions and Statistical Problems* (Springer Netherlands, Dordrecht, 1974).

[56] U. Frisch, *Turbulence: the legacy of A N Kolmogorov* (Cambridge Univ. Press, Cambridge, 1995).

[57] J. Bec and K. Khanin, Physics Reports **447**, 1 (2007).

[58] (PUBLISHER, ADDRESS, YEAR).

[59] H. Deng, H. Haug, and Y. Yamamoto, Rev. Mod. Phys. **82**, 1489 (2010).

[60] M. Born and E. Wolf, *Principles of Optics: Electromagnetic Theory of Propagation, Interference and Diffraction of Light (7th Edition)*, 7th ed. (Cambridge University Press, Cambridge, 1999).

[61] I. Carusotto and C. Ciuti, Rev. Mod. Phys. **85**, 299 (2013).

[62] V. Savona *et al.*, Phase Transitions **68**, 169 (1999).

[63] A. Imamoglu, R. J. Ram, S. Pau, and Y. Yamamoto, Phys. Rev. A **53**, 4250 (1996).

[64] J. J. Baumberg *et al.*, Phys. Rev. B **62**, R16247 (2000).

[65] R. M. Stevenson *et al.*, Phys. Rev. Lett. **85**, 3680 (2000).

[66] C. Ciuti, P. Schwendimann, B. Deveaud, and A. Quattropani, Phys. Rev. B **62**, R4825 (2000).

[67] C. Ciuti, P. Schwendimann, and A. Quattropani, Phys. Rev. B **63**, 041303 (2001).

[68] D. M. Whittaker, Phys. Rev. B **63**, 193305 (2001).

[69] I. Carusotto and C. Ciuti, Phys. Rev. B **72**, 125335 (2005).

[70] K. G. Lagoudakis *et al.*, Nature Physics **4**, 706 EP (2008).

[71] A. Amo *et al.*, Nature Physics **5**, 805 EP (2009).

[72] A. Amo *et al.*, Nature **457**, 291 EP (2009).

[73] A. Amo *et al.*, Science **332**, 1167 (2011).

[74] G. Roumpos *et al.*, Proceedings of the National Academy of Sciences **109**, 6467 (2012).

[75] G. Dagvadorj *et al.*, Physical Review X **5**, 041028 (2015).

[76] D. Caputo *et al.*, Nature Materials **17**, 145 EP (2017), article.

[77] H. Deng *et al.*, Phys. Rev. Lett. **97**, 146402 (2006).

[78] Y. Sun *et al.*, Phys. Rev. Lett. **118**, 016602 (2017).

[79] M. Wouters and I. Carusotto, Phys. Rev. Lett. **99**, 140402 (2007).

[80] M. Wouters and V. Savona, Phys. Rev. B **79**, 165302 (2009).

[81] L. P. Pitaevskii and S. Stringari, *Bose-Einstein condensation*, *Internat. Ser. Mono. Phys.* (Clarendon Press, Oxford, 2003).

[82] J. J. Hopfield, Phys. Rev. **112**, 1555 (1958).

[83] F. Baboux *et al.*, Optica **5**, 1163 (2018).

[84] L. M. Sieberer, M. Buchhold, and S. Diehl, Reports on Progress in Physics **79**, 096001 (2016).

[85] A. Trichet *et al.*, Phys. Rev. B **88**, 121407 (2013).

[86] T. Kloss, L. Canet, B. Delamotte, and N. Wschebor, Physical Review E **89**, (2013).

[87] S. Mathey *et al.*, Physical Review E **95**, (2017).

[88] H. Fröhlich, Advances in Physics **3**, 325 (1954).

[89] H. J. Carmichael, in *Statistical Methods in Quantum Optics 1: Master Equations and Fokker-Planck Equations* (Springer Berlin Heidelberg, Berlin, Heidelberg, 1999).

[90] I. G. Savenko, T. C. H. Liew, and I. A. Shelykh, Phys. Rev. Lett. **110**, 127402 (2013).

[91] M. Werner and P. Drummond, Journal of Computational Physics **132**, 312 (1997).

[92] G. R. Dennis, J. J. Hope, and M. T. Johnsson, Computer Physics Communications **184**, 201 (2013).

[93] E. Medina, T. Hwa, M. Kardar, and Y.-C. Zhang, Phys. Rev. A **39**, 3053 (1989).

[94] P. Meakin and R. Jullien, EuroPhys. Lett. **9**, 71 (1989).

[95] T. Halpin-Healy, Phys. Rev. A **42**, 711 (1990).

[96] Y.-C. Zhang, Phys. Rev. B **42**, 4897 (1990).

[97] H. G. E. Hentschel and F. Family, Phys. Rev. Lett. **66**, 1982 (1991).

[98] J. G. Amar, P.-M. Lam, and F. Family, Phys. Rev. A **43**, 4548 (1991).

[99] C.-K. Peng, S. Havlin, M. Schwartz, and H. E. Stanley, Phys. Rev. A **44**, R2239 (1991).

[100] N.-N. Pang, Y.-K. Yu, and T. Halpin-Healy, Phys. Rev. E **52**, 3224 (1995).

[101] M. S. Li, Phys. Rev. E **55**, 1178 (1997).

[102] A. K. Chattopadhyay and S. M. Bhattacharjee, Europhys. Lett. **42**, 119 (1998).

[103] E. Katzav and M. Schwartz, Phys. Rev. E **60**, 5677 (1999).

[104] E. Frey, U. C. Täuber, and H. K. Janssen, Europhys. Lett. **47**, 14 (1999).

[105] H. K. Janssen, U. C. Täuber, and E. Frey, Eur. Phys. J. B **9**, 491 (1999).

[106] M. K. Verma, Physica A **277**, 359 (2000).

[107] E. Katzav, Phys. Rev. E **68**, 046113 (2003).

[108] Hanfei and B. Ma, Phys. Rev. E **47**, 3738 (1993).

[109] E. Katzav and M. Schwartz, Phys. Rev. E **70**, 011601 (2004).

[110] P. Strack, Phys. Rev. E **91**, 032131 (2015).

[111] C.-H. Lam, L. M. Sander, and D. E. Wolf, Phys. Rev. A **46**, R6128 (1992).

[112] T. Song and H. Xia, Journal of Statistical Mechanics: Theory and Experiment **2016**, 113206 (2016).

[113] N. V. Antonov, N. M. Gulitskiy, M. M. Kostenko, and A. V. Malyshev, Phys. Rev. E **97**, 033101 (2018).

[114] L. Canet, H. Chaté, B. Delamotte, and N. Wschebor, Phys. Rev. Lett. **104**, 150601 (2010).

[115] T. Kloss, L. Canet, and N. Wschebor, Phys. Rev. E **86**, 051124 (2012).

[116] T. Halpin-Healy, Phys. Rev. E **88**, 042118 (2013).

[117] T. Halpin-Healy, Phys. Rev. E **88**, 069903 (2013).

[118] T. Kloss, L. Canet, and N. Wschebor, Phys. Rev. E **90**, 062133 (2014).

[119] B. Delamotte, in *Renormalization Group and Effective Field Theory Approaches to Many-Body Systems*, edited by A. Schwenk and J. Polonyi (Springer Berlin Heidelberg, Berlin, Heidelberg, 2012), pp. 49–132.

[120] L. Canet, B. Delamotte, O. Deloubrière, and N. Wschebor, Phys. Rev. Lett. **92**, 195703 (2004).

[121] C. Duclut and B. Delamotte, Phys. Rev. E **95**, 012107 (2017).

[122] J. Berges and D. Mesterházy, Nuclear Physics B - Proceedings Supplements **228**, 37 (2012), physics at all scales: The Renormalization Group, Proceedings of the 49th Internationale Universitätswochen für Theoretische Physik.

[123] J.-P. Blaizot, R. Méndez-Galain, and N. Wschebor, Physics Letters B **632**, 571 (2006).

[124] I. Balog *et al.*, arXiv e-prints arXiv:1907.01829 (2019).

[125] D. F. Litim, Phys. Rev. D **64**, 105007 (2001).

[126] L. Canet, eprint arXiv:cond-mat/0509541 (2005).

[127] L. Canet, H. Chaté, B. Delamotte, and N. Wschebor, Phys. Rev. E **84**, 061128 (2011).

[128] A. Pagnani and G. Parisi, Phys. Rev. E **92**, 010101 (2015).

[129] E. Altman *et al.*, Phys. Rev. X **5**, 011017 (2015).

[130] M. Marsili, A. Maritan, F. Toigo, and J. R. Banavar, Rev. Mod. Phys. **68**, 963 (1996).

[131] L. Onsager and S. Machlup, Phys. Rev. **91**, 1505 (1953).

[132] C. Gardiner, *Stochastic methods: a handbook for the natural and social sciences; 4th ed.*, *Springer Series in Synergetics* (Springer, Berlin, 2010), the book can be consulted by contacting: BE-ABP: Giovannozzi, Massimo.

[133] A. Altland and B. Simons, *Condensed matter field theory; 2nd ed.* (Cambridge Univ. Press, Cambridge, 2010).

[134] A. Kamenev, *Field Theory of Non-Equilibrium Systems* (Cambridge University Press, Cambridge, 2011).

[135] J. Zinn-Justin, Int. Ser. Monogr. Phys. **113**, (2002).

[136] A. Zee, *Quantum Field Theory in a Nutshell*, *Nutshell handbook* (Princeton Univ. Press, Princeton, NJ, 2003).